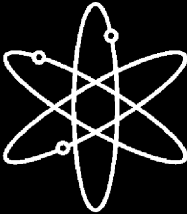


Experimental Measurements of Pressure Drop Across Sump Screen Debris Beds in Support of Generic Safety Issue 191



Pacific Northwest National Laboratory



**U.S. Nuclear Regulatory Commission
Office of Nuclear Regulatory Research
Washington, DC 20555-0001**



AVAILABILITY OF REFERENCE MATERIALS IN NRC PUBLICATIONS

NRC Reference Material

As of November 1999, you may electronically access NUREG-series publications and other NRC records at NRC's Public Electronic Reading Room at <http://www.nrc.gov/reading-rm.html>.

Publicly released records include, to name a few, NUREG-series publications; *Federal Register* notices; applicant, licensee, and vendor documents and correspondence; NRC correspondence and internal memoranda; bulletins and information notices; inspection and investigative reports; licensee event reports; and Commission papers and their attachments.

NRC publications in the NUREG series, NRC regulations, and Title 10, "Energy," in the *Code of Federal Regulations* may also be purchased from one of these two sources:

1. The Superintendent of Documents
U.S. Government Printing Office
Mail Stop SSOP
Washington, DC 20402-0001
Internet: <http://bookstore.gpo.gov>
Telephone: 202-512-1800
Fax: 202-512-2250
2. The National Technical Information Service
Springfield, VA 22161-0002
<http://www.ntis.gov>
1-800-553-6847 or, locally, 703-605-6000

A single copy of each NRC draft report for comment is available free, to the extent of supply, upon written request as follows:

Address: Office of the Chief Information Officer
Reproduction and Distribution
Services Section
U.S. Nuclear Regulatory Commission
Washington, DC 20555-0001

Email: DISTRIBUTION@nrc.gov
Facsimile: 301-415-2289

Some publications in the NUREG series that are posted at NRC's Web site address <http://www.nrc.gov/reading-rm/doc-collections/nuregs> are updated periodically and may differ from the last printed version. Although references to material found on a Web site bear the date the material was accessed, the material available on the date cited may subsequently be removed from the site.

Non-NRC Reference Material

Documents available from public and special technical libraries include all open literature items, such as books, journal articles, and transactions; *Federal Register* notices; Federal and State legislation; and congressional reports. Such documents as theses, dissertations, foreign reports and translations, and non-NRC conference proceedings may be purchased from their sponsoring organizations.

Copies of industry codes and standards used in a substantive manner in the NRC regulatory process are maintained at the following:

The NRC Technical Library
Two White Flint North
11545 Rockville Pike
Rockville, MD 20852-2738

These standards are available in the library for reference use by the public. Codes and standards are usually copyrighted and may be purchased from the originating organization or, if they are American National Standards, from the following:

American National Standards Institute
11 West 42nd Street
New York, NY 10036-8002
<http://www.ansi.org>
212-642-4900

Legally binding regulatory requirements are stated only in laws; NRC regulations; licenses, including technical specifications; or orders, not in NUREG-series publications. The views expressed in contractor-prepared publications in this series are not necessarily those of the NRC.

The NUREG series comprises (1) technical and administrative reports and books prepared by the staff (NUREG-XXXX) or agency contractors (NUREG/CR-XXXX), (2) proceedings of conferences (NUREG/CP-XXXX), (3) reports resulting from international agreements (NUREG/IA-XXXX), (4) brochures (NUREG/BR-XXXX), and (5) compilations of legal decisions and orders of the Commission and Atomic and Safety Licensing Boards and of Directors' decisions under Section 2.206 of NRC's regulations (NUREG-0750).

Experimental Measurements of Pressure Drop Across Sump Screen Debris Beds in Support of Generic Safety Issue 191

Manuscript Completed: December 2006
Date Published: February 2007

Prepared by
C.W. Enderlin, B.E. Wells, M. White, F. Nigl,
D.R. Rector, T.J. Peters, A.D. Guzman

Pacific Northwest National Laboratory
Richland, WA 99352

W.J. Krotiuk, NRC Project Manager

Prepared for
Division of Risk Assessment and Special Projects
Office of Nuclear Regulatory Research
U.S. Nuclear Regulatory Commission
Washington, DC 20555-0001
NRC Job Code N6106



Abstract

The U.S. Nuclear Regulatory Commission (NRC) Generic Safety Issue-191 deals with the possibility that, during a loss of coolant accident in a pressurized water reactor, thermal insulation and other materials may be damaged and the debris transported to accumulate on the sump screens of the emergency core cooling system and containment sump. Over time, a debris bed could form, blocking the sump screen, increasing the pressure drop across the sump screen, and reducing the available suction head for the recirculation pumps resulting in the safety margins for pump operations being exceeded.

Pacific Northwest National Laboratory (PNNL) conducted experiments to help the NRC predict the flow through debris beds consisting of fiberglass and calcium silicate particulate. The effects of debris preparation on debris bed formation and pressure drop were evaluated and a metric developed for characterizing the preparation. Testing consisted of forming the debris bed within the test loop and obtaining a steady-state pressure drop at the bed formation velocity. The velocity was then changed incrementally through several cycles—increasing and decreasing—with a steady pressure measurement obtained at each flow set point. The loop temperature was then changed and the velocity variation sequence repeated.

The test setup, data acquisition system, procedures, experimental results, and observations are presented. In situ measurements and photographs show the debris beds contracting and relaxing with the cycling of flow velocity.

Foreword

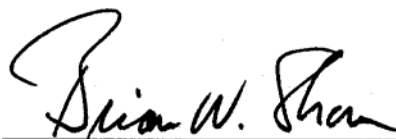
During a loss-of-coolant accident (LOCA) at a nuclear power plant, the impingement of a high-energy steam-water jet or exposure to the high containment temperature, pressure, and humidity environment may dislodge thermal insulation, coatings, and other material. Some dislodged debris may fall near the containment sump or be transported in the containment water pool to the vicinity of the sump. After recirculation starts, the debris may accumulate on the sump screen surface and increase the pressure drop (i.e., head loss) across the sump screens. The increased head loss could challenge the ability of the recirculation pumps to provide adequate long-term cooling water to the emergency core cooling system (ECCS) and the containment spray system pumps.

The nuclear industry has recognized this phenomenon. The United States and other countries have performed tests to characterize the pressure drop across a debris clogged sump screen. An October 1995, U.S. Nuclear Regulatory Commission (NRC) study documented in NUREG/CR-6224, *Parametric Study of the Potential for BWR ECCS Strainer Blockage Due to LOCA-Generated Debris*, used test data to develop a head loss correlation to evaluate suppression pool strainer performance in boiling-water reactors but did not address the range of potential debris characteristics postulated for accidents in pressurized-water reactors (PWRs). A significant number of PWR plants use calcium silicate (CalSil) thermal insulation, often in combination with other materials such as fiberglass (i.e., NUKON™) or reflective metal insulation.

Consequently, NRC sponsored another study to provide test data for head losses resulting from the accumulation of CalSil-laden insulation debris on a PWR sump screen and to evaluate the suitability of the NUREG/CR-6224 correlation for application to PWR plants that can accumulate CalSil insulation in combination with other debris on a sump screen. This study was documented in NUREG/CR-6874, *GSI-191 Experimental Studies of Loss-of-Coolant-Accident-Generated Debris Accumulation and Head Loss with Emphasis on the Effects of Calcium Silicate Insulation*, dated May 2005.

NRC's Advisory Committee on Reactor Safeguards (ACRS), Thermal-Hydraulic Subcommittee, raised concerns regarding the application of the NUREG/CR-6224 methodology for calculating head loss through debris-clogged PWR sump screens in letter ACRSR-2096, "Safety Evaluation of the Industry Guidelines Related to Pressurized Water Sump Performance," dated October 18, 2004. As a result of these technical comments, the staff of NRC's Office of Nuclear Regulatory Research concluded that the head loss methodology should be redeveloped and correlated against test data. NRC recognized that the available head loss test data did not include the effects of water temperature on a debris laden sump screen, did not provide data for a broad enough range of CalSil and NUKON concentrations on a sump screen to address a large portion of expected PWR sump screen conditions, and did not address head loss resulting from accumulation of coating debris on a sump screen. In addition, previous testing was performed using a woven metal screen to represent the sump screen, while many of the proposed PWR sump designs use perforated metal plates instead and are designed for lower water approach velocities.

NRC sponsored additional testing to address these concerns and to support development of an improved head loss correlation, as described in this document. The data provided can be used to develop a conservative bounding methodology for calculating pressure drop across a porous medium that might be present on a debris laden sump screen.



Brian Sheron, Director
Office of Nuclear Regulatory Research
U.S. Nuclear Regulatory Commission

Contents

Abstract	iii
Foreword	v
Abbreviations and Acronyms	xvii
Executive Summary	xix
1.0 Introduction	1.1
1.1 Background	1.1
1.2 Objectives	1.3
1.3 Report Outline	1.4
2.0 Test Setup	2.1
2.1 Design Requirements	2.1
2.2 Test Screen Materials	2.2
2.3 Benchtop Loop Setup	2.4
2.3.1 Benchtop Loop Description	2.5
2.3.2 Benchtop Test Section Description	2.7
2.4 Large-Scale Loop	2.9
2.4.1 Large-Scale Loop Description	2.9
2.4.2 Test Section	2.11
2.4.3 Debris Injection System	2.14
2.5 Instrumentation and Measurements	2.15
2.5.1 Large-Scale Test Loop Instrumentation and Data Acquisition	2.16
2.5.2 Benchtop Test Loop Instrumentation	2.17
2.5.3 Additional Instrumentation and Equipment	2.17
2.5.4 Supporting Post-Test Measurements	2.18
3.0 Test Debris Preparation	3.1
3.1 Debris Bed Formation Criteria and Target Characteristics Identification	3.1
3.1.1 Debris Bed Formation Criteria	3.2
3.1.2 NUKON Slurry Target Characteristics	3.2
3.1.3 CalSil Slurry Target Characteristics	3.5
3.2 Target Characteristics and Formation Criterion Testing	3.5
3.2.1 NUKON Slurry Preparation Characteristic Testing	3.6
3.2.2 CalSil Slurry Preparation Characteristic Testing	3.12
3.2.3 Debris Bed Criteria Testing	3.15
3.3 Debris Preparation Summary	3.30
3.3.1 NUKON Debris Preparation	3.31

3.3.2	CalSil Debris Preparation.....	3.31
4.0	Coating Characterization and Preparation.....	4.1
4.1	Requirements and Target Characteristics Identification	4.1
4.1.1	ALK Coating Preparation.....	4.1
4.1.2	ZE Coating Preparation Results	4.5
4.2	Coatings Preparation Summary.....	4.5
5.0	Test Matrix and Approach.....	5.1
5.1	Test Matrix	5.1
5.1.1	Series 1 Test Matrix	5.2
5.1.2	Benchmark Series Test Matrix	5.3
5.1.3	Series 2 Test Matrix	5.4
5.1.4	Coatings.....	5.4
5.1.5	Benchtop Tests	5.6
5.2	Approach for Developing Test Procedures	5.6
5.3	Overview of Test Procedure.....	5.8
5.3.1	Pretest Preparation.....	5.9
5.3.2	Test Procedure.....	5.12
5.3.3	Post-Test Procedures	5.14
6.0	Phenomenological Results and Discussion	6.1
6.1	Debris Preparation.....	6.1
6.1.1	Test Conditions	6.1
6.1.2	Test Results	6.2
6.2	Sump Screen Material Comparison.....	6.7
6.2.1	Test Conditions	6.8
6.2.2	Test Results	6.8
6.3	Debris Loading Sequence.....	6.10
6.3.1	Benchtop Loop Investigation	6.14
6.3.2	Investigation Conclusions	6.32
6.4	Debris Bed Sectioning.....	6.32
6.5	Flow History.....	6.39
6.5.1	Test Conditions	6.39
6.5.2	Test Results	6.39
7.0	Results of Large-Scale Tests	7.1
7.1	Large-Scale Results of Screen-Only Tests	7.4
7.1.1	Temperature Effects for Bare Perforated Plate	7.6
7.2	Large-Scale Results of NUKON Debris Beds.....	7.8
7.2.1	Debris Bed Height Measurements from NUKON-Only Tests.....	7.15

7.2.2	Temperature Effects on NUKON-Only Debris Beds	7.21
7.3	Results of CalSil-Only Debris Bed Tests	7.26
7.3.1	CalSil Debris Bed Formation	7.26
7.3.2	Pressure Measurements for CalSil-Only Debris Beds.....	7.33
7.3.3	Temperature Effects on CalSil-Only Debris Beds	7.35
7.4	Large-Scale Results for Debris Beds Containing NUKON and CalSil.....	7.36
7.4.1	Overview of the NUKON/CalSil Test Matrix.....	7.38
7.4.2	Results of Debris Bed Dissolution to Assess CalSil Mass Content	7.41
7.4.3	Debris Bed Height for NUKON/CalSil Test Cases.....	7.47
7.4.4	Head Loss Measurements for NUKON/CalSil Debris Beds at Ambient Temperature	7.53
7.4.5	Head Loss Measurements for NUKON/CalSil Debris Beds at Elevated Temperatures	7.63
7.5	Coating Debris Bed Results	7.66
7.5.1	Coating Debris Bed Formation.....	7.67
7.5.2	Coating Debris Bed Results	7.69
8.0	Discussion of Large Scale Results.....	8.1
9.0	Conclusions	9.1
10.0	References	10.1
Appendix A – Test Screens.....		A.1
Appendix B – Drawings.....		B.1
Appendix C – Test Loop Measurement and Equipment Listing.....		C.1
Appendix D – Large-Scale Data Acquisition System Worksheets		D.1
Appendix E – Debris Preparation Procedures.....		E.1
Appendix F – Benchtop Test Results.....		F.1
Appendix G – Screen-Only Quick Look Reports		G.1
Appendix H – NUKON-Only Quick Look Reports.....		H.1
Appendix I – CalSil-Only Quick-Looks		I.1
Appendix J – NUKON/CalSil Quick Looks		J.1
Appendix K – Quick-Look Report for PNNL Series 2 Coating Priority 5 and Associated Benchtop Tests		K.1
Appendix L – Test Plan for Comparison Benchmark Testing of PNNL and ANL Test Loops Used to Measure Debris Bed Head Loss for Reactor Sump Pump Screens		L.1
Appendix M – Test Matrix of NUKON-only Tests Conducted in the Benchtop Test Loop		M.1
Appendix N – Test Matrix of NUKON/CalSil Tests Conducted in the Benchtop Test Loop		N.1
Appendix O – Particle Size Characterization Photos for ALK and ZE Coatings		O.1

Figures

2.1	Screen Materials Used for Testing	2.3
2.2	Simplified Schematic of the Benchtop Loop.....	2.6
2.3	Photo of the Benchtop Loop Test Section	2.7
2.4	Upstream Portion of Benchtop Test Section Showing Pressure Tap Location	2.8
2.5	Downstream Portion of Benchtop Test Section Showing Pressure Tap Location.....	2.8
2.6	Large-Scale Test Loop Schematic	2.11
2.7	Large-Scale Transparent Test Section.....	2.12
2.8	Schematic Detailing the Dimensions of the Transparent Test Section.....	2.13
2.9	Schematic of the Optical Triangulation Technique	2.20
2.10	Schematic of Plan View Setup of Optical Triangulation System for Large-Scale Test Loop.....	2.20
2.11	Photos of Optical Triangulation System Installed on the Large-Scale Test Loop.....	2.21
2.12	Calibration Wedge Used for the Optical Triangulation System.....	2.21
3.1	R4 as a Function of NUKON Mass	3.7
3.2	R4 as a Function of Preparation Time for Constant 1449.5 g/m ² Target Debris Loading.....	3.8
3.3	R4 as a Function of Water Volume and Preparation Time.....	3.10
3.4	R4 as a Function of the Blender Used	3.11
3.5	Effect of Mixing Time on R4 Values for 1449.5 g/m ² NUKON Debris Loading Case	3.12
3.6	PSD Results for Prepared CalSil Slurry	3.14
3.7	PSD Results for Prepared CalSil Slurry	3.15
3.8	NUKON Debris Bed for 1449.5 g/m ² Target Debris Loading	3.16
3.9	NUKON Debris Bed for 1449.5 g/m ² Target Debris Loading	3.16
3.10	NUKON Debris Bed for 1449.5 g/m ² Target Debris Loading	3.17
3.11	NUKON Debris Bed for 107.3 g/m ² Target Debris Loading	3.17
3.12	NUKON Debris Bed for 107.3 g/m ² Target Debris Loading	3.18
3.13	NUKON Debris Bed for 107.3 g/m ² Target Debris Loading	3.18
3.14	NUKON Debris Bed for 217.4 g/m ² Target Debris Loading	3.19
3.15	NUKON Debris Bed for 724.7 g/m ² Target Debris Loading	3.19
3.16	NUKON and CalSil Debris Bed for 1811.9 g/m ² Target Debris Loading.....	3.20
3.17	Representative Debris Bed Heights and Recovery Fraction.....	3.21
3.18	NUKON Debris Bed Head Loss as Function of Screen Approach Velocity.....	3.22
3.19	Approximate NUKON Debris Bed Head Loss as a Function of Slurry Preparation.....	3.23
3.20	NUKON Debris Bed Head Loss as a Function of Screen Approach Velocity.....	3.24
3.21	NUKON Debris Bed Head Loss as a Function of Screen Approach Velocity.....	3.25
3.22	NUKON Debris Bed Loss Coefficients as Functions of the Screen Approach Velocity	3.26
3.23	NUKON Debris Bed Loss Coefficients as Functions of the Screen Approach Velocity	3.26
3.24	Fraction of Initial NUKON Mass Retained in Debris Bed as a Function of R4.....	3.27
3.25	Example NUKON Debris Bed for R4A	3.28
3.26	Example NUKON Debris Bed for R4C	3.28
3.27	Example NUKON Debris Bed for R4D2	3.29
3.28	NUKON Debris Bed for R4D2 Subjected to 0.29 m/s Screen Approach Velocity.....	3.29
3.29	NUKON Debris Bed Height as a Function of R4.....	3.30
4.1	ALK, R4 ~ 3.3	4.2
4.2	ALK, R4 ~ 2.2	4.3

4.3	ALK, R4 ~ 1.4	4.3
4.4	R4 as a Function of Initial ALK Coating Mass	4.4
4.5	“1/4 in. Square Coating” for ALK Prepared Coating Debris in the Range 0.157 to 0.265 in.	4.4
4.6	ZE, R4 ~ 1.5	4.6
4.7	ZE, R4 ~ 0.9	4.6
4.8	ZE, R4 ~ 0.5	4.7
4.9	“1/4 in. Square Coating” ZE Prepared Coating Debris in the Range 0.157 to 0.265 in.	4.7
6.1	Debris Bed Head Loss as a Function of R4	6.4
6.2	060228_NO_1363_BP2, Nonboiled.....	6.5
6.3	060421_NO_1363_BP1, Nonboiled.....	6.6
6.4	060327_NO_1363_BP1, Boiled.....	6.6
6.5	060328_NO_1363_BP1, Boiled.....	6.7
6.6	060523_NO_1363_BAP1, Boiled	6.7
6.7	060223_NO_1363_B1, 5-Mesh.....	6.11
6.8	060228_NO_1363_B1, 5-Mesh.....	6.11
6.9	060228_NO_1363_BP2, Plate.....	6.12
6.10	060421_NO_1363_BP1, Plate.....	6.12
6.11	Debris Bed Head Loss as a Function of Screen Approach Velocity for NUKON/CalSil Debris Beds Formed in the PNNL Large-Scale Loop During Series 1 Tests.....	6.13
6.12	Debris Bed Head Loss as a Function of Screen Approach Velocity for Debris Beds Formed in the PNNL Benchtop Loop.....	6.16
6.13	Test 051227_CO_0411x_B1 CalSil Debris Bed for Case 3	6.18
6.14	Test 051227_CO_1763_B2 CalSil Debris Bed for Case 3	6.18
6.15	Test 051228_NC_1234_B1 NUKON/CalSil Debris Bed for Case 4	6.20
6.16	Test 051228_NC_1234_B2 NUKON/CalSil Debris Bed for Case 4	6.20
6.17	Test 051214_NC_1234_B1 NUKON/CalSil Debris Bed for Case 1	6.21
6.18	Test 051214_NC_1234_B1 NUKON/CalSil Debris Bed for Case 1	6.21
6.19	Test 051214_NC_1234_B2 NUKON/CalSil Debris Bed for Case 1	6.22
6.20	Test 051214_NC_1234_B2 NUKON/CalSil Debris Bed for Case 1	6.22
6.21	Test 051215_NC_1234_B1 NUKON/CalSil Debris Bed for Case 2	6.23
6.22	Test 051228_NC_1234_B3 NUKON/CalSil Debris Bed for Case 4	6.23
6.23	Comparison of Debris Bed Head Loss as a Function of Screen Approach Velocity for NUKON/CalSil Debris Beds Formed in the PNNL Large-Scale and Benchtop Loops.....	6.24
6.24	Final Ramp up Debris Bed Head Loss as a Function of Screen Approach Velocity for Case 4 Lag Time Investigation.....	6.26
6.25	060207_NC_1234_B1 NUKON/CalSil Debris Bed for Case 4 Lag Time	6.27
6.26	060303_NC_1234_B2 NUKON/CalSil Debris Bed for Case 4 Lag Time	6.27
6.27	Screen Approach Velocity as a Function of Test Time, Case 4 Tests.....	6.28
6.28	Schematic of Debris Bed Cross-Section Used for SEM Imaging	6.34
6.29	Mounted Debris Bed Samples Used for SEM Imaging.....	6.34
6.30	SEM Image of the NUKON Fiber Region in Debris Bed 060303_NC_1234_B2	6.35
6.31	SEM Image of NUKON Fiber Region in Debris Bed 060303_NC_1234_B2 Showing Gap or Void Region.....	6.35
6.32	SEM Image of the CalSil Surface Layer for Debris Bed 060303_NC_1234_B2	6.36
6.33	High Magnification SEM Image of the CalSil Surface Layer for Debris Bed 060303_NC_1234_B2	6.36

6.34	NUKON Fibers Near Metal Grid for Debris Bed 060516_NC_1234_B1.....	6.37
6.35	NUKON Fibers Near Surface Region for Debris Bed 060516_NC_1234_B1	6.37
6.36	Cross-Section of Surface Region for Debris Bed 060516_NC_1234_B1	6.38
6.37	060418_NO_1363_B1 Head Loss as a Function of Velocity Cycle Count	6.41
6.38	060419_NO_1363_B1 Head Loss as a Function of Velocity Cycle Count	6.41
6.39	060418_NO_1363_B1 Flow History Test.....	6.42
6.40	060419_NO_1363_B1 Flow History Test.....	6.43
7.1	Pressure Drop as a Function of Approach Velocity for Bare Screen and Perforated Plate Without Error Bars	7.5
7.2	Pressure Drop as a Function of Approach Velocity for Bare Screen and Perforated Plate with Error Bars	7.6
7.3	Comparison of Head Loss Across Bare Perforated Plate with 1/8-in. Holes as a Function of Approach Velocity for Nominal Temperatures of 83°, 131°, and 179°F Without Error Bars	7.7
7.4	Comparison of Head Loss Across Bare Perforated Plate with 1/8-in. Holes as a Function of Approach Velocity for Nominal Temperatures of 83°, 131°, and 179°F With Error Bars	7.7
7.5	Head Loss Across Debris Bed as a Function of Screen Approach Velocity for Test Case NO4. The NUKON-only debris bed has a retrieved debris loading of 1788 g/m ² . The plot contains only head loss measurements obtained during the ramp up portions of the velocity sequence at ambient temperature (a and b are the same plot with and without error bars, respectively).	7.11
7.6	Comparison of Head Loss as a Function of Screen Approach Velocity for Repeat Test Cases NO4 and NO5. The retrieved mass loadings for NO4 and NO5 were 1788 and 1719 g/m ² , respectively. The data presented are from the first two velocity cycles for each test.....	7.12
7.7	Comparison of Large-Scale and Benchtop Loop Results for NUKON-Only Test Condition 1a.	7.12
7.8	Head Loss Across the NUKON-Only Debris Beds as a Function of Screen Approach Velocity During the Ramp up 2 Portion of Each Velocity Sequence.....	7.14
7.9	Head Loss Across the NUKON-Only Debris Beds as a Function of Screen Approach Velocity During the Ramp up 2 Portion of Each Velocity Sequence.....	7.15
7.10	Center Height of Debris Beds from Tests NO1, NO2, and NO3 as a Function of Screen Approach Velocity.....	7.19
7.11	Center Height of Debris Beds from Tests NO1, NO2, NO3a, and NO5 as a Function of Screen Approach Velocity. Tests NO1, NO2, and NO3a were all formed at a constant screen approach velocity of 0.1 ft/sec and test NO5 at an initial velocity of 0.2 ft/sec.....	7.19
7.12	Debris Bed Dry Bulk Density as a Function of Mass Loading for the NUKON-Only Debris Beds Created and Tested at Ambient Temperature.....	7.20
7.13	Pressure Drop Across Debris Beds as a Function of Dry Bulk Density for the NUKON-Only Debris Beds Created and Tested at Ambient Temperature.....	7.21
7.14	Head Loss as a Function of Screen Approach Velocity for the NUKON-Only Debris Bed Formed at 24°C	7.23
7.15	Head Loss as a Function of Screen Approach Velocity for the NUKON-Only Debris Bed Formed at 54°C	7.23
7.16	Head Loss as a Function of Screen Approach Velocity for the NUKON-Only Debris Bed Formed at 82°C	7.24
7.17	Head Loss as a Function of Screen Approach Velocity for the NUKON-Only Debris Bed Tests Conducted at Ambient Temperature	7.24
7.18	Head Loss as a Function of Screen Approach Velocity for the NUKON-Only Debris Bed Tests Conducted at Approximately 54°C	7.25

7.19	Head Loss as a Function of Screen Approach Velocity for the NUKON-Only Debris Bed Tests Conducted at Approximately 82°C	7.25
7.20	Underside of Incomplete Debris Bed from COBT3 Showing How CalSil Material Has Become Completely Entangled with Some of the Screen Wires in Test 051227_CO_0411x_BP1	7.27
7.21	Incomplete debris bed from COBT1, Test 060406_CO_1176_BP1	7.28
7.22	Incomplete Debris Bed from COBT2, Test 060510_CO_1469_BP1.....	7.29
7.23	Incomplete Debris Bed from COBT5, Test 060510_CO_1763_BP2.....	7.29
7.24	Incomplete Debris Bed from COBT6, Test 060510_CO_2351_BP3.....	7.30
7.25	Incomplete debris bed from COBT7, Test 060511_CO_3527_BP2	7.31
7.26	Incomplete Debris Bed from Test Condition CO1, Test 060510_CO_8108_LP1 Through LP3.....	7.31
7.27	Underside of COBT7.....	7.32
7.28	Side Views of the Debris Bed and Perforated Plate for Benchtop and Large-Scale Test Cases CO1 and COBT7	7.32
7.29	Pressure Drop as a Function of the Screen Approach Velocity for CO1a, with a Target CalSil Mass Loading of 4350 g/m ² and a Retrieved Mass Loading of 434 g/m ²	7.34
7.30	Pressure Drop as a Function of Screen Approach Velocity for Benchtop Tests COBT2, COBT5, COBT6, and COBT7 and large-scale test CO1a.....	7.34
7.31	Pressure Drop as a Function of Retrieved Mass Loading at Constant Screen Approach Velocities of 0.1 and 0.2 ft/sec.	7.35
7.32	Pressure Drop as a Function of Screen Approach Velocity for Test Condition CO1 with a target CalSil mass loading of 4350 g/m ² and retrieved mass loading of 434 g/m ²	7.36
7.33	Incomplete Debris Bed Retrieved from Test NC1 with a Retrieved Mass Loading of 56.3 g/m ²	7.39
7.34	Incomplete Debris Bed Retrieved from Test NC2 with a Retrieved Mass Loading of 94.4 g/m ²	7.39
7.35	Upstream View of Top of Debris Bed from Test Condition NC16.....	7.40
7.36	Plots of the Percent Target CalSil Mass and Percent Total Target Mass Loading Retained in the Debris Bed as a Function of the Retrieved Dry Mass Loading	7.45
7.37	Plots of Percent Target CalSil Mass and CalSil to NUKON Retrieved Mass Ratio Obtained from the Retrieved Debris Bed as a Function of the Total Retrieved Dry Debris Bed Mass Loading.....	7.45
7.38	Debris Bed Center Height as a Function of Screen Approach Velocity for Three Retrieved Mass Loadings.....	7.50
7.39	Debris Bed Dry Bulk Density as a Function of the Retrieved Debris Bed Mass Loading for Constant Screen Approach Velocities of 0.02, 0.1, and 0.2 ft/sec from Series 2 Test Cases with Debris Beds Formed at Ambient Temperature.....	7.52
7.40	Debris Bed Bulk Density as a Function of the Predicted CalSil Mass Loading for Constant Screen Approach Velocities 0.02, 0.1, and 0.2 ft/sec from the Series 2 Test Cases with Debris Beds Formed at Ambient Temperature.....	7.52
7.41	Debris Bed Bulk Density as a Function of the Predicted CalSil to NUKON Mass Ratio for Constant Screen Approach Velocities of 0.02, 0.1, and 0.2 ft/sec from Series 2 Test Cases with Debris Beds Formed at Ambient Temperature.....	7.53
7.42	Debris Bed Head Loss from NC7 as a Function of Screen Approach Velocity for Five Ramp ups in the Screen Approach Velocity and the First Two Ramp Downs in Velocity	7.56

7.43	Debris Bed Head Loss from NC9 as a Function of Screen Approach Velocity for Four Ramp ups in the Screen Approach Velocity and the First Ramp Down in Velocity	7.56
7.44	Plot of the Pressure Drop Across the Debris Bed as a Function of the Retrieved Debris Bed Mass Loading for Constant Screen Approach Velocities of 0.02, 0.1, and 0.2 ft/sec	7.57
7.45	Plot of Debris Bed Pressure Drop as a Function of the Relative Debris Bed Bulk Density for Constant Screen Approach Velocities of 0.02, 0.1, and 0.2 ft/sec from the Series 2 Test Cases with Debris Beds Formed at Ambient Temperature.....	7.58
7.46	Pressure Drop Across the Debris Bed as a Function of the Retrieved CalSil to NUKON Mass Ratio for Constant Screen Approach Velocities of 0.02, 0.1, and 0.2 ft/sec	7.59
7.47	Pressure Drop Across the Debris Bed as a Function of the Screen Approach Velocity for Group 1 NUKON/CalSil Test Cases. Test Cases NC4, NC5a and NC6a are from Series 2 and were formed at ambient temperature with a screen approach velocity of 0.1 ft/sec	7.60
7.48	Pressure Drop Across the Debris Bed as a Function of the Screen Approach Velocity for Group 1, Series 2, NUKON/CalSil Test Cases.....	7.60
7.49	Pressure Drop Across the Debris Bed as a Function of the Screen Approach Velocity for Group 2 NUKON/CalSil Test Cases	7.61
7.50	Pressure Drop Across Debris Bed as a Function of Screen Approach Velocity for Group 3, Series 1, NUKON/CalSil Test Cases.....	7.62
7.51	Plot of Pressure Drop Across the Debris Bed as a Function of Screen Approach Velocity for Group 1 Debris Beds Subjected to Testing at Elevated Fluid Temperatures.....	7.65
7.52	Pressure Drop Across Debris Bed as a Function of Screen Approach Velocity for Group 2 Debris Beds Associated with Elevated Temperature Test NC17a	7.66
7.53	ALK1a Debris Bed After Retrieval from Test Section, Top View	7.70
7.54	ALK2 Debris Bed After Retrieval from Test Section, Top View	7.70
7.55	Head Loss Results for ALK1a and ALK2	7.71
7.56	Head Loss Results for ALK1a and ALK2, Repeat Velocity Cycles	7.72
7.57	ALKBT Debris Bed After Retrieval from Test Section, Top View	7.72
7.58	Head Loss Results for ALK1a and ALKBT	7.73
7.59	ZE1 Debris Bed After Retrieval from Test Section, Top View.....	7.74
7.60	Head Loss Results for ALK1a and ZE1	7.74
7.61	Head Loss Results for ALK1a and ALK1b.....	7.75
8.1	Pressure Drop Across the Debris Bed as a Function of the Retrieved Mass Loading for NUKON-Only” and CalSil-Only Test Cases at Constant Velocities of 0.1 and 0.2 ft/sec.....	8.3
8.2	Pressure Drop Across the Debris as a Function of the Retrieved Mass Loading for NUKON-Only, CalSil-Only, and NUKON/CalSil Test Cases at Constant Velocities of 0.1 and 0.2 ft/sec..	8.5
8.3	Pressure Drop Across the Debris Bed as a Function of the Debris Bed Relative Bulk Density for NUKON-Only and NUKON/CalSil Test Case at Constant Velocities of 0.1 and 0.2 ft/sec	8.6

Tables

2.1	Characteristics of Sump Screen Materials Tested	2.2
2.2	Observed Deflections in 5-Mesh Screen Assembly After Applying Distributed Load.....	2.4
3.1	Preliminary NUKON Slurry Preparation Tests	3.3
3.2	NUKON Slurry Preparation Test NS6 R4 Results	3.5
3.3	Repeatability of R4 Values with Different Preparation Times.....	3.8
3.4	Distinction in R4 and R1 Values and Boiling Effect	3.9
3.5	Requirement 4 Testing NUKON Preparation.....	3.24
4.1	Description of Coatings Materials Used in PNNL Testing	4.1
4.2	ALK R4 Test Data.....	4.2
4.3	Prepared and Sieved ALK Coating Mass by Sieve Size from Two 6.52-g Preparations	4.5
4.4	ZE R4 Test Data	4.5
4.5	Prepared and Sieved ZE Coating Mass by Sieve Size from Three ~ 25 g Preparations for a Total Amount of 75 g	4.7
5.1	PNNL Series 1 Test Matrix	5.3
5.2	PNNL Benchmark Series Test Matrix.....	5.4
5.3	PNNL Series 2 Test Matrix	5.5
5.4	PNNL Coatings Materials Test Matrix.....	5.5
5.5	PNNL Benchtop Tests Directly Associated with Large-Scale Test Conditions.....	5.6
5.6	Truncated Velocity Sequence for an Incomplete Debris Bed.....	5.12
5.7	Velocity Sequence for the Benchmark Tests.....	5.13
5.8	Velocity Sequence for the PNNL Series 2 Tests.....	5.14
5.9	Parameter List for Developing the ISE Probe Performance Curves.....	5.16
6.1	Benchtop Nonboiled and Boiled Debris Results for Test Condition NOBT1a	6.3
6.2	Comparison of Results for Benchtop Non-Boiled and Boiled Debris Results for Test Condition NOBT1a.....	6.4
6.3	Benchtop Nonboiling and Boiling Preparation Debris Bed Data for Test Condition NOBT1a.....	6.5
6.4	Benchtop 5-Mesh and Plate Test Results for Test Condition NOBT1a	6.9
6.5	Benchtop 5-mesh Screen and Perforated Plate Debris Bed Data for Test Condition NOBT1a ...	6.11
6.6	Summary of Test Cases Conducted in the Benchtop Loop to Evaluate the Effects of the Debris Loading Sequence	6.15
6.7	Lag Time Benchtop Test Summary	6.25
6.8	Benchtop Investigation NUKON/CalSil Debris Bed Approximate Measured Body Height	6.29
6.9	Benchtop Investigation NUKON/CalSil Debris Bed Measured Mass	6.30
6.10	060418_NO_1363_B1 and 060419_NO_1363_B1 Flow History Tests Data.....	6.40
6.11	Average Change in Head Loss per Velocity Cycle	6.42
6.12	060418_NO_1363_B1 and 060419_NO_1363_B1 Flow History Tests Debris Bed Data.....	6.42
7.1	Velocity Range in Which a Transition Flow Regime May Exist for Each Nominal Test Temperature.....	7.3
7.2	PNNL Large-Scale Screen-Only Tests Conducted.....	7.4
7.3	PNNL Large-Scale Plate-Only Tests Conducted	7.4
7.4	Comparison of Head Loss Measurements for Bare Screen and Bare Plate at Selected Screen Approach Velocities	7.6

7.5	Comparison of Head Loss Measurements of Bare Plate at 83°F , 131°F , and 179°F for Selected Screen Approach Velocities.....	7.8
7.6	PNNL Large-Scale, NUKON-Only Sump Screen Debris Tests.....	7.10
7.7	Comparison of Measured Head Loss at Selected Velocities for Test Condition 1a Debris Beds Generated in Both the Large-Scale and Benchtop Loops at Ambient Temperature.....	7.13
7.8	Comparison of Measured Head Loss at Selected Velocities for NUKON-Only Debris Beds Generated and Evaluated at Ambient Temperature	7.15
7.9	In Situ Debris Bed Height Measurements and Calculated Density Obtained from Optical Triangulation Measurements	7.17
7.10	PNNL Large-Scale CalSil-Only Sump Screen Debris Tests Conducted.....	7.26
7.11	PNNL Benchtop, CalSil-Only Sump Screen Debris Tests Conducted.....	7.26
7.12	Test Matrix of the PNNL Large-Scale NUKON/CalSil Sump Screen Debris Bed Tests Conducted.....	7.37
7.13	Retrieved Mass Loading of CalSil in the CalSil/NUKON Debris Beds.....	7.43
7.14	Comparison of Percent of Target CalSil Retained in Debris Bed with Target CalSil to NUKON Mass Ratio for a Target NUKON Mass Loading of 217 g/m ²	7.46
7.15	Comparison of Percent of Target CalSil Retained in Debris Bed with Target CalSil to NUKON Mass Ratio for Target NUKON Mass Loading of 724 g/m ²	7.46
7.16	In Situ Debris Bed Height Measurements and Calculated Density Obtained from Optical Triangulation Measurements	7.48
7.17	Post-Test Manual Measurements of Debris Bed Height and Corresponding Calculated Relative Density Compared to In Situ Measurements and Calculated Density from Optical Triangulation Measurements	7.51
7.18	NUKON/CalSil Group 1 Test Case Debris Bed Properties with Total Mass Loadings Between 160 and 297 g/m ²	7.54
7.19	NUKON/CalSil Group 2 Debris Bed Properties with Total Mass Loadings Between 646 and 811 g/m ²	7.54
7.20	NUKON/CalSil Group 3 Debris Bed Properties with Total Mass Loadings Between 1034 and 1924 g/m ²	7.55
7.21	Comparative Ranking of the Group 1 Test Cases with Respect to Head Loss Across the Debris Bed, Total Mass Loading, CalSil Mass Loading, CalSil to NUKON Mass Ratio, and Relative Bulk Density	7.61
7.22	Comparative Ranking of the Group 2 Test Cases with Respect to Head Loss Across the Debris Bed, Total Mass Loading, CalSil Mass Loading, CalSil-to-NUKON Mass Ratio, and Relative Bulk Density	7.62
7.23	Comparative Ranking of the Group 3 Test Cases with Respect to Head Loss Across the Debris Bed, Total Mass Loading, CalSil Mass Loading, and CalSil-to-NUKON Mass Ratio	7.63
7.24	PNNL Coating Debris Tests Conducted.....	7.67

Abbreviations and Acronyms

A/D	analog to digital
ACRS	Advisory Committee on Reactor Safeguards
ALK	Ameron's Amercoat 5450 alkyd topcoat
ANL	Argonne National Laboratory
BAP	boiled after preparation
BPP	boiled prior to preparation
BT	benchtop
BWR	boiling water reactor
CalSil	calcium silicate
CO	CalSil only
CSS	containment spray system
DAS	data acquisition system
DP	differential pressure
ECCS	emergency core cooling system
ENS	European Nuclear Society
ft	feet
ft/sec	feet per second
g/m ²	grams per square meter
gpm	gallons per minute
GSI	Generic Safety Issue
Hp	horsepower
Hz	Hertz
ID	inner diameter
in.	inches
Inc.	incorporated
ISA	ionic strength adjuster
ISE	ion selective electrode
L	liter
L/D	length/diameter; nondimensionalized distance expressed in terms of number of diameters
LANL	Los Alamos National Laboratory
LOCA	loss-of-coolant accident
m	meters
M&TE	measurement and testing equipment
m/s	meters/second
mA	milliamperes
mL	milliliters
mm	millimeters
mV	millivolts

NA	not applicable
N/A	not applicable
NC	NUKON and CalSil combined
NO	NUKON only
NPSH	net positive suction head
NPT	National Pipe Thread
NRC	U.S. Nuclear Regulatory Commission
NRR	NRC Office of Nuclear Reactor Regulation
PC	personal computer
PNNL	Pacific Northwest National Laboratory
PNPP	Perry Nuclear Power Plant
PO	perforated plate only
PSD	particle size distribution
psi	pounds per square inch
PVC	polyvinyl chloride
PWR	pressurized water-reactor
Re	Reynolds Number
RES	NRC Office of Nuclear Regulatory Research
RHR	residual heat removal
RTD	resistive temperature device
RWST	refueling water storage tank
SEM	scanning electron microscopy
SO	screen only
TC	thermocouple
TTS	transparent test section
V	volts
VFD	variable frequency drive
ZE	Ameron's Dimetecote 6 inorganic zinc primer with Amercoat 90 epoxy topcoat

Executive Summary

In 1996, the U.S. Nuclear Regulatory Commission (NRC) established Generic Safety Issue (GSI) 191, “Assessment of Debris Accumulation on PWR Sump Performance,” to identify, prioritize, and resolve concerns regarding the blockage of sump screens following a loss-of-coolant accident (LOCA). The primary concern associated with GSI-191 is the possibility that, during a LOCA within the containment of a pressurized water reactor (PWR), thermal insulation and other materials (e.g., coatings and concrete) may be damaged and dislodged. Dislodged material (i.e., debris) may subsequently be transported and accumulate on the sump screens of the emergency core cooling system and containment spray system sump. Over time, a debris bed could form on the sump screen that progressively restricts flow, inducing a head loss that could reduce the available net positive suction head below that required for these pumps.

Pacific Northwest National Laboratory (PNNL) was tasked with conducting experiments to obtain data for the pressure drop across debris beds as a function of the approach velocity. The data will assist the NRC in developing correlations for predicting the pressure drop for flow through a compressible porous-medium debris bed composed of NUKON™ (a fiberglass insulation) low-density fiberglass and calcium silicate (CalSil) particulate.

Two test loops with test sections 4 and 6 inches in diameter were constructed for generating debris beds and measuring the associated pressure drop. Debris beds were generated and pressure drop measurements made for beds consisting of NUKON fiberglass, CalSil particulate, and combinations of fiberglass and particulate.

During the test program, the effects of debris preparation on debris bed formation and pressure drop were evaluated and a metric developed for characterizing the disassociation of the debris after preparation. Testing consisted of forming the debris bed within the test loop and obtaining a steady-state pressure drop at the bed formation velocity. The approach velocity was then changed incrementally through several cycles of increasing and decreasing velocity with a steady pressure measurement obtained at each flow set point. The loop temperature was then changed and the velocity variation sequence repeated.

During testing, in situ measurements of the debris bed height were taken using an optical triangulation system developed for the test program. Selected retrieved debris beds were impregnated with epoxy and sectioned, and subsequently imaged using scanning electron microscopy to evaluate the debris bed structure. A process for assessing the CalSil mass in a NUKON/CalSil debris bed was employed using chemical dissolution and a calcium ion selective electrode. The test program also evaluated the effects of the debris loading sequence and flow history through the debris bed on the resulting pressure drop.

The initial set of tests conducted by PNNL was performed at test conditions similar to those of tests performed at the University of New Mexico under the direction of Los Alamos National Laboratory in 2004. Limited testing was also conducted using coating materials (Ameron’s Amercoat 5450 alkyd topcoat and Ameron’s Dimetcote 6 inorganic zinc primer with Amercoat 90 epoxy topcoat) as debris. The test setup, data acquisition system, procedures, experimental results, and observations are described in this report.

The preparation of the debris material and the constituent loading sequence during debris bed formation were shown to strongly influence the resulting pressure drop and physical integrity of a debris bed. NUKON/CalSil debris beds were formed by:

- CalSil being deposited on an existing NUKON debris bed (referred to as NUKON bed first)
- NUKON being introduced into a flow stream with CalSil already well dispersed in the flow (referred to as NUKON time lag)
- Premixing the NUKON and CalSil material before introducing it into the flow stream (referred to as premixed).

The debris loading sequences of NUKON bed first and NUKON time lag yielded pressure drops approximately 3 orders of magnitude higher than those achieved from the premixed condition, with the NUKON time lag yielding the larger pressure drop.

PNNL-generated debris beds consisting only of fiber material yielded relatively repeatable results. Complete debris beds were generated at debris loadings $\geq 171 \text{ g/m}^2$ in the 6-in.-diameter test loop and $\geq 56 \text{ g/m}^2$ in the 4-in.-diameter loop. Complete debris beds consisting of only calcium silicate particulate material were not formed at loadings up to 4350 g/m^2 .

In situ measurements of debris bed height and accompanying photographs show the debris beds contracted and relaxed with continued cycling of the approach velocity. For most cases, the pressure drop decreased with increased temperature; however, the flow history to which the debris bed had been subjected affected the measured pressure drop. Negligible differences in the measured pressure drop were obtained for similar debris loadings between debris beds generated on 5-mesh woven wire and 1/8-in. perforated plate.

A relative bulk density was calculated for the debris beds based on the in situ bed height measurements obtained with the optical triangulation system. For both the NUKON-only and the NUKON/CalSil debris beds, the pressure drop across the debris bed increased with an increase in the relative bulk density of the debris bed. For each elevated temperature case in which the head loss increased with temperature, the relative bulk density of the debris was observed to be significantly higher.

1.0 Introduction

This report details experimental work conducted by Pacific Northwest National Laboratory (PNNL) for the U.S. Nuclear Regulatory Commission (NRC) Office of Nuclear Regulatory Research (RES). The experiments focused on measuring the pressure drop as a function of approach velocity across debris beds formed on a section of 5-mesh screen or 1/8-inch perforated plate. The test conditions were intended to be representative of a section of pressurized water reactor (PWR) sump strainer debris beds following a loss-of-coolant accident (LOCA). The work was performed as part of the NRC's effort to resolve Generic Safety Issue 191 (NRC 1996).

Two test loops with test sections 4 and 6 inches in diameter were constructed for generating debris beds and measuring the associated pressure drop as a function of the upstream approach velocity. Debris beds consisting of NUKON™ low-density fiberglass, calcium silicate particulate, and combinations of fiberglass and particulate were generated. A limited number of tests were also conducted using coatings (e.g., epoxy paint) as the debris.

During the test program, the effects of debris preparation on debris bed formation and pressure drop were evaluated and a metric developed for characterizing the disassociation (preparation) of the prepared debris. This effort also investigated the impact of the debris loading sequence (i.e., the order in which debris components arrive at the screen) on the measured pressure drop. The work was initiated in May 2005, and large-scale tests were conducted between November 2005 and August 2006.

A brief background of the circumstances that have led to this test effort is given in Section 1.1. The objectives for this body of work are presented in Section 1.2, and an outline of the rest of this report is provided in Section 1.3.

1.1 Background

During a design basis LOCA, the emergency core cooling system (ECCS) provides water to the reactor core, and the containment spray system (CSS) sprays water into (to avoid excluding scrubbing radio-nuclide function) the containment atmosphere. To provide sufficient cooling to the reactor core, the ECCS is required to operate for the extended period required by the long-lived radioactivity in the core (often assumed to be 30 days for analytical purposes). The cooling water is initially obtained from the refueling water storage tank (RWST). When the RWST liquid is depleted, water from the sump pool that accumulates at the bottom of the reactor containment is circulated through the core. In the event of a LOCA within the containment, the potential exists for insulation, coatings, and other materials to be dislodged and introduced into the sump water. The accumulation of such debris after a LOCA may adversely affect the flow paths necessary for proper operation of the ECCS and CSS. In particular, the accumulation of debris on the sump screens upstream of the pump inlets could result in a head loss that reduces the available net positive suction head required for operation of the ECCS and/or CSS pumps.

In 1979, the NRC established USI A-43, "Containment Emergency Sump Performance," to study safety issues related to the ability of PWRs and boiling water reactors (BWRs) to circulate water to the reactor core following a LOCA.

In July of 1992, Barsebäck-2, a Swedish BWR, experienced the clogging of two ECCS pump suction strainers from the accumulation of fibrous insulation. The clogging occurred following the release of steam from a safety valve that inadvertently opened at low power (ENS 1992). In 1993, the Perry Nuclear Power Plant, with a BWR/6 reactor, experienced two instances of ECCS strainer plugging (PNPP 1993). One of the events resulted in deformation of the pump suction strainers due to the buildup of debris and subsequent pressure drop. Based on these events, the NRC issued NRC Bulletin 93-02 in May 1993, which requested PWR and BWR licensees identify fibrous air filters and other temporary sources of fibrous material in the containment not specifically designed to withstand a LOCA, and to remove the material and ensure the functional capability of the ECCS.

As a result of these occurrences in Europe and the United States, the NRC initiated a study of BWR strainer blockage based on plant surveys. Findings from European experiences were used to identify possible deficiencies in the suction strainers employed in U.S. BWRs. In September 1993, as a result of the initial study, the NRC undertook a plant-specific study using a BWR/4 reactor with a Mark I containment. The results of this plant specific study were documented in *Parametric Study of the Potential for BWR ECCS Strainer Blockage due to LOCA Generated Debris* (Zigler et al. 1995).

In August 1994, a draft of NUREG/CR-6224 was released for public comment. Based on the lack of relevant experimental data available during the preparation of the draft NUREG/CR-6224, the NRC sponsored a series of experiments (Brinkman and Brady 1994, Rao and Souto 1995) to investigate the behavior of debris in the suppression pool and obtain debris bed pressure drop data. The bulk of the experimental work used NUKON™ (a fiberglass insulation) as the fibrous debris material. Particulate material consisted of simulated BWR sludge composed primarily of iron oxide. The new experimental data and revised models for debris transport and pressure drop were presented in the final NUREG/CR-6224 (Zigler et al. 1995). NUREG/CR-6224 concluded that debris blockage could result in a rapid loss of available net positive suction head (NPSH) for most postulated occurrences of pipe breaks.

In 1996, the NRC established *Generic Safety Issue (GSI) 191, Assessments of Debris Accumulation on PWR Sump Performance* (NRC 1996) to identify, prioritize, and resolve concerns regarding the blockage of PWR sump screens following a LOCA. Specifically, GSI-191 deals with the possibility that, during a LOCA within the containment of a PWR, thermal insulation and other materials (e.g., coatings and concrete) may be damaged and dislodged. Dislodged material (debris) may subsequently be transported and accumulate on the sump screens for the ECCS and CSS pumps. Over time, a debris bed could form that progressively blocks the screen, inducing a head loss that could reduce the available net positive suction head below that required for these pumps. Excessive debris bed head loss will reduce the flow rate and discharge pressure of the pumps, potentially terminating the flow of coolant water if the blockage is sufficiently severe.

As part of NRC's efforts to resolve GSI-191, RES contracted with Los Alamos National Laboratory (LANL) to perform additional experiments to determine the pressure drop associated with debris beds on sump screens. LANL was tasked with evaluating the performance of the head loss correlation derived in NUREG/CR-6224 for NUKON and iron oxide particulate on debris beds containing calcium silicate. The test results from LANL are presented in NUREG/CR-6874, *Experimental Studies of Loss-of-Coolant-Accident-Generated Debris Accumulation and Head Loss with Emphasis on the Effects of Calcium Silicate Insulation* (Shaffer et al. 2005).

The NRC's Advisory Committee on Reactor Safeguards (ACRS), Thermal-Hydraulic Subcommittee raised concerns regarding the application range of the NUREG/CR-6224 methodology for calculating head loss through debris clogged sump screens (Bonaca 2004). In September 2004, the RES staff was also provided two documents written by Graham Wallis, the Chairman of the ACRS: *NUREG/CR-6224 Head Loss Correlation*, dated Sept. 3, 2004, and *Flow Through a Compressible Mat: Analysis of the Data Presented in Series 6 Test Reported by LANL in LA-UR-04-1227*, dated Sept 3, 2004, which reviewed and critiqued the head loss correlations presented in NUREG/CR-6224. These documents criticized the NUREG/CR-6224 head loss equation and the associated compression relation for the debris bed. The ACRS indicated that the head loss calculation method should not be based on variances in the specific surface area of the debris and should not use a "thin bed" effect, which was not theoretically based. These documents further indicated that the NUREG/CR-6224 compression relation for the debris bed was inconsistent with the limited test data available and that additional test data were needed.

As a result of the ACRS' technical comments, the RES staff concluded that the existing head loss methodology should be redeveloped and correlated with additional test data. To assist in this task, RES contracted with PNNL to fabricate a test loop and obtain experimental data of the pressure drop across debris beds as a function of approach velocity and temperature. During the experimental effort, data was transmitted to RES staff as it became available. Using these data, RES revised the method for calculating head loss across a debris bed. The revised methodology and comparative results are presented in NUREG-1862 (Krotiuk 2006).

1.2 Objectives

The primary objectives of this task were to:

- Obtain experimental data characterizing the pressure drop associated with debris deposition on sump screen material to be used by RES to develop a methodology for predicting pressure drop for flow through a compressible porous medium debris bed composed of fiberglass and calcium silicate (CalSil) particulate.
- Characterize the head loss as a function of debris composition, loading, and thermal-hydraulic conditions.
- Design experiments for measuring the debris bed pressure drop that have controllable conditions that
 - Minimize the experimental uncertainty
 - Assess the true variability associated with debris bed formation for a given debris composition and loading.
 - Maximize the repeatability of debris bed pressure drop measurements.

To accomplish these objectives, PNNL performed the following activities:

- Fabricated a test loop for generating debris beds and taking pressure drop measurements for approach velocities of 0.02 to 2 ft/sec (0.01 to 0.61 m/s) at temperatures between 68° and 185°F (20° and 85°C).
- Developed debris preparation procedures and defined metrics for assessing the degree of debris preparation (disassociation of fibrous material).

- Developed a system for taking in situ debris bed height measurements as a function of approach velocity.
- Conducted experiments in which debris beds were generated from vendor provided insulation and coating materials; steady state pressure drop measurements were taken as a function of approach velocity. The following sets of debris beds were evaluated.
 - Eleven tests were conducted for particulate-only (CalSil) debris for target debris loadings of 1451 to 4350 g/m².
 - Eighty-six tests were conducted for fibrous-only (NUKON) debris for target debris loadings of 105 to 1681 g/m² with debris bed thicknesses measured between 0.11 to 0.63 inches.
 - Thirty-nine tests were conducted for debris beds generated with a combination of particulate and fiber. The target total debris loadings ranged from 135 to 2421 g/m². The target mass ratio of particulate to fibrous material ranged from 0.25 to 1.25. The measured debris bed thicknesses ranged from 0.04 to 0.36 inches.
 - Three tests of coating chips were conducted with Ameron's Amercoat 5450 alkyd topcoat (ALK) for a target debris loading of 1400 g/m².
 - One test of coating chips was conducted Ameron's Dimetcote 6 inorganic zinc primer with Amercoat 90 epoxy topcoat (ZE) for a target debris loading of 1400 g/m².

1.3 Report Outline

An overview of the test setup and instrumentation is contained in Section 2. Schematics of the two head loss test loops constructed are included. Detailed drawings of the test loop are contained in Appendix B.

Section 3 describes the development of the debris preparation procedure and associated metrics used to verify the process for specific debris mass loadings. This section defines the criteria used for establishing the debris preparation process. The results of testing to evaluate the effects of debris preparation on the debris bed pressure drop are included. The description of the preparation and characterization of the coatings materials tested is contained in Section 4.

Section 5 contains the test matrix for the large-scale loop tests and an overview of the test procedures and approach. The test matrixes for the tests completed in the benchtop loop are included in Appendix C.

Phenomenological results for the effect of parameters associated with initial conditions on the measured pressure drop are presented in Section 6. These parameters are potential sources of variability in the results and were investigated to aid in the development of the test matrix and test procedures. These parameters include debris preparation, screen material, debris loading sequence, and flow history.

The results of the pressure drop tests are included in Section 7, and the associated discussion of these results is presented in Section 8. Section 9 presents the discussion and conclusions of the entire test effort. All references for the report are included in Section 10.

Details of the test setup are included in Appendices A and B. The instrumentation and data acquisition system details are provided in Appendices C and D. Appendix E contains the debris preparation procedures and results from the benchtop test loop are included in Appendix F. The Quick Look reports

used to transmit the data from individual tests to the NRC are provided in Appendices G through K. The benchmark test plan used by PNNL and ANL to conduct comparative tests is in Appendix L. The test matrices completed in the benchtop test loop for NUKON only and NUKON/CalSil debris beds are contained in Appendices M and N, respectively. Photographs for the characterization of the coatings debris are included in Appendix O.

2.0 Test Setup

This section provides an overview of the test setup, measurements, and instrumentation used for obtaining the experimental measurements. Two test loops, the benchtop and the large-scale, were constructed for obtaining pressure drop measurements across a debris bed. The benchtop and large-scale loops are described in Sections 2.3 and 2.4, respectively.

The original and final design requirements are discussed in Section 2.1. The specifications for the test screen materials and how they were incorporated into the test loops are presented in Section 2.2. The instrumentation and associated measurements taken during the test program are described in Section 2.5.

2.1 Design Requirements

The original specifications provided by the NRC for performing the tests included:

- Data should be recorded at steady state flow conditions for screen approach velocities from 0.1 to 2 ft/sec (0.03 to 0.61 m/s)
- Screen diameter between 8 and 12 in. (20.3 and 30.5 cm)
- Accommodate and measure debris bed thicknesses of 0.25 to 8 in. (0.6 to 20.3 cm)
- Debris bed pressure drop measurements up to 34 ft H₂O (14.7 psi)
- Water temperature from 68° to 185°F (20° to 85°C).

After procurement and construction of the large-scale test loop had been initiated, the specified screen diameter was reduced to 6 in. (15.2 cm). Preliminary testing conducted in the benchtop loop provided insight as to the range of pressure drops, debris bed thicknesses, and associated approach velocities that would be required to achieve the initial proposed test matrix provided by the NRC. The preliminary benchtop tests indicated the following:

- Debris bed thickness would be less than 1 in.
- For the range of debris loadings evaluated, pressure drops in excess of 14.7 psi, which would be an upper-bound limit for typical plant pumps (not possible to draw a suction from less than -14.7 psig), were measured at approach velocities less than 1 ft/sec (0.3 m/s). Therefore, a maximum approach velocity of 1 ft/sec (0.30 m/s) would be sufficient for conducting the tests.
- Discontinuities and crevices in the main-line flow path should be minimized to reduce the settling and accumulation of debris material in the test loop.

Based on the PNNL test approach, the following additional design criteria for the large-scale test loop were specified:

- The maximum loop pressure should be 100 psig. Increasing the loop static pressure aids in maintaining dissolved gas in solution, thus ensuring single-phase fluid flow through the debris bed with no holdup of gas within the debris bed.
- To allow fully developed flow to be established, 20 length/diameters (L/D s) of straight, constant diameter piping should be provided upstream of the test screen.

- To ensure the downstream pressure tap is located in a region with a fully developed velocity profile, 10 L/Ds of straight, constant-diameter piping should be provided between the test screen and the downstream pressure tap.
- The entire test section should have a constant diameter with no obstructions or discontinuities.
- The test screen material should extend to the pipe wall with no support lip or collar protruding into the flow stream.
- The test section immediately upstream of the debris bed should be transparent to allow for direct viewing, taking in situ debris bed height measurements, and photography. It was preferred but not mandatory that the test section immediately downstream of the test screen be transparent to make observations associated with debris material passing through or being extruded from the test screen and to determine if gas was coming out of solution in the flow discharged from the debris bed.
- The debris injection system should produce a repeatable process that yields similar debris beds.
- The debris injection system should have the capability to introduce debris constituents separately so there is no mixing of the constituents prior to introduction into the loop.
- The debris bed should be able to be removed from the test loop while still on the screen and within a section of piping (i.e., undisturbed).
- The loop should have sufficient filtering capability to remove suspended debris material under test condition flow rates.

2.2 Test Screen Materials

The primary goal of the project was to characterize the differential pressure across a debris bed formed on sump screen material as a function of approach velocity. Two screen materials were tested, 5-mesh wire cloth and perforated sheet metal with 1/8-in. openings. Table 2.1 provides the specifications of the screen materials tested.

Table 2.1. Characteristics of Sump Screen Materials Tested

Tested Screen Geometries (304-Stainless Steel)					
Type	Pattern	Thickness (in.)	Penetration Size (in.) and Shape	Hole Pitch (in.)	Flow Area (%)
Perforated Metal (perforated plate)	Hexagonal	0.063 plate	0.125 ID round	0.188	40
Wire Cloth (5-mesh screen)	Orthogonal	0.072 wire interwoven (total thickness x 2)	0.128 square	0.20	41

The 5-mesh wire cloth (woven wire) represents one configuration of screen material that has been employed at PWRs. The material was selected as the closest fit to the description of the screen material used for previous debris bed tests at LANL (obtained via email from Bruce Letellier of LANL, May 24, 2005). The 5-mesh wire cloth will be referred to as 5-mesh screen. The 1/8-in.-opening perforated metal sheet was selected by the NRC staff as a representative configuration of what may be installed in PWRs following the resolution of GSI-191. The perforated metal will be referred to as perforated plate.

For the benchtop loop, test screens consisted of a 6-in.-diameter circular piece of the screen material cut from stock sheets using an abrasive water jet. The circular pieces were sandwiched between two annular rubber gaskets with inner diameter (ID) equal to that of the test section. The screen and gaskets were then secured between two PVC pipe flanges bolted together.

For the large-scale loop, screen assemblies were fabricated by securing the screen material between two stainless steel annular rings. The screen material was tack welded to the annular rings and then the outside of the screen assembly was seal welded. The ID of the annular rings was the same as for Schedule-40 6-in. pipe, 6.065 in. (15.4 cm). The screen assemblies were fabricated to avoid distortion of the screen during testing and handling. Custom-cut Gorlock[®] gaskets were used to secure and seal a screen assembly within the transparent test section (see Section 2.4.2). Figure 2.1 contains photos of the two screen materials and a wire-mesh screen assembly. Refer to Appendix A for details on the geometry and fabrication of the test screens.

For a pressure drop of 14.7 psi (101.3 kPa) across a debris bed, the 6.065-in.- (15.4-cm-) diameter screen would be subjected to a total load of approximately 425 lb (1890 N). Because in situ debris-bed height measurements were to be taken, the deflection of the 5-mesh material in a screen assembly was evaluated under load.

During the deflection test, the screen assembly was uniformly supported by the stainless steel annular rings by placing the assembly over a 6-in. pipe flange. The screen assembly was marked such that the load would be applied to the same side each time. A pad of 1/16-in silicone gasket material was placed over the screen material followed by a circle of 3/8-in.-thick plywood to distribute the test load and prevent point loads. The test loads were applied to the top of the plywood circle.

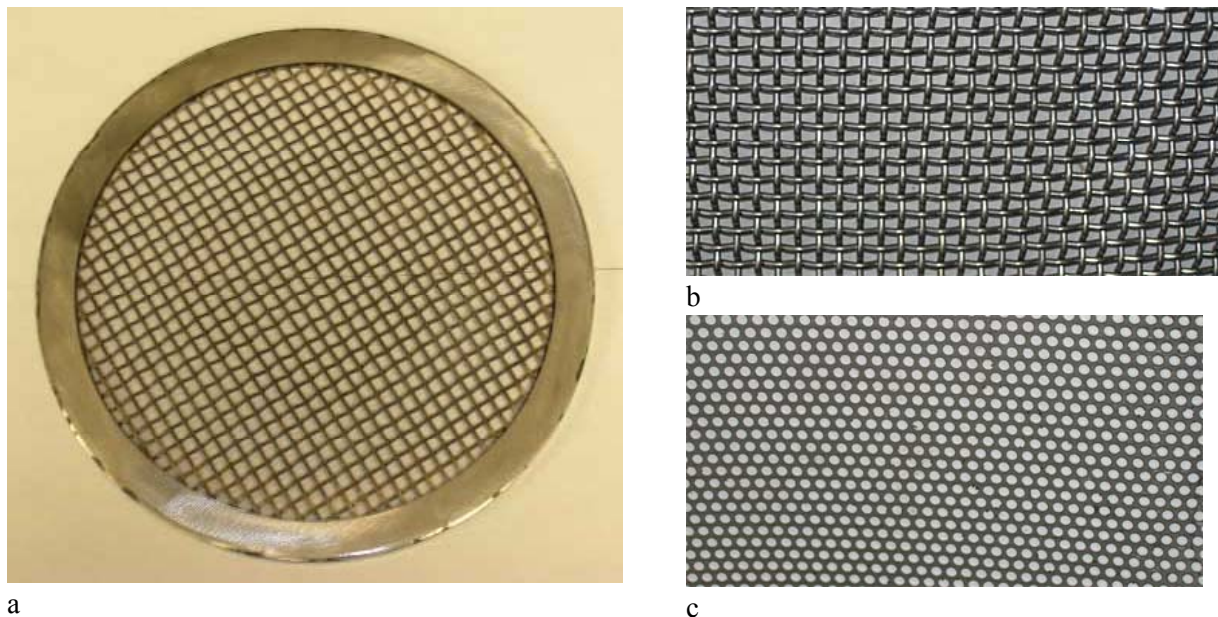


Figure 2.1. Screen Materials Used for Testing: a) screen assembly for large-scale loop with 5-mesh woven wire, b) 5-mesh woven wire material, c) perforated plate material

The test was conducted by adding the desired load, waiting 5 minutes, removing the load, measuring deflection and inspecting for damage. Table 2.2 contains the results of the deflection tests. The perforated plate was much stiffer material and no deflections were measured for the test loads applied.

Table 2.2. Observed Deflections in 5-Mesh Screen Assembly After Applying Distributed Load

Applied Load (lb)	Observations Following Removal of Load
25	No observed or measured change
75	No observed or measured change
125	No observed or measured change
175	One region of screen shows deflection of approximately 0.12 in.(3.2 mm)
225	Depressed region still approximately 0.12 in. (3.2 mm) but larger in diameter.
275	Approximately 40% of screen area is depressed 0.12 in. (3.2 mm). Depressed region is not symmetrical about center of screen and appears shifted to one side.
325	Approximately 40% of screen area is depressed 0.12 in. (3.2 mm). Depressed region is not symmetrical about center of screen and appears shifted to one side. About the same as observations made for 275 lb load except a visually obvious ripple/dimple effect where the screen is not uniformly deformed.
375	No change from 325 load observations
425	Approximately 50% of screen area is depressed 0.12 in. (3.2 mm). Some individual wires indicate a deflection of 0.25 in.

2.3 Benchtop Loop Setup

The benchtop loop was fabricated prior to the large-scale loop to meet the following objectives:

- Evaluate holdup of debris material within the test loop under various operating scenarios. Results and observations from these tests were used to improve the design of the large-scale test loop.
- Develop a debris introduction system and debris bed formation procedure that was controllable, yielded relatively repeatable results, and satisfied the debris bed formation criteria (see Section 3.1.1).
- Aid in developing a debris preparation process and investigate the effects of debris introduction and preparation on debris bed pressure drop.
- Provide feedback on the design of the large-scale test loop by providing test experience associated with debris introduction, debris bed formation, data acquisition, and debris bed retrieval.
- Provide insight into the trends, range of pressure drops, and debris loadings required to form complete debris beds that could be expected during tests in the large-scale loop. Results and observations obtained in the benchtop loop were used to refine the test matrix and prioritize test conditions.
- Develop, evaluate, and refine the test procedures for the large-scale loop.

Because a major objective of the benchtop loop was to assist in developing the final design and procedures for the large-scale loop, the benchtop loop had several modifications incorporated during the test program. The description of the benchtop loop is for the final configuration of the loop. Two additional benchtop loops were used to evaluate debris introduction, debris material holdup, filtration requirements, and CalSil particle size information. These loops did not contain debris screens and no detailed descriptions are provided.

The benchtop loop contained no heating capability or cover gas for increasing the static pressure. Therefore, all tests in the benchtop loop were performed at ambient temperature. With no cover gas system, the static pressure of the loop could not be raised to maintain gas in solution. Therefore, at increased pressure drops across the debris bed, the potential existed for gas bubbles to be generated.

The filter installed in the benchtop loop was not used during testing; therefore, the potential existed for debris to be added to the debris bed throughout a test. The potential sources of additional mass were suspended debris that passed through the debris bed or resuspended debris that had previously settled within the loop. As the approach velocity is increased following the initial test debris bed formation, the debris bed compresses and becomes more efficient at filtering suspended material from the flow. The increased approach velocity also has the potential to resuspend debris that may have settled within the test loop at the lower approach velocities used for the test debris bed formation.

The intent of the benchtop loop was to obtain comparative results for evaluating trends associated with changes in test parameters or procedures. When comparing pressure drop measurements from the benchtop loop with test data from the large-scale loop or other test programs, two limitations of the benchtop loop should be considered.

- The configuration of the test loop piping did not ensure a fully developed flow profile upstream of the test screen.
- The taps used to obtain pressure drop measurements across the debris bed were not located at ideal positions.

An overview of the benchtop loop description is presented in Section 2.3.1. The test section containing the test screen is described in Section 2.3.2.

2.3.1 Benchtop Loop Description

The benchtop loop was assembled on the minus-12-ft level of the 336 Building at PNNL. The test section containing the test screen for the benchtop loop is 4 in. in diameter (see Section 2.3.2 for details). The loop is fabricated mostly of 2-in. flex hose interconnected by Camlock quick-disconnect fittings and Schedule-40 pipe fittings. Kuriyama Tigerflex Series WH, a transparent PVC suction hose, made up the majority of the hoses. The loop is configured for closed-loop testing. The total length of the benchtop loop pipe run is approximately 53 ft, and the volume of the main line is approximately 13 gal.

A 3-hp pump driven by an electronic variable frequency drive (VFD) provides motive power for the test fluid. A combination of the pump VFD and a throttle valve (2-in. gate valve) control the flow rate through the test section. The maximum flow rate of the loop is approximately 50 gpm, which provides a maximum approach velocity of approximately 1.3 ft/sec (0.4 m/s).

Two parallel pipe runs, which bypass the main-line throttle valve, exist for introducing debris material into the loop and are referred to as the debris injection lines. Each 1-in.-diameter injection line includes a Coriolis flow meter and a throttle valve (1-in. gate valve) at the upstream end so that the flow through the individual injection lines can be controlled and monitored. Each injection line contains a section of 1-in. transparent flex hose downstream of the throttle valve that can be removed from the system and loaded with debris material. The two debris injection lines are connected to the main line using pipe crosses. The main-line throttle valve is located between the upstream inlet to the injection lines and the

downstream discharge of the injection lines. This configuration allows adjustment of the main line throttle valve to generate a backpressure sufficient to cause flow through the injection lines. The transparent flex hoses allow the debris to be observed during the injection process to ensure the debris is distributed throughout the length of the injection line and is not clumping or settling.

Between the discharge of the test section and the inlet of the pump, two alternative flow paths were plumbed. One of the alternative paths was added for reducing entrained gas bubbles. The flow passed through a small tank exposed to the ambient air. The open tank and reduced velocity allowed gas bubbles to rise to the surface. The flow was passed through the degassing loop prior to debris injection and after the bed formation had been completed. The second alternative path included a filter for polishing the test loop water prior to debris injection. Filtration was not performed during test operations. Figure 2.2 is a simplified schematic of the benchtop loop.

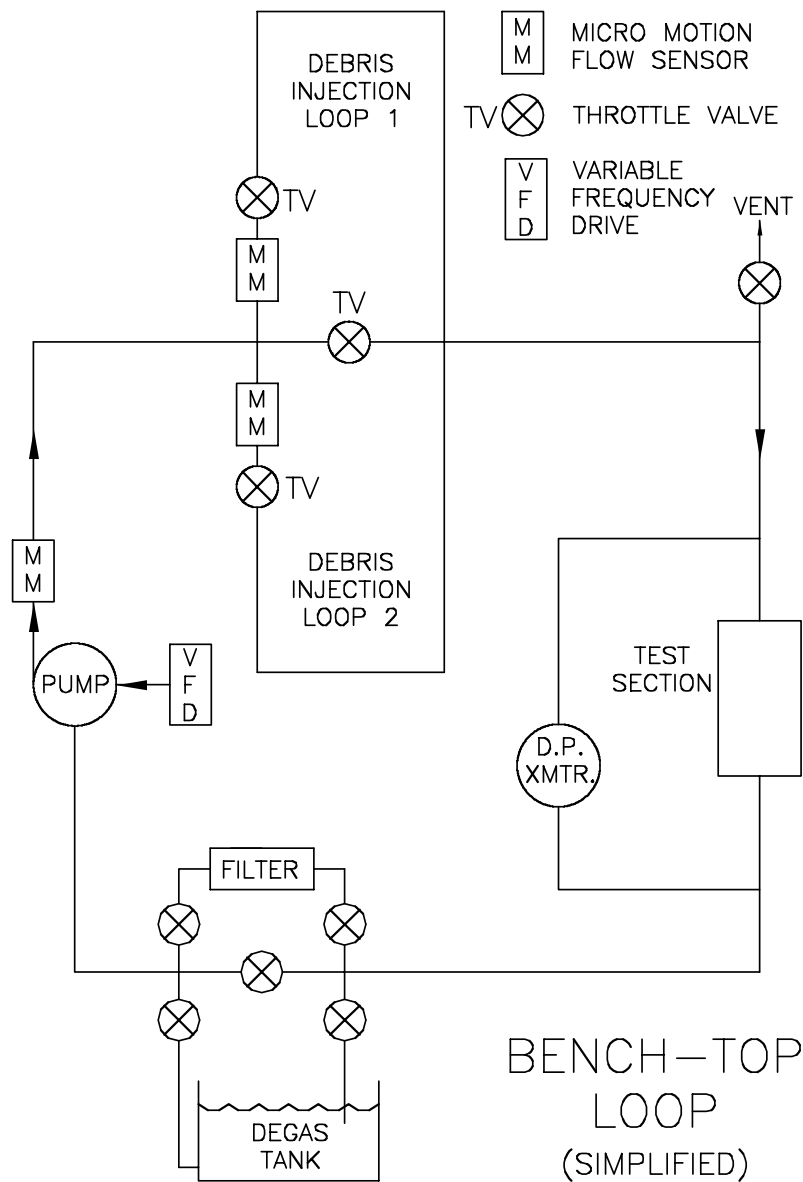


Figure 2.2. Simplified Schematic of the Benchtop Loop

While the benchtop loop could not be pressurized or heated like the large-scale loop, the duration of tests and associated cleanup and turn-around time was much less. Thus tests were conducted, data were provided to the NRC, and decisions were made regarding large-scale testing fairly quickly.

2.3.2 Benchtop Test Section Description

The test section of the benchtop loop was fabricated from 4-in. Schedule-40 transparent PVC pipe glued into 4-in. PVC pipe flanges in the form of pipe spool pieces. Two of these spool pieces form the test section, which has an overall length of 41.5 in. (Figure 2.3).



Figure 2.3. Photo of the Benchtop Loop Test Section. The test screen is sandwiched in the center set of pipe flanges.

Ninety-degree pipe elbows exist at the inlet and discharge of the test section. Due to the relatively short length (5.2 pipe diameters) and the proximity of the pipe elbows, fully developed flow is not ensured just upstream of the test screen. The taps used to obtain the pressure drop measurements across the debris beds are located upstream and downstream of the 4-in test section, which are not ideal locations. The locations of the pressure taps are shown in Figures 2.4 and 2.5.

The screen materials and geometries tested in the benchtop loop were the same as those used for the large-scale loop described in Section 2.4. For the benchtop loop, the cut screen material is sandwiched between the flanges of the two spool pieces forming the test section. The screen material contains no annular support ring, is sealed with silicone rubber gaskets custom cut to fit, and is held in place by tightening the bolts of the PVC pipe flanges. This configuration results in the screen material penetrating the test section wall and creates no discontinuity in the test section cross-sectional area, such as with a ledge or other protruding support structure.

The upstream (inlet) pressure port is 10.5 in. (26.7 cm) above the top gasket of the test section assembly. The downstream (outlet) pressure port horizontal “T” run is 11.5 in. (29.2 cm) below the bottom gasket of the test section assembly.



Figure 2.4. Upstream Portion of Benchtop Test Section Showing Pressure Tap Location



Figure 2.5. Downstream Portion of Benchtop Test Section Showing Pressure Tap Location

2.4 Large-Scale Loop

The large-scale test loop was designed and fabricated to facilitate testing of larger diameter screens than possible in the benchtop loop and to include the following features:

- Temperature control (heating) from ambient to 194°F (90°C).
- Loop pressurization to 100 psig (689 kPa) to maintain gas in solution.
- Filtering at test condition flow rates.
- Fully developed flow upstream of the test screen.
- Sufficiently long test section to allow pressure taps to be placed in ideal locations.
- In situ debris bed height measurements.

This loop was assembled on the main floor level of the 336 Building high bay. The overall height of the test loop is 36 ft. The loop is accessible at four levels.

An overview of the large-scale loop design is presented in Section 2.4.1. The test section containing the test screen and pressure taps is described in Section 2.4.2, and the debris injection system is described in Section 2.4.3.

2.4.1 Large-Scale Loop Description

The initial specifications for the large-scale test loop included a 10-in.- (25-cm-) diameter test screen and a maximum screen approach velocity of 2 ft/sec (0.6 m/s), which would have required a flow rate of 490 gpm (3.1E-2 m³/s). After design and procurement activities for the test loop had been initiated, the NRC made changes in loop performance specifications. The final requirements specified a test screen diameter of 6 in. (15 cm) and a maximum screen approach velocity of 2 ft/sec (0.6 m/s), which requires a flow rate of 180 gpm (1.1E-2 m³/s). The initial flow rate requirements specified were used to size the large-scale loop lines so 3- and 4-in. lines were used to fabricate the main line. For the 6-in. test section, smaller line sizes could have been used. This would increase the velocity in the horizontal runs and reduce the potential for debris settling.

The final design had a test section ID of 6.065 in. (15.405 cm), matching that of 6-in. Schedule-40 pipe. The test section is described in detail in Section 2.4.2. The maximum flow rate of the system was not determined due to the range selected for the mass flow meter. A flow rate of 240 gpm (1.5E-2 m³/s) was achieved with just the test screen in place and no debris material. A 25 hp (19 kW) centrifugal pump driven by an electronic VFD provided motive power for the loop. The pump was located on the ground level at the lowest point in the system. The pump had a 3-in. inlet and a 1.5-in. discharge. Immediately downstream of the pump discharge, the discharge line expanded to 3-in. pipe.

Other than the 6-in. piping of the test section, the main loop consisted of 3- and 4-in. piping and 3- and 4-in. flex hose. All piping was 304-stainless steel. Main loop flex hoses were Goodyear FlexwingTM White, Hi-Temp (FDA-3A), with 3-in. (8 cm) and 4-in. (10 cm) ID, chosen for its pressure and temperature ratings. Fittings were stainless steel, aluminum, or brass.

Observations and measurements made during preliminary testing in the benchtop loop indicated that debris was readily deposited in any small crevices or behind discontinuities in the pipe wall. Negligible quantities of debris were observed to settle in or adhere to continual lengths of piping or hose. The deposited material was an issue at joints and couplings. The deposited debris was not readily resuspended or flushed from the system; therefore, the design of the large-scale loop attempted to reduce available locations for debris deposits. Most of the pipe fittings were butt-welded, and where flanges were required, custom-cut Gorlock gaskets were used.

Several 3-in. full-port ball valves were installed for isolating various portions of the loop. These ball valves are manipulated during filling, draining, and debris bed retrieval operations. During test operations, the three valves used to control flow through the filter unit and by-pass line were manipulated as needed to either the “full-open” or “full-closed” position. The ball valve just downstream of the pump was maintained in a partially closed position to provide additional backpressure to the pump to eliminate cavitation. All of the other main-line ball valves remained full open during testing.

Downstream of the pump discharge was a 4-in. stainless steel pipe vertical riser with clamshell band heaters attached. The band heaters provided a maximum output of 32 kW. Heater control was via a Chromalox 1601E temperature controller and a Chromalox 10100 over-temperature controller mounted in a cabinet, which were controlled by means of the time-proportional on-off method.

The 4-in. vertical riser transitioned to horizontal pipe via 4-in. flex hose at the top of the test loop where the debris injection lines were located. The debris injection lines are described in Section 2.4.3. The upper horizontal portion of the loop was a combination of 4-in. pipe and flex hose and contained the expansion tank and main-line throttle valve, a 4-in. neoprene pinch valve. The water flow rate through the test screen was controlled by varying the output frequency of the VFD and/or by throttling the 4-in. pinch valve. The pinch valve allowed throttling without any internal parts that may collect debris material.

The expansion tank allowed for fluid expansion and contraction and was connected to the highest point of the loop. Static line pressure in the loop was controlled by means of adjusting the headspace pressure in the expansion tank using an argon cover gas. The argon cover gas was used to reduce the dissolved gas in the working fluid.

The downstream side of the upper horizontal portion of the loop connected to the vertical test section fabricated from 6-in. Schedule-40 pipe. The transparent portion of the test section containing the test screen was accessible from the first level. At the discharge of the vertical test section, the line size reduced to 3-in. piping, which contained the main loop flow meter. A Micro Motion CMF-300 Coriolis flow sensor measures mass flow rate and density in the main line.

Downstream of the flow sensor was a filter with a bypass loop. The filter unit contained an 8-in.-diameter filter bag housing with 4-in. pipe flanges. The filter housing was connected to the main line with custom machined blank flanges to reduce potential crevices; 10- μ m filters were used in the filter housing. The bag filters were dried at 194°F (90°C) and then weighed prior to installation in the loop. Following test operations, the bag filters were removed and dried to determine the mass of debris filtered from the loop. During formation of the debris bed, the filter was “valved-out” of the loop to allow debris to circulate and be captured by the test screen. Following the formation of the debris bed, the flow was increased to 0.2 ft/sec (0.06 m/s) and passed through the filter to remove suspended debris. Filtering the flow after

bed formation reduced the amount of debris that could be added to the debris bed after steady-state measurements were initiated. The filter unit was also used to polish the test fluid before initiating a test.

No filters existed in the loop during the Series-1 tests; the discharge of the flow meter was connected via 3-in. flex hose directly to the pump inlet. The filter unit and associated by-pass line were installed prior to the Benchmark tests.

Between the discharge of the test section and the inlet of the pump, several drain ports are provided for filling and draining the loop. Figure 2.6 is a schematic of the large-scale test loop.

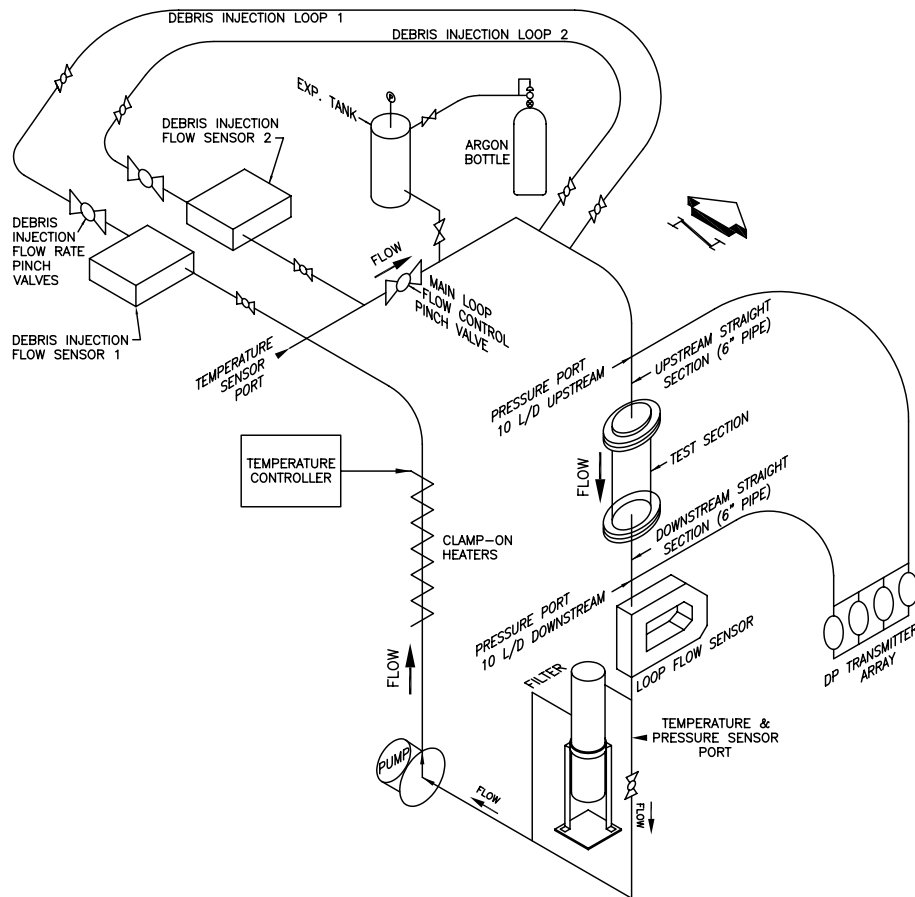


Figure 2.6. Large-Scale Test Loop Schematic (see Appendix B for detailed drawings of the large-scale loop configuration)

2.4.2 Test Section

The test section consisted of the entire vertical run of 6-in. pipe and contained the upstream section, the transparent test section (TTS), which housed the test screen, and the downstream section. The upstream and downstream sections were fabricated from seamless Schedule-40, 6-in., 304-stainless steel pipe. Inside flange welds were butt type with no annular gaps or protrusions to disrupt flow or collect debris material.

The upstream straight section was 9.7 ft (2.96 m) long, allowing for at least 20 L/D of straight pipe to allow a fully developed flow profile to exist upstream of the test screen. The downstream section was 5.6 ft (1.71 m) long, allowing 12 L/D of straight pipe prior to a reduction in pipe size.

The TTS was machined from 8-in. round stock of polycarbonate. The ID was machined to match that of Schedule-40, 6-in. pipe. The test section was designed for operations at 150 psi (1034 kPa) and 200°F (93°C), resulting in a wall thickness of 0.87in. (2.21 cm). Three TTSs were fabricated, allowing the entire section to be removed from the test loop with the debris bed intact and another clean unit to be installed immediately.

The TTS consisted of two parts, an upstream portion and a downstream portion, which cradled the test screen assembly in a socket in the top of the downstream portion. The two halves of the TTS were clamped together by threaded studs and nuts, securing two modified 6-in., 150# blind flanges. These flanges also mounted the TTS assembly to the upstream and downstream straight pipe sections. Photos of the large-scale TTS are presented in Figure 2.7, and the dimensions and assembly details are presented in Figure 2.8.

To obtain pressure drop measurements across the debris beds, ports were drilled and tapped for 1/8-in. national pipe thread (NPT) in the upstream and downstream test sections. At axial locations for the pressure ports, a port was drilled and tapped on each side of the pipe to form a set. The ports were then connected as needed to the manifold for the pressure transmitter array. In the upstream section, ports existed at locations of 2, 5, and 10 L/D upstream of the test screen. Initially it was anticipated that debris beds several inches thick would be generated. To allow pressure measurements to be taken 2 L/D upstream of the debris bed surface, five additional sets of ports were located at 2-in. (5.1-cm) increments upstream of the port located 2 L/D from the surface of the test screen for a total of eight sets of ports upstream of the test screen. In the downstream section, the ports existed at locations of 5 and 10 L/D downstream of the test screen.

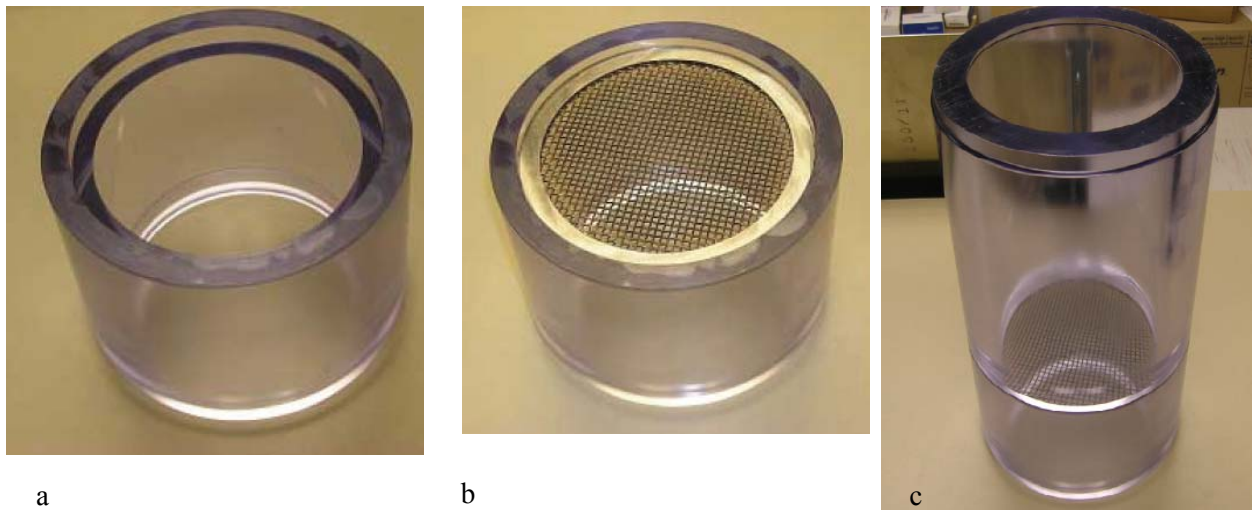


Figure 2.7. Large-Scale Transparent Test Section: a) downstream (bottom) section with no screen assembly, b) downstream (bottom) section with screen assembly installed, c) assembled test section.

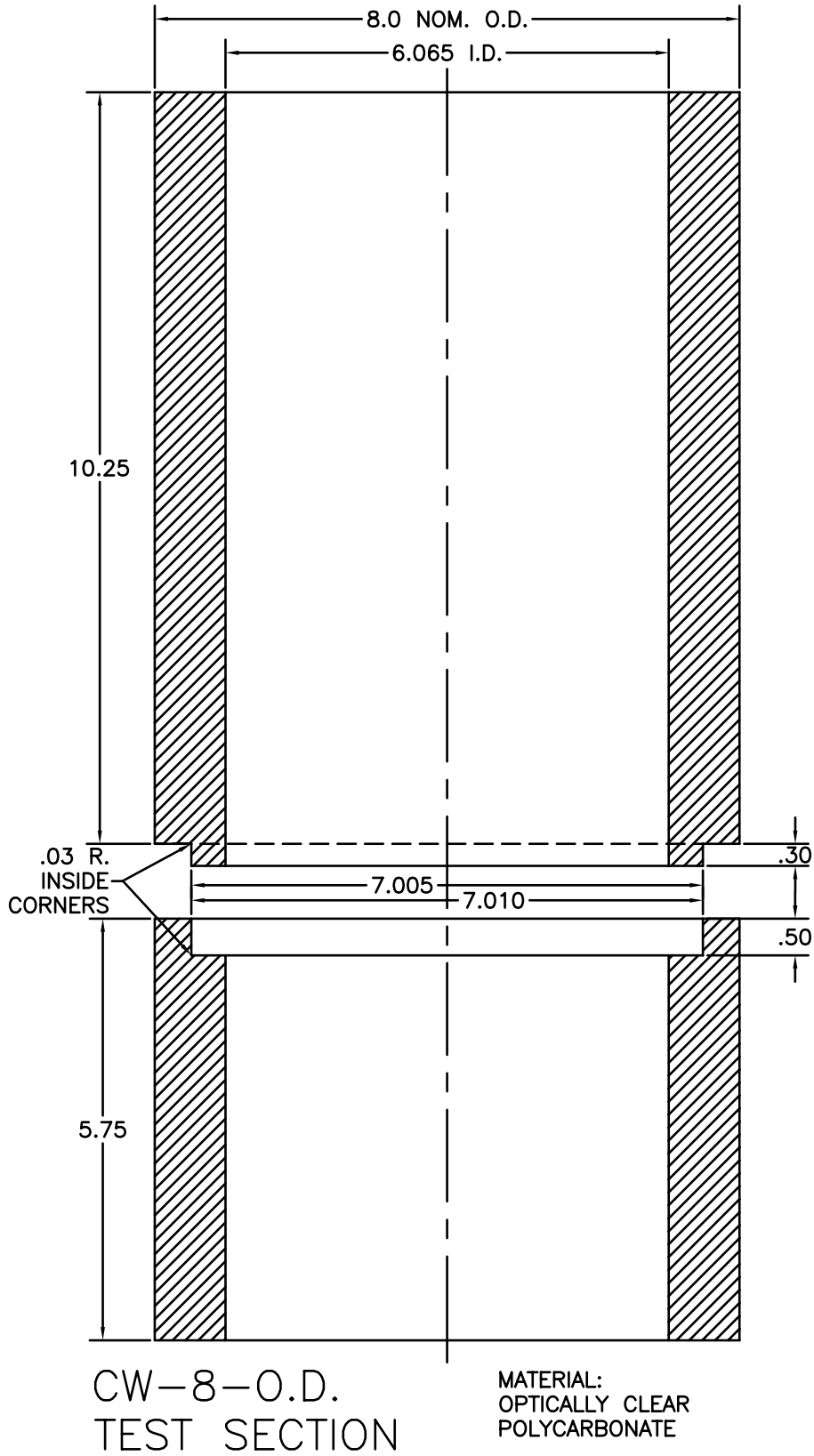


Figure 2.8. Schematic Detailing the Dimensions of the Transparent Test Section

2.4.3 Debris Injection System

To reduce the variability associated with debris bed formation, a debris injection system was developed for introducing debris material into the loop in a manner that could be controlled and repeated. The debris injection system was also designed with the option to introduce debris constituents separately so that they did not mix until after they had been introduced into the test loop. The debris injection system and associated procedure (Section 5.3.1) were developed concurrently.

Significant factors that were taken into consideration in designing the debris injection system included:

- The consistency of the rate at which debris material was introduced into the test loop. The objective was to introduce the debris into the loop at a relatively constant rate to avoid highly concentrated slugs of debris material reaching the test screen. The main reason to avoid slugs of high debris concentration is the difficulty associated with reproducing the flow of debris to the screen from one test to the other. The concentration at which the debris arrives at the test screen may also affect the formation of the debris bed and its resulting structure.
- The ability of the debris injection system to deliver all of the prepared material to the loop. It was desired that no residual debris be left in the injection system.
- No agglomeration of debris in the injection system. Initial work with NUKON demonstrated that if prepared debris was allowed to settle the material would clump, changing its behavior.
- Maintaining debris concentrations in the debris injection system of less than 7.4 g of debris per liter of water (personal communication from BC Letellier, LANL, to CW Enderlin and F Nigl, PNNL, June 17, 2005, providing guidance for concentrations of debris used for blending during debris preparation and debris introduction into the loop).

The final method of debris injection consisted of filling a transparent flexible hose with prepared debris and then connecting the flexible hose to a line that bypassed the main throttle valve. By diverting a portion of the main-line flow through the injection line, the debris material was introduced into the main line. This type of system was originally developed for the benchtop loop and proved very successful in generating debris beds that yielded repeatable head loss test results.

The debris injection system consisted of two parallel, identical lines located on the third level, 29.5 ft above the main floor. Two loops facilitated simultaneous or phased injection of two different debris recipes. The upstream end of an injection line was 1-in. piping and contained in series a Micro Motion CMF 100 Coriolis mass flow sensor, a 1-in. ball valve, and a 1-in. pinch valve. Downstream of the injection-line pinch valve was a 2-in. ID, 13.3-ft- (4.1-m-) long transparent flex hose connected to the loop via isolation valves (1-in. ball valves) and Camlock quick-disconnect fittings. The transparent hose was Kuriyama Tigerflex™ Series WH PVC hose with a rated working pressure of 35 psig (241 kPa) at 68°F (20°C). The schematic of the large-scale test loop shown in Figure 2.8 includes the debris injection lines.

The mass flow sensors installed in each injection line allowed precise monitoring of the injection line inlet mass flow rate. The original design had the mass flow sensors located at the discharge of each debris injection line to monitor the rate at which debris entered the test loop. However, testing of this configuration in the benchtop loop demonstrated that the flow path through the smaller range mass flow

sensors could result in the accumulation of debris and even plugging. Therefore, the mass flow meters were located at the upstream end of the injection lines to monitor the inlet flow rate.

Testing in the benchtop loop determined that a fluid velocity of 0.8 ft/sec (0.2 m/s) through the injection line hoses was sufficient to mobilize the debris for the range of NUKON/CalSil loadings prescribed in the proposed test matrix.

The main-line pinch valve was used to adjust the flow rate through the debris injection lines. The main-line pinch valve was partially closed to generate backpressure to drive flow through the injection line. The main-line and injection-line pinch valves were adjusted in combination to obtain the desired debris bed formation velocity at the screen and the desired velocity through the injection lines. The ball valves allow the injection line to be isolated when the flexible hose was disconnected.

The size and length of the flexible hose was selected based on:

- The physical location of the upstream and downstream connections to the main line. The space limitations of the platform dictated the configuration of loop components, which generated a minimum distance that had to be spanned by the debris injection line hose.
- The need to produce a velocity of 0.8 ft/sec (0.2 m/s) in the injection line while generating a screen approach velocity of 0.20 ft/sec (0.06 m/s) during debris bed formation (the debris bed formation velocity was later reduced to 0.10 ft/sec (0.03 m/s) by the NRC, as discussed in Section 5.3).
- Ensuring that a maximum debris concentration of 7.4 g of debris per liter of water was not exceeded for any case in the test matrix.

The flexible hose could be manipulated manually to disperse the debris within the hose and prevent the material from settling between the time of loading and the time flow was initiated (usually only several minutes). The transparency of the hose allowed the following:

- Observation to ensure the debris was distributed throughout the length of the hose.
- Determination of whether settling or clumping of the debris was occurring and if additional agitation was required.
- Determination of the time at which the debris was completely discharged from the injection line.

Because of its low temperature and pressure ratings, the transparent hose was isolated prior to increasing the static pressure of the loop or heating the loop. For the tests conducted with the debris injected at an elevated temperature, 2-in. Goodyear FlexwingTM White, Hi-Temp (FDA-3A) hose replaced the transparent hose.

2.5 Instrumentation and Measurements

Experimental data were obtained from manual measurements, digital readouts, electronic outputs captured on a data acquisition system (DAS), post-test analysis of digital photographs, and scanning electron microscopy (SEM). The DAS and electronic instrumentation connected to the large-scale loop are described in Section 2.5.1, and the instrumentation connected to the benchtop loop is described in Section 2.5.2. Additional instrumentation used to support the experimental loops is discussed in Section 2.5.3. Section 5.4 presents post-test measurements and the analysis associated with optical

triangulation to determine in situ debris bed heights, ion selective probe readings to determine the mass of CalSil within debris beds, and SEM to assess the debris bed structure. Refer to Appendix C for the detailed project measurement and testing equipment (M&TE) listings.

2.5.1 Large-Scale Test Loop Instrumentation and Data Acquisition

The DAS recorded the following large-scale loop measurements to an electronic file:

- Specific gravity of the main-line flow
- Mass flow rate through the test screen. The mass flow rate and fluid density were used to calculate the screen approach velocity.
- The pressure drop across the debris bed/test screen.
- Fluid temperature
- Mass flow rate entering each debris injection line
- Specific gravity of the flow entering each debris injection line.
- The main line pressure
- Ambient temperature
- Temperature of the differential pressure (DP) manifold tube bundle for assessing temperature corrections.

The DAS computer and associated hardware are presented in Section 2.5.1.1 and the instruments connected to the DAS in Section 2.5.1.2. Large-scale M&TE are listed in Appendix C.

2.5.1.1 Large-Scale Test Loop Data Acquisition System

A personal computer (PC)-based DAS with a standard Dell tower model GX280 was used for the project. The operating system was Microsoft Windows XP[®] Professional.

Signals from instrument sensors were first fed to industry-standard 5B analog signal conditioning modules mounted on motherboards designed to accept them. Specific versions of 5B modules were available for input voltage, current, thermocouple (TC), and resistive temperature device (RTD) signals. 5B32-02 modules were used for signals transmitted on standard 4~20 mA current loops. All sensors except the three TCs used 4~20 mA loops. Type J TC signals were handled by 5B47J-02 modules. All 5B modules used in the system output in the 0~5V range, which was linearly proportional to the input range of the module. Voltage signals from the 5B modules were fed to the PC-based DAS. The analog-to-digital (A/D) converter circuit board was a Measurement Computing PCI-DAS6402-16. This 16-bit peripheral component interconnect bus board could handle up to 64 analog input channels.

The DAS software was DasyLAB 7, a flexible, graphical user interface based system. Individual signals were sampled by the 6402 board at a 100-Hz rate. Each input signal was run through a running 1-second average and scaled to engineering units. Signals were displayed on meters or charts, run through specific calculations, and logged to an ASCII text data file that facilitated post-processing and analysis using Microsoft Excel[®] and other software. Appendix D contains screen prints of the worksheet layout.

The DAS software was also used to perform real time calculations to assess the data with respect to meeting the steady-state criterion (see Section 5.3.). The value of the acceptance criterion was displayed on a DAS meter and could be readily evaluated by the test operators.

2.5.1.2 Large-Scale Test Loop Instrumentation

The mass flow rate and specific gravity were measured using Micro Motion Elite series Coriolis mass flow (CMF) sensors. A CMF 300 sensor measured flow in the main loop downstream of the test section, and a CMF 100 sensor in each of the two debris injection loops measured the injection line inlet mass flow rate and specific gravity. Transmitters for these sensors were Micro Motion model RFT 9739. An Ametek 88F005A2SCSSM pressure transmitter sensed the line pressure at the lower elevation of the loop.

Four Rosemount 115-series DP transmitters were connected to a DP valve manifold that facilitated quickly valving in or out (bring on- or off-line) individual transmitters based on the magnitude of the pressure drop across the test screen or flushing gas bubbles from the DP manifold and associated tubing. The array of DP transmitters had ranges of 5, 30, 150, and 750 in. of H₂O.

Temperature sensors monitored temperature in the top and bottom of the loop, ambient air temperature near the top of the loop, and the temperature of the bundle of DP lines near the DP manifold. The upper loop sensor was an RTD, while the others were Type J TCs. Further details for the large-scale instrumentation can be found in the M&TE listing in Appendix C.

2.5.2 Benchtop Test Loop Instrumentation

The same DAS used for the large-scale test loop was also used for the benchtop loop. Different analog input channels were allocated for the large-scale and benchtop loops. Two versions of DasyLAB worksheet or setup files were produced, one to acquire and process the benchtop instrument signals and the other for the large-scale instruments. Appendix D portrays the graphical layout of the benchtop DAS worksheet. Benchtop instruments connected to the DAS were:

- Micro Motion D100 Coriolis mass flow sensor sensing main loop flow rate and fluid density
- Micro Motion DH03S Coriolis mass flow sensor sensing debris injection loop-1 flow rate and fluid density
- Micro Motion DH025S Coriolis mass flow sensor sensing debris injection loop-2 flow rate and fluid density
- Honeywell Y41104 DP transmitter with a span of 1000-in. H₂O sensing DP across the test screen
- Type J TC sensing loop fluid temperature.

Each of the Micro Motion sensors was connected to Micro Motion RFT9739 transmitters that perform calculations and produce 4~20 mA analog outputs.

2.5.3 Additional Instrumentation and Equipment

To conduct the tests and evaluate the debris material and debris beds, additional instrumentation that was not connected to the DAS computer was used. This section provides an overview of the instrumentation and equipment that is not discussed in other sections.

Several laboratory benchtop digital scales were used for taking general mass measurements such as mass of debris constituents and dry debris beds. The Sartorius BP 3100 S was the most frequently used scale for debris preparation.

Manual measurements of the debris bed under flow conditions in the large-scale loop were made with a tape measure fastened to the outside of the test section. The zero of the scale was aligned with the top of the screen assembly ring. More substantial in situ bed height measurements were taken using optical triangulation (Section 2.5.4.1). Post-test measurements of the debris bed height were made using a commercially available ruler with centimeters and millimeter graduations. With the retrieved debris bed in the TTS, a straight edge was placed across the top of the test section and the measurements made by lowering the ruler into the test section until it touched the debris bed. Section 5.3 contains details of the post-test bed-height measurements.

Relative moisture content measurements of the debris beds were taken using a Delmhorst BD-2100 moisture content probe (property No. 35519). These measurements were taken for managing the drying of the debris beds and to obtain comparative measurements. These measurements were taken and recorded for indication only and are not reported.

Particle size analysis was performed with an S3000 Microtrac particle size analyzer (ID No. N830468) per PNNL Waste Treatment Plant procedure TPR-RPP-WTP-222, Rev. 2 (2005). A variable-speed recirculating pump setting of 45 was used for the measurements. An Ultrameter II 6P Serial No. 6203236 was used to monitor the conductivity of the large-scale test loop water.

To prepare the debris materials, blenders and a 3-in. ceramic mortar and pestle were used to disassociate or break up the debris material from its as-received condition. Four blenders were used in the course of the test program; three Waring (7011HS Model HGB2WTS3) commercial blenders and one Kitchen Aid (Model KSB50B4). The blenders were not interchangeable. The Waring blenders were designated 1, 2, and 4 (see Appendix C). Section 3.2 contains a discussion of the blender effects on debris preparation.

Still and video digital cameras were used to photograph various aspects of testing including debris bed formation. Appendix C shows details.

2.5.4 Supporting Post-Test Measurements

Following the completion of tests and the drying of debris beds, additional evaluations were performed on selected debris beds. This section describes the three main activities of:

- Obtaining in situ debris bed height measurements using optical triangulation. Following the Series-1 tests, a system was developed and installed as part of the large-scale transparent test section that allowed digital pictures to be taken with an array of spaced lines projected across the surface of the debris bed. Post-test analysis of the pictures allowed the bed height and topography of the debris bed to be determined. The test procedures, Section 5.3, called for taking the optical triangulation pictures at each steady-state test condition. However due to cost constraints, post-test analysis was only conducted on a limited set of photos. Section 2.5.4.1 explains the methodology used to obtain the bed height measurements, and Section 7.0 presents the results.
- Assessing the CalSil mass contained in debris beds consisting of both NUKON and CalSil. A procedure was developed for dissolving the debris beds and determining the mass of CalSil retained

in the bed based on relative measurements of CalSil performance standards (mixtures containing known masses of CalSil) obtained with a Ca^{++} ion selective electrode (ISE). An overview of the method is discussed in Section 2.5.4.2.

- To assess the structure of debris beds formed under selected conditions, these retrieved beds were prepared and sectioned for imaging by SEM. Section 2.5.4.3 discusses the preparation and scanning of the debris bed sections.

2.5.4.1 Debris Bed Height Measurements Using Optical Triangulation

The NRC wanted debris bed heights to be measured as a function of velocity throughout the test without disrupting the flow upstream of the debris bed. Optimally, this objective would involve measuring the topography of the debris bed. The transparent test section allowed manual measurements to be made by visually sighting across the top of the debris bed and estimating the elevation using a scale fixed to the pipe wall. However, manual measurements were complicated by the existence of a raised rim of deposited debris material that formed at the wall of the test section around the entire outer edge of the debris bed. The fluid velocity profile across the test section along with the characteristics of the fiber debris contributed to the formation of a raised rim. For debris beds of smaller mass loading with less pronounced rims, the position of the interface between the two halves of the TTS and the associated gasket interfered with manual measurements.

PNNL investigated using ultrasonic and optical methods and had the greatest success using optical triangulation, which is an established method to determine the position of an object. A schematic describing the technique is presented in Figure 2.9. A light beam shines on a surface and is imaged onto a detector array. As the surface position (i.e., debris bed thickness) changes, Δz , the image of the reflected beam, moves on the detector, Δx . The light beam could be a white light source or a laser beam and can be a dot, a line, or an array of dots or lines, depending on the item to be measured. The detector array can be a linear detector or a two-dimensional array (video camera). The sensitivity of the technique depends on the angle between the input beam and the detector, the size of the pixels in the array, and the focal length of the imaging lens.

For the tests performed in this study, a series of light and dark lines on a grid (50 lines per inch) was projected onto the test bed through the TTS. The detector was a video camera. The camera detector array was 3264 x 2448 pixels. Figure 2.10 is a diagram of the test setup, and Figure 2.11 presents pictures of the system installed on the test bed. The light source and digital camera were attached directly to the test section to reduce any relative motion of the debris bed and camera. In the course of the testing, several changes had to be made to the setup. For example, the camera position had to be moved back and made more secure so it would not be in the way during loading and unloading operations. Also, the light source had to be raised to minimize the shadow of the rim on the test bed. The position of the camera was changed to minimize the obscuration of parts of the debris bed due to the support posts.

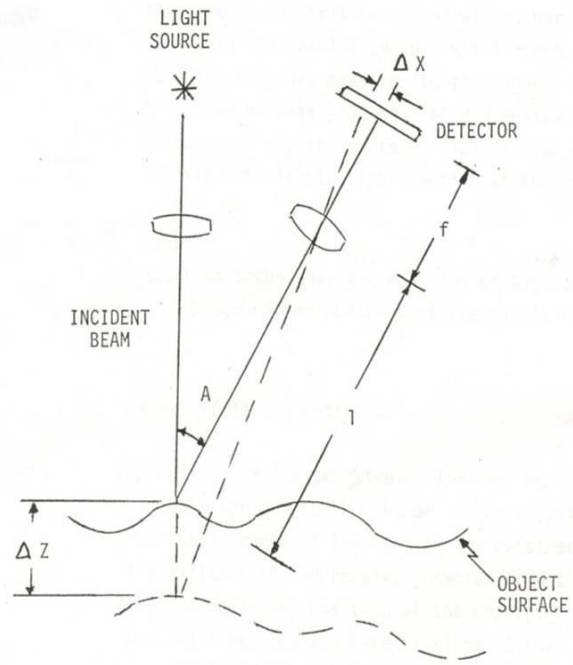


Figure 2.9. Schematic of the Optical Triangulation Technique

System Dimensions

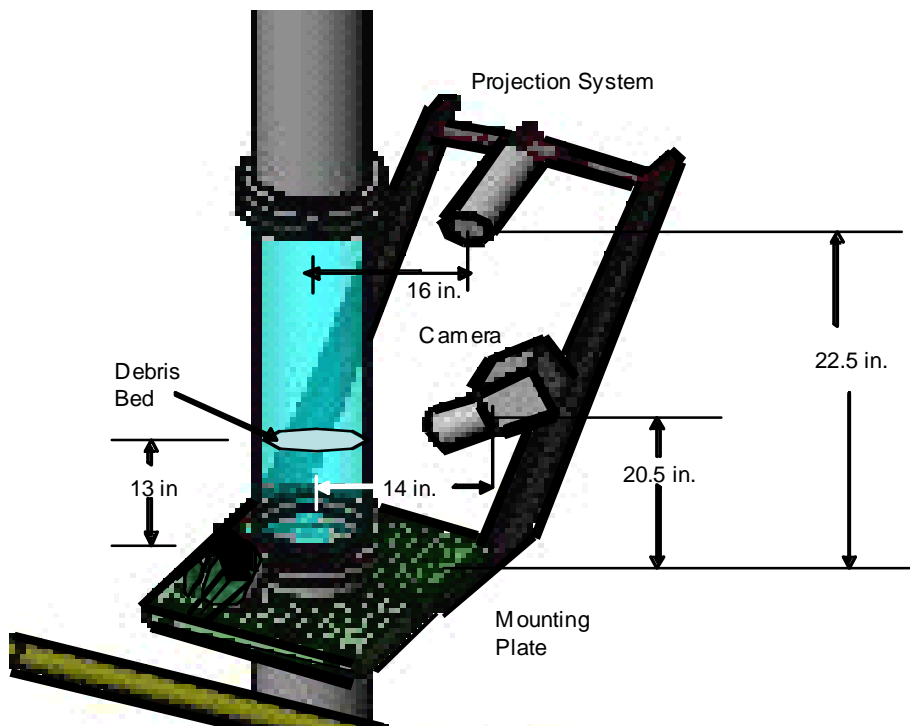


Figure 2.10. Schematic of Plan View Setup of Optical Triangulation System for Large-Scale Test Loop



Figure 2.11. Photos of Optical Triangulation System Installed on the Large-Scale Test Loop

To determine the thickness of the debris bed, it was necessary to calibrate the system. A calibrated step wedge, shown in Figure 2.12, was placed in the system, and a picture was taken with the same setup as was used when the actual unknown debris beds were measured. From this calibration, the amount of movement (in camera pixels) that corresponds to a certain height of the debris bed can be correlated. Additional reference points were provided by a line placed on the inside of the TTS at a measured height of 1.6 in. (40 mm) above the screen and the interface 0.4 in. (10 mm) above the screen where the top and bottom pieces of the TTS meet. When possible, the rim height from the manual measurements was also provided as an additional reference. These values allowed a calibration constant to be determined over a wide range of thicknesses. Based on this calibration wedge, the resolution of the system was determined to be 0.025 in. (0.63 mm).



Step Heights: 0.04 0.03 0.02 0.10 in.

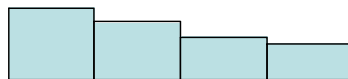


Figure 2.12. Calibration Wedge Used for the Optical Triangulation System

To measure the bed height, digital photos of the debris bed with the set (grid) of lines projected across the bed surface were taken at each test condition after a steady-state pressure drop had been achieved. The distance from the edge of the debris bed to the reference elevations on the inside of the pipe wall were determined (in camera pixels) and then translated through the calibration constant to an edge height. Similarly, the distance to the edge of the bed plane (flatter area of the bed surface inside the outer rim) was determined. By using the projected grid lines, one could determine the change in bed height from the edge to any point on the bed.

The analysis could not be performed if the complete surface of the debris bed was not in focus. Occasionally, changes in lighting or suspended debris caused a change in focus, resulting in some photos being corrupted with respect to the optical triangulation analysis.

2.5.4.2 Assessment of CalSil Mass in Debris Beds

The CalSil mass in debris beds was assessed using chemical dissolution and calcium ISEs. The CalSil insulation material used for testing was primarily composed of calcium silicate. By dissolving the entire debris bed in hydrochloric acid (HCl), the concentration of the calcium ions was detected by the ISE probe. The potential (millivolts) measured by the probe were correlated to a CalSil concentration.

Probe readings are not fixed in relation to Ca^{++} concentration. The readings may vary with time, temperature, and probe usage. Thus, the Ca^{++} concentration readings of unknown CalSil masses in debris bed samples were compared to a performance curve, which was a curve fit of Ca^{++} concentration readings to CalSil masses of performance curve samples. The performance curve samples consisted of known CalSil masses. Because of the potential shift of the performance curves with changes in time, temperature, and probe usage, the performance curve standards were generated at approximately the same time that the debris beds were dissolved. The ISE readings for the performance curve samples were taken each time readings were made of debris bed samples.

Before taking measurements using the ISE probe, the dissolved CalSil and debris bed solutions were diluted in deionized (DI) water, the pH was adjusted to 7, and ionic strength adjuster (ISA) was added. The dilution, pH adjustment, and ISA were added to obtain better results with the ISE probe.

2.5.4.3 Debris Bed Sectioning

To perform SEM analysis of a debris bed, the bed must first be dried, impregnated with an epoxy resin, and sectioned. The sectioned sample is then polished to provide a uniform smooth surface for SEM analysis. For this process the debris bed was not removed from the screen, and the screen material was also sectioned.

After a debris bed was retrieved from the test loop, it was dried in an oven at 194°F (90°C) until constant mass readings were obtained. For impregnating the debris bed with epoxy, a rubber mold was fabricated to hold the debris bed and test screen. Because of the weak structure of the debris bed, care was taken not to distort it while adding the epoxy. The epoxy was poured into the mold and degassed by placing it in a vacuum chamber to remove as much air as possible. The debris bed was then carefully lowered into the mold, taking care to not disturb the bed or entrap additional air in the epoxy. The epoxy filters into the debris bed and was then allowed to set at room temperature, which required several hours.

After the epoxy was set, forming a solid disk, the disk was cut using a circular saw with a silicon carbide abrasive disk. The bed was cut along two lines running through the center of the bed: one along the center wire of the 5-mesh woven-cloth screen (Section 2.2), and the other cut along a diagonal with respect to the screen grid. A thin section was taken from along each cut and mounted. Because of the fragile nature of the debris bed, the entire bed could not be placed in a vacuum chamber to remove all of the trapped air. Therefore, the surface of the slice was examined to find a section with no or minimal air pockets. The surface was then polished and examined.

A JEOL GSM-5900LV SEM was used to obtain detailed images of the debris bed structure and identify any distinct regions. The technique used was backscattered imaging at 20 kV and 100X magnification. Images were also taken at higher magnification as needed to examine the detailed structure of regions of interest. A series of images was taken traversing the height of the debris bed and along the top surface for each sample. The images in each series were relatively evenly spaced. The preliminary analysis performed on the selected images is presented in Section 6.5.

3.0 Test Debris Preparation

Debris bed head loss testing at PNNL was conducted using both NUKON and CalSil insulation. To introduce the debris to the test loop, NUKON and CalSil slurries were prepared. The target NUKON and CalSil slurry criteria, characteristics, quantification methods, and associated evaluations are elucidated in this section. The proposed test matrix specified target debris loadings in terms of mass of debris constituent per unit area of screen. The target mass loading was used to determine the amount of material to introduce to the test loop. Because all of the debris material was not necessarily retained on the screen, the target mass loadings generally differ from the retained mass loadings.

The debris material received for the formal testing conducted by PNNL was the following:

- NUKON material received from Performance Contracting Inc., Lot No. 09/06/5ND5, BS-4813, shipped on 10/8/05. The vendor/manufacturer subjected the NUKON to a 12- to 14-hr heat-treating process and then shredded the material in a wood chipper prior to shipment. G. Hunter, of Performance Contracting Inc., described in phone conversations to Carl Enderlin of PNNL the heat-treating process and “average effective fiber diameter.” The fiberglass “blankets” were placed in direct contact with a hot plate surface that was maintained at approximately 600°F. During the heat-treating process only one side of a blanket was brought in direct contact with the heated surface. The average effective fiber diameter of the NUKON had been measured by Performance Contracting Inc. at 2.6e-4 in. for virgin material and 2.8e-4 in. for fiber with the binder applied. The effective diameter was determined for a “fiber pack” via an air resistance test to an uncertainty of $\pm 2E-5$ in. and does not necessarily match the physical diameter of the individual fibers.
- CalSil material received from Johns Manville, Lot No. 017-276, BS-4823, shipped on 9/28/05. The CalSil material was not subjected to any heat treatment and was in the form of 3 x 12 x 48-in. blocks.

The debris material used for the preliminary PNNL testing conducted to evaluate the debris preparation methodology as described herein was ordered in June 2005 from the vendors listed above. The initial order of CalSil was from Lot No. H 14 RP. The initial order of NUKON was received in two forms; the 3-in.-thick sheets (blankets) of material were from Lot No. 03/30/4ND5 BS-4700, and the shredded material was not from a specific lot but was made up of leftover materials saved by the vendor for shredding. The material may have been from two to four lots of material.

In Section 3.1, the target slurry criteria and defining characteristics are identified. Testing results for the formation criteria and techniques to quantify these characteristics are presented in Section 3.2, and the debris preparation techniques are summarized in Section 3.3.

3.1 Debris Bed Formation Criteria and Target Characteristics Identification

The debris bed head loss testing at PNNL was conducted to provide data useful for developing and validating a head loss correlation that can be applied in safety basis-type applications for varying debris-loading conditions. To obtain data useful to the development of a correlation, the debris preparation process should produce debris material with an initial condition that can be verified (characterized) and repeated. Failure to do so makes it difficult to determine whether differences in the test results should be attributed to variations in the test parameters or variations in the initial condition of the debris. In Section 3.1.1, the PNNL-defined NUKON and CalSil slurry-generated debris bed criteria are listed.

Guidance for the target characteristics, as defined by previous related work, is discussed in Sections 3.1.2 and 3.1.3 for NUKON and CalSil debris material, respectively. These criteria and target characteristics were agreed to by NRC staff and NRC contracted national laboratories [LANL and Argonne National Laboratory (ANL)].

3.1.1 Debris Bed Formation Criteria

The current debris bed head loss correlation, as presented in NUREG/CR-6224 (Zigler et al. 1995), assumes that the debris bed is uniform in thickness as well as composition. To assess possible accident scenarios, conditions should be created for different debris loading scenarios to provide statistically significant and repeatable results. Additionally, given the safety aspects of the applications of the developed correlations, evaluated conditions should consider the effect of slurry preparation on the resulting debris bed head loss.

The objective of this experimental task was to study debris conditions that form a complete (entire screen covered with debris with no channeling present) debris bed. Obtaining pressure drop measurements for incomplete or partial debris beds was outside the scope of this effort. Elevated pressure drops are present only if a complete debris bed was formed. Consequently, the tested debris beds should have certain standard characteristics that provide repeatable data for developing a method for calculating the pressure drop. Actual debris beds formed in a nuclear plant following a LOCA may not possess these standard characteristics; however, a calculational method can address only known, specified debris bed conditions. Variations from non-standard bed conditions may be handled using probability techniques. The five NUKON and CalSil debris bed formation criteria for the debris beds generated and tested at PNNL are listed below:

1. Material should form a complete debris bed on the specified metal screen or perforated plate.
2. Debris beds should be uniformly thick and internally as homogeneous as possible in the radial direction.
3. Uniform debris beds should be formed over the range of debris loadings specified by the NRC proposed test matrix (NRC 2005).
4. The debris beds generated for a given composition and target debris loading should yield repeatable physical and performance characteristics.
5. The debris beds should meet NRC specifications for debris bed composition and criteria for head loss measurements (e.g., formed at specified bed formation velocity and temperature).

3.1.2 NUKON Slurry Target Characteristics

The target NUKON slurry characteristics provided by investigators from previous related work (Shaffer et al. 2005) were approximately defined by specifying the slurry preparation conditions. These slurry preparation conditions were obtained through personal communications with previous investigators such as B.C. Letellier of LANL. The NUKON slurry preparation was performed using vendor-supplied NUKON material. G. Hunter of Performance Contracting Inc., the supplier of NUKON, stated that the preparation of the shredded NUKON was achieved by passing NUKON “blankets” through a commercially available wood chipper. Mr. Hunter stated that shredded NUKON previously supplied to investigators had been created by passing the blankets through a leaf shredder.

The preparation of the shredded NUKON was defined by previous LANL investigators as follows: 25 g of shredded NUKON and 1,000 mL of water were added to a Black and Decker blender (550W BL6000) operated at the “middle” setting for 10 minutes.

To establish baseline characteristics, PNNL prepared a slurry consisting of 25 g of wood-chipper-shredded NUKON and 1,000 mL of water in a Waring commercial blender (model 31BL41, 840 W) operated for 10 minutes on the “low” setting. The slurry was poured through an 8-in.-diameter 5-mesh screen. The material retained on the screen as well as the collected material that passed through the screen were dried and weighed separately. The required blender preparation time and NUKON mass/water volumes were subsequently evaluated.

The results of the preliminary NUKON slurry preparation tests are presented in Table 3.1. In this table, as well as in all subsequently presented results of Section 3, the practice of maintaining the significant digits in numerical values is not followed.

Table 3.1. Preliminary NUKON Slurry Preparation Tests

Test	Initial NUKON Mass (g)	Water Vol. (mL)	Prep. Time (min)	Blender Speed	Dried NUKON on Screen (g)	Dried NUKON Through Screen (g)	R1	R2	R3
NS2	25	1000	10	low	18.03	4.83	0.72	0.19	0.27
NS3	25	1000	3	low	18.64	4.69	0.75	0.19	0.25
NS4	12.5	500	10	low	7.72	3.4	0.62	0.27	0.44
NS5	12.5	500	3	low	8.99	1.86	0.72	0.15	0.21
NS6	12.5	500	3	high	8.82	2.8	0.71	0.22	0.32

Test NS2 used the same debris concentration, water volume, and blender time in an attempt to mimic, as closely as possible, the NUKON slurry preparation definition provided by LANL investigators, and replicate the baseline test.

Although no metrics were provided from the previous work for characterizing the prepared debris material, the current results were quantified by measuring the mass after drying of both the NUKON on the screen and the mass that passed through the 5-mesh screen. Visual observations showed that test NS2 produced an apparent homogenous slurry with no clumps. It was expected that a homogeneous slurry would support Criterion 2 from Section 3.1.1. The measured quantities were related to the initial NUKON mass of the test as well as to each other by computing the following ratios:

$$R1 = \frac{\text{dried NUKON mass on screen}}{\text{initial NUKON mass}} \quad (3.1)$$

$$R2 = \frac{\text{dried NUKON mass through screen}}{\text{initial NUKON mass}} \quad (3.2)$$

and

$$R3 = \frac{\text{dried NUKON mass through screen}}{\text{dried NUKON mass on screen}} \quad (3.3)$$

Before drying, liquid was decanted from the material that had passed through the screen. Thus, the sum of defined parameters R1 and R2 may yield results less than unity due to the loss of suspended fines with the decanted liquid.

Following test NS2, test NS3 was conducted to determine whether shorter preparation times could achieve similar results. It was determined by a comparison of the computed mass ratios in Table 3.1 that the shorter preparation time produced similar slurry and consequently also matched baseline conditions.

The range of debris loadings specified by the proposed test matrix dictated that a lower NUKON mass would be needed. Therefore, test NS4 evaluated the effect of a lower initial NUKON mass. (A secondary consideration for evaluating a reduced amount of slurry was the working capacity [volume] of the blender). A 10-minute blender-operation time (referred to as preparation time) was used, and the ratio of the initial NUKON mass to the water volume was held constant. A lower R1 with higher R2 and R3 values, neglecting the possible loss of fines, indicated that more material passed through the screen; the slurry had changed characteristics (more fines were possibly produced). It was therefore determined that the preparation time was too long to replicate the baseline results, and a reduced preparation time (same as for test NS3) was evaluated in test NS5.

Although metric results similar to the baseline test NS2 were achieved with test NS5, it was determined from R2 and R3 (again neglecting possible decanted fines) that the amount of NUKON that passed through the screen was low (possibly fewer fines were produced), and the “high” preparation speed in the blender was thus considered for test NS6. Metric results for NS6 were determined to be reasonably similar to those for baseline test NS2. The procedure to produce the slurry of test NS6 was therefore chosen as the preliminary procedure to evaluate the potential to achieve Criteria 1 through 5 listed in Section 3.1.1. In subsequent tests in the benchtop loop, this preparation procedure was indeed shown to form and produce uniform debris beds on a 5-mesh screen. Thus, 12.5 g of NUKON and 500 mL of water prepared for 3 minutes on “high” in a Waring commercial blender (model 31BL41) was selected as the baseline slurry to be evaluated in the benchtop loop.

To facilitate slurry preparation and development, a simple metric was developed to relate the slurry preparation to that of test NS6. The metric used wet conditions, relating the NUKON and water mass retained on an 8-in.-diameter 5-mesh screen immediately after the slurry was poured through the screen to the initial dry NUKON mass or

$$R4 = \frac{\text{NUKON and water mass on screen}}{\text{initial NUKON mass}} \quad (3.4)$$

Excess water was removed from the screen before the mass was measured by tapping the screen five times on the rim of the collection container, rotating it 90° counter-clockwise, and then tapping five more times. When pouring the slurry through the 5-mesh screen, care was taken to ensure that the operator continually moved the pour across the screen such that the material was continually poured onto an unused (clean) portion of the screen. After the bulk of the slurry was poured out, sufficient water was added to the blender (on the order of 100 mL) to flush all of the debris material out and through the screen. The R4 procedure is presented in detail in Appendix E.

The value of R4 was determined for the Test NS6 NUKON slurry preparation to establish a baseline criterion. The conditions of Test NS6 were reproduced two times, resulting in R4 values of 11.8 and 10.6. The specifics for these tests are reported in Table 3.2.

Table 3.2. NUKON Slurry Preparation Test NS6 R4 Results

Condition/Debris Loading (g/m²)	Initial NUKON Mass (g)	Water Volume (mL)	Prep. Time (min)	Blender Speed Setting	Mass of NUKON and Water on Screen (g)	R4
Baseline	12.5	500	3	high	147.11	11.8
Test NS6	12.5	500	3	high	132.66	10.6

3.1.3 CalSil Slurry Target Characteristics

As with the NUKON characteristics (Section 3.1.2), the target CalSil slurry characteristics for previous related work (Shaffer et al. 2005) were approximately defined by specifying the slurry preparation conditions obtained through personnel communication with previous investigators such as B.C. Letellier of LANL. The CalSil debris preparation procedure was defined as using a mortar and pestle to completely disassociate the particulate CalSil from the fibrous binder material.

The simple R4 metric developed for the NUKON slurry preparation (Eq. (4)) was used to provide a rapid means of approximate quantification of the CalSil slurry preparation. Visual observation of the prepared CalSil material was also made such that it appeared to be relatively homogenous with no clumps. The disassociated fibrous material was visually observable. As with NUKON, homogeneity was expected to support Criterion 2 from Section 3.1.1.

To establish a baseline criterion, an R4 value was determined for CalSil material that was first disassociated by using a mortar and pestle and then wetted. Particle size distribution (PSD) analyses were subsequently conducted on the debris after being further fragmented in a blender. Evaluations of the effects of CalSil debris preparation techniques have also been made using various sieves. The baseline preparation conditions as well as results from the additional analyses are presented in Section 3.2.2.

3.2 Target Characteristics and Formation Criterion Testing

NUKON and CalSil materials were prepared to meet the target characteristics defined in Section 3.1. These prepared materials were then evaluated in regards to meeting the five criteria listed in Section 3.1.1. Actual debris masses for all target debris loadings presented herein correspond to the 4-in. test section of the PNNL benchtop loop. In Section 3.2.1, target characteristic testing of the NUKON slurry is discussed. CalSil debris preparation is discussed in Section 3.2.2. In Section 3.2.3, the prepared slurries are tested against the five debris bed criteria. Testing against these criteria was conducted in the PNNL benchtop loop. Note that the benchtop loop does not have the degassing capability of the PNNL large-scale loop; the quantity of gas in the test section was visually observed to vary to some degree between the test cases. The instrumentation in the benchtop loop had greater uncertainties and less resolution compared to the instrumentation of the large-scale loop. Data from the benchtop loop was recorded electronically. However, the data presented within Section 3 were obtained from manual recordings taken from the DAS screen meters.

3.2.1 NUKON Slurry Preparation Characteristic Testing

The test NS6 slurry R4 values were used to develop slurry preparation procedures for NUKON-only debris loadings. Relative homogeneity of the prepared NUKON debris was also confirmed by visual observation. The R4 metric is a function of the preparation time, blender and associated speed setting used, initial debris mass, and the added water volume. The initial condition of the NUKON may also impact the preparation time required to reach a specific R4 with all other parameters held constant. Additionally, the R4 metric can be shown to have a range of NUKON masses and dilution ratios in which it is most applicable. Subsection 3.2.1.1 has an explanation for this phenomenon.

3.2.1.1 R4 Metric Applicability

The 5-mesh screen used for the NUKON slurry R4 tests was 8 in. in diameter, which allowed for all of the slurry (within the 1-L blender operational limit) to be poured through an unused (clean) portion of the screen, as specified in Section 3.1, with no overflow (such that no liquid or slurry flowed beyond the edge of the screen). The mass of the material retained on the screen is

$$m_{SM} = \text{NUKON} + \text{water retained in NUKON} + \text{water retained on screen} \quad (3.5)$$

For a constant water volume, it may be expected from Eq. (3.5) that slurries with different R4 values and NUKON masses may in fact have similar slurry characteristics. The reverse may also be true because the water retained on screen will have a comparatively more significant effect on the R4 ratio for lower NUKON masses. Tests were thus conducted to evaluate this effect. Four cases were considered:

1. Constant water volume (800 mL) with no blender operation
2. Constant dilution ratio of 0.025 g/mL (NUKON mass per water volume) with no blender operation
3. Constant dilution ratio of 0.015 g/mL with no blender operation
4. Constant water volume (800 mL) with 1-minute preparation time.

Within the relative grossness of the R4 metric itself, the test case results presented in Figure 3.1 suggest that the effects of the mass of the “water retained on the screen” are reduced for tests with at least approximately 10 g of NUKON (see subsection 3.2.1.2.1 regarding R4 variability for repeated tests). Thus, a rough applicability range of the R4 metric can be defined such that the NUKON mass should be greater than 10 g. The R1, R2, and R3 metrics are not affected by water retained on the screen. They do, however, require extended evaluation times to obtain dry masses.

The R4 data shown in Figure 3.1 may also be considered in terms of the dilution ratio (grams of NUKON per mL of water). For Cases 1 and 4, with a constant water volume of 800 mL, the possible limit of 10 g translates to approximately a 0.01 g/mL dilution ratio, suggesting that the water retained on screen dominates at lower dilution. However, from Figure 3.1, R4 may also be observed to approach a relatively constant value only after the mass is increased for the constant dilution ratio tests (Cases 2 and 3). Therefore, for the evaluated R4 tests, it appears that both the mass of the NUKON and the dilution ratio provide similar applicability limits; nominally greater than 10 g and 0.01 g/mL, respectively. For dilution ratios on the order of 0.01 g/mL and lower and the 1 L capacity of the blenders, the mass of the NUKON is the critical parameter.

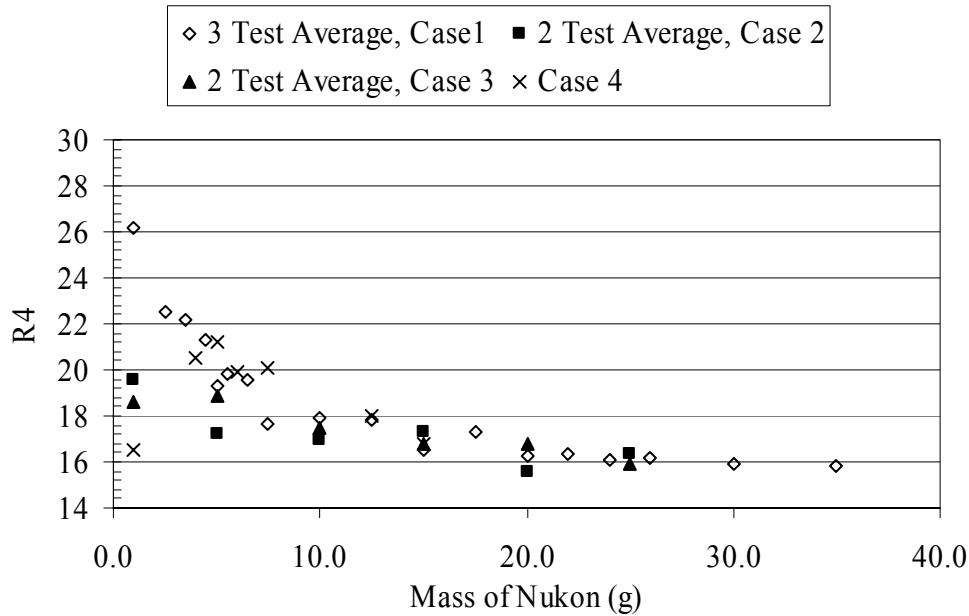


Figure 3.1. R4 as a Function of NUKON Mass

The proposed test matrix specified that NUKON be prepared in quantities less than 10 g (NRC 2005). Therefore, with the possible 10-g applicability limit, it may be suggested that (1) the R4 metric is not useful or (2) the effect of NUKON mass on the R4 value as indicated by Figure 3.1 should be accounted for in the slurry preparation determination. However, the intent of the metric is to provide a rapid, simple, and repeatable means whereby slurry that meets the five debris bed criteria in Section 3.1.1 may be produced. Therefore, although the water retained on the screen issue presented by Eq. (3.5) is acknowledged, reliance is placed on the slurry characteristic testing for debris bed formation (see Section 3.2.3), and the indicated R4 metric applicability range is ignored in light of this testing.

3.2.1.2 Effect of Preparation Conditions on the R4 Metric

The R4 metric has been shown to be a function of the blender preparation time, water volume added, debris mass (see subsection 3.2.1.1), and blender and associated operating speed used. Thus, slurry preparation for the target R4 value should be evaluated for each new condition (including different blenders of the same make and model or for a blender that may have aged due to use).

3.2.1.2.1 Preparation Time (Blender Operation Time)

Figure 3.2 illustrates R4 as a function of blender preparation time for a debris loading of 1449.5 g/m² (corresponding to 11.75 g of NUKON in the PNNL benchtop loop) with 470 mL of water in a Waring commercial blender (model 31BL41) operated on the high setting. For the cases evaluated, R4 decreases with increases in the preparation time (see Figure 3.2).

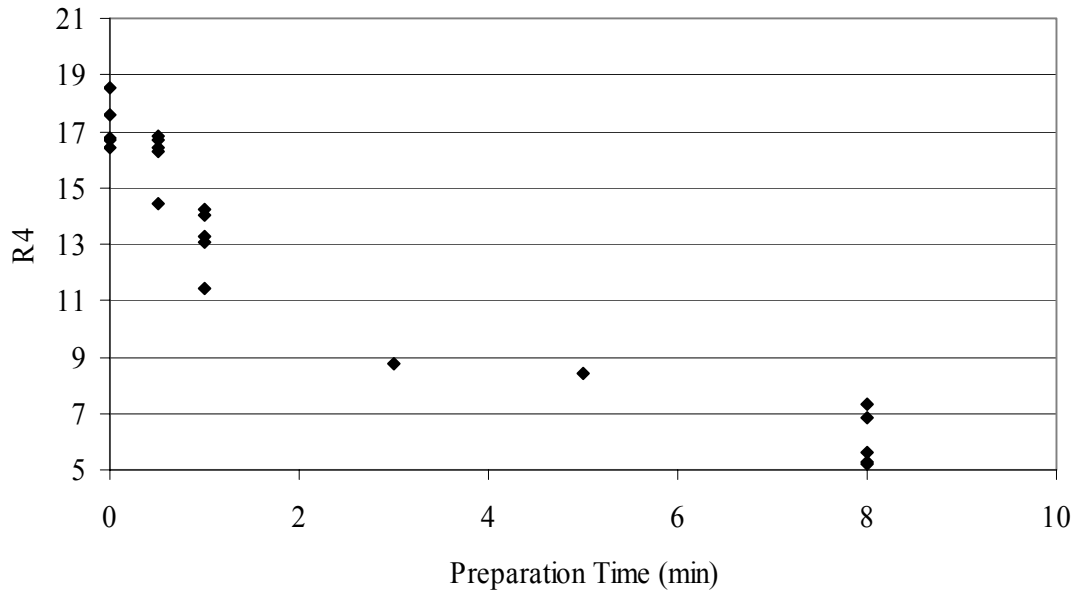


Figure 3.2. R4 as a Function of Blender Preparation Time for Constant 1449.5 g/m² Target Debris Loading

The repeatability of the tests depicted in Figure 3.2, as determined by the standard deviation, is similar for all the tests (see Table 3.3). Distinction between the R4 values as a function of blender preparation time is also apparent. For the tested conditions, the only overlap for maximum and minimum values is between the 0- and 0.5-minute preparation times. Given the visually observable difference in the NUKON slurry (see Sections 3.2.3.1 and 3.2.3.3), this apparent overlap is not considered to render these slurries similar in terms of the debris bed criteria listed in Section 3.1.1. The NUKON slurry with no blender preparation is primarily made up of up to 1-in.³ chunks or clumps of NUKON fiber, while the NUKON slurry with 0.5-minute blender preparation time has no chunks larger than about 0.25 in.³. Relatively long fibers are apparent in the former. This indicates that the blenders may be chopping (reducing in size) some of the fiber as well as separating the fibers (disassociation).

Table 3.3. Repeatability of R4 Values with Different Preparation Times

Statistical Properties for Sets of Repeated Tests	Blender Preparation Time (min)			
	0	0.5	1	8
Median	16.78	16.39	13.26	5.63
Average	17.20	16.14	13.19	6.04
Maximum	18.57	16.81	14.24	7.33
Minimum	16.41	14.45	11.41	5.18
Standard Deviation	0.88	0.97	1.11	0.97
Data Points	5	5	5	5

The apparent distinction of R4 with blender preparation time was confirmed by analyzing R1 (see Eq. 3.1 in Section 3.1.2) for three distinct nominal R4 values. A distinction in the R4 values is also apparent in the R1 values for the non-boiled and boiled tests (see below), Table 3.4.

Previous investigations of NUKON debris bed head loss (Shaffer et al. 2005) have prepared the debris by boiling it for 10 to 15 minutes before introducing it to the loop. Other researchers have subjected the debris material to a presoak, which consists of soaking the material in 140°F water for 30 minutes before placing it into the loop. The 30-minute presoak is intended to simulate the approximately 30-minute delay between the occurrence of a LOCA and the start of the circulation pump. The soaking of NUKON material in the water at an elevated temperature is predicted to affect the characteristics of the NUKON's binder. PNNL investigated the effect of boiling the NUKON material both before and after blender preparation to determine if this would affect R4 results. The target debris loading tested was 1681.4 g/m², and the NUKON material was boiled for 10 minutes.

Testing was conducted to repeat the middle of the three blender preparation times (median R4 of 10.6) of the non-boiled tests shown in Table 3.4. In Table 3.4, BPP denotes boiling the as-received material for 10 minutes, oven drying at 194°F (90°C) until constant mass was reached (within the accuracy of the scale), resaturating it, and then blender preparing it for the R4 tests. Boiled after preparation (BAP) means that the material was first prepared in the blender, boiled for 10 minutes, and then the R4 test was conducted immediately. The variability of the R4 values between the boiled and non-boiled tests does not exceed that typical of repeated R4 tests (Tables 3.3 and 3.4), although a trend of lower R4 values may be indicated from non-boiled to BAP to BPP. The apparent opposite trend in R1 values from non-boiled to BAP may suggest that more water was retained on the screen (Eq. 3.5) for the non-boiled test (lower R1 values indicate less NUKON mass is retained on the screen (Eq. 3.1).

Table 3.4. Distinction in R4 and R1 Values and Boiling Effect (1681.4 g/m² target debris loading)

Test ID (blender prep. time in minutes, boiling distinction)	R4	R1
0.25	14.34	N/A ^(a)
0.25	14.82	N/A
0.25	14.20	0.88
0.25	13.96	0.89
0.75	10.02	N/A
0.75	11.10	N/A
0.75	10.68	0.76
0.75	10.59	0.75
0.75, BPP ^(b)	8.63	N/A
0.75, BPP	9.26	N/A
0.75, BPP	8.10	N/A
0.75, BAP ^(c)	9.73	0.77
0.75, BAP	10.15	0.81
0.75, BAP	9.85	0.79
1.75	6.85	N/A
1.75	6.01	N/A
1.75	7.15	0.62
1.75	6.52	0.55
(a) N/A: Not available.		
(b) BPP: boiled prior to preparation.		
(c) BAP: boiled after preparation.		

However, the BAP tests were conducted by preparing the material, immediately boiling the slurry and then pouring the slurry through the screen while it was still hot. Thus it may be argued that the water mass is lost through accelerated evaporation. This argument may not be made for the BPP results, however, because the NUKON debris was first boiled and then dried prior to resaturation and preparation. Therefore, although boiling has not been demonstrated to significantly alter the R4 test results with regard to the anticipated variability, there is some indication that boiling the material may alter the prepared slurry's physical properties.

3.2.1.2.2 Water Volume for Blender Preparation

Data relating to the effect of the water volume used for blender preparation is illustrated in Figure 3.3 for a target debris loading of approximately 363 g/m^2 (corresponding to 1.76 g of NUKON in the PNNL benchtop loop). A Waring commercial blender (model 31BL41) operated on the high setting was again used. Within the variability of the R4 measurements themselves and the limited data, it appears that the R4 value decreases with increasing water volume. Also apparent from Figure 3.3 is the effect of blender preparation time on the R4 value. The results indicate that changes in the water volume and associated ratio to debris mass should be accompanied by an evaluation of the R4 metric.

3.2.1.2.3 Blender Effects

Differences in R4 values for NUKON slurries with similar debris loading (1449.5 to 1541.8 g/m^2) prepared in different blenders with the same preparation time (3 minutes) and ratio of NUKON mass to water volume (Section 3.1.2) are illustrated in Figure 3.4. Blenders 1, 2, and 4 are the same make and model, and blender 4 differs from blenders 1 and 2 only in that the blades may have been dulled due to extensive intermediate use with an alternative potentially abrasive material. Based on the observed results, consideration should be given to periodically assessing the R4 for a given slurry with continued use of a blender or if a change in blenders is made.

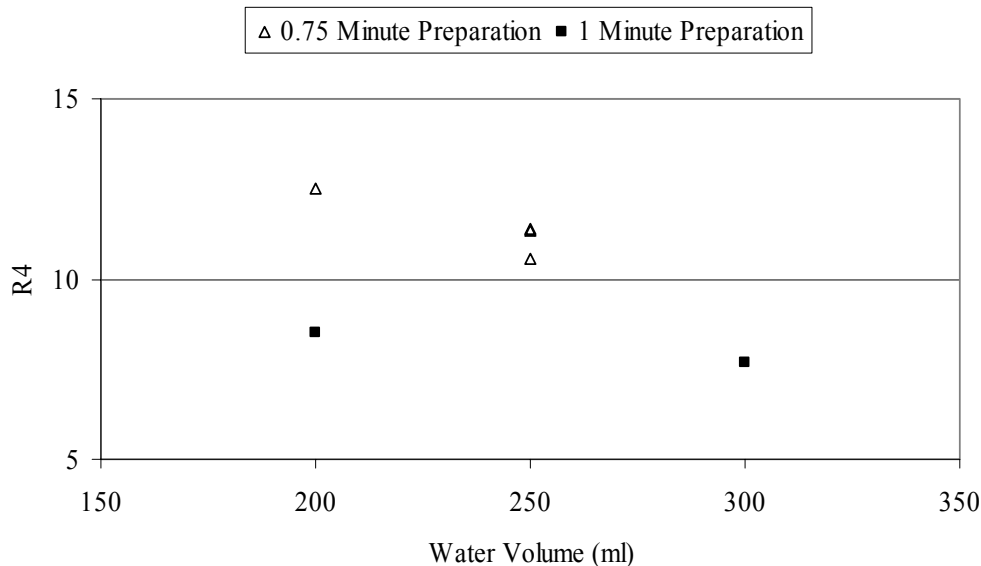


Figure 3.3. R4 as a Function of Water Volume Used for Blender Preparation for Blender Preparation Times of 0.75 and 1.0 minutes. Constant target debris loading is 363 g/m^2 (1.76 g of NUKON in the PNNL benchtop loop).

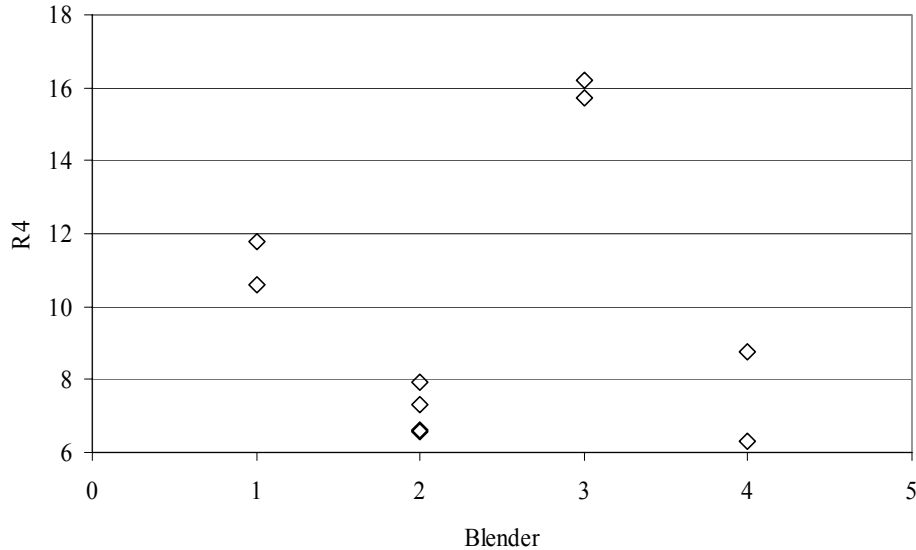


Figure 3.4. R4 as a Function of the Blender Used for Target Debris Loading of 1449.5 to 1541.8 g/m² in the Benchtop Loop (3-minute blender preparation time)

3.2.1.2.4 Visual Observation of Homogeneity

When evaluating/determining a slurry preparation technique using the R4 metric, visual observation of the slurry consistency should be considered. As described in Section 3.1.2, visual confirmation of slurry homogeneity (no clumps) may be desirable to meet the specified (Section 3.1.1) debris bed criteria. It has been observed that similar NUKON slurry R4 values from different blenders may produce slurries with different visually observable characteristics. That is, although the same amount of material is retained on a 5-mesh screen during a “pour-through” test, visual observation of the slurry condition indicates a different consistency.

The variation of R4 results with blender preparation time for a potentially altered blender is used for illustration. Before potentially dulling the blades of a specific blender, a preparation time of 0.75 minutes at “high” was used for the 1449.5 g/m² target debris loading to achieve the desired R4 value. Increasing the preparation time to 1 and 3 minutes resulted in lower R4 values, as shown in Figure 3.5. The “non-dulled” case is denoted by “Blender A” in the figure.

The variation in the R4 value with blender preparation time for the altered blender (blades were potentially dulled over time due to abrasiveness of the debris material), denoted by Blender B, is also shown in Figure 3.5. Operating Blender B for 0.75 minutes produced similar R4 values, but the response of R4 to various mixing times was different. The slurry from Blender A appeared to be uniform, while in Blender B clumps were observed for the same R4 values (approximately 10–12) until the mixing time was increased to 1.25 minutes. Visual observation of the homogeneity of the slurry should therefore be considered.

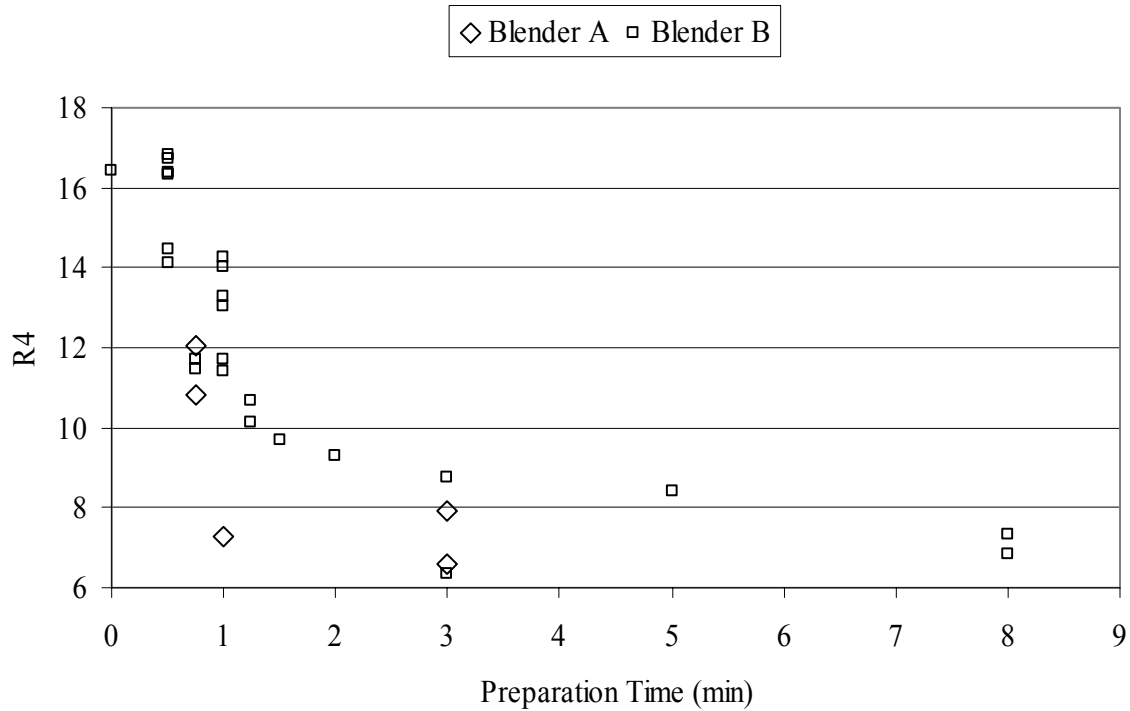


Figure 3.5. Effect of Mixing Time on R4 Values for 1449.5 g/m² NUKON Debris Loading Case

3.2.2 CalSil Slurry Preparation Characteristic Testing

The target CalSil slurry characteristics for previous related work (Shaffer et al. 2005) were approximately defined by specifying the slurry preparation conditions. The simple R4 metric developed for NUKON slurry preparation (Eq. 3.4) was used to provide a rapid means of approximate quantification of the CalSil slurry prepared by completely disassociating the particulate CalSil from the fibrous binder material using a mortar and pestle. The prepared CalSil material was also processed until visual observation showed it to be relatively homogenous with no clumps.

For initial evaluation, a relatively large target debris loading for CalSil of 725 g/m² was chosen from the proposed test matrix. For the PNNL large-scale test loop, this debris loading equates to 13.22 g. Material was separated from the as-received CalSil blocks using a saw. Irregularly shaped chunks of approximately 0.2 to 0.8 in. (5 to 20 mm) in diameter were broken off from the separated material with pliers until the desired mass was obtained.

To establish the CalSil baseline for criterion 2 (see Section 3.1.3), a mortar and pestle were used to completely disassociate the particulate from the fibrous binder material. The prepared fibrous binder and CalSil particulate were then diluted with 530 mL of water (arbitrarily chosen to match the 12.5-g debris to 500-mL water dilution ratio for the NUKON) (Section 3.1.2), and the resulting slurry was poured through an 8-in.-diameter 5-mesh screen to obtain a value of R4 (Eq. 3.4). Minimal debris was observed retained on the screen. The bulk of the retained material consisted of the fiber material added to the CalSil during manufacturing to provide structural integrity of the formed shapes (e.g., sheets, pipe shells). Particulate was held up in this fibrous material as well as on the screen mesh itself. Relatively repeatable R4 values

were achieved over three tests with a median value of 1.82. As expected from the debris preparation procedure, no clumps of particulate were observed. This visually observable relative homogeneity was used as the primary guideline for CalSil material preparation. The R4 metric, given the lack of significant quantities of debris on the screen, was used as a secondary consideration.

Testing showed that blender-prepared (no mortar and pestle preparation) CalSil with a median R4 value less than approximately 1.55 is relatively homogeneous, while CalSil slurries with R4 values greater than a median value of approximately 1.82 have clumps and chunks of undisturbed CalSil particulate. (The equivalence of the mortar-and-pestle-prepared median R4 with that of the blender-prepared median R4 with clumps and chunks was considered coincidental and not investigated further.)

Data were also taken that suggested that longer blender preparation times may alter the CalSil particulate from that expected using a mortar and pestle. CalSil material was ground with a mortar and pestle to disassociate the fibrous material from the particulate. The bulk material was then separated by sieving through a 212- μm -opening screen mesh, which was visually observed to segregate the CalSil particulate from the fiber. Three separate samples of 13.22 g from this visually inspected fiberless CalSil particulate were diluted with 530 mL of water. The first sample was the as-prepared material. The second was prepared for 0.75 minutes in a KitchenAid blender (Model No. KSB50B4) set to “Liquefy,” and the third sample was similarly prepared for 6 minutes. R4 type tests using a 150- μm sieve for the pour-through test were then conducted. The 150- μm sieve R4 results were 1.3, 0.88, and 0.37, respectively, suggesting that extended preparation times can affect the CalSil material’s properties.

PSD analyses were conducted on the prepared CalSil material using a MicroTrac S3000 particle size analyzer to determine whether this measurement method could be used to provide quantifiable insight. Instrumentation and configuration, as well as conditions such as particulate/ agglomeration shape, can affect and potentially distort PSD results. Given the presence of fibrous material in the CalSil and sampling effects, the PSD results should not be considered highly accurate. However, the PSD results provide an understanding of the relative distribution of the particle size and insight into the possible effect of varying the blender preparation time. Three cases of blender-prepared CalSil were generated for a constant mass loading with one case having a blender preparation time of 1 minute and the other two cases a preparation time of 3 minutes. The cases were evaluated to:

- Determine the effectiveness of using PSD analysis to characterize the CalSil debris
- Evaluate the repeatability of the CalSil debris preparation process
- Evaluate the distinguishability between blender preparation times.

The results are presented in Figure 3.6. There was no discernable definitive trend in the PSD-determined CalSil particulate size with preparation time (Figure 3.6) for the limited cases evaluated.¹

In practice, a minimum preparation time in the KitchenAid blender of approximately 0.5 minutes was required for 13.22 g of the as-received bulk CalSil in 530 mL of water to achieve an R4 value of

¹ Aliquots of prepared CalSil slurry were taken from the bulk sample for the preparation-time PSD analysis using a pipette. For some aliquots, the visually observed fibrous material plugged the pipette, causing the samples to be redrawn. For other aliquots, the observed fibrous material did not plug the pipette. Thus, fibrous material is present in the analyzed samples and the amount of fibrous material may not be constant from aliquot to aliquot.

nominally less than 1.55 on a 5-mesh screen and visually exhibit no chunks. The minimum preparation time was desired to reduce the potential blender effects on the particulate. CalSil slurry preparation was therefore roughly standardized by visually determining the minimum mixing time required to produce a homogeneous slurry using the maximum R4 value as a guideline.

PSD analyses were conducted for the upper and lower range of the target CalSil debris loadings specified in the proposed test matrix, 135 and 724 g/m² (Section 5.1). The blender preparation time for the CalSil debris was determined based on the criteria:

- An R4 value of nominally less than 1.55 for a 5-mesh screen
- Blender operations continued until visual observation of slurry indicated no chunks present.

The results for the two cases are plotted in Figure 3.7. While PSD by itself was not conclusive, no discernable difference was identified for the two conditions presented in Figure 3.7, indicating that the level of debris fragmentation was similar. The blender preparation time used for generating the CalSil debris associated with the data in Figure 3.7 was determined as the point at which chunks were no longer visually observed, while the blender preparation time for the CalSil used to produce the data in Figure 3.6 exceeded this time.

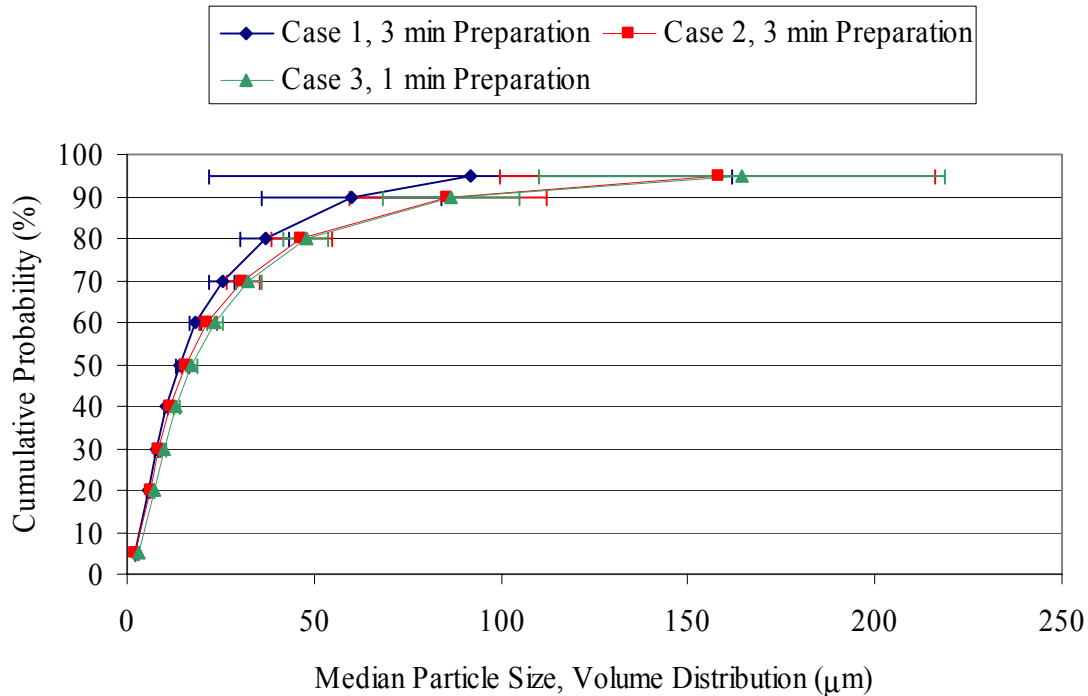


Figure 3.6. PSD Results for Blender Prepared CalSil Slurry for Blender Preparation Times of 1 and 3 minutes (median of at least 5 repeated samples; error bars indicate ±1 standard deviation; results are comparative and do not represent actual particle size)

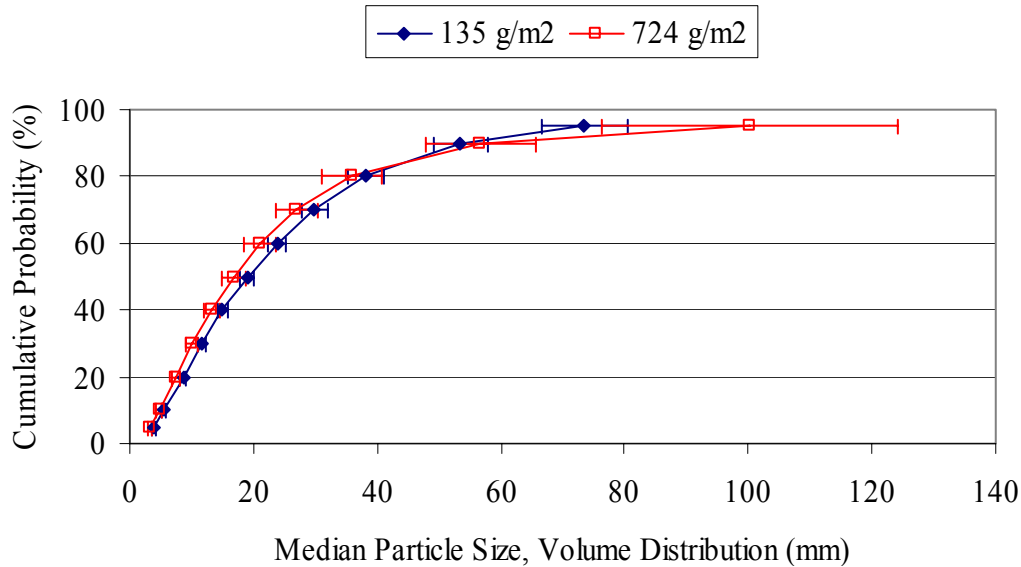


Figure 3.7. PSD Results for Blender Prepared CalSil Slurry. Blender preparation time determined from visual observation of “no chunk” condition (median of three repeated samples; error bars indicate ± 1 standard deviation; results are comparative and do not represent actual particle size)

3.2.3 Debris Bed Criteria Testing

Five specific debris bed criteria are listed in Section 3.1.1. The PNNL benchtop loop was used to determine the applicability of debris prepared to these criteria, as described in Sections 3.2.1 and 3.2.2.

3.2.3.1 Debris Bed Formation Criteria 1–3

As shown in Figure 3.8, NUKON debris prepared to the test NS6 R4 conditions (R4 ~ 11, see Table 3.2) forms a complete debris bed (Criterion 1) when introduced into the PNNL benchtop loop. When the debris preparation process is altered for the same target debris loading to produce higher R4 values, the surface uniformity is lost, as observed for debris beds in Figures 3.9 (R4 ~ 17, no blender preparation) and 3.10 (R4 ~ 16, 0.5-minute blender preparation time). Each of these debris beds had a target debris loading of 1449.5 g/m² and was formed at an initial screen approach velocity of 0.2 ft/sec. NUKON debris beds for a target debris loading of 1449.5 g/m² at R4 ~ 11 were formed at varied screen approach velocities (0.07 to 0.36 ft/sec). At a lower target debris bed loading, 107.3 g/m², the ability to form a complete debris bed (0.2 ft/sec screen approach velocity) as well as debris bed surface uniformity were lost at higher (R4 ~ 20, no blender preparation) and lower (R4 ~ 6) R4 values (Figures 3.11 and 3.12, respectively). Examples of complete uniform debris beds formed for an R4 value of approximately 11 and debris loadings of 107.3, 217.4, and 724.7 g/m² are shown in Figures 3.13 through 3.15, respectively.

Visual comparison of the NUKON debris beds shown in Figures 3.8 and 3.13–3.15 demonstrate the achievement of Criterion 1, produce a complete debris bed on the screen; Criterion 2, uniform thickness; and Criterion 3, uniform debris beds over the specified debris loading range. The NUKON debris beds shown were formed at the same nominal screen approach velocity of 0.2 ft/sec on a 5-mesh screen. Formation of these beds has been shown to be repeatable based on visual observation and debris bed height (Section 3.2.3.2).

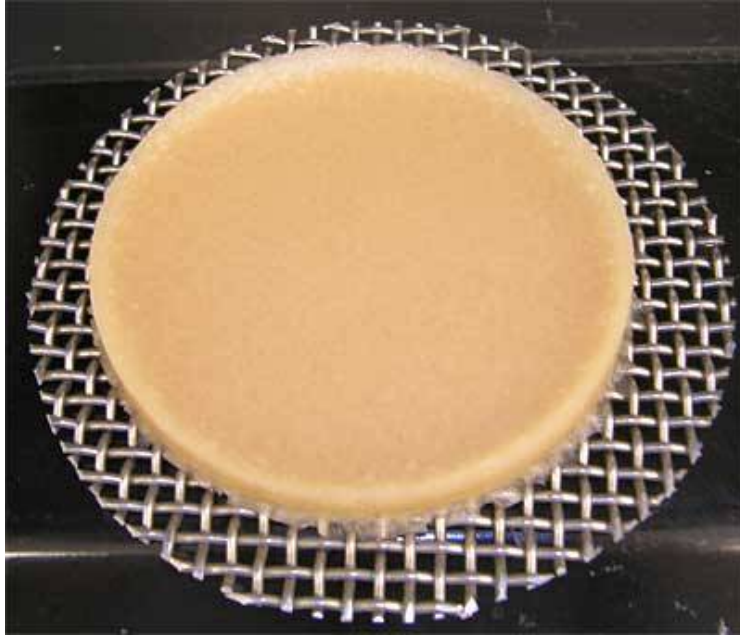


Figure 3.8. NUKON Debris Bed for 1449.5 g/m² Target Debris Loading (R4 ~ 11)



Figure 3.9. NUKON Debris Bed for 1449.5 g/m² Target Debris Loading (R4 ~ 17 as-received material/no blender preparation)



Figure 3.10. NUKON Debris Bed for 1449.5 g/m^2 Target Debris Loading (R4 ~ 16)



Figure 3.11. NUKON Debris Bed for 107.3 g/m^2 Target Debris Loading (R4 ~ 20, no blender preparation)

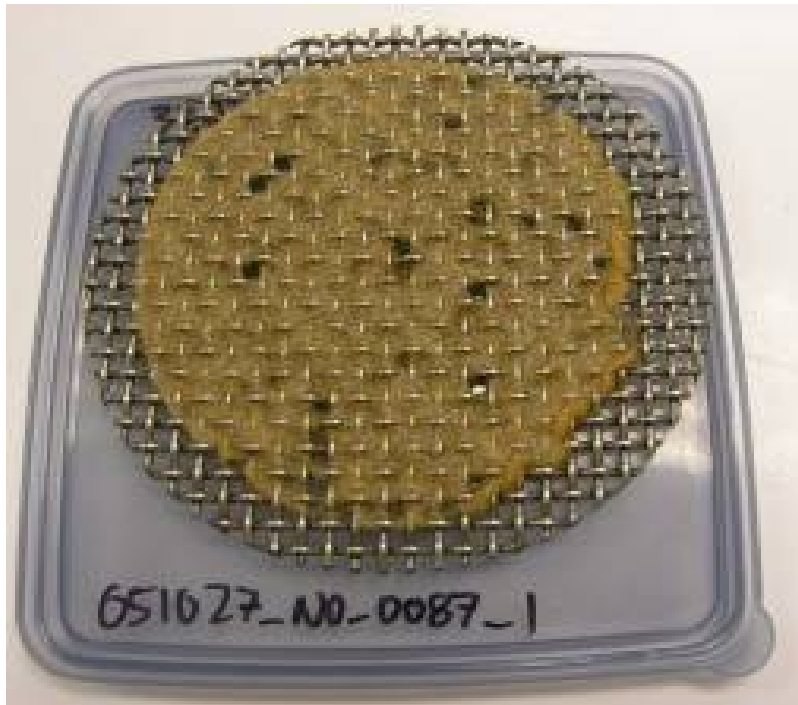


Figure 3.12. NUKON Debris Bed for 107.3 g/m^2 Target Debris Loading (R4 ~ 6)

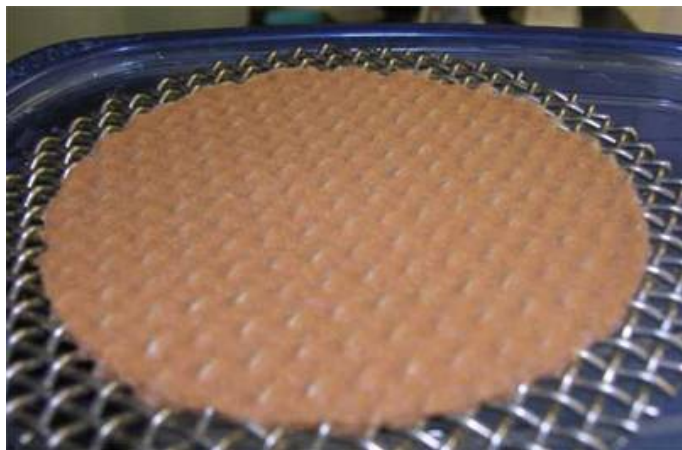


Figure 3.13. NUKON Debris Bed for 107.3 g/m^2 Target Debris Loading (R4 ~ 11)



Figure 3.14. NUKON Debris Bed for 217.4 g/m² Target Debris Loading (R4 ~ 11)

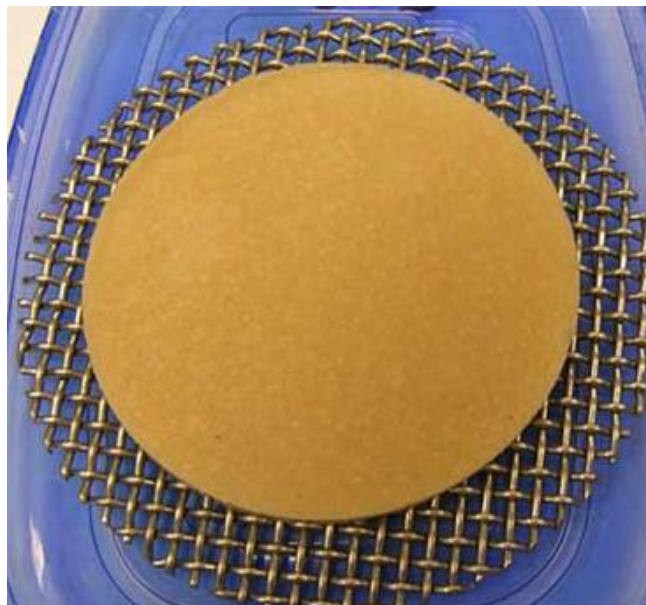


Figure 3.15. NUKON Debris Bed for 724.7 g/m² Target Debris Loading (R4 ~ 11)

The visually uniform NUKON and CalSil (referred to as NUKON/CalSil) debris bed shown in Figure 3.16 was formed at an initial screen approach velocity of 0.2 ft/sec. Uniform NUKON/CalSil debris beds were formed at screen velocities of 0.1 ft/sec as well. Additional photos of the debris beds can be seen in the “Quick Look” reports in Appendixes H through K and in the discussion of debris loading sequences in Section 6.3. The NUKON and CalSil slurries prepared to the guidelines presented in Sections 3.2.1 and 3.2.2 produced complete debris beds (Criterion 1) that were uniform in thickness (Criterion 2) over the specified debris loading range (Criterion 3). Criteria 1 through 3 were satisfied for



Figure 3.16. NUKON and CalSil Debris Bed for 1811.9 g/m² Target Debris Loading (NUKON R4 ~ 11, CalSil R4 < 1 = 1.55) (see Section 3.2.2)

both methods of debris injection; premixed (NUKON and CalSil slurries mixed together just prior to introduction into the test loop) and independent introductions (the CalSil and NUKON are introduced via separate injection lines and do not come in contact until they are in the main line of the test loop).

Investigation of the internal uniformity of debris beds (second part of Criterion 2) was made via sectioning of a limited number of the debris beds (see Section 6.5). Visual observation of the sectioned beds does not provide compelling evidence that this requirement has not been met. Observation of the sectioned beds using SEM provided a more definitive assessment with regard to this requirement than visual observation alone.

3.2.3.2 Debris Bed Formation Criterion 4

Determination of the achievement of Criterion 4 (the formed debris beds should yield repeatable physical and performance characteristics) is made by examining a representative debris bed height, surface appearance, and head loss history for debris beds of equivalent target debris loading and the same debris preparation procedure. Based on the results presented in Section 3.2.3.1, NUKON and CalSil debris slurries were prepared to achieve R4 ~ 11 and R4 ≤ 1.55, respectively (Sections 3.2.1 and 3.2.2). All debris beds formed under these preparation conditions exhibited a uniform surface appearance.

Representative retrieved NUKON debris bed heights are relatively repeatable at a target debris loading of 1449.5 g/m² (Figure 3.17). All debris beds for this evaluation were formed at an initial screen approach velocity of 0.2 ft/sec. The debris bed body measurements (plane area of the bed, not the outer rim; see Figure 3.8 for example) are inferred from a 1-mm-increment ruler placed vertically beside the debris bed. (The measured debris bed heights are referred to as representative because of the limitations of the described measurement technique. This gross technique is only employed for the benchtop evaluations and provides a qualitative means of comparison.) The reported debris bed heights are taken post-retrieval and thus represent no-flow conditions. Different methodologies were employed for obtaining the heights of debris beds formed in the large-scale test loop.

The observable variations in the approximate heights are deemed appropriate for the different time at flow (the debris beds were subjected to varying numbers of circulations, 4 to 103), as evidenced by the recovery fraction. The recovery fraction shown in Figure 3.17 for target NUKON debris loading of 1449.5 g/m² is computed from the dry retrieved debris bed mass divided by the initial mass added to achieve the target debris loading. The observed debris bed height variation is deemed reasonable given the measurement technique. Aside from a single outlier, similar variation is observed for NUKON/CalSiI debris beds formed with a target debris loading of 1811.9 g/m². In summary, the physical characteristics of the debris bed thickness and uniform surface appearance indicate that relatively repeatable debris beds have been produced.

The performance characteristics of debris beds formed from the specified debris preparations were shown to be repeatable as judged by their head loss history. An example comparison is provided in Figure 3.18. The head-loss history is taken from tests of two NUKON debris beds (1681.4 g/m² target debris loading) that included incremental cycling of the screen approach velocity. Only the first ramp up from each case is shown for approximately equivalent screen approach velocities (i.e., not all of the test data are plotted). The median difference in head loss was 12%. Additional comparison of the repeatable performance of debris beds was made in the PNNL large-scale loop, resulting in a median difference of 2% for the head

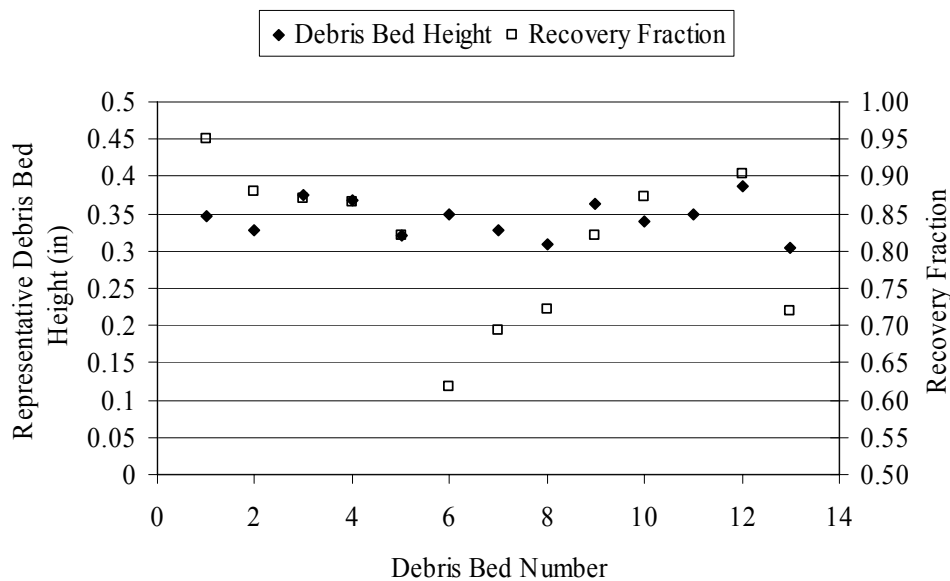


Figure 3.17. Representative Debris Bed Heights and Recovery Fraction (1449.5 g/m² target NUKON debris loading)

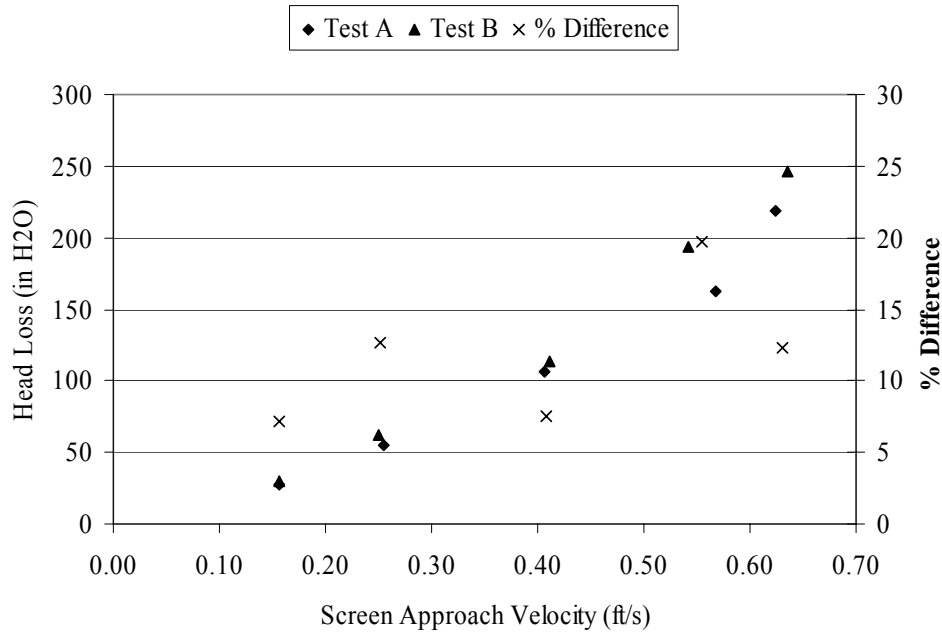


Figure 3.18. NUKON Debris Bed Head Loss as Function of Screen Approach Velocity (1681.4 g/m² target NUKON debris loading)

loss measured during the first ramp up. Reasonably comparable results were achieved for the same target debris loading in the benchtop and large-scale PNNL test loops (refer to Quick Look report for PNNL Test 060125_NO_3067_L1 in Appendix H).

The repeatability of the measured head loss as a function of screen approach velocity has been investigated for NUKON/CalSil debris beds generated with the debris prepared as specified. Test results indicate the head loss was strongly affected by the debris loading sequence (i.e., the order in which NUKON and CalSil debris was introduced into the test loop), but carefully controlled similar loading sequences yielded relatively repeatable results (refer to Section 6.3).

3.2.3.3 Debris Bed Formation Criterion 5

Tests have shown that the debris preparation procedure can affect the measured head loss. At a target debris loading of 1681.4 g/m², the measured head loss can be doubled depending on the slurry preparation procedure. For the NUKON-only tests depicted in Figure 3.19, the R4 values were approximately 18.6 (no blender preparation) and 10.4. Only the ramp up portions of the tests are shown. The percent difference is computed from the subsequent data pairs, neglecting the apparent screen approach velocity differences; the percent difference is plotted at the pair-averaged screen approach velocity.

At the average debris bed formation velocity, the NUKON debris bed (R4~10.4) had a head loss that was approximately 13% larger than that of the debris bed formed with NUKON with no blender preparation (R4~18.6). A nominal 50% increase in screen approach velocity raised the difference to approximately 28%. The maximum difference observed was almost 60%, corresponding to the maximum tested screen approach velocities for each case (these peak velocities were different, as shown in Figure 3.19). The initial debris bed formation velocity was the same, but the actual screen approach velocity after introducing the NUKON slurry into the loop varied, as depicted in Figure 3.19.

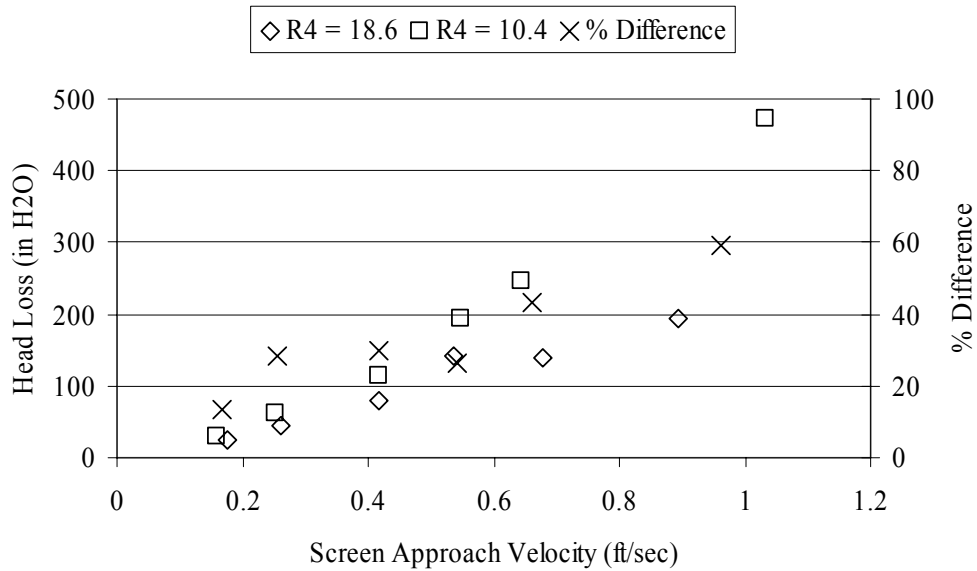


Figure 3.19. Approximate NUKON Debris Bed Head Loss as a Function of Slurry Preparation (target debris loading of 1681.4 g/m²)

When evaluating Criterion 5, it is important to consider Criteria 1 through 3 as well. If the NUKON slurry is not prepared in a blender, debris bed surface uniformity is markedly reduced (see, for example, Figure 3.9).

Based on the apparent variance in debris bed head loss associated with the slurry preparation procedure presented above, further tests were conducted in which the R4 value for the debris preparation was varied. As suggested in Section 3.1.2, it may be expected that NUKON slurry with no blender preparation will have the highest R4 value, and that successively longer blender preparation times will yield lower R4 values as the debris is disassociated or ground to a finer state. It may also be expected that nonuniform clumping of NUKON in a debris bed will result in a reduced head loss for a given debris loading and flow compared with a uniformly packed debris bed. However, excessively long blender preparation time may produce debris with characteristics insufficient to form a debris bed with significant flow resistance, resulting in a low head loss. Thus, the function relating head loss to R4 can be expected to have a maximum at some intermediate R4 value.

To establish the repeatability of producing debris batches with the same R4 value, multiple debris preparation tests were conducted by different researchers at varied blender preparation times. Tests were conducted with debris masses corresponding to target debris bed loadings of 107.3 and 1449.5 g/m² in the benchtop loop (4-in. diameter), which bound the proposed test matrix. The resulting R4 values are presented in Table 3.5. R4 decreases with increasing blender preparation time, as can be observed in Figure 3.2.

The debris bed head loss at various screen approach velocities for NUKON slurries prepared to match the R4 values of Table 3.5 are shown in Figure 3.20 and 3.21 for target debris bed loadings of 107.3 g/m² and 1449.5 g/m², respectively. At the lower target debris loading, the R4A1 and R4D1 slurries did not produce complete debris beds (see Figures 3.11 and 3.12). The R4C1 debris beds developed ruptures (channeling) as the screen approach velocity exceeded 0.6 ft/sec (0.2 m/s). The ruptures occurred as gas

Table 3.5. Criterion 4 Testing NUKON Preparation

Debris Loading (g/m ²)	Parameters	NUKON Preparation			
		R4A1	R4B1	R4C1	R4D1
107.3	Slurry Name	R4A1	R4B1	R4C1	R4D1
	Preparation Time (min)	0	0.75	1.5	2
	Median R4	20.3	14.5	8.6	5.9
1449.5	Slurry Name	R4A2	R4B2	R4C2	R4D2
	Preparation Time (min)	0	0.5	1	8
	Median R4	16.8	16.4	13.3	5.6

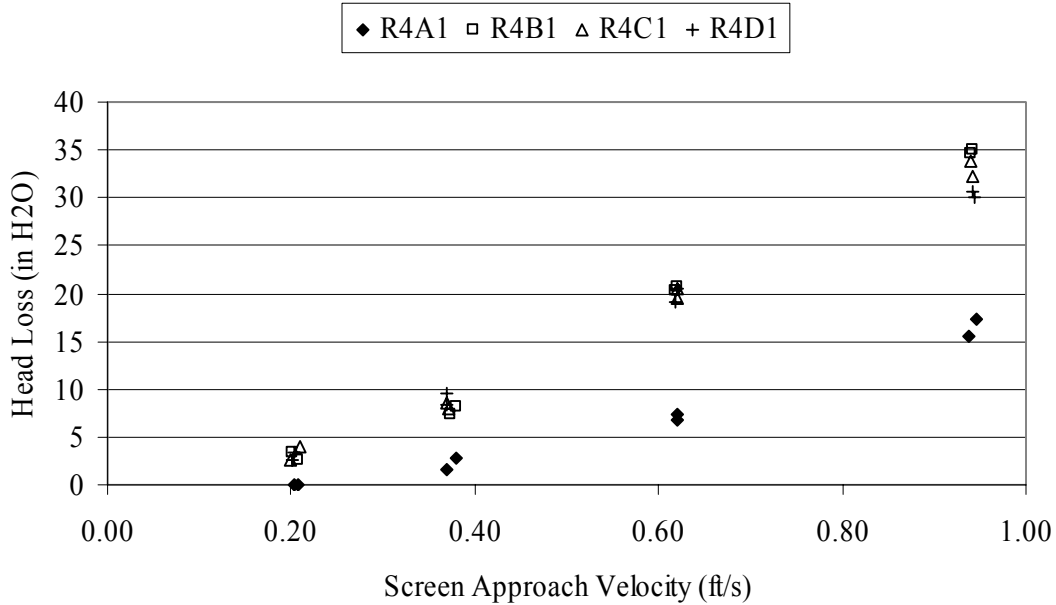


Figure 3.20. NUKON Debris Bed Head Loss as a Function of Screen Approach Velocity (R4 values from Table 3.5; target debris loading of 107.3 g/m²)

came out of solution and bubbles were formed on and around the debris bed and opened less than approximately 5% of the screen area to flow based on visual observation.

Regardless of the ruptures observed in the R4C1 beds, for each debris loading, the data indicate that the head loss at each screen approach velocity tested is at a minimum for R4A, and at higher velocities appears to peak for values of R4 with less blender preparation time than R4D. A clearer quantitative comparison of the effect of R4 on the debris bed head loss can be made by evaluating a loss coefficient for the debris bed. The head loss produced by the debris bed can be expressed by

$$\Delta H = K \frac{\rho V^2}{2} \quad (3.6)$$

where K is the loss coefficient for the debris bed, ρ is the fluid (water) density, and V is the screen approach velocity. With the data from Figures 3.20 and 3.21, the loss coefficient may be expressed as

$$\frac{K\rho}{2} = \frac{\Delta H}{V^2} \quad (3.7)$$

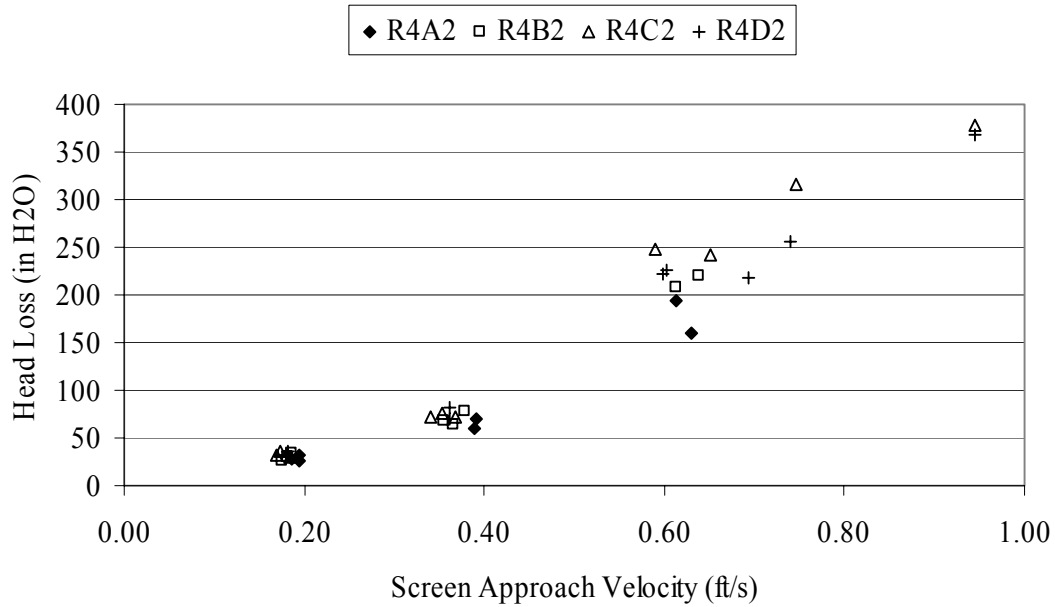


Figure 3.21. NUKON Debris Bed Head Loss as a Function of Screen Approach Velocity (R4 values from Table 3.5; target debris loading of 1449.5 g/m²)

The loss coefficients (from Eq. 3.7 including ρ and $1/2$) for the debris beds of Figures 3.20 and 3.21 are plotted as a function of the screen approach velocity in Figures 3.22 and 3.23. The apparent variation of K with the screen approach velocity is briefly addressed. The indicated transition or decrease from high to low K with increasing screen approach velocity apparent in Figures 3.22 and 3.23 is most likely the result of the potential transition of the flow regime upstream of the debris bed relative to laminar/transitional/fully turbulent flow (Reynolds number dependent) and compression of the debris bed with changes in the screen approach velocity. Another potential factor affecting the loss coefficient with changes in screen approach velocity is the transition of flow regime occurring at the debris bed surface, assuming predominantly laminar flow through the pores in the debris bed.

The increase of K with increasing screen approach velocity for the no-blender preparation cases at 107.3 g/m² (R4A1 in Figure 3.22) may be due to the incomplete coverage of the debris bed (see example in Figure 3.11), which allows for a redistribution of the flow through open areas with increasing velocity. The longer fibers and clumped material associated with NUKON debris having no blender preparation may form debris beds with relatively high porosity that undergo a greater degree of compression than the blender prepared material, which could also increase the resistance of flow at higher velocities.

Based on the results observed in Figure 3.23, it is arguably evident that the highest K value (i.e., the highest head loss) was achieved for the debris beds with R4C (for the approach velocities tested). Regardless, in conjunction with achieving Criterion 5 (which at the time the debris preparation process was being developed was assumed to include the maximum head loss), Criteria 1–4 should also be met, as is addressed below.

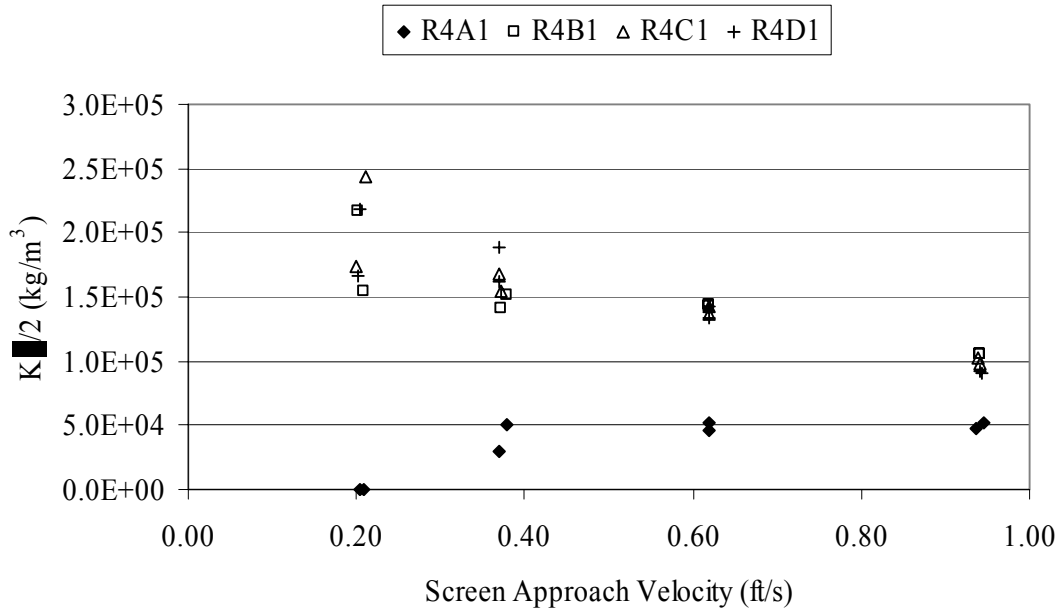


Figure 3.22. NUKON Debris Bed Loss Coefficients as Functions of the Screen Approach Velocity (R4 values from Table 5; target debris loading of 107.3 g/m²)

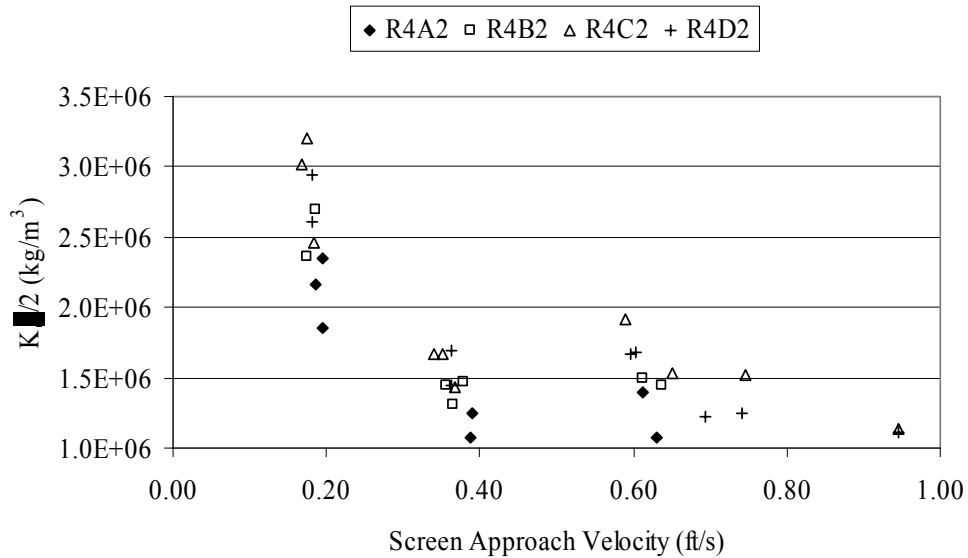


Figure 3.23. NUKON Debris Bed Loss Coefficients as Functions of the Screen Approach Velocity (R4 values from Table 3.5; target debris loading of 1449.5 g/m²)

First, however, consider the target debris loading 1449.5 g/m² results with regard to potential contributors other than debris preparation to the apparent head loss differences and whether the differences are due to actual differences in the formed debris bed or to a reduction of actual debris loading of the debris bed. That is, for a given preparation, less mass on a debris bed would be expected to result in a lower measured head loss.

The calculated fraction of the NUKON mass added to the test loop that was retained in selected debris beds is presented in Figure 3.24. The calculated mass fraction trend from R4A to R4C is the opposite of that for head loss. The decrease in the calculated mass fraction from a median of 0.97 to a median of 0.96 for R4C and R4D, respectively, is essentially negligible. These results suggest that the difference in head loss is predominantly due to the different NUKON preparation procedures, which changed the structure of the debris beds.

The Test Set labels in Figure 3.24 refer to the order in which the tests were performed. They are important because the debris beds from Test Sets 2 and 3 were tested for longer durations and at higher flow rates. Thus, the increase in retention of debris on the screen over Test Set 1 is expected. Ideally the ratio of the dry retrieved debris mass to the initial debris mass should not exceed a value of 1.0. However, in practice (Cases for R4A2 in Figure 3.24) some contamination from residual construction materials (e.g., pipe dope) was experienced during early tests in the benchtop loop.

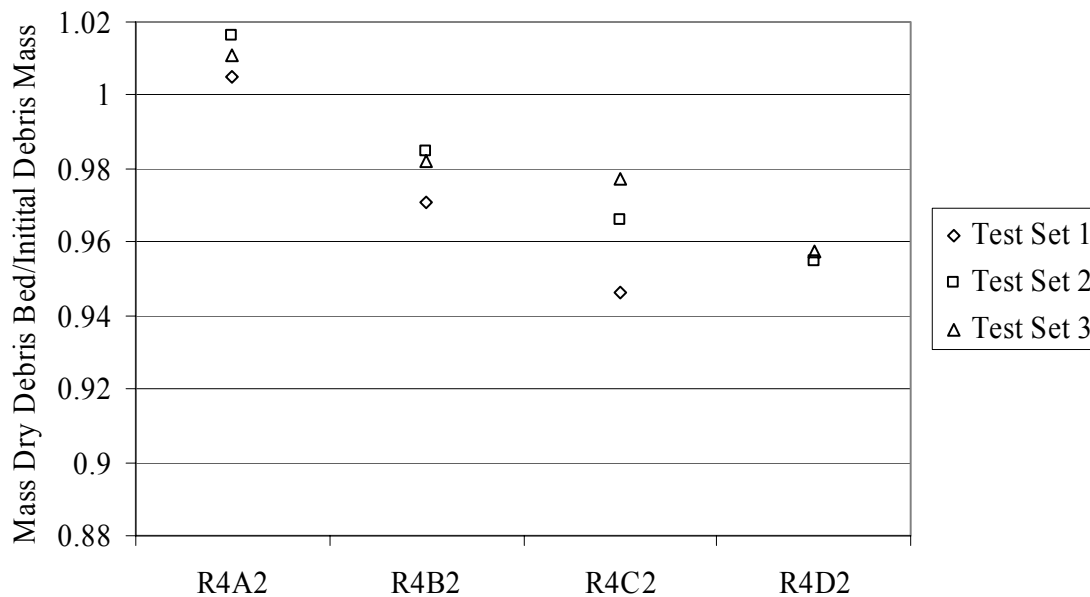


Figure 3.24. Fraction of Initial NUKON Mass Retained in Debris Bed as a Function of R4 (target debris loading of 1449.5 g/m²)

The negligible decrease in the retained mass fraction of initial NUKON on the debris bed from R4C2 to R4D2 is briefly compared in terms of expected head loss using the NUREG/CR-6224 (Zigler et al. 1995) correlation. Based on the correlation, a 1% decrease in fiber mass results in a 1% decrease in head loss at a screen approach velocity of approximately 0.95 ft/sec (0.29 m/s). Considering the retrieved debris bed mass, the data from Figures 3.21 and 3.24 for R4C and R4D at 0.95 ft/sec (0.29 m/s) indicate that a 1% reduction in mass (0.97 to 0.96) results in a 3% decrease in head loss (379 to 368 in. H₂O) that is not fully accounted for by the correlation. The results of the correlation suggest that the approximately 3% decrease in head loss from R4C2 to R4D2, as observed in Figure 3.21, is due predominantly to differences in the slurry preparation and not to a reduction in the debris-bed mass loading.

In Figures 3.11 and 3.12, Criterion 1 was not satisfied for R4A2 and R4D2 (target debris loading of 107.3 g/m²). Debris bed formation was not an issue for the 1449.5 g/m² target debris loading in Figures 3.9 and 3.25 (R4A2), 3.10 (R4B2), 3.26 (R4C2), and 3.27 (R4D2)]. It is readily apparent,

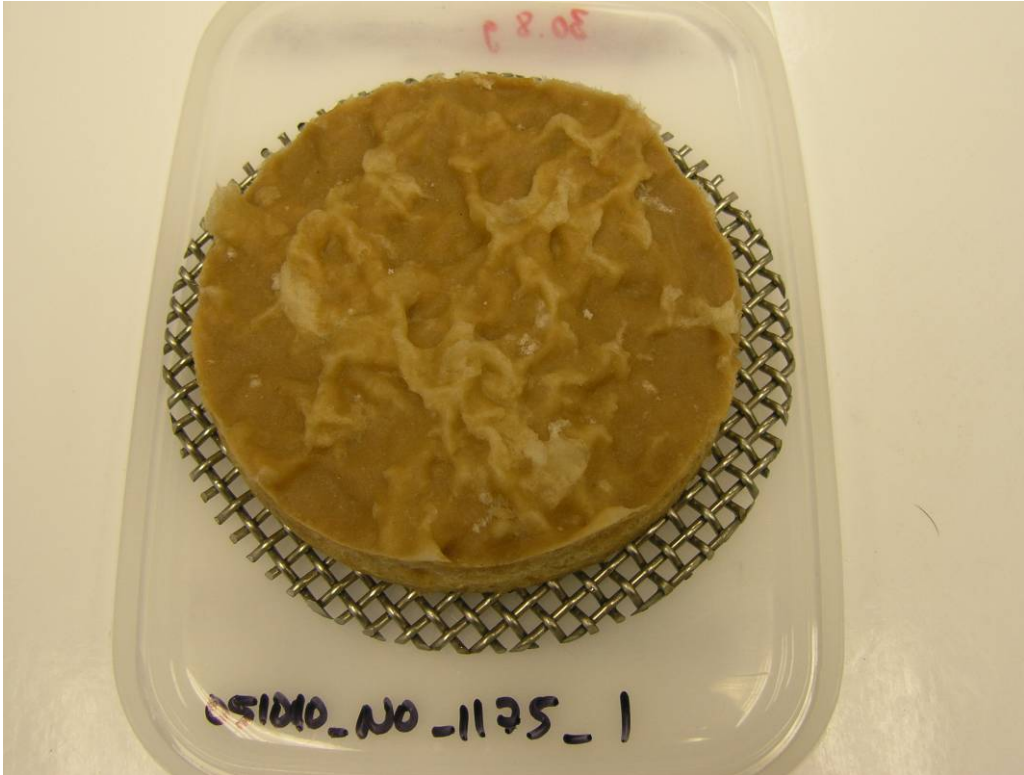


Figure 3.25. Example NUKON Debris Bed for R4A (target debris loading of 1449.5 g/m^2)

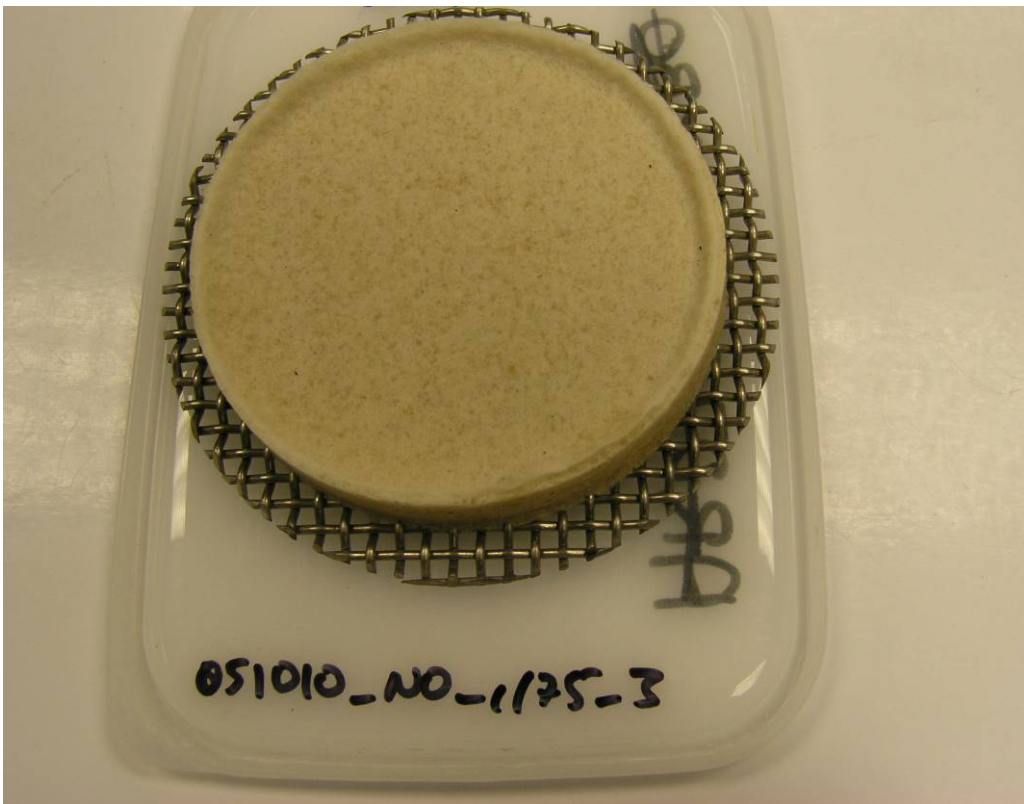


Figure 3.26. Example NUKON Debris Bed for R4C (target debris loading of 1449.5 g/m^2)



Figure 3.27. Example NUKON Debris Bed for R4D2 (target debris loading of 1449.5 g/m^2)

however, that surface uniformity, Criterion 2, is reduced for R4A and, to a much lesser extent, for R4B (Figure 3.10). The surface uniformity of an R4D2 debris bed was affected after being subjected to higher screen approach velocities. The screen surface (pattern) was telegraphed through the debris bed (Figure 3.28).



Figure 3.28. NUKON Debris Bed for R4D2 Subjected to 0.29 m/s Screen Approach Velocity (target debris loading of 1449.5 g/m^2 ; screen pattern perceptible on surface)

The representative debris bed height (see Section 3.2.3.2) was also affected by varying the R4 metric. For discussion, the debris beds having a target debris loading of 1449.5 g/m^2 are considered. Not surprisingly, the NUKON with no blender preparation (R4A2) resulted in the thickest debris bed, as shown in Figure 3.29. The thickness reported for R4A2 and R4B2 debris beds are the visually observed “average” heights; surface irregularities up to 1.2 and 0.2 in., respectively, were observed.

Based on the discussions in Sections 3.2.3.1 through 3.2.3.3, a NUKON debris preparation procedure that achieves an R4 of approximately 11, similar to test NS6, appears to be the best candidate to meet the debris bed criteria specified in Section 3.1.1.

The effect of debris preparation procedures on head loss for NUKON/CalSil debris beds has only been directly considered with regard to the NUKON preparation procedure as discussed above. CalSil preparation has only been indirectly examined based on a single test with the actual particulate content of the material altered, not the subsequent debris preparation. It is deemed reasonable to expect that the trend of the individual constituents, as presented for the NUKON debris, will dictate the combined debris bed response. Further, as described in Sections 3.2.3.2 and 6.3, the debris loading sequence appears to have a dominant effect on the resulting debris bed head loss. Therefore, the potential for debris preparation interaction to significantly affect the head loss of the NUKON/CalSil debris beds was not evaluated further.

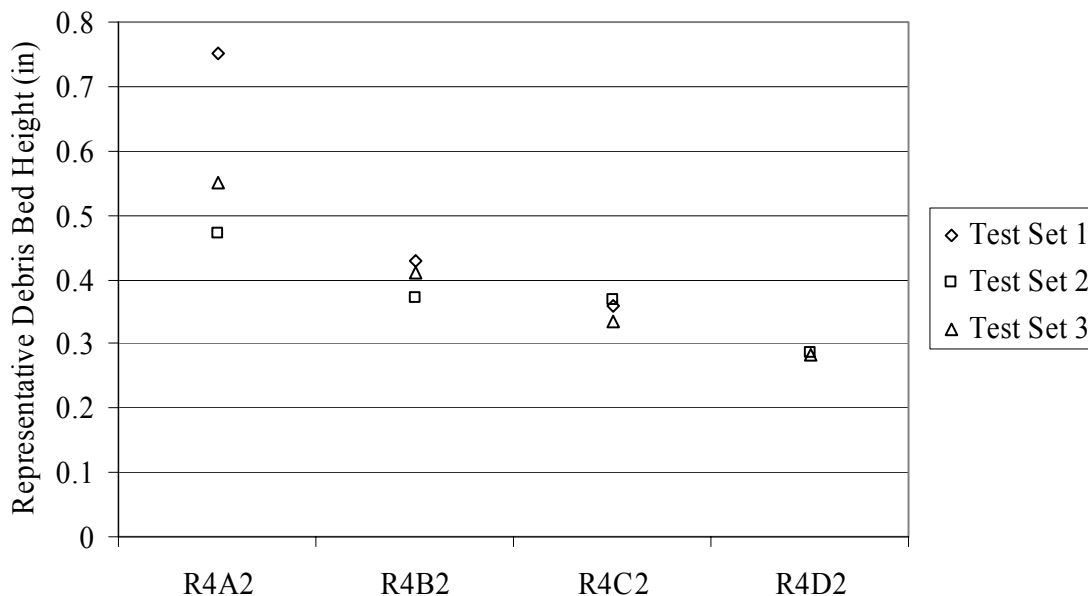


Figure 3.29. NUKON Debris Bed Height as a Function of R4 (target debris loading of 1449.5 g/m^2)

3.3 Debris Preparation Summary

The debris preparation techniques, procedures, and associated criteria developed and tested at PNNL (Sections 3.1 and 3.2) are summarized in this section. NUKON debris is addressed in Section 3.3.1, and CalSil debris is addressed in Section 3.3.2.

3.3.1 NUKON Debris Preparation

The as-received NUKON debris material was subjected to a 12- to 14-hr heat-treating process and shredded in a wood chipper by the vendor/manufacturer prior to shipment (Section 3.1). The following steps have been developed to prepare the as-received NUKON for testing. The NUKON preparation procedure is included in Appendix E.

1. Dry a quantity of as-received NUKON in an oven at a nominal temperature of 194°F (90°C) until a constant mass (within the uncertainty of the scale) is reached.
2. Select the required mass for testing from the dried material of step 1.
3. Based on a dilution ratio of 12.5 g of NUKON to 500 mL of water and the blender volume limits, and considering the indicated applicability range of the R4 metric (Section 3.2.1.1), determine the mass of NUKON to be prepared and its associated water volume. Multiple preparations of sub-batches may be required to reach a target debris loading.
4. Determine the debris preparation time necessary to achieve the desired R4 value (Section 3.1.2) and establish repeatability. To meet the debris bed criteria listed in Section 3.1.1, testing has established that the target R4 value should be 11 ± 1 . The resulting slurry should be observed to have a homogeneous consistency. The procedure for conducting the R4 test is provided in Appendix E.
5. The necessary blender preparation time should be reevaluated for each blender used. Additionally, the required blender preparation time should be periodically reevaluated for a given blender.

3.3.2 CalSil Debris Preparation

The as-received CalSil material was not subjected to any heat treating and was in the form of 3 x 12 x 48-in. blocks. The following steps have been developed to prepare CalSil for testing. The CalSil preparation procedure is included in Appendix E.

1. Separate material from the as-received CalSil blocks using a saw.
2. Dry the CalSil from step 1 in an oven at a nominal temperature of 194°F (90°C) until a steady mass (within the uncertainty of the scale) is reached.
3. Break off irregularly shaped chunks of approximately 0.25 to 0.75 in. in diameter from the dried material of step 2 with pliers until the required mass for testing is obtained.
4. Based on a dilution ratio of 12.5 g of CalSil to 500 mL of water and the blender volume limits, determine the mass of CalSil to be prepared and its associated water volume. Multiple preparations of sub-batches may be required to reach a target debris loading.
5. Determine the minimum mixing time necessary to produce a homogeneous slurry using the maximum R4 value of 1.55 as a guideline (Section 3.2.2) and establish repeatability.
6. The necessary preparation time should be reevaluated for each blender used. In addition, the necessary preparation time should be periodically reevaluated for a given blender.

4.0 Coating Characterization and Preparation

PNNL staff prepared Ameron's Amercoat 5450 alkyd topcoat (ALK) and Ameron's Dimetcote 6 inorganic zinc primer with Amercoat 90 epoxy topcoat (ZE) coating to serve as debris for head loss testing. Descriptions of the two tested coatings are presented in Table 4.1. The ALK and ZE coatings purchased by Ameron were applied to plastic sheets during preparation by the vendor. The plastic sheets with the coating materials attached were folded and shipped to PNNL. In Section 4.1, the preparation target slurry requirements and defining characteristics are identified. Like the insulation material, the coatings preparation procedure was referenced to an R4 criterion. Testing results for the criterion and quantification techniques for the characteristics are presented in Section 4.2. A summary of the debris preparation techniques is provided in Section 4.3.

Table 4.1. Description of Coatings Materials Used in PNNL Testing

Designation	Vendor Name/Specification	Description
ALK	Ameron's Amercoat 5450 alkyd topcoat	Single layer low density alkyd topcoat; unqualified nuclear containment coating; manufacturer, Ameron; coating name, Amercoat 5450; density, 1.35 g/cc; thickness, one coat of 1.5 mils ^(a)
ZE	Ameron's Dimetcote 6 inorganic Zn primer with Amercoat 90 epoxy topcoat	Inorganic zinc primer with epoxy-phenolic topcoat; qualified nuclear containment coating; manufacturer, Ameron; coating name, primer, Dimetcote 6; topcoat, Amercoat 90; primer density, 1.5 g/cc, topcoat, 1.75 g/cc; thickness, one primer of 2.5 mils, two topcoats of 4 mils per coat
(a) 1 mil = 0.001 in. (0.0254 mm).		

4.1 Requirements and Target Characteristics Identification

ALK and ZE coatings were prepared to conditions specified by the NRC. Unlike the insulation preparation (Section 3), specific performance criteria were not identified. The NRC defined target characteristics for "processed coating" and "coating chips" (sieving process [1/4-in. square coating]).

4.1.1 ALK Coating Preparation

"Processed coating" preparation tests used 6.52 g of ALK (mass corresponds to 0.35 kg/m² debris loading in the PNNL large-scale loop) and 260 mL of water prepared in a Waring blender. The coating was peeled from the plastic backing, torn into pieces smaller than 6 in. square, and pressed into the bottom of the blender. Water was then added and the blender operated at low speed for three specific times. R4 tests (see Section 3) were then conducted using an 8-in.-diameter 5-mesh screen (Table 4.2). Duplicate results are provided. Figures 4.1, 4.2, and 4.3 are photographs of the debris on the screen representing each R4 test. As agreed to by the NRC, the ALK processed coating was prepared to an R4 target value of 1.4.

Table 4.2. ALK R4 Test Data

Test No.	ALK Mass (g)	Water Volume (mL)	Blender Preparation Time (sec)	R4
PN1L0	6.52	260	1	3.1
PN1L1	6.52	260	1	3.4
5N1L1	6.52	260	5	2.3
5N1L2	6.52	260	5	2.0
15N1L0	6.52	260	15	1.4
15N1L1	6.52	260	15	1.3



Figure 4.1. ALK Debris Poured onto 5-Mesh Screen for R4 Evaluation, R4 ~ 3.3

R4 testing of prepared ALK coating debris was also conducted for target debris loadings of 0.7 kg/m^2 (corresponds to 13.05 g in the PNNL large-scale loop and 5.68 g in the benchtop loop) and 1.4 kg/m^2 (corresponds to 26.10 g in the PNNL large-scale loop [two batches with 13.05 g ALK each to produce quantity of 26.10 g] and 11.35 g in the benchtop loop). The water volume used for each ALK mass was determined from a constant 500-mL H_2O per 12.5-g debris mass ratio (Section 3). The R4 results are shown to be essentially independent of debris mass (compared to blender preparation time in Table 4.2), as shown in Figure 4.4.

For the 1/4-in.-square coating (paint chips), the ALK coating was peeled from the plastic backing, torn into pieces less than 6 in. square, and pressed into the bottom of the blender. The blender was pulsed on high for 1 second. No water was used. A constant ALK coating mass of 6.52 g was used each time. Coating pieces larger than a 50-cent piece were separated and reprocessed in the blender with a 1-second pulse on high. The bulk coating debris was then passed through a stack of progressively smaller sieves with 0.5-, 0.265-, 0.157-, and 0.111-in. openings. To agitate the material, the sieve stack was dropped from about 2 in. onto a flat surface five times. The resulting coating mass of each size from each sieve and in the bottom receptacle are listed in Table 4.3. Figure 4.5 is a photograph of the prepared coating debris in the range 0.17 to 0.265 in.



Figure 4.2. ALK Debris Poured onto 5-Mesh Screen for R4 Evaluation, R4 ~ 2.2

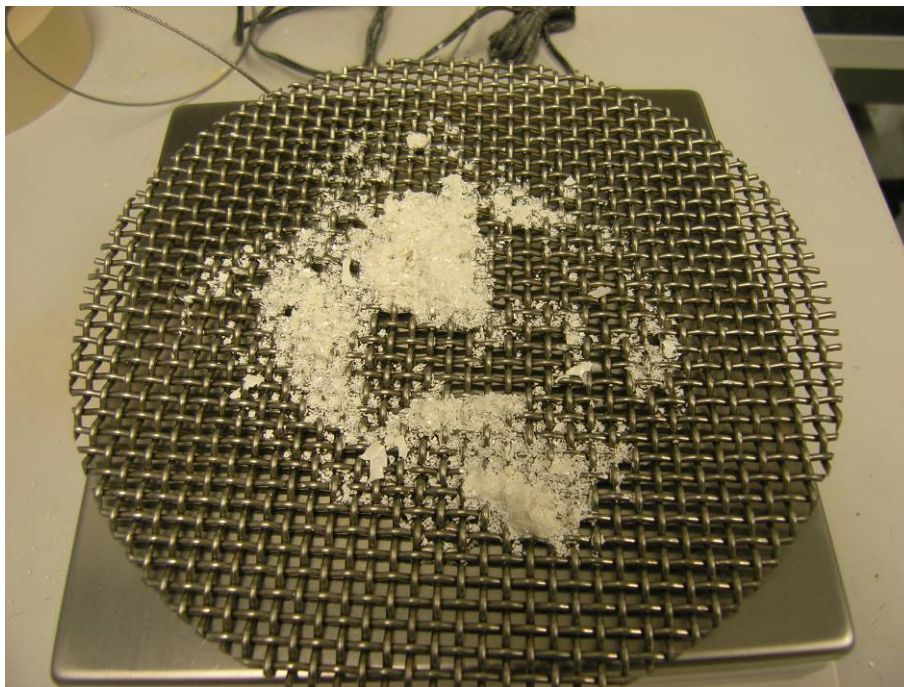


Figure 4.3. ALK Debris Poured onto 5-Mesh Screen for R4 Evaluation, R4 ~ 1.4

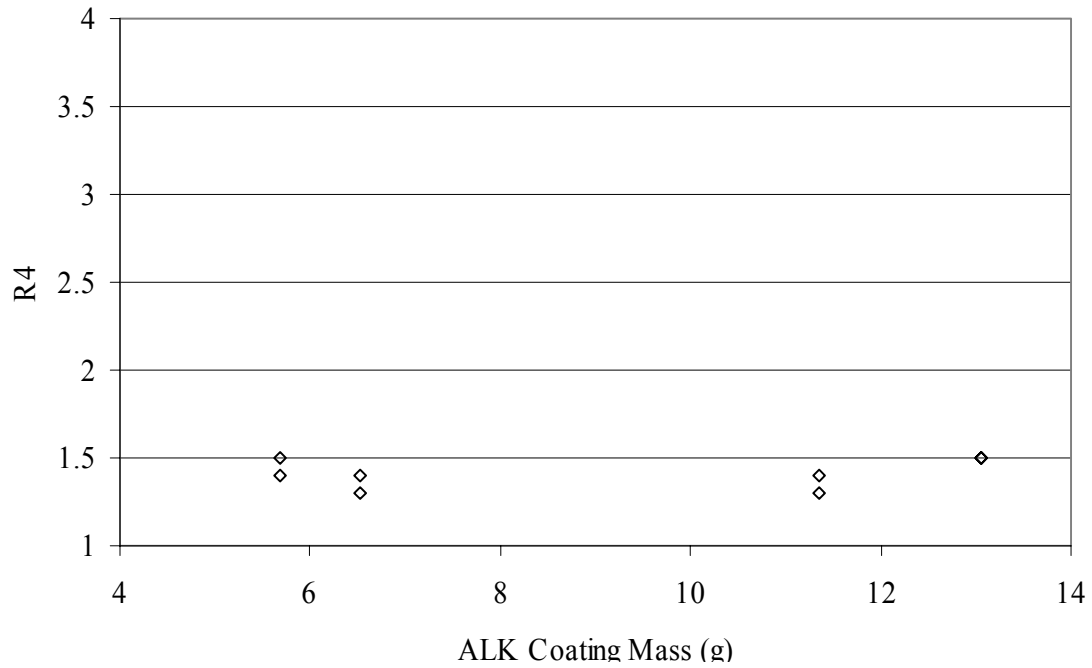


Figure 4.4. R4 as a Function of Initial ALK Coating Mass (constant 15-second blender preparation time and constant dilution ratio)



Figure 4.5. “1/4 in. Square Coating” (paint chips) for ALK Prepared Coating Debris in the Range 0.157 to 0.265 in.

4.1.2 ZE Coating Preparation Results

The “Processed Coating” tests used 13.05 g of ZE (mass equivalent to 0.7 kg/m² loading in the PNNL large-scale loop) and 520 mL of water prepared in a Waring blender. The coating typically broke into pieces smaller than 6 in. square when it was removed from its plastic backing. The coating was then placed into the blender, the water added, and the blender operated at low speed for three specific times. R4 tests (see Section 3) were then conducted using an 8-in.-diameter 5-mesh screen (Table 4.4). Photographs of the debris on the screen representing each R4 test are provided in Figures 4.6, 4.7, and 4.8. In agreement with the NRC, the ZE processed coating was prepared to an R4 target value of 0.5.

Table 4.3. Prepared and Sieved ALK Coating Mass by Sieve Size from Two Preparations of 6.52-g Each

Sieve Size (in.)	Mass ^(a) (g)
0.500	1.31
0.265	1.39
0.157	1.09
0.111	0.76
bottom receptacle	8.67
(a) Mass sums to greater than initial amount (13.04 g) due to measurement error associated with segregated samples.	

Table 4.4. ZE R4 Test Data

Test No.	ZE Mass (g)	Water Volume (mL)	Blender Preparation Time (s)	R4
PN1L0	13.05	520	1	1.5
PN1L1	13.05	520	1	1.4
5N1L0	13.05	520	5	0.9
15N1L0	13.05	520	15	0.4
15N1L	13.05	520	15	0.6

For the ¼-in. square coating (paint chips), the coating was removed from the plastic backing, placed into a container, and then grasped 10 times with a rubber-gloved hand to break the material into finer chips. No water was used in the preparation. The process was repeated for three separate samples of nominally 25 g ZE coating. The bulk coating debris (75 g total) was then sifted through a stack of progressively smaller sieves of 0.5, 0.265, 0.157, and 0.111-in. openings. To agitate the material, the sieve stack was shaken back and forth 4 times and dropped about 2 in. onto a flat surface. The shaking and dropping sequence was repeated 5 times. The resulting coating masses of each size from each sieve and in the bottom receptacle are listed in Table 4.5. Figure 4.9 is a photograph of the prepared coating debris in the range 0.157 to 0.265 in.

4.2 Coatings Preparation Summary

The processed coating ALK and ZE coatings debris were prepared to attain R4 values of 1.4 and 0.5, respectively. The 1/4 in. square coating ALK and ZE coatings debris were prepared by sieving through progressively smaller sieves. The material in the range 0.157 to 0.265 in. was used for testing. Photos of the four different coatings debris were prepared and sent to Naval Surface Warfare Center (NSWC) for particle size characterization. The prepared photos and associated particle size distributions are included in Appendix O.

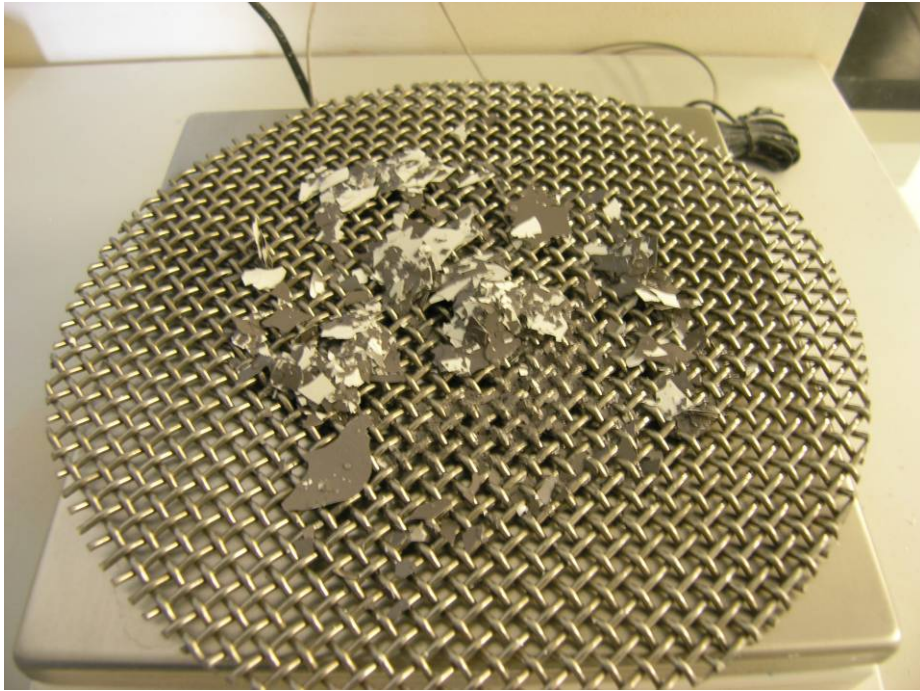


Figure 4.6. ZE Debris Poured onto 5-Mesh Screen for R4 Evaluation, R4 ~ 1.5

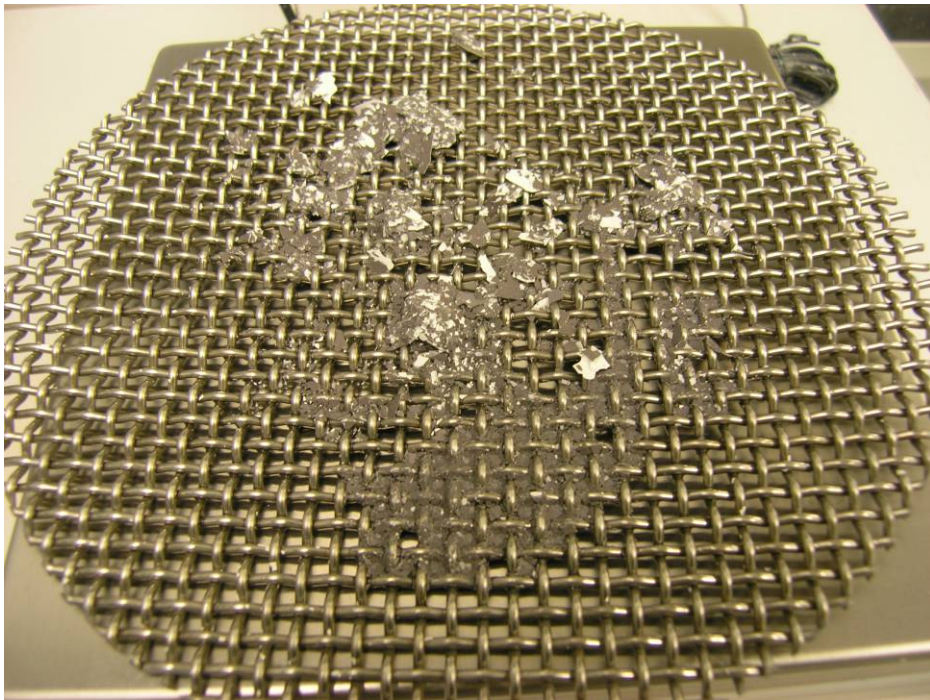


Figure 4.7. ZE Debris Poured onto 5-Mesh Screen for R4 Evaluation, R4 ~ 0.9

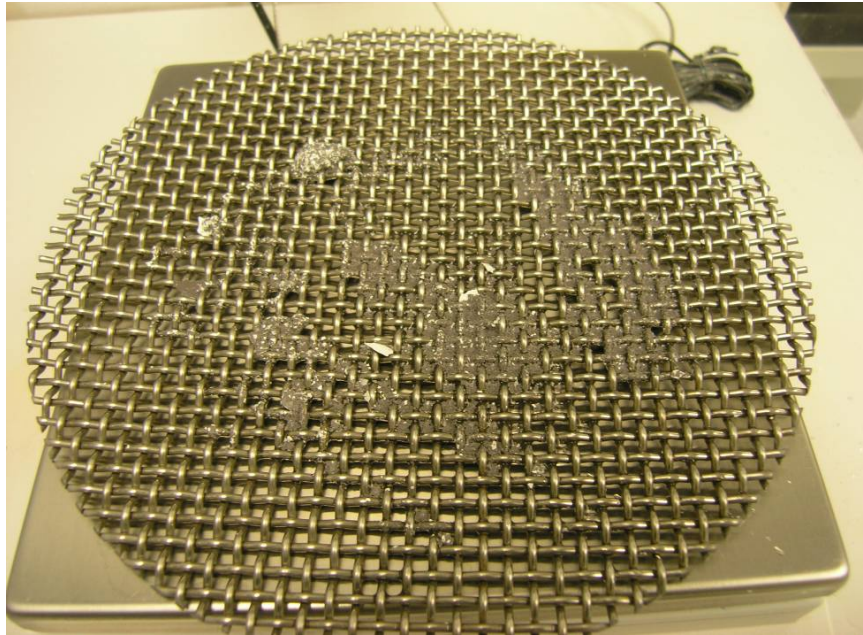


Figure 4.8. ZE, R4 ~ 0.5

Table 4.5. Mass of Prepared and Sieved ZE Coating Debris by Sieve Size from Three Preparations of ~ 25 g each for a Total Processed Mass of 75 g

Sieve Size (in)	Mass (g)
0.500	1.11
0.265	22.58
0.157	23.08
0.111	14.33
bottom receptacle	14.00



Figure 4.9. ¼-in. Square Coating ZE Coating Debris with Particle Dimensions of 0.157 to 0.265 in.

5.0 Test Matrix and Approach

This section presents the test matrix that was conducted for the PNNL debris bed head loss measurement effort in Section 5.1, discusses key factors considered in developing the test program and test procedures in Section 5.2, and in Section 5.3 provides an overview of the test procedures used to conduct the tests.

5.1 Test Matrix

Testing in the large-scale test loop was performed based on four separate test matrixes, which are referred to as Series 1, Benchmark, Series 2, and Coatings and are presented in Sections 5.1.1, 5.1.2, 5.1.3, and 5.1.4, respectively. In each section, the test matrix is described in tabular form along with a brief description of the associated test program.

In each table describing a test matrix, a test case number, test identification, mass loading for the individual debris constituents, total debris loading, nominal fluid temperature, and the screen material used are listed. The test case number was assigned to each test after the majority of the testing was completed and is intended to provide unified, simple labels that relate the tests from the separate matrixes.

For the test labels, the various test conditions are identified as SO = screen only, PO = perforated plate only, CO = CalSil only, NO = NUKON only, NC = NUKON and CalSil (denoted as NUKON/CalSil), BT = benchtop test, ALK = Ameron's Amercoat 5450 alkyd topcoat, and ZE = Ameron's Dimetcote 6 inorganic Zn primer with Amercoat 90 epoxy topcoat. The test cases are numbered in ascending order of the mass loading for each individual test condition. For the NUKON/CalSil cases (NC) the test cases are numbered according to the ascending order of the NUKON mass loading followed by the ascending order of the CalSil loading.

Some test case numbers end with a lower case letter, indicating that the same debris bed was used to conduct multiple tests. The alphabetical order of the letters indicates the order in which the tests were conducted. Thus those test cases with an "a" were conducted immediately after debris bed formation.

NO6a through NO7b and NC15a through NC17b are exceptions to the numbering order of the test cases. These test cases were added to the Series 2 test matrix after the writing of the report had been initiated, and therefore were provided sequential numbers in the order the tests were completed.

The test identification is the test name created at the time the test was executed. The test identification is the same name given to the electronic DAS file used to record the instrument readings. The associated data sheets and Quick Look reports are labeled with the test identification (ID) number. The test ID number is created from the date of the test, the test condition, the total mass of debris being introduced to the test loop, the test loop being used, screen material installed in the test loop, and the number of the test run for a given day. The test ID is written as *YYMMDD_tc_WWWW_LS#*

where

- YY* = two digits indicating year. (2005 = 05)
- MM* = two-digit number of month (August = 08)
- DD* = two digits representing day of the month

Tc =two-letter designation of the test condition as listed for the test case numbers above with the following exceptions used for the coatings tests:

- P is used to designate that processed (finer sized coating particles, refer to Section 4) coating is included in the debris
- Q is used to designate that ¼-inch chips are included in the debris
- ALK is replaced with a “C” for coating
- ZE is replaced with a “Z”

WWWW= four digits representing the total dry target material mass in grams being introduced to loop with two digits to the right of the decimal place (e.g., 12.03 g = 1203). Note: this is the sum of the masses for all of the debris constituents being introduced to the test loop.

L = designation of test loop. “L” for large-scale loop and “B” for benchtop loop.

S = screen material. “P” for the perforated plate with 1/8-inch holes and no indication if the 5-mesh woven-wire cloth is installed.

= the sequential number of the test being conducted that day: 1 = first test of the day, 2 = second test of the day, etc.

Examples of test identifications used are:

- 051123_NC_2181_L1 – This was the first test, conducted on November 23, 2005. The test was conducted in the large-scale loop with the 5-mesh woven wire cloth installed. A total of 21.81 g of debris containing both NUKON and CalSil debris material was introduced into the test loop.
- 060501_PQC_2609_LP2 – This was the second test, run on May 1, 2006. The test was conducted in the large-scale loop with the perforated plate installed. A total of 26.09 g of debris consisting of both ALK processed and ¼-inch chip material was introduced into the test loop.

The bulk of the tests conducted in the benchtop loop were performed to develop procedures and evaluate trends in the data. However, a number of benchtop loop tests were used for direct comparison to the large-scale results. These benchtop loop tests are listed in Section 5.1.5 and the associated results presented in Section 7.

In Section 7, the results of the large-scale tests are presented in separate sections for each type of test condition (e.g., NO, NC). The test series of a particular test is pertinent because slight changes were made to the test procedures for each series of tests. The variations in the test procedures for each test series are discussed in Section 5.3.

5.1.1 Series 1 Test Matrix

The Series 1 tests are listed in Table 5.1 and were the first suite of tests conducted in the large-scale test loop. The test conditions selected for the matrix were based on conditions used in a previous study of the head loss associated with sump screen debris beds (Shaffer et al. 2005). Both the initial debris loadings and the test velocity sequence from the previous study were matched for the Series 1 tests. Section 5.3 discusses the test procedures unique to the Series 1 tests. Comparisons to the pressure drop measurements obtained in the previous study are not made in this report, but some comparisons have been included in the Quick Look reports of Appendixes H and J. The far right column of Table 5.1 contains the test identification numbers used by the previous study and the Quick Look reports.

Table 5.1. PNNL Series 1 Test Matrix

Test Case No.	Test ID	Target Debris Bed NUKON Loading (g/m ²)	Target Debris Bed CalSil Loading (g/m ²)	CalSil to NUKON Mass Ratio	Total Target Debris Bed Loading (g/m ²)	Target Fluid Temperature (°C)	Screen Material Used ^(a)	Corresponding Test Case ID from Previous Study ^(b)
SO1	051114 SO 0000 L1	0	0	N/A	0	21	screen	N/A
SO2	051128 SO 0000 L1	0	0	N/A	0	21	screen	N/A
NO4	051108 NO 3067 L1	1645	0	0.00	1645	21	screen	1a
NO5	060125 NO 3067 L1	1645	0	0.00	1645	21	screen	1a
NC3	051110 NC 0595 L1	213	106	0.50	326	21	screen	6h
NC7	051121 NC 1586 L1	568	284	0.50	851	21	screen	6f
NC11	051123 NC 2181 L1	780	390	0.50	1170	21	screen	6i
NC12	051117 NC 2776 L1	993	496	0.50	1489	21	screen	6e
NC13	051128 NC 2776 L2	993	496	0.50	1489	21	screen	6e2
NC14	051115 NC 4098 L1	1419	780	0.55	2199	21	screen	6b

(a) Screen = 5-mesh woven wire cloth, plate = perforated plate with 1/8-inch holes.
(b) Test conditions were intended to match those from the previous test study conducted at the University of New Mexico under the direction of LANL (Shaffer et al. 2005).

All of the Series 1 tests used the 5-mesh woven wire and were conducted at ambient temperature. The Series 1 tests were the only large-scale tests that did not premix the debris constituents prior to introduction to the test loop. The Series 1 tests used two debris injection lines to simultaneously inject the debris constituents into the main line of the test loop.

5.1.2 Benchmark Series Test Matrix

The three Benchmark test cases listed in Table 5.2 were selected by NRC staff to be run in parallel in both the ANL and PNNL test loops. The results were to be used by the NRC to compare the two loops and evaluate the variability in the pressure drop measurements associated with multiple test loops. The results of the ANL Benchmark tests and a comparison to the PNNL results are included in NUREG/CR-6913 (Kasza et al. 2006). The R4 metric was used by both organizations to determine and monitor the debris preparation for the tests to ensure that similar material consistency was used for both suites of tests.

To match the R4 metric for both tests, ANL conducted R4 tests first and provided data to PNNL. PNNL in turn adjusted the blender mixing time to match the data from ANL. While PNNL was able to match the R4 values produced at ANL, ANL had deviated from the baseline procedure for conducting the R4 tests. The ANL operators used higher dilution rates (2500 mL water) than the base point of 12.5 g NUKON/500 mL water defined by PNNL. After matching the ANL results using 2500 mL of water, PNNL then reevaluated the R4 values immediately after blending operations in 1000 mL of water. For BM-2, the PNNL NUKON preparation provided an R4 ~ 10.8, and for BM-1 and BM-3 the R4 was ~16.4. These results suggest the NUKON preparation for BM-2 was similar to the R4 values used by PNNL for the other test series and that BM-1 and BM-3 were not. However, the debris mass-to-water volume ratio used in the final PNNL evaluations of the Benchmark R4 metric were still significantly different than the 12.5g/500 mL used as the PNNL base point. The results presented in subsection 3.2.1.2.2 indicate the R4 value decreases with increased dilution.

Table 5.2. PNNL Benchmark Series Test Matrix

Test Case No.	Test ID	Target Debris Bed NUKON Loading (g/m ²)	Target Debris Bed CalSil Loading (g/m ²)	CalSil to NUKON Mass Ratio	Total Target Debris Bed Loading (g/m ²)	Target Fluid Temp. (°C)	Screen Material Used ^(a)	Corresponding Test Case ID from Benchmark Test Plan ^(b)
NO1	060321_NO_0405_LP1	217	0	0.00	217	21	plate	BM-1
NO2	060313_NO_1349_LP1	724	0	0.00	724	21	plate	BM-2
NC8	060323_NC_1619_LP1	724	145	0.20	869	21	plate	BM-3

(a) Screen = 5-mesh woven wire cloth, plate = perforated plate with 1/8-inch holes.
(b) The Benchmark test plan was used by both PNNL and ANL to conduct the Benchmark tests and is included in Appendix **.

The final evaluations of the R4 values used for the Benchmark tests indicate that the consistency of the NUKON debris for the ANL and PNNL tests should be relatively close within the limits of the R4 metric. However, comparison of the NUKON-debris consistency between the Benchmark tests and the other PNNL test series cannot be quantified with the R4 metric due to the difference in the dilutions used for blender preparations (refer to Section 3 for effect of dilution on R4 metric). It is therefore uncertain whether the NUKON debris preparation of the Benchmark tests matches that of the other PNNL tests. The R1 through R3 metrics (Section 3) were not evaluated for comparing the ANL and PNNL Benchmark tests debris preparation.

The ANL test loop did not contain filters; therefore, the PNNL loop filters were bypassed for the benchmark tests. The far right column of Table 5.2 contains the test identification for the Benchmark tests that is used in the Benchmark test plan of Appendix L and the Quick Look reports in Appendixes H and J.

5.1.3 Series 2 Test Matrix

The Series 2 tests make up the bulk of the PNNL large-scale tests and all of the elevated temperature tests. All Series 2 tests were conducted with the perforated plate installed in the test loop, and the test fluid was filtered after ramp up 1 in the screen approach velocity. Table 5.3 lists all Series 2 tests. The far right column of the table contains the test priority number provided in the NRC proposed test matrix from the “Modification to the Statement of Work,” JCN: N6106, for the performance period of 4/1/05 to 12/30/06. Reference is made to the test priority numbers in the Quick Look reports in the appendixes.

For the CalSil-only test condition CO1 (priority 2 +200%), the initial target debris loading proposed by the NRC was 1450 g/m². Initial tests in the benchtop loop (Sections 5.1.4 and 7.3) indicated that the original mass loading was insufficient to form a complete debris bed. Therefore, based on the results of the benchtop testing, the mass loading for the CalSil-only test condition was increased by an additional 200% over the original priority 2 mass loading.

5.1.4 Coatings

Table 5.4 contains a list of the Coatings tests, which were conducted the same way as the Series 2 tests except for changes in the screen approach velocity used for debris bed formation. Screen approach velocities as high as 0.8 ft/sec were required to transport the debris material from the debris injection tubes to the test screen.

Table 5.3. PNNL Series 2 Test Matrix

Test Case No.	Test ID	Target Debris Bed NUKON Loading (g/m ²)	Target Debris Bed CalSil Loading (g/m ²)	CalSil to NUKON Mass Ratio	Total Target Debris Bed Loading (g/m ²)	Target Fluid Temperature (°C)	Screen Material Used ^(a)	NRC Priority No. for Test ^(b)
PO1	060804 PO 0000 LP1	0	0	N/A	0	21	plate	13
PO2	060804 PO 0000 LP2	0	0	N/A	0	54	plate	13
PO3	060805 PO 0000 LP1	0	0	N/A	0	82	plate	13
NO3a	060425 NO 2703 LP1	1450	0	0.00	1450	21	plate	1
NO3b	060425 NO 2703 LP2	1450	0	0.00	1450	54	plate	1
NO3c	060425 NO 2703 LP3	1450	0	0.00	1450	82	plate	1
NO6a ^(c)	060731 NO 2703 LP1	1450	0	0.00	1450	54	plate	1
NO6b ^(c)	060731 NO 2703 LP2	1450	0	0.00	1450	21	plate	1
NO7a ^(c)	060802 NO 2703 LP1	1450	0	0.00	1450	82	plate	1
NO7b ^(c)	060802 NO 2703 LP2	1450	0	0.00	1450	54	plate	1
CO1a	060512 CO 8108 LP1	0	4350	N/A	4350	21	plate	2 +200% ^(d)
CO1b	060512 CO 8108 LP2	0	4350	N/A	4350	54	plate	2 +200% ^(d)
CO1c	060512 CO 8108 LP3	0	4350	N/A	4350	82	plate	2 +200% ^(d)
NC1	060427 NC 0252 LP1	108	27	0.25	135	21	plate	7
NC2	060428 NC 0453 LP1	108	135	1.25	243	21	plate	8
NC4	060509 NC 0505 LP1	217	54	0.25	271	21	plate	9
NC5a	060426 NC 0708 LP1	217	163	0.75	380	21	plate	6
NC5b	060426 NC 0708 LP2	217	163	0.75	380	82	plate	6
NC6a	060517 NC 0808 LP1	217	217	1.00	434	21	plate	N/A
NC6b	060517 NC 0808 LP2	217	217	1.00	434	82	plate	N/A
NC9	060331 NC 2024 LP1	724	362	0.50	1086	21	plate	4
NC10	060404 NC 2698 LP1	724	724	1.00	1448	21	plate	5
NC15a ^(c)	060807 NC 0708 LP1	217	163	0.75	380	54	plate	6
NC15b ^(c)	060807 NC 0708 LP2	217	163	0.75	380	21	plate	6
NC16a ^(c)	060809 NC 0708 LP1	217	163	0.75	380	82	plate	6
NC16b ^(c)	060809 NC 0708 LP2	217	163	0.75	380	54	plate	6
NC17a ^(c)	060817 NC 2024 LP1	724	362	0.50	1086	54	plate	4
NC17b ^(c)	060817 NC 2024 LP2	724	362	0.50	1086	21	plate	4

(a) Screen = 5-mesh woven wire cloth, plate = perforated plate with 1/8-inch holes.
(b) Test Priority number from the “Modification to the Statement of Work” for the performance period of 4/1/05 to 12/30/06.
(c) Debris bed formed at an elevated fluid temperature.
(d) The initial priority 2 test called for a CalSil mass loading of 1450 g/m². Benchtop testing demonstrated this to be insufficient mass loading to form a complete debris bed. Therefore, the mass loading for the large-scale test was increased an additional 200% (refer to Section 7.3).

Table 5.4. PNNL Coatings Materials Test Matrix

Test Case No.	Test ID	Target Debris Bed Processed Coating Loading (g/m ²)	Target Debris Bed 1/4 in. Square Coating Loading (g/m ²)	Total Target Debris Bed Loading (g/m ²)	Target Fluid Temperature (°C)	Screen Material Used ^(a)
ALK1a	060501 PQC 2609 LP1	700	700	1,400	21	plate
ALK1b	060501 PQC 2609 LP2	700	700	1,400	82	plate
ALK2	060502 POC 2609 LP1	1400	0	1,400	21	plate
ZE1	060504 PQZ 2609 LP1	700	700	1,400	21	plate
ALKB	060428 PQC 1136 BP1	700	700	1,400	21	plate

(a) Screen = 5-mesh woven wire cloth, plate = perforated plate with 1/8-inch holes.

5.1.5 Benchtop Tests

The PNNL test program used the benchtop loop to conduct 79 NUKON-only, 8 CalSil-only, 25 NUKON/CalSil tests, and 1 Coatings test. These tests were conducted to assess debris preparation procedures and associated metrics; develop the debris loading system design, technique, and procedures; investigate the effects of the debris loading sequence; evaluate repeatability and data trends such as with flow history; and provide initial scoping results to help refine the test matrix and velocity sequence. The bulk of the benchtop results are discussed in Sections 3 and 6.

Table 5.5 includes a list of benchtop tests that were conducted in the same manner as the large-scale tests and whose results are included in the presentation of large-scale results in Section 7. The head loss measurements from these tests are included in the Quick Look reports for the related large-scale test cases listed in the far right column of Table 5.5. The test matrixes for the additional NUKON-only and NUKON/CalSil tests conducted in the benchtop loop are included in Appendixes M and N.

Table 5.5. PNNL Benchtop Tests Directly Associated with Large-Scale Test Conditions

Test Case No.	Test ID	Target Debris Bed NUKON Loading (g/m ²)	Target Debris Bed CalSil Loading (g/m ²)	CalSil to NUKON Mass Ratio	Total Target Debris Bed Loading (g/m ²)	Target Fluid Temperature (°C)	Screen Material Used ^(a)	Related Large-Scale Test Case No.
NOBT1	060223_NO_1363_B1	1681	0	0	1681	21	screen	NO6, NO7
NOBT1	060228_NO_1363_B1	1681	0	0	1681	21	screen	NO6, NO7
COBT1	060406_CO_1176_BP1	0	1450	N/A	1450	21	plate	CO1a, CO1b, CO1c
COBT2	060510_CO_1469_BP1	0	1812	N/A	1812	21	plate	CO1a, CO1b, CO1c
COBT3	051227_CO_0411x_B1	0	2174	N/A	2174	21	screen	CO1a, CO1b, CO1c
COBT4	051227_CO_1763_B2	0	2174	N/A	2174	21	screen	CO1a, CO1b, CO1c
COBT5	060510_CO_1763_BP2	0	2175	N/A	2175	21	plate	CO1a, CO1b, CO1c
COBT6	060510_CO_2351_BP3	0	2900	N/A	2900	21	plate	CO1a, CO1b, CO1c
COBT7	060511_CO_3527_B2	0	4350	N/A	4350	21	plate	CO1a, CO1b, CO1c

(a) Screen = 5-mesh woven wire cloth, plate = perforated plate with 1/8-inch holes.

5.2 Approach for Developing Test Procedures

The test preparation procedure is specified in an attempt to control the initial conditions at which the debris bed is formed on the screen. Test preparation consists of establishing the test loop conditions, preparing of the debris material, introducing the debris to the test loop, and forming the debris bed.

This section summarizes the approach taken to meet the objectives presented in Section 1.2. The primary driver in developing the test setup and test procedures was to maximize the repeatability of the head loss measurements obtained from separate debris beds having the same debris mass loading, ratio of debris constituents, and flow conditions (screen approach velocity and fluid temperature). To accomplish this,

an attempt was made to identify the parameters to which the resulting pressure drop across the debris bed may be sensitive and then to ensure those parameters were monitored and controlled. The goal was to ensure that scatter obtained in the measured data would be due to random uncertainty and variability in the debris bed formation as opposed to changes in a critical parameter not being monitored or held constant.

The main parameter postulated to have a significant impact on the head loss was the structure of the debris bed. In other words, given the same quantity of debris materials, it was assumed that a wide range of pressure drops could be obtained for a given screen approach velocity depending how the material was loaded onto the screen. Therefore, controlling the initial conditions of the test that may influence the debris bed formation or structure of the final debris bed was given significant attention. These parameters included:

- The size or consistency of the debris material introduced into the loop. Repeatable debris preparation procedures and methods for characterizing the resulting debris were determined to be critical for obtaining repeatable results. Therefore, a significant effort was put forth to develop debris preparation procedures, evaluate the impact of changes to the debris preparation procedures, and monitor or characterize the prepared debris materials. The goal was to introduce the same material into the loop each time.
- The rate, concentration, and order in which debris reaches the test screen. It was postulated that the structure of the debris bed (and thus the resulting pressure drop) might vary if the order in which the various components of the debris were applied to the screen was altered. Therefore, significant emphasis was placed on developing a debris injection system and associated procedures that provided repeatable injection of the debris material into the flow stream upstream of the test screen. Emphasis was also placed on ensuring that the process could be monitored.
- The test screen configuration. To eliminate pressure drops associated with discontinuities in the flow path or complications associated with an unsecured screen, the test screen was designed so the screen material terminated at the pipe wall with no support structure affecting the flow path and no crevice in the pipe wall to retain debris material. To ensure the test screen could not flutter, vibrate, or change configuration, the screen was secured in a support collar that was sandwiched between the two halves of the custom-fabricated TTS.

The intent was to use the same material for each test and apply it to the test screen in the same manner each time. Therefore, the structure of the debris beds for repeat tests would only differ due to the variability associated with the deposition of the debris on the screen.

The second priority was to ensure that the measured pressure drop across the debris bed corresponded to known conditions on the screen. After debris bed formation, numerous data points were recorded as the screen approach velocity was varied. The desire was to ensure the measured pressure drop could be associated with a well-characterized debris bed. To assist with improving the characterization of the debris, the following issues were addressed:

- Continual formation of the debris bed. Initial benchtop tests indicated that a significant fraction (on the order of 0.15 to 0.4) of the target mass loading was not being retained on the screen during the duration of loop operation. It was postulated that debris material may continue to be deposited on the debris bed as the capture efficiency of the debris bed improved with increased debris accumulation. If this were the case, the concern existed that for most of the pressure drop measurements made

across the debris bed, the mass loading would be unknown. To address this issue, minimum debris bed formation criteria (e.g., number of loop circulations) were specified in the procedures, and a bag filter system was added to the test loop. The filter system allowed suspended debris material to be filtered from the flow at any prescribed point during a test, thus reducing the potential for mass addition to occur during a test.

- In situ characterization of the debris bed. To obtain characterization of the debris bed at each velocity point, several systems for in situ characterization of the debris bed and flow stream were investigated. The development of an optical triangulation system for obtaining in situ debris bed height measurements was pursued, and a system was installed at the end of the Series 1 tests. The in situ bed height measurements allowed changes in the debris bed thickness to be monitored at each velocity point.
- Determining mass loading of individual constituents on the test screen. With the benchtop result indicating that 15 to 40% of the target mass would not be retained on the test screen, mass measurements indicated that the uncertainty in the CalSil mass loading for NUKON/CalSil debris beds would exceed 100%. These high uncertainties would make it difficult to evaluate trends in the debris bed pressure drop associated with the CalSil mass loading. To resolve the issue, Ca^{++} ISE probes were employed to determine the concentration of CalSil from HCl solutions used to dissolve the retrieved debris beds.

The following additional issues were addressed to reduce the variability in the test results:

- The presence of gas in the fluid and potentially the debris bed as the pressure drop within the test loop is increased. To eliminate pressure drop associated with a gas phase and the variability that could exist if the presence of gas was periodic, an argon cover gas system was applied to the expansion tank so that the static pressure of the entire test loop could be raised to maintain gas in solution.
- Flow profile upstream of the test screen. To minimize changes or disruptions to the flow field as the screen approach velocity is varied (e.g., swirl component) 20-plus diameters of straight seamless pipe were installed upstream of the test screen. To ensure steady, true pressure-drop measurements, 10-plus diameters of straight seamless pipe were installed downstream of the test section allowing for the downstream pressure tap to be located 10 diameters downstream of the test section.
- Contamination from settled debris and cleaning of the test loop. The benchtop testing demonstrated that insulation debris materials that settled in sections of pipe or flex hose were readily mobilized and flushed at higher fluid velocities. However, the testing also indicated that the debris materials, especially CalSil, had an affinity for crevices such as those created by flanged joints. This created the potential for contamination from settled materials and having to perform extensive, time-consuming cleaning operations. To reduce the impact of this issue, the pipe was butt-welded as much as possible, and flex hoses that were readily removed for inspection and cleaning were used in the large-scale loop.

5.3 Overview of Test Procedure

This section provides an overview of the procedures used to conduct the head loss tests. Each series of tests was conducted with a fixed set of procedures with several exceptions:

- The screen approach velocity during the Series 1 tests was changed from 0.2 ft/sec to 0.1 ft/sec (refer to Section 5.3.2).

- During the test program, several changes were made to the debris bed retrieval procedure in an attempt to increase the reliability of the process to recover the debris bed intact.

Slight changes were made to some procedures between test series. These changes will be summarized in the following sections. Unless otherwise noted, the description of the procedures applies to all of the test series described in Section 5.1.

There are several instances where the test operators deviated from the test procedures due to extenuating circumstances related to the individual tests. Examples include:

- Omitting the velocity sequence from Test Case NC10 due to the high head loss encountered at the completion of the debris bed formation.
- Repeating the velocity sequence for ALK2 after the peak screen approach velocity was increased to mobilize material and allow the bed formation process to continue.

Instances where a deviation from the test procedure occurred are explained in the individual Quick Look Reports, which are in Appendixes G through K. Section 5.3.1 discusses the pretest preparations, Section 5.3.2 discusses the test procedure used to obtain the head loss measurements, and Section 5.3.3 discusses the post-test operations and debris bed assessment.

5.3.1 Pretest Preparation

The Series 1 tests used laboratory process water and the Benchmark and Series 2 tests used DI water with a conductivity $< 2 \mu\text{S}/\text{cm}$. After each Series 1 test, the entire inventory of water was drained from the loop for disposal. For the Series 2 and Benchmark tests, the DI water was drained to a holding tank and reused. The conditioning of the water after each test consisted of circulating the water for multiple passes through a 10- μm bag filter. To control biological growths in the test fluid, the loop inventory was treated periodically with Mt. Hood 480 biocide, as prescribed in vendor instructions. Because of the rubber flex hoses used in the test loop, the conductivity of the DI water was increased using potassium chloride (KCl) to ensure protection of the instrumentation from the buildup of static charge. The salt was added to reach a target conductivity on the order of $80 \mu\text{S}/\text{cm}$. Approximately 32 g of KCl were added to an inventory of approximately 200 gal of DI water. Periodic adjustments were made as water inventory was lost, and additional DI water was added. The conductivity of the process water was measured to be approximately $160 \mu\text{S}/\text{cm}$.

Prior to testing, the screen material was placed in the TTS and the loop filled with water. When the perforated plate was installed, the rounded edges of the perforations were placed facing upstream. The loop was degassed by circulating the loop inventory through the main line with the isolation valves partially closed to increase the local pressure drop and drive gas out of solution. The flow rate through the loop was periodically reduced and passed through the bag filter housing where the configuration of the filter housing and the filter itself helped to scrub gas bubbles from the flow. The accumulated gas was then bled/purged from the top of the filter housing.

DAS instrument checks included:

- Purging the delta-pressure transmitter manifold, isolating each transmitter and using the transmitter bypass valves to check the true instrument zero readings.

- Isolating the high-pressure side of the delta-pressure transmitter array manifold and comparing the water column readings for all of the transmitters installed.
- Isolating the Micro Motion flow meters and performing zero checks.
- Closing the main line throttle valve so that all main line flow passed through the injection lines, this flow configuration put the main line Micro Motion in Series with the injection line Micro Motions. The mass flow readings for the main line Micro Motion were compared for consistency to those from the injection line units through the upper range limit of the injection line Micro Motions.

DAS zero readings were recorded and the screen approach and injection line velocities adjusted to 0.1 ft/sec and 0.8 ft/sec, respectively except as noted above. After the adjustment of the flow rates, the test loop was considered ready for debris injection.

5.3.1.1 Debris Preparation

The NUKON debris preparation for all test series except the Benchmark series targeted an R4 value of 11 ± 1 . The debris preparation was conducted as specified in Section 3.3. The variations to the debris preparation for the Benchmark tests are discussed in Section 5.1.2.

The debris preparation was always performed after the test loop had been prepared for testing and the initial screen approach and injection line velocities had been set. Following preparation, the debris slurry was continually agitated as it was taken from the wet lab to the test loop.

5.3.1.2 Debris Injection and Debris Bed Formation

For the Series 1 tests, the CalSil and NUKON materials were prepared separately and introduced into the loop using independent injection loops for each constituent. The constituents were introduced into the test loop simultaneously but had no interaction before entry into the test loop. Based on the variation in the head loss measurements obtained between tests from the Series 1 tests, it was postulated that the Series 1 debris introduction procedure created variability in the sequence at which debris material arrived at the test screen. To investigate the variation observed in the Series 1 head loss measurements, the debris loading sequence investigation presented in Section 6.3 was conducted. Following the investigation of the loading sequence, the NRC staff decided that future tests would be conducted by premixing the debris constituents prior to introduction into the test loop.

For the Benchmark and Series 2 NUKON/CalSil tests, the debris material was prepared separately but then mixed together prior to introduction into the debris injection line. For NUKON-only and CalSil-only tests, no difference existed in the debris injection procedures.

To introduce the debris slurry to the debris injection lines, the flow through the injection line(s) was terminated and the injection-line flex hose isolated. The debris slurry was then poured into the debris injection-line flex hose and water added to fill the hose. The connection of the injection line hose allowed an air bubble to be trapped in the injection line flex hose. With the injection line hose isolated from the rest of the injection line, the air bubble was used to continually agitate (performed manually) and disperse the debris material within the flex hose.

The debris injection system contained two parallel injection lines so that debris constituents could be loaded separately or with a lag time between debris introductions. If the second line was used, the first hose was manually manipulated while the second hose was filled and similarly manipulated. To initiate the introduction of debris to the test loop the debris injection line isolation valves were opened.

The first Series 1 tests were conducted with the screen approach velocity initially set to 0.2 ft/sec, and the pump speed was held constant as debris accumulated on the test screen. The pressure drop across the screen increased with the accumulation of debris on the screen, and the resulting screen approach velocity was allowed to decline. Tests NO4, NC3, and NC14 were conducted in this manner. Following test NC14, NRC staff determined that the debris beds should be formed at a constant screen approach velocity of 0.1 ft/sec. Therefore, for the remainder of the test program, the screen approach velocity was set to 0.1 ft/sec and the pump speed adjusted as needed to maintain the constant screen approach velocity.

Because of the slow buildup in head loss observed during debris bed formation in the benchtop loop, a minimum requirement of 20 loop circulations was specified before the steady-state criterion could be evaluated for the completion of the debris bed formation process. For the first three tests of Series 1, the minimum circulation requirement took approximately 95 minutes, which was extended to 185 minutes (20 circulations at 0.1 ft/sec) for the remainder of the Series 1 tests and the Benchmark tests.

In reviewing the test data for debris bed formation from the Benchmark tests, it was observed that the head loss across the debris bed was fairly constant after approximately 6 to 7 calculated circulations through the loop—approximately one hour. A more substantial impact to the head loss appeared to be created by cycling the screen approach velocity. Therefore, for the Series 2 tests, the minimum bed formation time was reduced to one hour at 0.1-ft/sec screen approach velocity from the time the debris material initially reached the screen/plate.

The DAS recorded instrument readings throughout the debris bed formation process. However, transient head loss associated with debris bed formation is beyond the scope of this report and is not presented. Following the minimum number of circulations (debris bed formation time) required for bed formation, the steady-state criterion was evaluated for acceptance.

The Series 1 tests were conducted at higher screen approach velocities and therefore at higher-pressure drops than the rest of the tests. The Series 1 steady-state criterion used for debris bed formation was less than a 2-in. change in the head loss over a span of 10 minutes.

For the Benchmark and Series 2 tests, the steady-state head loss criterion for debris bed formation following the completion of the minimum number of circulations was an absolute change in head loss of less than 2% over 10 minutes based on a 1-minute running average. The criterion is expressed as

$$0.02 \geq \left| \frac{\Delta P_{t_1} - \Delta P_{t_2}}{\Delta P_{t_1}} \right|$$

where

ΔP_{t_1} = the measured head loss across the bed at time t_1 .

ΔP_{t_2} = the measured head loss across the bed at time t_2 .

$t_1 - t_2 \geq 10$ minutes

Following the completion of the minimum bed formation time and achieving the steady-state criterion, the debris bed was visually observed to determine whether a complete debris bed was formed. A complete debris bed was defined as a debris bed that covered the entire screen leaving no open channels for preferential flow. If a complete debris bed had been formed, the pretest procedure was considered complete, and the test procedure was initiated.

If a complete debris bed had not formed, the following steps were executed:

1. Head loss measurements were taken at 0.1 ft/sec after the bed formation criteria with respect to steady state head loss had been met.
2. The screen approach velocity was increased to 0.2 ft/sec for 20 minutes and observations made as to whether the debris bed formation process was continuing such that channeling would be mitigated. After 20 minutes at 0.2 ft/sec:
 - a. If the visual observation of the debris bed surface indicated the channeling was being mitigated, the head loss was monitored for acceptance of the bed formation criterion assuming time zero started at the completion of the initial 20-minute duration at 0.2 ft/sec.
 - i. If a complete debris bed had formed and no channeling existed, then steady-state data were recorded for test point No. 2 (refer to Table 5.8 in Section 5.3.2), filtering was initiated, and execution of the normal test procedure continued from the point of filtration.
 - ii. If the bed formation criteria were met but channeling existed, proceed to item b.
 - b. If visual observation of the debris bed surface indicated that the channeling was not being reduced and minimal change in the head loss was observed (steady state criterion < 0.05), then filtering was initiated. The velocity sequence matrix in Table 5.8 was replaced with the velocity sequence presented in Table 5.6.

Table 5.6. Truncated Velocity Sequence for an Incomplete Debris Bed

Test Point	Velocity (ft/sec)	Test Phase
Initial condition	0.10	Bed formation
1	0.10	Increase in static pressure of test loop ramp up 1
2 (prefiltering)	0.20	Ramp up 1 (prefiltering)
2 (post-filtering)	0.20	Ramp up 1 (post-filtering)
3	0.10	Ramp down 1
5	0.02	Ramp down 1
6	0.10	Ramp up 2

5.3.2 Test Procedure

While data was recorded throughout the entire debris injection and debris bed formation process, the actual testing was considered to begin after the debris bed had been formed. At the completion of bed formation the following were recorded:

- Optical triangulation photographs of the debris bed (optical triangulation system not available for the Series 1 tests)
- Manual in situ measurements of the debris bed thickness
- Time duration between debris introduction and steady-state head loss readings.

After the minimum bed formation time and the steady-state criterion for debris bed formation had been met, the static pressure of the test loop was increased using the cover gas pressure in the expansion tank. To maintain gas in solution and avoid gas bubbles during testing, the pressure was raised approximately 2.5 atm (37 psi [253 kPa]). After the loop pressure had been set, execution of the velocity sequence was initiated.

For the Series 1 tests, the velocity sequence for each test was determined from the velocities used in the past study (Shaffer et al. 2005). Therefore, the velocity sequence used for each Series 1 test was unique. Tables 5.7 and 5.8 contain the velocity sequences used for the Benchmark and Series 2 tests.

At each test point in the velocity sequence, the head loss was monitored for steady-state conditions. The steady-state criteria were the same as those specified for bed formation with the time duration cut in half. For the peak velocity at the end of each velocity ramp up, the steady-state criterion was the same as that for debris bed formation. After steady-state conditions were reached at each test point, the debris bed was photographed with the optical triangulation system, and in situ manual measurements of the debris bed height were recorded.

For the Series 1 and Benchmark tests, no filtering of the test fluid was performed during the test. For the Series 2 tests, after steady-state conditions were reached at the completion of ramp up 1 (0.2 ft/sec), the entire main line flow was diverted through the 10- μ m bag filter. Filtering was conducted for a minimum of 20 minutes and was maintained until the steady-state criterion for a peak flow was reached. After reaching steady-state conditions, the main-line valve configuration was returned to bypassing the bag filter housing. Testing continued through the remainder of the velocity sequence with no additional filtering.

Table 5.7. Velocity Sequence for the Benchmark Tests

Test Point	Velocity (ft/sec)	Test Sequence
Initial condition	0.10	Bed Formation
1	0.10	Increase in static pressure of test loop Ramp down 1
2	0.05	Ramp down 1
3	0.02	Ramp down 1
4	0.05	Ramp up 1
5	0.10	Ramp up 1
6	0.05	Ramp down 2
7	0.02	Ramp down 2
8	0.10	Ramp up 2
9	0.15	Ramp up 2
10	0.20	Ramp up 2
11	0.15	Ramp down 3
12	0.10	Ramp down 3
13	0.15	Ramp up 3
14	0.20	Ramp up 3
15	0.10	Ramp down 4
16	0.05	Ramp down 4
17	0.02	Ramp down 4
18	0.10	Ramp up 4

Table 5.8. Velocity Sequence for the PNNL Series 2 Tests

Test Point	Velocity (ft/sec)	Test Phase
Initial condition	0.10	Bed Formation
1	0.10	Ramp up 1
2 (prefiltering)	0.20	Ramp up 1 (prefiltering)
2 (post-filtering)	0.20	Ramp up 1 (post-filtering)
3	0.10	Ramp down 1
4	0.05	Ramp down 1
5	0.02	Ramp down 1
6	0.10	Ramp up 2
7	0.20	Ramp up 2
8	0.10	Ramp down 2
9	0.02	Ramp down 2
10	0.10	Ramp up 3
11	0.20	Ramp up 3
12	0.10	Ramp down 3
13	0.02	Ramp down 3
14	0.10	Ramp up 4

At the completion of the velocity sequence, if the test fluid was not to be heated, the test was considered complete, and the post-test procedure was initiated to retrieve the debris bed.

If the test fluid was to be heated, the heaters were turned on to the desired temperature set point. The screen approach velocity was maintained at 0.1 ft/sec, and the fluid temperature was monitored. At the completion of the heat up, the velocity sequence was repeated.

5.3.3 Post-Test Procedures

At the completion of testing, the main objective was to recover the debris bed intact. Debris bed retrieval is discussed in Section 5.3.3.1. The post-test evaluation of the debris bed consisted of obtaining post-test debris bed height measurements with the debris bed still in the TTS and obtaining the dry retrieved mass of the debris bed. The post-test measurements are described in Section 5.3.3.2

The intact NUKON/CalSil debris beds were dissolved to determine the retrieved CalSil mass loading. The CalSil assessment is discussed in Section 5.3.3.3. The other possible post-test evaluation consisted of sectioning the debris bed (see Sections 2.5.4.3 and 6.4). Only debris beds from the benchtop loop were sectioned. No sectioning of the large-scale debris beds was performed, and the sectioning process is not described in this section. The current methodology does not allow a debris bed to be both sectioned and assessed for CalSil content. Both processes use and consume the entire debris bed.

5.3.3.1 Debris Bed Retrieval

The debris bed retrieval procedure will not be described in detail because it was continually being refined to enhance the chances of recovering the intact debris bed. The critical requirements for successfully retrieving the debris beds were:

- Maintaining a positive flow through the debris bed until the water was drained below the debris bed
- Avoiding the release of gas bubbles or exposure of the bed to pressure pulses, either of which could rupture the debris bed or cause the bed to lift off the screen.

Initially, the argon cover gas was used to generate flow through the debris bed and ensure a positive differential pressure existed across the debris bed until the loop was successfully drained and vented. Later in the test program an additional drain valve was added to the discharge of the test loop pump. The drain line allowed the loop's main pump to be used to continually draw flow through the debris bed while discharging fluid from the loop. After the test loop was drained and vented, the TTS was removed from the test loop with the debris bed still intact within the TTS.

5.3.3.2 Post-Test Evaluation

While the debris bed was still intact in the TTS, the top of the TTS was used as a reference plane to obtain a coarse topography of the retrieved debris bed. A metal scale was used to obtain measurements from the debris bed surface to the reference plane at the top of the TTS. The measurements were taken along two perpendicular diameters of the TTS. The reference position of the screen was used to transform the measurements into debris bed heights.

The debris bed and test screen were then removed from the TTS, and the debris bed was photographed. The wet debris bed mass was obtained. The debris bed was placed in a fume hood and allowed an initial drying period at ambient conditions for several hours to several days. Final drying consisted of placing the debris in a 194°F (90°C) oven and periodically measuring the debris bed mass until constant readings were obtained.

5.3.3.3 CalSil Assessment

For the NUKON/CalSil debris beds, the effects of the CalSil mass loading and the CalSil-to-NUKON mass ratio on the resulting pressure drop across the debris bed were to be evaluated. Benchtop testing demonstrated that for some of the proposed NUKON/CalSil mass loadings, the test screen only retained approximately 60 to 85% of the target mass loading based on mass measurements of the initial constituents introduced into the loop and the dry mass of the retrieved debris bed. The benchtop results indicated that for some of the proposed NUKON/CalSil test cases, the uncertainty in the CalSil mass loading based on the mass measurements would be well over 100%.

Therefore, a method was desired to either separate the CalSil from the NUKON or detect the concentration of one of the constituents. After a preliminary investigation, the process of dissolving the debris beds in an HCl solution consisting of 37.6% HCl diluted in DI water at a ratio of 2:3 and detecting the concentration of calcium using a calcium ion selective electrode (ISE) was chosen (see Section 2.5.4.2).

The ISE probe voltage is a function of the calcium concentration in solution. However, there may be other factors (i.e., constituents) that influence the resulting ISE probe reading when submerged in an unknown solution. The approach used for assessing the CalSil mass content was to correlate the CalSil concentration in performance standards with the ISE probe voltage. To develop the performance curve, performance standards of varying CalSil concentrations in HCl solutions were generated over the range of interest defined by the spectrum of target CalSil mass loadings in the varying test series. Based on the effective concentration range of the ISE probe, which is ion specific, aliquots were prepared from the performance standards. The process of preparing the aliquots included adding sodium hydroxide (NaOH) to neutralize them to a pH of 7 and adding potassium chloride (KCl) as an ionic strength adjuster.

Because the ISE probe readings can change with time due to aging or contamination of the membrane, a fixed performance curve was not used. The aliquots from the performance standards were measured at the time that aliquots from the debris beds were evaluated. Therefore, the performance curves were generated for a specific set of measurements taken at a specific time. The objective was to obtain relative probe readings from known samples and correlate the readings to the CalSil concentration. The probe reading from the debris bed sample was then used to predict a CalSil concentration in the debris bed aliquot through inverse linear regression. Knowing the dilution used to generate the debris bed aliquot, the concentration of CalSil in the dissolved debris sample can then be calculated.

In developing the performance curve for the ISE probe, the following parameters should be considered:

- the number of CalSil concentrations at which performance standards are made
- the number of performance standards made for each concentration
- the number of aliquots drawn from each performance standard
- the number of readings taken in each aliquot
- the number of ISE probes used to obtain the readings.

Based on the time and resources required to perform the assessment, it is much more efficient to evaluate a suite of debris beds at one time rather than one debris bed at a time. The assessment of the Series 1 debris beds was performed based on the experience of the initial evaluation used to assess the methodology and develop the initial procedures. The assessment of the Series 2 debris beds was able to take advantage of the lessons learned from the Series 1 debris bed assessment. Based on the results of the Series 1 CalSil assessment, statistical modeling was used to optimize the test plan for generating the performance curves to reduce the uncertainty of the results. The modeling took into account the resources available to conduct the test, so that the uncertainty was optimized with respect to the resources allocated for the task. For the parameters listed above, Table 5.9 lists the values used for the Series 1 and Series 2 CalSil assessments of the NUKON/CalSil debris beds.

This optimization is the reason for the significant difference between the 95% upper and lower inverse confidence limits reported for the Series 1 and 2 CalSil mass loadings reported in Section 7.4. Not all of the measurements obtained for the Series 1 data were fully analyzed; therefore, additional analyses of the Series 1 data could reduce the difference between the upper and lower confidence limits reported for the Series 1 results.

Table 5.9. Parameter List for Developing the ISE Probe Performance Curves

Parameter Description	Values for Series 1 CalSil Assessment Performance Curve	Values for Series 2 CalSil Assessment Performance Curve
Number of CalSil concentrations used to generate performance curve	5	5
Number of performance standards generated for each CalSil concentration	1	4
Number of aliquots prepared from each performance standard	1	3
Number of probe readings made in each aliquot	1	1
Number of ISE probes used to take readings	2	1

6.0 Phenomenological Results and Discussion

To ensure the adequacy of the data obtained from tests performed on the large-scale loop, testing was conducted in the benchtop loop to evaluate the effect of parameters associated with the initial conditions on the measured pressure drop across debris beds. These parameters are potential sources of variability and may explain differences observed between the results of the PNNL tests and other testing efforts. An example of such a parameter is the degree of debris disassociation or fragmentation discussed in Section 3.2.1.2. This section discusses the results obtained for the following four parameters:

- Debris preparation associated with presoaking fiber material at elevated temperature to simulate a 30-minute lag time between the occurrence of a LOCA and the start of the sump recirculation (Section 6.1).
- Sump screen material (Section 6.2).
- The debris loading sequence used to generate the debris bed. Section 6.3 contains the pressure drop measurements for various debris loading sequences, and Section 6.4 presents observations made using SEM.
- The flow history to which the debris bed has been subjected (Section 6.5). The effects of time at flow and the cycling of the approach velocity are discussed.

6.1 Debris Preparation

Section 3.2.3.3 shows that NUKON debris preparation accomplished by mixing in a blender can significantly affect debris bed formation and subsequent head loss results. The degree of disassociation or fragmentation of the insulation material to create debris is quantified using the R4 metric discussed in Section 3. Previous investigations of the head loss associated with NUKON debris beds prepared the debris by boiling it for 10 to 15 minutes to break down organic binders before introducing it to the loop (Shaffer et al. 2005). Based on conversations with Dr. W.J. Shack at ANL, other researchers presoaked the debris material in 140°F water for 30 minutes before introducing it into the loop to simulate the approximately 30-minute delay that would exist between the occurrence of a LOCA and the start of the sump recirculation. Boiling the NUKON debris, both before and after blender preparation, apparently reduces the R4 metric for the debris, as discussed in Section 3.1.2.

Debris bed loading conditions similar to Test Case 1a from NUREG/CR-6874 (Shaffer et al. 2005), which was a NUKON-only test with a debris loading of 1681.4 g/m², have been used to study some effects of varying debris preparation procedures. This test condition will be referred to as NOBT1a. Repeat tests in the benchtop loop for test condition NOBT1a using both boiled and non-boiled debris material are considered to evaluate the effects on resulting debris bed formation and head loss.

6.1.1 Test Conditions

Tests were conducted in the PNNL benchtop loop (Section 2.3) using the test procedures similar to those summarized in Section 5.3. All NUKON debris (the bulk of the benchtop loop tests were conducted using the initial shredded NUKON that had no specific lot number; see Section 3) was prepared to an R4 value of 10–12 for each test. Some of the debris was tested without prior boiling; other samples of debris were boiled at 212°F (100°C) for 10 minutes, allowed to cool to approximately 86°F (30°C) with frequent

mixing using a kitchen spatula, then introduced into the loop. The target debris loading of 1681.4 g/m^2 corresponds to 13.63 g of NUKON debris for the 4 in.-diameter test section of the benchtop loop. All of these tests employed a perforated plate as the sump screen material, which is described in Section 2.2.

An initial screen approach velocity of 0.20 ft/sec (0.06 m/s) was used to form the debris bed. The velocity was allowed to decay over the 20-minute bed formation time (constant pump speed), resulting in approximately 27 circulations through the loop. Debris bed formation was considered complete when steady conditions were achieved for the preset pump speed. The steady-state criterion for bed formation and at each recorded velocity was assumed to be achieved when the pressure drop exhibited a change of less than 2-in. of H_2O over a 5-minute period. All reported pressure drop measurements are for steady-state conditions. Pressure drops are reported in inches of H_2O at a reference temperature of 68°F (20°C).

The velocity sequence used for Test Case 1a (Shaffer et al. 2005) was used as the basis for selecting the velocity sequence to be used for test condition NOBT1a. This is the same velocity sequence used for large-scale test cases NO6 and NO7. To reduce the test time, the velocity sequence was truncated. Also the limitations of the benchtop loop precluded testing at the peak velocities obtained for Test Case 1a during previous work (Shaffer et al. 2005). The tables presented in Sections 6.1.2 and 6.2.2 contain blank lines to represent Test Case 1a test points that were skipped during the individual benchtop loop tests.

Two non-boiled tests, 060228_NO_1363_BP2 and 060421_NO_1363_BP1, and three BAP tests, 060327_NO_1363_BP1, 060328_NO_1363_BP1, and 060523_NO_1363_BAP1 were conducted. An additional BAP test, 060324_NO_1363_BP1, was conducted, but contamination of the debris bed with rust particulate rendered the data suspect, and those results are not included in this evaluation. The rust contamination consisted of flakes of material that were readily visible. Visual observation of the retrieved bed determined whether contamination was present. The replacement of some loop components and a change in the loop preparation procedures greatly reduced the occurrence and severity of contamination.

6.1.2 Test Results

Head-loss results as a function of screen approach velocity for the non-boiled and boiled prepared NUKON debris for test condition NOBT1a are presented in Table 6.1. The percent difference and average of the measured head loss for corresponding velocities for the non-boiled and boiled tests are provided in Table 6.2. Comparison is made based on the averages.

The differences in the non-boiled and boiled results are similar to the respective non-boiled and boiled differences. However, the results of the boiled tests are typically lower. Thus, the results indicate that boiling the debris results in lower head loss for the same preparation conditions.

Different results may be obtained due to boiling if the debris preparation procedures are different than those described for the non-boiled and boiled tests (consider debris preparation results in Section 3). It was shown, as depicted in Figure 6.1, as a function of the R4 metric, that the head loss increased with increasing blender preparation time (lower R4) to a point approximately coincident with the chosen PNNL NUKON debris preparation target R4 value and then began to decrease. It was also shown that boiling the debris reduced the R4 metric result. Thus, boiling, which has been shown to decrease the R4 metric, might be expected to increase head loss if a larger initial value of R4 was used (right side of Figure 6.1). In contrast, for PNNL testing with debris prepared near peak head loss with respect to R4, boiling (i.e., decreasing R4) would be expected to reduce the head loss (left side of Figure 6.1).

Table 6.1. Benchtop Non-Boiled and Boiled Debris Results for Test Condition NOBT1a^(a)

Test Preparation	060228_NO_1363_BP2 Non-Boiled		060421_NO_1363_BP1 Non-Boiled		060327_NO_1363_BP1 Boiled		060328_NO_1363_BP1 Boiled		060523_NO_1363_BAP1 Boiled	
Test Phase	Screen Approach Velocity (ft/sec)	Head Loss (in. H ₂ O) ^(b)	Screen Approach Velocity (ft/sec)	Head Loss (in. H ₂ O) ^(b)	Screen Approach Velocity (ft/sec)	Head Loss (in. H ₂ O) ^(b)	Screen Approach Velocity (ft/sec)	Head Loss (in. H ₂ O) ^(b)	Screen Approach Velocity (ft/sec)	Head Loss (in. H ₂ O) ^(b)
Ramp up 1	0.13	23	0.14	30	0.14	27	0.14	31	0.15	34
	0.20	39	0.20	46	0.20	40	0.20	41	0.20	46
	0.40	86	0.40	103	0.40	103	0.40	104	0.40	118
	0.57	164	0.57	167	0.57	160	0.57	157	0.57	183
	0.70	227	0.70	226	0.70	215	0.70	195	0.70	237
	0.88	322	0.88	343	0.88	293	0.88	266	0.88	326
Ramp down 1	Point skipped	NA	Point skipped	NA	Point skipped	NA	Point skipped	NA	Point skipped	NA
	0.70	245	0.70	257	0.70	219	0.70	199	0.70	244
	0.56	187	0.56	196	0.56	165	0.56	149	0.56	185
	0.41	129	0.41	134	0.41	113	0.41	102	0.41	126
	0.20	55	0.20	57	0.20	47	0.20	42	0.20	54
Ramp up 2	0.30	90	0.30	93	0.30	77	0.30	69	0.30	88
	0.41	129	0.41	134	0.41	113	0.41	103	0.41	130
	0.56	193	0.56	198	0.56	166	0.56	152	0.56	187
	0.71	263	0.71	269	0.71	225	0.71	208	0.71	250
	0.88	355	0.88	362	0.88	302	0.88	278	0.88	336
Ramp down 2	Point skipped	NA	Point skipped	NA	Point skipped	NA	Point skipped	NA	Point skipped	NA
	Point skipped	NA	Point skipped	NA	Point skipped	NA	Point skipped	NA	Point skipped	NA
	Point skipped	NA	Point skipped	NA	Point skipped	NA	Point skipped	NA	Point skipped	NA
	Point skipped	NA	Point skipped	NA	Point skipped	NA	Point skipped	NA	Point skipped	NA
	Point skipped	NA	Point skipped	NA	Point skipped	NA	Point skipped	NA	Point skipped	NA
	Point skipped	NA	Point skipped	NA	Point skipped	NA	Point skipped	NA	Point skipped	NA
Ramp up 3	0.30	93	0.30	96	0.30	79	0.30	71	0.30	88
	0.88	360	0.88	372	0.88	304	0.88	284	0.88	341
	Point skipped	NA	Point skipped	NA	Point skipped	NA	Point skipped	NA	Point skipped	NA
Ramp down 3	Point skipped	NA	Point skipped	NA	Point skipped	NA	Point skipped	NA	Point skipped	NA
	Point skipped	NA	Point skipped	NA	Point skipped	NA	Point skipped	NA	Point skipped	NA
	Point skipped	NA	Point skipped	NA	Point skipped	NA	Point skipped	NA	Point skipped	NA
	Point skipped	NA	Point skipped	NA	Point skipped	NA	Point skipped	NA	Point skipped	NA
	0.2	57	0.2	60	0.2	48	0.2	44	0.2	54
Ramp up 4	Point skipped	NA	Point skipped	NA	Point skipped	NA	Point skipped	NA	Point skipped	NA
	Point skipped	NA	Point skipped	NA	Point skipped	NA	Point skipped	NA	Point skipped	NA
	Point skipped	NA	Point skipped	NA	Point skipped	NA	Point skipped	NA	Point skipped	NA
Ramp down 4	Point skipped	NA	Point skipped	NA	Point skipped	NA	Point skipped	NA	Point skipped	NA
	Point skipped	NA	Point skipped	NA	Point skipped	NA	Point skipped	NA	Point skipped	NA
	Point skipped	NA	Point skipped	NA	Point skipped	NA	Point skipped	NA	Point skipped	NA
	Point skipped	NA	Point skipped	NA	Point skipped	NA	Point skipped	NA	Point skipped	NA
	Point skipped	NA	Point skipped	NA	Point skipped	NA	Point skipped	NA	Point skipped	NA
Ramp up 5	Point skipped	NA	Point skipped	NA	Point skipped	NA	Point skipped	NA	Point skipped	NA
	Point skipped	NA	Point skipped	NA	Point skipped	NA	Point skipped	NA	Point skipped	NA

(a) The blank lines represent velocity points in the original test case 1a velocity sequence that were skipped during the individual benchtop loop tests.

(b) In. of H₂O are for a reference temperature of 68°F (20°C).

Table 6.2. Comparison of Results for Benchtop Non-Boiled and Boiled Debris Results for Test Condition NOBT1a^(a)

Test Phase	Screen Approach Velocity (ft/sec)	% Difference Between PNNL Non-Boiled Tests (%)	Non-Boiled Average (in. H ₂ O) ^(a)	% Difference Boiled Test 1 to 2	% Difference Boiled Test 1 to 3	% Difference Boiled Test 2 to 3	Boiled Average (in. H ₂ O) ^(a)	% Difference Non-Boiled to Boiled
Ramp up 1	0.14	30	27	15	26	10	31	16
	0.20	18	43	3	15	12	42	0
	0.40	20	95	1	15	13	108	15
	0.57	2	166	-2	14	17	167	1
	0.70	0	227	-9	10	22	216	-5
	0.88	7	333	-9	11	23	295	-11
Ramp down 1	0.70	5	251	-9	11	23	221	-12
	0.56	5	192	-10	12	24	166	-13
	0.41	4	132	-10	12	24	114	-14
Ramp up 2	0.20	4	56	-11	15	29	48	-15
	0.30	3	92	-10	14	28	78	-15
	0.41	4	132	-9	15	26	115	-12
	0.56	3	196	-8	13	23	168	-14
	0.71	2	266	-8	11	20	228	-14
	0.88	2	359	-8	11	21	305	-15
Ramp down 2	Point skipped	NA	NA	NA	NA	NA	NA	NA
Ramp up 3	0.30	3	95	-10	11	24	79	-16
	0.88	3	366	-7	12	20	310	-15
Ramp down 3	0.2	5	59	-8	13	23	49	-17
Ramp up 4	Point skipped	NA	NA	NA	NA	NA	NA	NA
Ramp down 4	Point skipped	NA	NA	NA	NA	NA	NA	NA
Ramp up 5	Point skipped	NA	NA	NA	NA	NA	NA	NA

(a) Inches. of H₂O are for a reference temperature of 68°F (20°C).

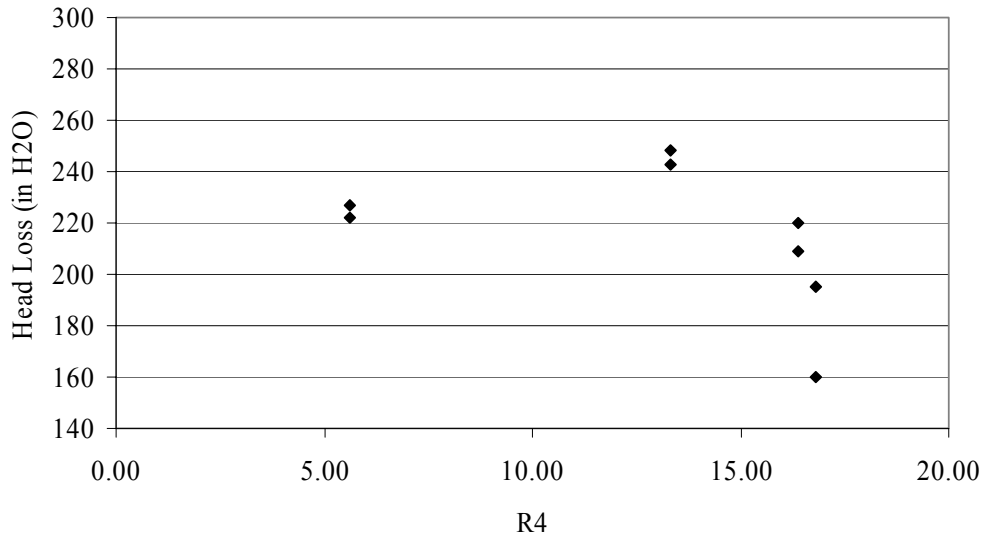


Figure 6.1. Debris Bed Head Loss as a Function of R4 for a Target Debris Loading of 1449.5 g/m²

The non-boiling to boiling test results were considered in regards to the readily quantifiable aspects of debris bed formation: height, mass, and appearance. The representative approximate debris bed body heights for the tests are given in Table 6.3 along with the dry retrieval debris bed mass and computed density. The measured debris bed heights are referred to as approximate because of the limitations of the measurement technique; the debris bed “body” measurements (plane area of the bed, not the outer rim) are inferred from a 1-mm-increment ruler placed beside the debris bed in a vertical orientation. This gross technique is only employed for the benchtop evaluations and provides a relative means of comparison. The dry retrieved debris bed mass is approximately equivalent across the tests, while the representative height apparently increases, thereby reducing the computed density. The highest head loss results are achieved for the highest density debris bed, 060421_NO_1363_BP1. Thus, considering the minimal differences and approximate nature of the results, boiling the debris is apparently discernable in the resulting height and mass of the debris bed.

The visual appearance of the debris beds in Figures 6.2, 6.3, 6.4, 6.5 and 6.6 does not provide any evidence that head loss differences may be expected (see Section 3.2.3.3 related debris bed appearance as a function of debris preparation to head loss).

Table 6.3. Benchtop Non-Boiling and Boiling Preparation Debris Bed Data for Test Condition NOBT1a

Test	Preparation	Approximate Measured Debris Bed Body Height (in.)	Dry Debris Bed Mass (g)	Computed Density (g/mL)
060228 NO 1363 BP2	Non-boiled	0.35	12.53	0.17
060421 NO 1363 BP1	Non-boiled	0.31	12.96	0.20
060327 NO 1363 BP1	boiled	0.39	12.93 ^(a)	0.16
060328 NO 1363 BP1	boiled	0.39	12.81 ^(a)	0.16
060523 NO 1363 BAP1	boiled	0.43	13.05	0.15

(a) Rust flakes from benchtop loop components were visually observable on the debris bed. The mass of this contaminant is not readily quantifiable.



Figure 6.2. 060228_NO_1363_BP2, Non-Boiled



Figure 6.3. 060421_NO_1363_BP1, Non-Boiled



Figure 6.4. 060327_NO_1363_BP1, Boiled



Figure 6.5. 060328_NO_1363_BP1, Boiled



Figure 6.6. 060523_NO_1363_BAP1, Boiled

6.2 Sump Screen Material Comparison

PNNL employed both 5-mesh screen and a perforated plate with 1/8-inch-diameter holes as sump screen material. (Refer to Section 2.2 for descriptions of the sump screen materials.) Repeat tests in the bench-top loop with test condition NOBT1a (NUKON-only, target debris loading 1681.4 g/m^2) using both the

5-mesh screen and the perforated plate as sump screen material are considered to evaluate the effect on the resulting debris bed formation and head loss.

6.2.1 Test Conditions

Tests were conducted in the PNNL benchtop loop using test procedures similar to those discussed in Section 5.3. All NUKON debris material (i.e., the initial shredded NUKON with no specified lot number, as discussed in Section 3), was prepared to an R4 value of 11 ± 1 for each test. The target debris loading of 1681.4 g/m^2 corresponds to 13.63 g of NUKON debris for the 4-in.-diameter test section of the benchtop loop.

An initial screen approach velocity of 0.20 ft/sec (0.06 m/s) was used to form the debris bed. The velocity was allowed to decay over the 20-minute bed formation time (constant pump speed), resulting in approximately 27 circulations through the loop. Debris bed formation was determined to be complete when steady-state conditions were achieved for the preset pump speed. The steady-state criterion for bed formation and at each recorded velocity was assumed to be achieved when the pressure drop exhibited a change of less than 2-in. H₂O over a 5-minute period. Pressure drop readings were taken after steady-state conditions were achieved after bed formation and after steady-state conditions were reached at a matrix of predefined velocities. All reported pressure drop measurements are for steady-state conditions. Pressures are reported in inches of H₂O at a reference temperature of 68°F (20°C).

The velocity sequence used for Test Case 1a (Shaffer et al. 2005) was used as the basis for selecting the velocity sequence to be used for test condition NOBT1a. This is the same velocity sequence used for the large-scale test cases NO6 and NO7. To reduce the test time, the velocity sequence was truncated. Also, the limitations of the benchtop loop precluded testing at the peak velocities obtained for Test Case 1a during previous work (Shaffer et al. 2005). The tables presented in Sections 6.1.2 and 6.2.2 contain blank lines to represent Test Case 1a test points that were skipped during the individual benchtop loop tests.

Two tests were conducted with the 5-mesh screen, 060223_NO_1363_B1 and 060228_NO_1363_B1, and two tests were conducted with the perforated plate, 060228_NO_1363_BP2 and 060421_NO_1363_BP1.

6.2.2 Test Results

Head loss results from the benchtop loop as a function of screen approach velocity for the 5-mesh screen and perforated plate conducted at test condition NOBT1a are presented in Table 6.4. The percent difference and average of the measured head loss for corresponding velocities for the two materials are also provided in Table 6.4. Average values are compared in the table.

The differences between the measured head loss for 5-mesh screen and perforated plate were not sufficiently distinct from the respective 5-mesh and plate differences to make a conclusion about whether the sump screen material significantly affected the debris bed head loss. These results are considered with regard to the readily quantifiable aspects of debris bed formation, height, mass, and appearance.

The representative approximate debris bed body heights for the tests are given in Table 6.5 along with the dry retrieval debris bed mass. (The measured debris bed heights are referred to as approximate because of the limitations of the measurement technique; the debris bed body measurements (plane area of the bed, not the outer rim) are inferred from a 1-mm-increment ruler placed vertically beside the debris bed. This

Table 6.4. Benchtop 5-Mesh and Plate Test Results for Test Condition NOBT1a

Test	060223_NO_1363_B1		060228_NO_1363_B1		060228_NO_1363_BP2		060421_NO_1363_BP1		Comparison				
Sump Screen	5-mesh		5-mesh		Plate		Plate						
Test Phase	Screen Approach Velocity (ft/sec)	Head Loss (in. H ₂ O) ^(a)	Screen Approach Velocity (ft/sec)	Head Loss (in. H ₂ O) ^(a)	Screen Approach Velocity (ft/sec)	Head Loss (in. H ₂ O) ^(a)	Screen Approach Velocity (ft/sec)	Head Loss (in. H ₂ O) ^(a)	% Difference 5-Mesh	5-Mesh Average (in. H ₂ O) ^(a)	% Difference Plate	Plate Average (in. H ₂ O) ^(a)	% Difference Plate to 5-mesh
Ramp up 1	0.16	35	0.16	28	0.13	23	0.14	30	-20.0	32	30.4	27	-15.9
	0.20	45	0.2	43	0.20	39	0.20	46	-4.4	44	17.9	43	-3.4
	0.40	112	0.4	89	0.40	86	0.40	103	-20.5	101	19.8	95	-6.0
	0.57	203	0.57	161	0.57	164	0.57	167	-20.7	182	1.8	166	-9.1
	0.70	246	0.7	206	0.70	227	0.70	226	-16.3	226	-0.4	227	0.2
	0.88	344	0.88	304	0.88	322	0.88	343	-11.6	324	6.5	333	2.6
	Point skipped	NA	Point skipped	NA	Point skipped	NA	Point skipped	NA	NA	NA	NA	NA	NA
Ramp down 1	Point skipped	NA	Point skipped	NA	Point skipped	NA	Point skipped	NA	NA	NA	NA	NA	NA
	0.70	265	0.7	226	0.70	245	0.70	257	-14.7	246	4.9	251	2.2
	0.56	202	0.56	168	0.56	187	0.56	196	-16.8	185	4.8	192	3.5
	0.41	147	0.41	122	0.41	129	0.41	134	-17.0	135	3.9	132	-2.2
	0.20	70	0.2	45	0.20	55	0.20	57	-35.7	58	3.6	56	-2.6
Ramp up 2	0.30	104	0.3	89	0.30	90	0.30	93	-14.4	97	3.3	92	-5.2
	0.41	148	0.41	126	0.41	129	0.41	134	-14.9	137	3.9	132	-4.0
	0.56	227	0.56	187	0.56	193	0.56	198	-17.6	207	2.6	196	-5.6
	0.71	297	0.71	246	0.71	263	0.71	269	-17.2	272	2.3	266	-2.0
	0.88	398	0.88	324	0.88	355	0.88	362	-18.6	361	2.0	359	-0.7
	Point skipped	NA	0.96	NA	Point skipped	NA	Point skipped	NA	NA	NA	NA	NA	NA
Ramp down 2	Point skipped	NA	0.88	NA	Point skipped	NA	Point skipped	NA	NA	NA	NA	NA	NA
	Point skipped	NA	0.69	236	Point skipped	NA	Point skipped	NA	NA	NA	NA	NA	NA
	Point skipped	NA	0.56	188	Point skipped	NA	Point skipped	NA	NA	NA	NA	NA	NA
	Point skipped	NA	0.4	127	Point skipped	NA	Point skipped	NA	NA	NA	NA	NA	NA
	Point skipped	NA	0.29	86	Point skipped	NA	Point skipped	NA	NA	NA	NA	NA	NA
	Point skipped	NA	0.2	47	Point skipped	NA	Point skipped	NA	NA	NA	NA	NA	NA
Ramp up 3	0.30	104	0.3	88	0.30	93	0.30	96	-15.4	96	3.2	95	-1.6
	0.88	416	0.88	322	0.88	360	0.88	372	-22.6	369	3.3	366	-0.8
	Point skipped	NA	0.96	NA	Point skipped	NA	Point skipped	NA	NA	NA	NA	NA	NA
Ramp down 3	Point skipped	NA	0.87	NA	Point skipped	NA	Point skipped	NA	NA	NA	NA	NA	NA
	Point skipped	NA	0.7	245	Point skipped	NA	Point skipped	NA	NA	NA	NA	NA	NA
	Point skipped	NA	0.41	126	Point skipped	NA	Point skipped	NA	NA	NA	NA	NA	NA
	Point skipped	NA	0.29	84	Point skipped	NA	Point skipped	NA	NA	NA	NA	NA	NA
	Point skipped	NA	0.2	55	0.2	57	0.2	60	NA	NA	5.3	58.5	NA
	Point skipped	NA	0.41	130	Point skipped	NA	Point skipped	NA	NA	NA	NA	NA	NA
Ramp up 4	Point skipped	NA	0.7	263	Point skipped	NA	Point skipped	NA	NA	NA	NA	NA	NA
	Point skipped	NA	0.96	NA	Point skipped	NA	Point skipped	NA	NA	NA	NA	NA	NA
	Point skipped	NA	0.69	NA	Point skipped	NA	Point skipped	NA	NA	NA	NA	NA	NA
	Point skipped	NA	0.41	130	Point skipped	NA	Point skipped	NA	NA	NA	NA	NA	NA
	Point skipped	NA	0.2	63	Point skipped	NA	Point skipped	NA	NA	NA	NA	NA	NA
	Point skipped	NA	0.1	31	Point skipped	NA	Point skipped	NA	NA	NA	NA	NA	NA
Ramp down 4	Point skipped	NA	0.05	6	Point skipped	NA	Point skipped	NA	NA	NA	NA	NA	NA
	Point skipped	NA	0.02	6	Point skipped	NA	Point skipped	NA	NA	NA	NA	NA	NA
	Point skipped	NA	0.1	31	Point skipped	NA	Point skipped	NA	NA	NA	NA	NA	NA
	Point skipped	NA	0.2	68	Point skipped	NA	Point skipped	NA	NA	NA	NA	NA	NA
	Point skipped	NA	0.1	31	Point skipped	NA	Point skipped	NA	NA	NA	NA	NA	NA
	Point skipped	NA	0.2	68	Point skipped	NA	Point skipped	NA	NA	NA	NA	NA	NA

(a) In. of H₂O are for a reference temperature of 68°F (20°C).

Note: The blank lines (point skipped) represent velocity points in the original Test "Case 1a velocity sequence that were skipped during the individual benchtop loop tests.

gross technique is employed only for the benchtop evaluations and provides a qualitative means of comparison.) For both the 5-mesh screen and the perforated plate, the head loss is elevated for those tests with more mass retained in the debris bed. The trend is not apparent between the sump screen materials; however, as the 5-mesh test 060228_NO_1363_B1 yielded lower head loss results than the plate test, 060421_NO_1363_BP1, which has a lower retained dry debris bed mass. (The unquantified contaminant mass [see Table 6.5] is ignored.) However, the indicated decrease in debris bed body height for test 060421_NO_1363_BP1 results in the greater computed density (see Table 6.5), suggesting that the discussed “mass-trend” discrepancy is therefore plausible. The “density effect” is not consistent (head loss trend with density) either, however. Thus, it is not possible to correct for debris bed formation conditions to further evaluate sump screen material effects.

Likewise, the visual appearance of the debris beds in Figures 6.7, 6.8, 6.9, and 6.10 does not provide any evidence that head loss differences may be expected (see Section 3.2.3.3 for related debris bed appearance as a function of debris preparation to head loss).

6.3 Debris Loading Sequence

As reported in *Quick-Look Report for PNNL Test 051128_NC_2776_L2, Test Case 6e2 Conditions*, in Appendix J, the values of the head loss measured during that test were significantly higher than those obtained from previous tests of debris beds with the same and similar target mass constituent ratios (0.5 and 0.55) and the same (1522 g/m²) and greater (up to 2246.7 g/m²) total target mass loadings (see Figure 6.11). The evaluation of the impact the debris loading sequence has on the head loss was initiated in an attempt to explain the elevated head loss measurements obtained for test 051128_NC_2776_L2. Test Cases 6e and 6e2 are identifications used by the previous head loss investigation reported in NUREG/CR-6874 (Shaffer et al. 2005) and are similar to tests replicated for the Series 1 test matrix (see Section 5.1). Test Cases 6e and 6e2 correspond to PNNL Test Cases NC12 and NC13; the target mass loadings for this test condition are 993 g/m² of NUKON and 496 g/m² of CalSil for a total mass loading of 1489 g/m²

The head loss measured for 051128_NC_2776_L2 (test case NC13) was approximately twice that of test 051117_NC_2776_L1 (test case NC12), even with approximately 6% less measured mass (based on post-test measurements) retained on the screen. Head loss results from test 051117_NC_2776_L1 (test case NC14) appear to trend, in terms of higher head loss with higher target debris loading, with tests 051110_NC_0595_L1 (test case NC3), 051121_NC_1587_L1 (test case NC7), and 051115_NC_4098_L1 (test case NC14). Based on the results presented in Figure 6.11, test 051123_NC_2181_L1 is observed to also have elevated (out of the trend) head loss results.

Initial benchtop tests (prior to the initiation of large-scale loop testing) with debris beds generated from the same target mass constituent ratio and a target debris loading of 2174.2 g/m² produced similar dramatic variations in the measured debris bed head loss. For two of these tests, the pump in the benchtop loop was effectively insufficient to provide flow through the bed, while for two other tests, flow was easily maintained. These four referenced tests, 050831_NC_1763_1, 050831_NC_1763_2, 050901_NC_1763_1, and 050901_NC_1763_2, were performed as part of an initial scoping evaluation to evaluate the suitability of the debris loading techniques; head loss as a function of screen approach velocity was not investigated.

Table 6.5. Benchtop 5-mesh Screen and Perforated Plate Debris Bed Data for Test Condition NOBT1a

Test	Screen Material	Approximate Measured Debris Bed Body Height (in)	Dry Debris Bed Mass (g)	Computed Density (g/mL)
060223 NO 1363 B1	5-mesh	0.35	13.45	0.18
060228 NO 1363 B1	5-mesh	0.35	13.30 ^(a)	0.18
060228 NO 1363 BP2	plate	0.35	12.53	0.17
060421 NO 1363 BP1	plate	0.31	12.96	0.20

(a) Rust flakes from benchtop loop components were visually observable on the debris bed. The mass of this contaminant is not readily quantifiable.



Figure 6.7. 060223_NO_1363_B1, 5-Mesh



Figure 6.8. 060228_NO_1363_B1, 5-Mesh. Flakes are rust from benchtop loop components.

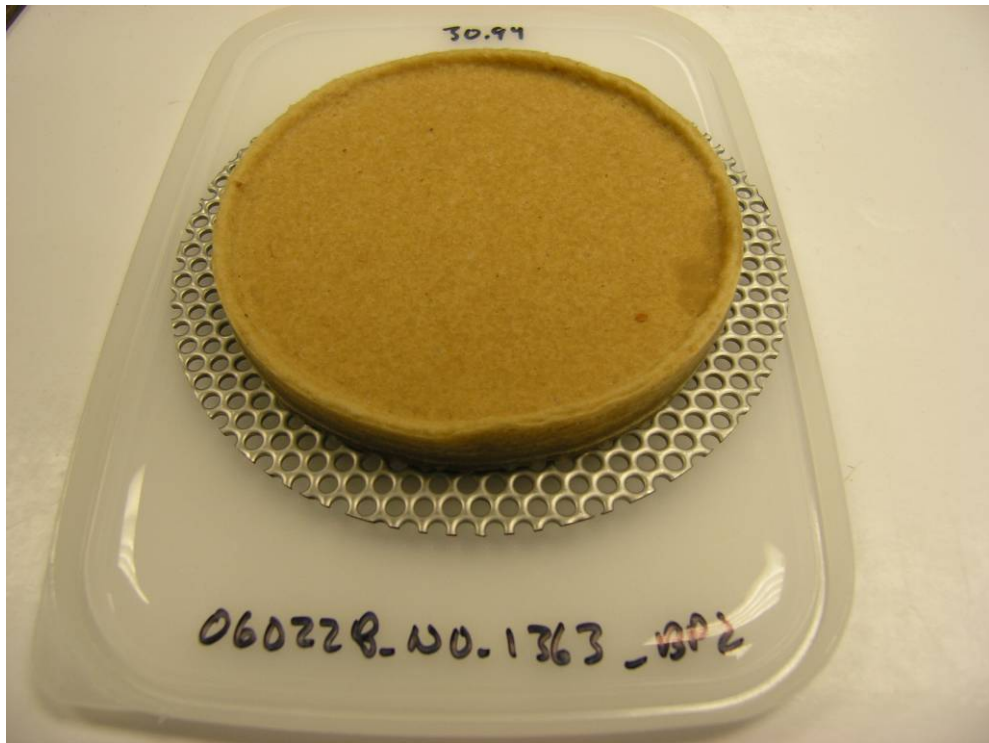


Figure 6.9. 060228_NO_1363_BP2, Plate

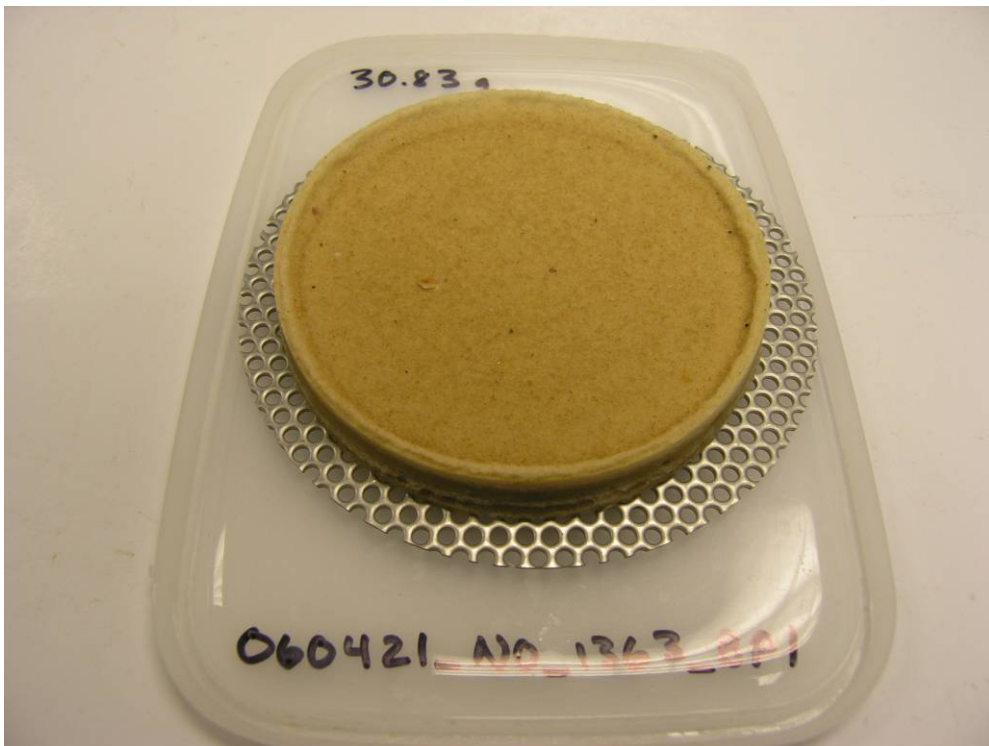


Figure 6.10. 060421_NO_1363_BP1, Plate

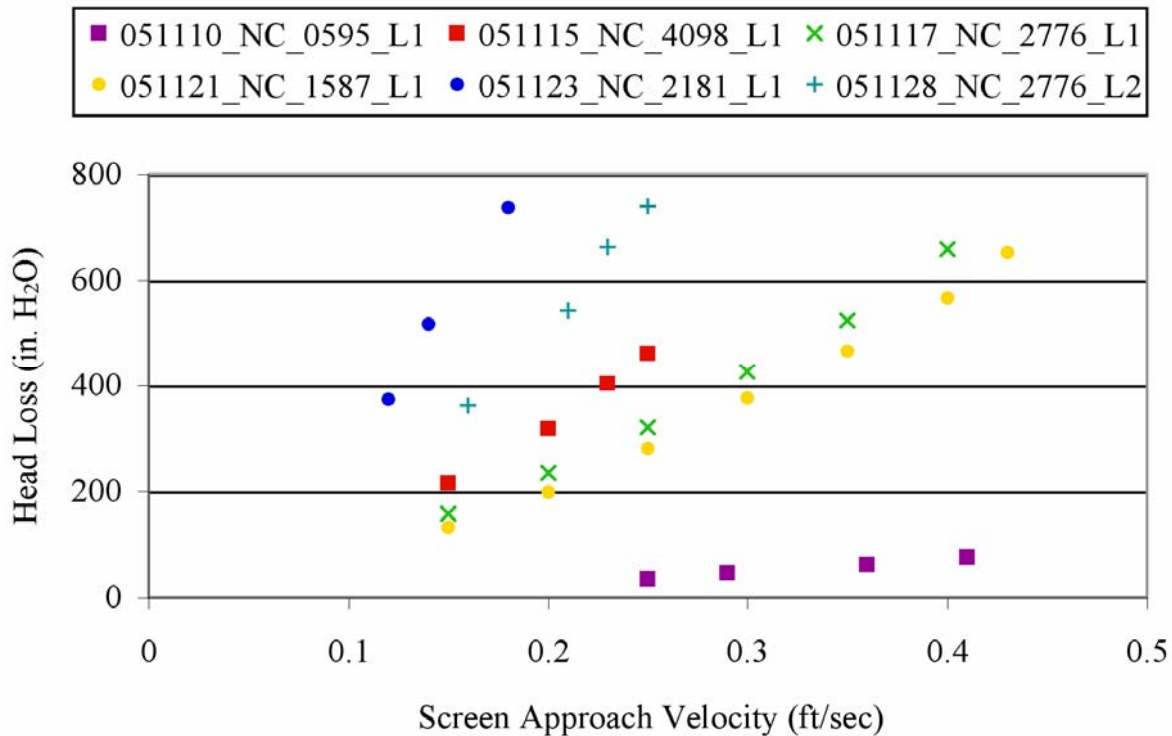


Figure 6.11. Debris Bed Head Loss as a Function of Screen Approach Velocity for NUKON/CalSil Debris Beds Formed in the PNNL Large-Scale Loop During Series 1 Tests. The data points plotted are all from ramp up 3 of each velocity sequence. All of the data are from PNNL Quick-Look Reports, related to each specific test, that are contained in Appendixes H and J.

As was subsequently done in the large-scale loop, the same procedures were followed for each of these benchtop tests, and extreme care was taken to ensure that initial conditions (sample preparation, handling, introduction into loop, etc.) were similar for each test. Simple and rapid out-of-loop tests were conducted to try to identify the cause of the altered debris bed head loss performance (mass to volume considerations depending on NUKON and CalSil slurry handling evaluated via R4 test). No readily apparent mechanisms were identified.

It was suggested by PNNL staff that the relatively high target CalSil to NUKON mass constituent ratio (0.5) may be the cause of the varied results; the extremely high head loss results were not repeated at a mass constituent ratio of 0.25 in the benchtop loop (Tests 050908_NC_1469_1, 050908_NC_1469_2, 050919_NC_1469_1, 051004_NC_1469_1, and 051006_NC_1469_1). These results possibly indicated that there is a critical amount of CalSil particulate that can fill the pore space of the NUKON fibers to drastically reduce the flow paths through a debris bed.

Visual observations made during and after large-scale tests 051123_NC_2181_L1 (Test Case NC13) and 051128_NC_2776_L2 (Test Case NC15) indicated that the initial material reaching the screen was CalSil and that the flow rate in the horizontal sections of the test loop at a screen approach velocity of 0.1 ft/sec (0.03 m/s) was not sufficient to keep the CalSil particulate well mobilized (fully suspended). It was therefore hypothesized that the relatively elevated head loss results discussed above for the large-scale loop were caused by the bulk of the CalSil reaching an already-formed NUKON debris bed. This

scenario could occur in the Series 1 debris introduction scheme if a significant portion of the CalSil were to reach the screen prior to a NUKON debris bed forming or if CalSil particulate settled and resuspended prior to initially reaching the screen. In each case, CalSil particulate that had not been captured by the debris bed would potentially be available to fill in the flow paths through and/or deposit onto a pre-existing NUKON debris bed. This hypothetical post-fibrous layer formation deposition of the particulate CalSil could form a relatively close-packed layer of particulate. The close-packed layer has the potential to have a high resistance to flow resulting in a higher head loss at low flow rates. Benchtop tests were conducted to evaluate the effect of these possible scenarios of debris loading sequence on the resulting debris bed head loss.

6.3.1 Benchtop Loop Investigation

The significantly varied head loss results for debris beds in both the benchtop and large-scale tests with the same target debris loading raised questions regarding both the ability to provide statistically meaningful results with regard to repeatability as well as conservatism of the results in terms of a safety-basis use. The postulated mechanisms whereby head loss results could be significantly altered were therefore investigated. These mechanisms include the following:

- A critical particulate-to-fiber mass ratio exists at which the packing minimizes the bulk debris bed porosity. Depending on debris bed formation conditions, CalSil particulate may deposit more densely into the debris bed flow paths.
- The formation of a closely packed layer of particulate (layer of relatively small diameter particulate having a lower porosity than a layer of relatively large fibers) on the surface of the debris bed. The layer of small particulate forming on the top of the bed is readily conceived. However, it is possible that the close-packed layer could form at the discharge side or exit surface depending on how the bed was formed and how long the bed has been in existence. Loop operation for a longer time period could tend to push the particulates to the outlet end of the debris bed.

6.3.1.1 Benchtop Test Cases

Investigations to assess the potential effects of these postulated mechanisms were conducted in the benchtop loop. The introduced debris mass was scaled to match the target debris loading of tests 051117_NC_2776_L1 (Test Case NC14, Condition 6e) and 051128_NC_2776_L2 (Test Case NC15, Condition 6e2). CalSil-only debris beds with higher target loadings were also investigated. The NUKON and CalSil debris materials were prepared the same as for the Series 1 tests.

A 5-mesh screen was used in the benchtop loop. Debris beds were formed, when possible, at an initial screen approach velocity of 0.2 ft/sec. Two velocity cycles of ramp up and -down cycles were typically conducted. Note that the benchtop loop does not have the degassing capability of the large-scale loop; the quantity of gas in the test section was visually observed to vary to some degree between the test cases. Also, the data presented herein from the instrumentation of the benchtop loop should not be considered to have the same resolution as the Series 1 data from the large-scale loop. All of the test data were recorded electronically; however, the data presented here were recorded manually from the DAS meters displayed on the computer screen. The test cases considered and the associated tests are tabulated in Table 6.6. Individual tests for the same test case indicate repeated tests with the exception of the Case 3 tests and one Case 4 test, as described below.

Table 6.6. Summary of Test Cases Conducted in the Benchtop Loop to Evaluate the Effects of the Debris Loading Sequence

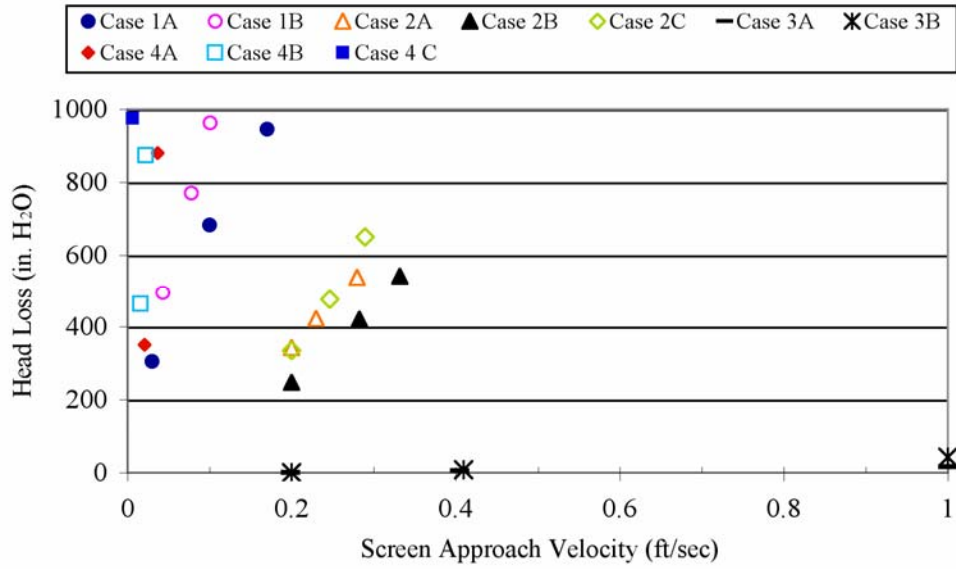
Test Number	Test Case	Test Case Description
051214_NC_1234_B1	1A	Introduction of the CalSil material after a NUKON debris bed has completely formed (steady-state criteria met).
051214_NC_1234_B2	1B	
051215_NC_1234_B1	2A	Introduction of the NUKON and CalSil material as pre-mixed slurry.
051215_NC_1234_B2	2B	
051216_NC_1234_B1	2C	
051227_CO_0411x_B1	3A	Introduction of the CalSil material only. If a CalSil-only debris bed could be formed, NUKON material would be added.
051227_CO_1763_B2	3B	
051228_NC_1234_B1	4A	Introduction of the NUKON material following the CalSil material being introduced into the flow loop. The duration between the CalSil being introduced and the initiation of the NUKON addition is referred to as the “lag time”
051228_NC_1234_B2	4B	
051228_NC_1234_B3	4C	

The possible effect of the delay or lag time for the introduction of the NUKON material for Case 4 has also been considered. In the Case 4 tests of Table 6.6, the NUKON material was introduced when, by visual observation, all of the CalSil material had been introduced into the flow loop. The results from the lag time analysis are presented in subsection 6.3.1.2.1.

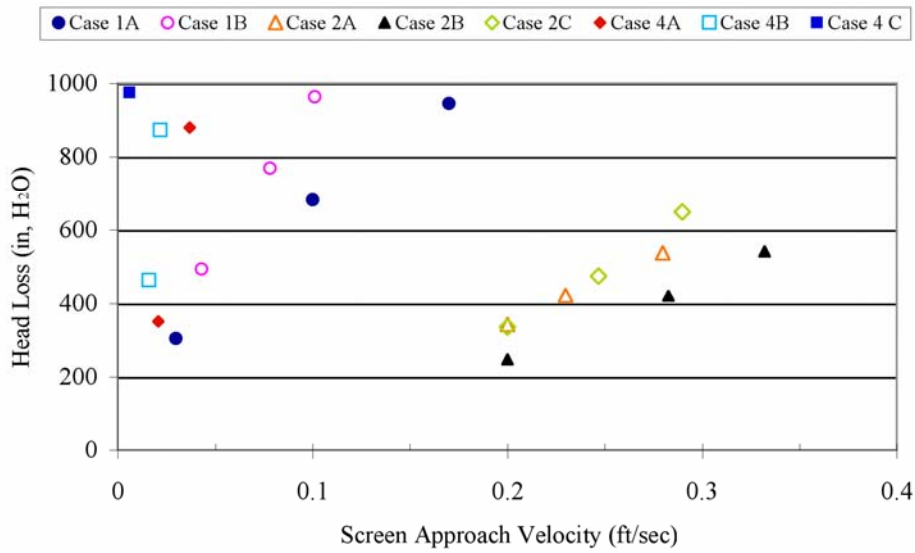
6.3.1.2 Benchtop Test Head Loss Results and Discussion

Initial results confirm that CalSil particulate introduced onto a pre-formed NUKON debris bed, either by post NUKON-debris bed formation or by initial pass-through, has significant effects on the resulting head loss (Figure 6.12). The data presented in Figure 6.12 are tabulated with the complete test results in Appendix F. (Due to the range [0 to 1,000 inches H₂O] of the pressure transducer used in the benchtop loop and the incomplete debris bed formation for the CalSil-only test cases, essentially no head loss was observed, and the data are therefore not reported in the Appendix.). Referring to Table 6.6, two repeat tests were performed for Case 1; 051214_NC_1234_B1 and 051214_NC_1234_B2. Three tests were performed for Case 2, 051215_NC_1234_B1, 051215_NC_1234_B2, and 051216_NC_1234_B1. As shown in Figure 6.12, the Case 1 head loss results were significantly higher than Case 2 results. This result is not surprising given that the Case 1 tests resulted in an observable layer of relatively fine particulate that could reasonably be expected to be packed such that flow paths were limited compared with the expectedly dispersed particulate tests of Case 2. As discussed, the variation in size and shape between the NUKON fibers and CalSil particulate may be expected to provide a tightly packed condition with subsequently limited flow paths, but there may be insufficient particulate to reach this condition when it is dispersed throughout the fibrous debris layer.

Two tests were performed for Case 3. For test 051227_CO-0411x_B1 (Case 3A), the initial CalSil mass introduced to the benchtop loop was 4.11 g (target CalSil debris loading for Test Case-6e [NC12] and Test Case-6e2 [NC13]). A complete CalSil debris bed was not formed at this concentration due to the existence of exposed screen and open channels (debris bed formation criteria included no visually observable open screen mesh openings in the debris bed. Refer to Section 3). CalSil material was therefore subsequently added in an attempt to form a debris bed. Four incremental loadings of 3.38 g of CalSil was added to yield a peak target mass loading of 2175 g/m³. This mass loading was the maximum



(a)



(b)

Figure 6.12. Debris Bed Head Loss as a Function of Screen Approach Velocity for Debris Beds Formed in the PNNL Benchtop Loop. The data presented are for the final ramp up of each velocity sequence. The tests were conducted for various sequences of debris loading; (a) contains all four cases of the load sequence investigation; Case 3 has been excluded from (b) allowing greater resolution of the screen approach velocity to be shown.

CalSil debris loading from the NRC proposed test matrix. After each addition of CalSil, head loss measurements were monitored for steady-state conditions, and time was allowed for the debris bed to form. Although measurable head loss was achieved (Figure 6.12), a complete CalSil debris bed was not considered to have formed (Figure 6.13).

For the second Case 3 test 051227_CO_1763_B2 (Case 3B), the maximum CalSil debris loading from the proposed test matrix (2175 g/m³) was added in a single introduction. Again, a complete CalSil debris bed was not considered to have formed (Figure 6.14). The head loss measurements for the single addition of CalSil were higher than those obtained after the incremental introductions (see Figure 6.12). The head losses from these CalSil-only tests were negligible compared with the other debris loading scenarios evaluated.

Three tests were performed for Case 4: 051228_NC_1234_B1, 051228_NC_1234_B2, and 051228_NC_1234_B3. As shown in Figure 6.12, these tests resulted in the highest measured head loss of all the cases evaluated. This result may suggest that the postulated critical particulate-to-fiber mass ratio mechanism or conditions used for debris bed formation have more effect on the head loss than a distinct particulate layer (the apparent lack of a distinct particulate layer for these tests is discussed below). Conditions for debris bed formation include factors such as the initial screen approach velocity, control of the approach velocity during bed formation, sequence of debris introduction, rate of debris injection, fluid temperature, and concentration of debris as it reaches the test screen. This concept is corroborated by investigations of particulate filtration and related literature (Konstandopoulos 2000, Merkel et al. 2003, Mizuno and Suzuki 2004).

While both the benchtop and large-scale tests had elevated head loss with debris introduction possibly similar to the benchtop Case 4 tests, the large-scale head loss results (Test 051128_NC_2776_L2) at the same screen approach velocity are approximately 40 times less than those from the benchtop Case 4 tests. There are a number of possible explanations for this behavior discussed below, none of which were investigated.

- The introduction of CalSil first results in a larger percentage of the debris mass circulating through the entire loop. The differences in loop configurations and the significantly longer flow path with increased vertical rise of the large-scale loop allows for the possibility of greater segregation of the various size particles of debris. If a significant amount of segregation occurred, the difference in debris bed structure between the large-scale and benchtop loop beds may explain the variation in results. The debris beds from the benchtop loop would be expected to display a greater degree of uniformity from top to bottom compared with the large-scale beds, which would possess a greater degree of stratification.
- Variations in the concentration of the debris reaching the screen may also contribute to variations in the debris bed structure.
- The configuration of the large-scale loop may have allowed a significant portion of the CalSil to initially settle in the loop. Therefore, the ratio of CalSil to NUKON during the bed formation process was different from that of the benchtop loop tests. The settled CalSil may have then been deposited on the surface of the bed when the screen approach velocity was increased.

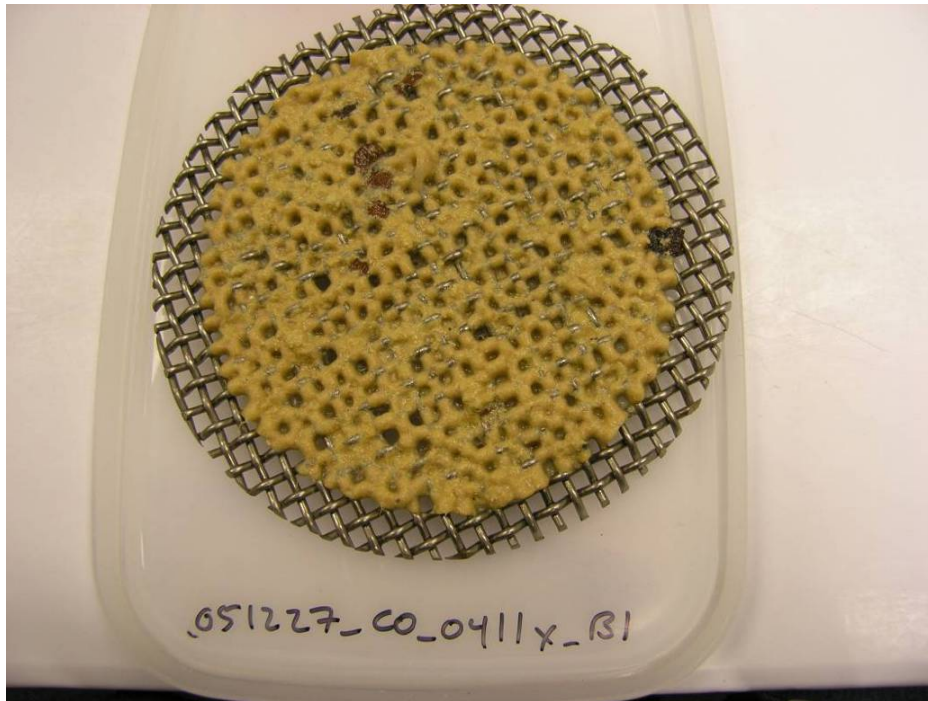


Figure 6.13. Test 051227_CO_0411x_B1 CalSil Debris Bed for Case 3A; target CalSil mass, 17.63 g; rust particulate and chunks from loop visible on surface.

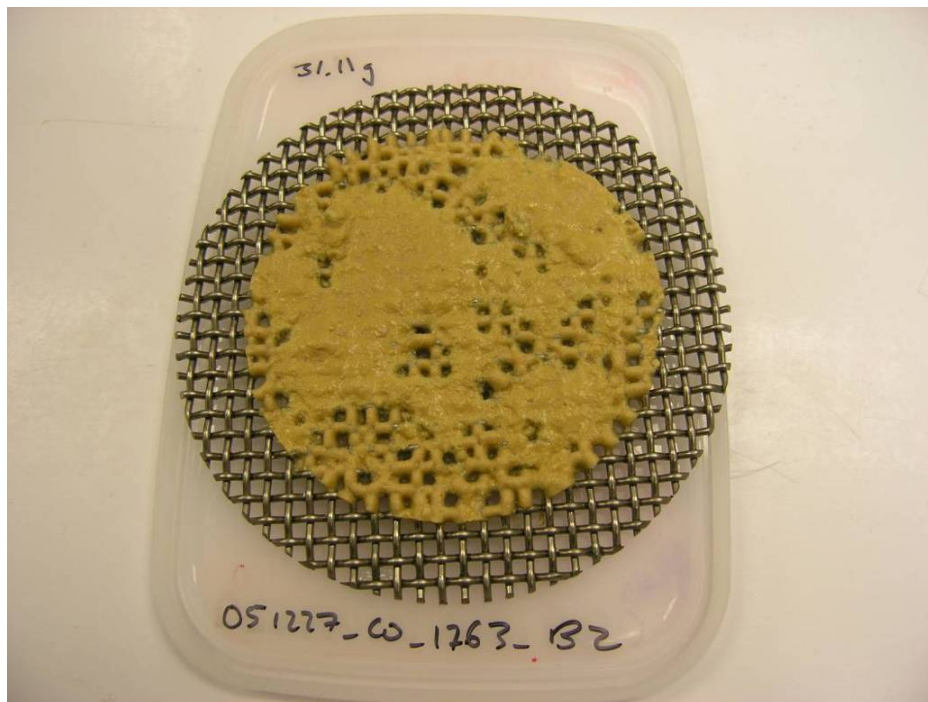


Figure 6.14. Test 051227_CO_1763_B2 CalSil Debris Bed for Case 3B

The high head loss of benchtop tests 051228_NC_1234_B1 and 051228_NC_1234_B2 (Cases 4A and 4B) occurred even with possible channeling in one location on the edge of the beds, as shown in Figures 6.15 and 6.16, respectively. The time or conditions at which these possible channels were formed are unknown, although the initial head loss at high velocity was approximately 10% higher for each debris bed than the subsequent head loss when the velocity was again ramped up.

It was suggested by PNNL investigators that the head loss for the Case 4 tests (CalSil immediately followed by NUKON) are higher than the Case 1 tests (CalSil introduced onto a preformed NUKON debris bed) as a result of the fibrous material in the CalSil. This fibrous material could be deposited on the debris bed surface during the Case 1 tests while the majority may be expected to be in the interior of the debris bed for the Case 4 tests (the fiber will hold up on the screen with or without NUKON fiber present). This fibrous material from the CalSil insulation may provide a structure or flow paths in the CalSil surface layer of the Case 1 tests. This potential effect was indirectly considered for test 051228_NC_1234_B3 (Case 4C). In this test, as-received CalSil was ground with a mortar and pestle to disassociate the fibrous material from the particulate. The bulk material was then separated by sieving through a 212- μm -opening screen mesh. The CalSil material for test 051228_NC_1234_B3 was then taken from this "fiber-less" CalSil and prepared as for the other tests. The maximum head loss of any of the benchtop tests was achieved for test 051228_NC_1234_B3; approximately 975 in. H₂O at a screen approach velocity of 0.006 ft/sec (0.002 m/s). It is not believed that the possible channels in the other two debris beds of the Case 4 tests were the sole reason for the observed difference. When debris bed formation was occurring, the attainable screen approach velocity at the maximum pump speed for debris bed B3 was 50 to 60% of that for debris beds B1 and B2.

As discussed, it may be expected that introducing CalSil particulate on top of a preformed NUKON debris bed will result in a higher head loss than a debris bed formed from premixed debris. Further, the suggestion above that the fibrous material in the CalSil may provide flow paths or reduce the packed density of CalSil appears plausible and may be supported, at first glance, by the results of test 051228_NC_1234_B3. However, the difference between the surface appearance of the debris beds for Case 1, those of Case 4A and 4B, and the one for Case 4C is striking and may indicate that the critical particulate to fiber mass ratio and formation conditions are more significant.

As postulated, the variation in particle size and shape between the NUKON and CalSil may be expected to provide a tightly packed uniformly distributed debris bed with limited flow paths, even more so than a particulate surface layer, when sufficient particulate is available. Visual observation of the debris beds in Figures 6.17 through 6.20 from Case 1 shows distinct CalSil layers. Visual observation of Case 4 debris beds 051228_NC_1234_B1 and 051228_NC_1234_B2 does not show such distinct CalSil layers (see Figures 6.15 and 6.16). In fact, these debris beds do not appear dissimilar to the Case 2 debris beds (see Figure 6.21). This is also true for Case 4C, 051228_NC_1234_B3 (see Figure 6.22), which produced the highest head loss during the evaluation of the debris load sequence.

Reasonably good agreement (relative to the magnitude of the head loss between different test cases) was achieved between the large-scale and benchtop results for relatively similar debris injection scenarios (simultaneous separate injection lines compared to premixed) as shown in Figure 6.23. Consider head loss results from tests 051127_NC_2776_L1 (NC12) and 051128_NC_2776_L2 (NC13) performed in the large-scale loop and contained in Figure 6.23. For these tests, the debris constituents were introduced separately but simultaneously according to the Series 1 procedures. The head loss results from



Figure 6.15. Test 051228_NC_1234_B1 NUKON/CalSil Debris Bed for Case 4A. Possible flow channel at 5:00 orientation.

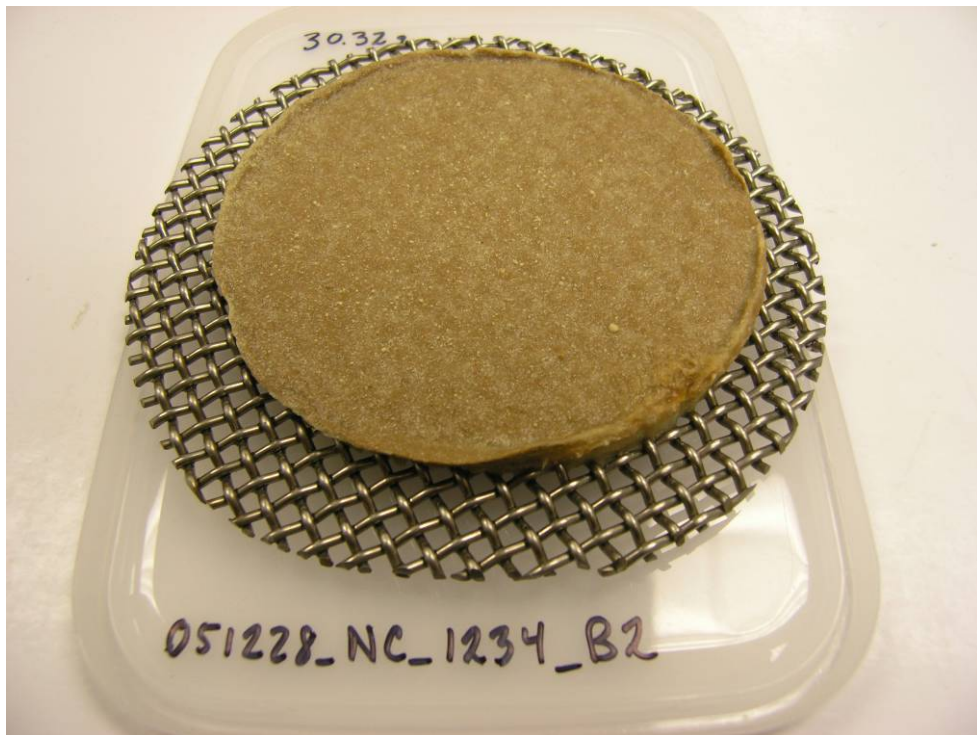


Figure 6.16. Test 051228_NC_1234_B2 NUKON/CalSil Debris Bed for Case 4B. Possible flow channel at 4:30 orientation.



Figure 6.17. Test 051214_NC_1234_B1 NUKON/CalSil Debris Bed for Case 1A. Debris Bed Surface is Mostly CalSil.



Figure 6.18. Test 051214_NC_1234_B1 NUKON/CalSil Debris Bed for Case 1A. Observation of CalSil Layer after attempt made to remove retrieved debris bed from the test screen. Brown “chunks” are rust from loop captured at screen surface.



Figure 6.19. Test 051214_NC_1234_B2 NUKON/CalSil Debris Bed for Case 1B. Debris Bed Surface is CalSil. Apparent Post-Test Rupture Caused After Drainage of the Test Loop During Separation of Test Section.



Figure 6.20. Test 051214_NC_1234_B2 NUKON/CalSil Debris Bed for Case 1B. Observation of CalSil Layer. Debris Bed Piece Tipped on Side. Brown “Specks” Are Rust From Loop Captured at Screen Surface.

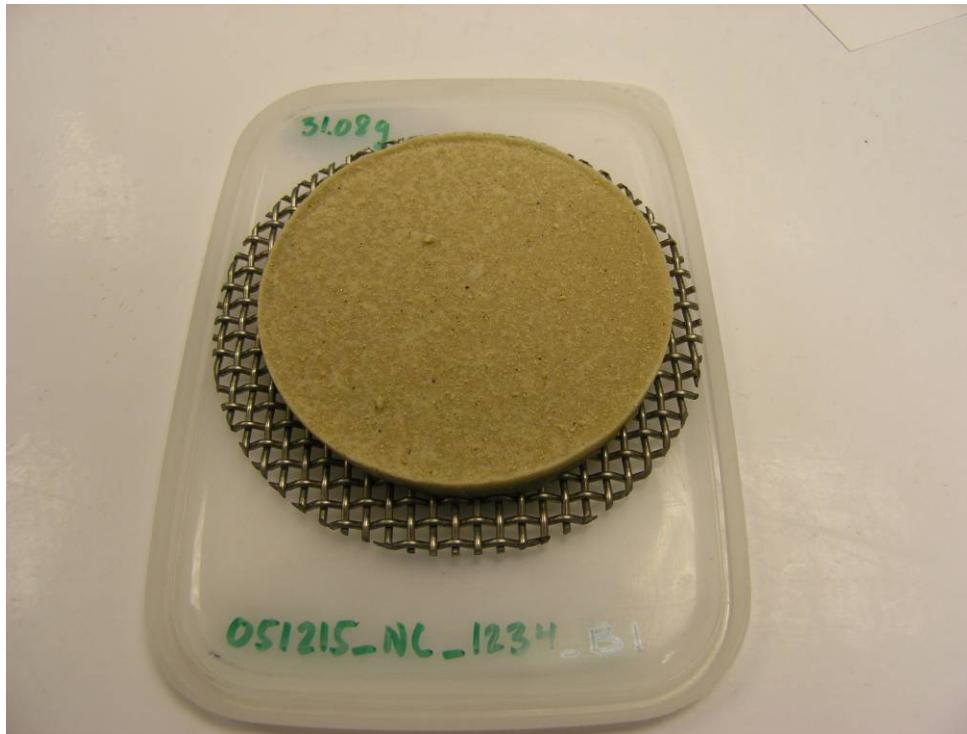


Figure 6.21. Test 051215_NC_1234_B1 NUKON/CalSil Debris Bed for Case 2A.

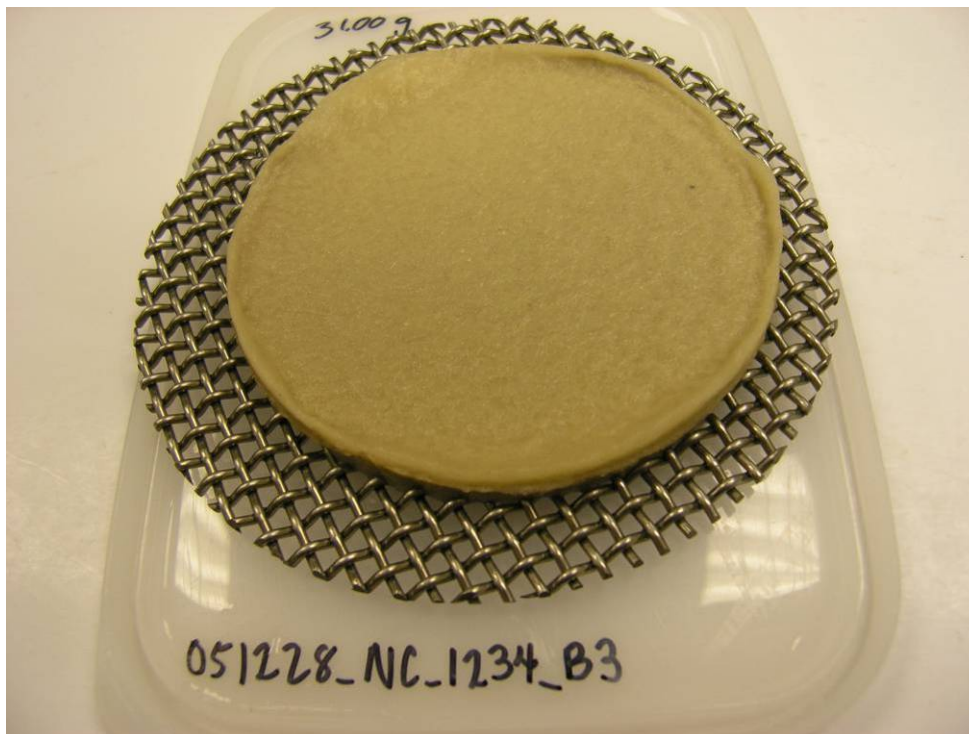


Figure 6.22. Test 051228_NC_1234_B3 NUKON/CalSil Debris Bed for Case 4C

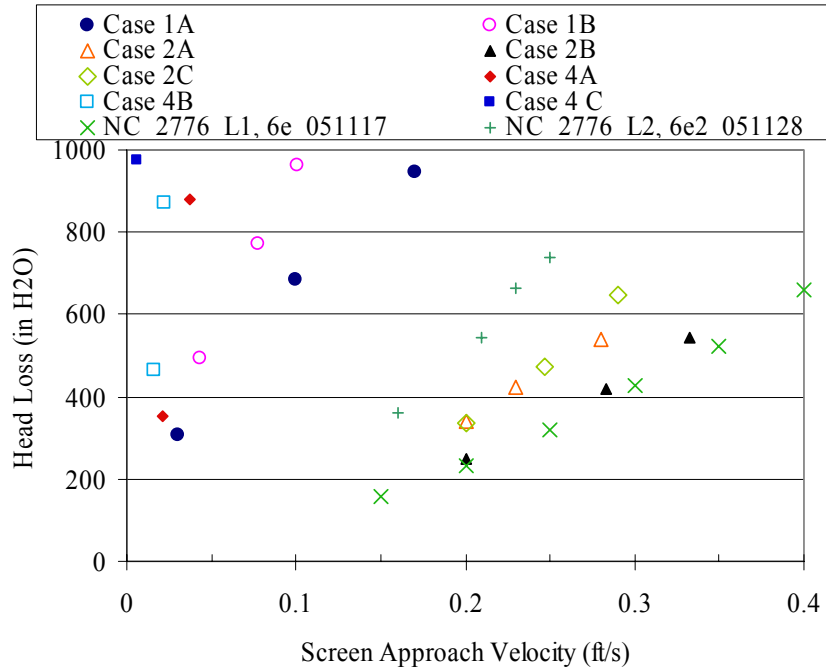


Figure 6.23. Comparison of Debris Bed Head Loss as a Function of Screen Approach Velocity for NUKON/CalSil Debris Beds Formed with Different Debris Loading Sequences in the PNNL Large-Scale and Benchtop Loops (data from Figures 6.11 and 6.12).

051127_NC_2776_L1 fall with the range of those obtained for the Case 2 tests, indicating the debris may have been well mixed before reaching the screen. The head loss results from 051128_NC_2776_L2 fall between those obtained for Case 2 (premixed debris) and Case 1 (CalSil introduced after NUKON-only bed formed). These results suggest the simultaneous injection of the NUKON and CalSil debris can result in premixed debris or allow for a fraction of the CalSil to be deposited on the surface of debris bed resulting in an elevated head loss for the same target mass loading.

The variation in the head loss results for the two Series 1 tests appears to be greater than for any of the other loading scenarios evaluated. Thus, the quantity of CalSil particulate potentially available for deposition on a preformed bed is at a maximum in the sequential introduction (Case 1), at a minimum in the premixed condition (Case 2), and somewhere in between for the simultaneous injection employed as the standard procedure for the Series 1 large-scale tests. However, as evidenced from the Case 4 tests, in particular test 051228_NC_1234_B3, significantly elevated head loss results are achievable without an apparent CalSil (particulate) top layer.

It may be that a critical particulate-to-fiber mass ratio is approached when the amount of particulate in the CalSil debris mass is increased by pre-sieving out the fiber (see above discussion of CalSil material preparation for test 051228_NC_1234_B3). This potential effect is addressed in subsection 6.3.1.2.1.

Furthermore, formation conditions such as CalSil particulate preferentially depositing into the flow path of a forming debris bed are believed to also play a significant role. For a given particle-to-fiber ratio, pre-mixing results in a lower head loss as the particulate distributes throughout the debris bed. Therefore, some of the particulate occupies pore space that is not in a flow path and therefore does not contribute to

flow resistance or blockage. When the CalSil particulate is introduced to the loop before the introduction of NUKON and allowed to become distributed throughout the flow (as in the Case 4 tests), CalSil particulate is available to be continually added to the forming debris bed, allowing it to be used more effectively and transported to block flow paths as the NUKON debris accumulates in the debris bed. This scenario may result in the particulate being more efficiently (optimally with respect to increasing flow resistance) distributed by the flow within the debris bed as the bed is formed, rather than:

- Being uniformly distributed within the debris bed and possibly having some particulate adhere to the NUKON prior to debris injection as a result of the premixed debris condition.
- The CalSil reaching the surface of the preformed NUKON debris bed thus limiting the dispersing of CalSil within debris bed to transport via flow from the debris surface through the packed NUKON fiber bed.

6.3.1.2.1 Case 4 Lag Time Investigation

As postulated, when the particulate is added during the bed formation, particulate may be used more effectively and transported to block flow paths. The possible effect of the delay or lag time for the introduction of the NUKON material for Case 4 has therefore been considered. Altering the lag time would potentially alter the distribution of the particulate through the debris bed and thus potentially alter the resulting head loss.

In the Case 4 tests of Table 6.6, the NUKON debris was introduced when, by visual observation, all of the CalSil material had been introduced into the flow loop. The actual lag time from the introduction of the CalSil to that of the NUKON for these tests is provided in Table 6.7 along with lag times for subsequently performed specific lag time tests.

The lag times of the 051228 Case 4 tests, 11, 17, and 19 seconds (Table 6.7), correspond to approximately 0.25, 0.39, and 0.43 of the calculated circulation time, respectively (subsequently referred to as the circulation fraction). To provide substantial differentiation to the 051228 tests as well as the calculated circulation time, a 30 second lag time, corresponding to an approximately 0.68 circulation fraction, was chosen for investigation.

The head loss results for tests 060207_NC_1234_B1 and 060303_NC_1234_B2 are provided in Figure 6.24. The 051228 Case 4 test results are included for comparison. All test data are tabulated in Appendix F. The results in Figure 6.24 indicate that increasing the lag time (i.e., increasing the circulation fraction) elevates the head loss for the tests considered. These results underscore the importance the debris bed formation conditions and process can have.

Table 6.7. Lag Time Benchtop Test Summary for Case 4 Conditions

Test Number	Lag Time (sec)	Circulation Fraction
051228_NC_1234_B1 (Case 4A)	11	0.25
051228_NC_1234_B2 (Case 4B)	17	0.39
051228_NC_1234_B3 (Case 4C)	19	0.43
060207_NC_1234_B1	30	0.68
060303_NC_1234_B2	30	0.68

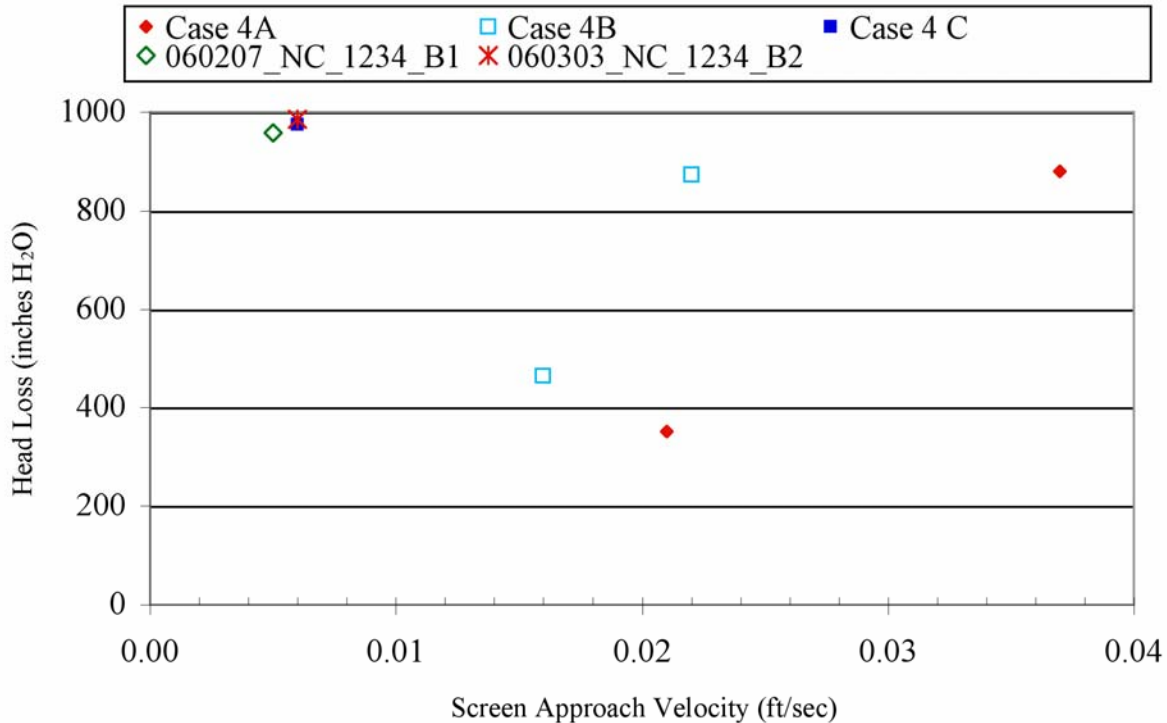


Figure 6.24. Debris Bed Head Loss as a Function of Screen Approach Velocity for Case 4 Lag Time Investigation. Data is for the final ramp up in velocity. Debris beds formed in the PNNL benchtop loop.

The essential replication of the 051228_NC_1234_B3 (Case 4C) head loss by the 060207_NC_1234_B1 and 060303_NC_1234_B2 tests indicate that closely approaching or perhaps reaching the critical particulate to fiber mass ratio by increasing the amount of particulate in the CalSil debris mass by pre-sieving out the fiber (see Section 6.3.1.2 discussion of CalSil material preparation for test 051228_NC_1234_B3) is not a strong contributor to the elevated head loss results. It does seem plausible however that the introduction of true particulate mass without fibers (due to sieving) may serve to increase the effect of the elevated circulation fraction (19 sec compared to 30 sec; refer to Table 6.7).

There is no visually observable difference in the 060207_NC_1234_B1 and 060303_NC_1234_B2 debris beds (Figures 6.25 and 6.26, respectively) compared with the 051228_NC_1234_B1, 051228_NC_1234_B2, and 051228_NC_1234_B3 debris beds (Figures 6.15, 6.16, and 6.22, respectively).

As discussed in subsection 6.3.1.2 regarding Figures 6.15 and 6.16, the 051228_NC_1234_B1 and 051228_NC_1234_B2 debris beds showed signs of channeling in one location at the test section wall. This raises the question as to whether the presence of these channels negates the apparent effect of the lag time depicted in Figure 6.24. As discussed, the time or conditions at which these possible channels were formed is unknown, although the initial head loss at high velocity was elevated by approximately 10% for each debris bed over the subsequent head loss when the velocity was again ramped up. Further, and more conclusively, an edge channel was visually observed to form during debris bed formation for the debris bed of benchtop test 060303_NC_1234_B1. (The 0.68 circulation fraction was being evaluated with test 060303_NC_1234_B1. The formation of the channel and the subsequent flow history resulted in the test



Figure 6.25. 060207_NC_1234_B1 NUKON/CalSil Debris Bed for Case 4 30 sec Lag Time

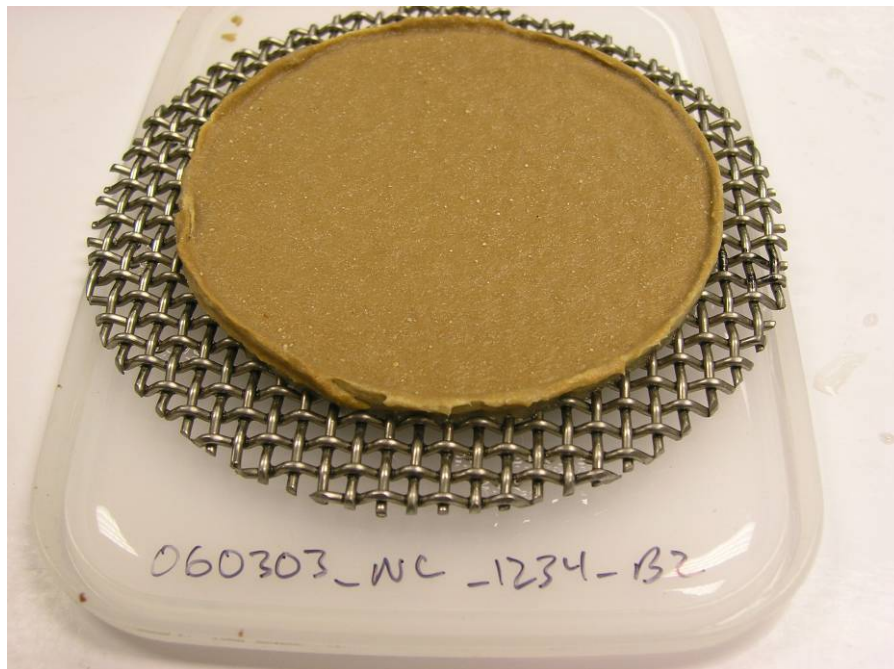


Figure 6.26. 060303_NC_1234_B2 NUKON/CalSil Debris Bed for Case 4 30 sec Lag Time

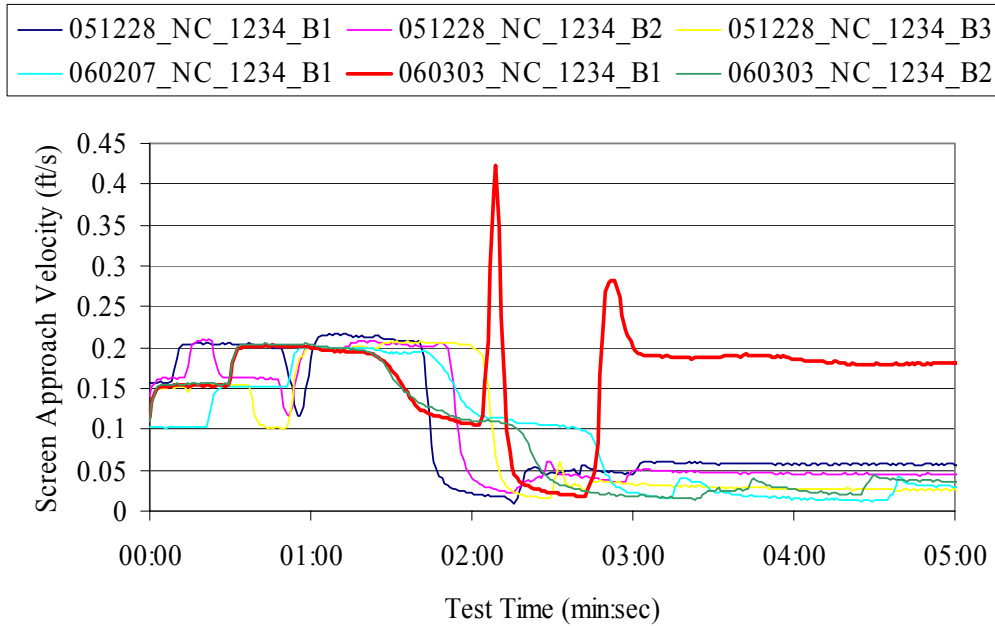


Figure 6.27. Screen Approach Velocity as a Function of Test Time, Case 4 Tests

being prematurely terminated and no head loss results are therefore presented.) The flow history during debris bed formation as illustrated by the attainable velocity of test 060303_NC_1234_B1 compared to all of the other Case 4 tests shows the effect of the observed channel, see Figure 6.27. (For each Case 4 test, the pump speed was maximized to maintain flow through the debris bed. The pump speed was reduced after the first velocity spike for test 060303_NC_1234_B1.) The similarity of the flow histories for the remaining tests suggests that the lag time effects evidenced in Figure 6.24 are real and not a result of channeling in the lower circulation fraction tests. Further lag time tests would support or negate this statement.

6.3.1.3 Post-Test Debris Bed Evaluation

Additional visual comparison may be made of the characteristics of the debris beds. The debris bed rim is not as pronounced in Case 1 (Figures 6.17 and 6.19) as in Cases 2 (Figure 6.21) and 4 (Figures 6.15, 6.16, 6.22, 6.25, and 6.26). (The lag time test debris beds of Section 6.3.1.2 are included with the Case 4 debris beds.) The approximate debris bed body heights for the test cases are given in Table 6.8. The appearance and visually observed thickness of the CalSil layers are also reported. The measured debris bed heights are referred to as “representative” because of the limitations of the measurement technique; the debris bed “body” measurements (plane area of the bed, not the outer rim, see Figure 6.16 for example) are inferred from a 1-mm-increment ruler placed vertically beside the debris bed. This gross technique is used only for the benchtop evaluations and provides a relative means of comparison.

The debris beds with elevated head loss results, Cases 1 and 4, had approximate measured debris bed body heights nominally 67% as thick as those from Case 2. As presented below, the Cases 1 and 4 dried debris beds had 86% of the mass of the Case 2 beds on average. Thus, the elevated head loss for the thinner debris beds may be expected due to the higher bulk densities for the debris beds. The manually measured approximate debris bed body heights for retrieved, dried beds from the Series 1 large-scale loop

Table 6.8. Relative Comparison of Approximate Debris Bed Body Height Measurements from Benchtop Investigation of NUKON/CalSil Debris Beds

Test	Approximate Measured Debris Bed Body Height (in.) (mm)	Approximate Measured CalSil Top Layer Height at Edge (in.) (mm)
051214_NC_1234_B1	0.20 (5.1)	0.04 (1.0)
051214_NC_1234_B2	0.22 (5.6)	0.06 (1.5)
051215_NC_1234_B1	0.31 (7.9)	No CalSil Layer Apparent
051215_NC_1234_B2	Rupture on Retrieval, N/A	No CalSil Layer Apparent
051216_NC_1234_B1	0.31 (7.9)	No CalSil Layer Apparent
051227_CO_0411x_B1	N/A	N/A
051227_CO_1763_B2	N/A	N/A
051228_NC_1234_B1	0.20 (5.1)	No CalSil Layer Apparent
051228_NC_1234_B2	0.22 (5.6)	No CalSil Layer Apparent
051228_NC_1234_B3	0.22 (5.6)	No CalSil Layer Apparent
060207_NC_1234_B1	0.24 (6.1)	No CalSil Layer Apparent
060303_NC_1234_B2	0.20 (5.1)	No CalSil Layer Apparent

tests exhibiting elevated head loss were 0.21 in (5.3 mm) for 051128_NC_2776_L2, and 0.24 in (6.1 mm) for test 051117_NC_2776_L1 (refer to Appendix J). This relatively minor thickness difference, 0.03 in. (0.8 mm), is the inverse of the expected result given the resultant head losses (similar mass quantities were retrieved). However, as shown in Figure 6.23, the head loss difference for these two large-scale tests is much less significant than for the benchtop results.

The relatively greater reduction in thickness of the benchtop Case 1 and 4 debris beds compared with the reduction in mass of the Case 2 debris beds may further support the significance of the formation conditions and the critical mass ratio of particulate on influencing the resultant head loss. Particulate packing into a flow path, while increasing the head loss, may not increase the bulk volume of the debris bed. As suggested, the diverse particle and fiber sizes in a premixed debris bed may pack relatively tightly. It may be, however, as suggested by the debris bed results, that the particulate intermingled with the fiber in the premixed condition causes a decrease in the bulk density despite a potential reduction in the local porosity.

It was observed that the Case 1 and Case 4 debris beds were significantly weaker structurally than those of Case 2, as judged by their behavior during removal from the screen. A flat metal ruler was used to remove and lift the debris beds off the screens. For debris from the Case 1 debris beds sagged and fell where it was not directly supported by the ruler. The Case 4 debris beds, while not actually removed from the screen, were evaluated on the debris bed edge, and similar behavior was observed. The Case 2 debris beds could be lifted in their entirety off the screen with the ruler, as could the NUKON-only debris. NUKON-only debris beds were easily removed from their screens and appeared to be stronger structurally than the Case 1 and 4 debris beds. This result is somewhat surprising, given the higher head loss of the Case 1 and 4 debris beds.

The relative structural strength of debris beds may be related to the water content of the debris bed, which may be compared using their computed immediate post-retrieval water mass fraction. The water mass fraction, w_H , is computed from

$$w_H = \frac{m_W - m_D}{m_W} \quad (6.1)$$

where m_D and m_W are the dry and wet retrieved debris bed masses, respectively. Essentially equivalent water mass fractions are computed for Cases 1 and 4 as well as for the Case 2 debris beds (see Table 6.9). Thus, the water content apparently does not contribute to the observed strength differences.

The total dry debris mass that accumulated on the test screen is also reported in Table 6.9. The dry debris bed mass is lower for the Case 1 and 4 debris beds compared with those from the Case 2 tests (approximately 0.82 dry solid retrieval fraction of the initial added mass compared to approximately 0.94). This result may be expected given the premixing of the debris for the Case 2 tests allows material interaction to occur prior to introduction. However, perhaps much more crucial is the fact that the extremely high head loss results achieved for the Case 1 and 4 tests limited the available flow rate, thus significantly decreasing the number of loop circulations completed during these tests. It is somewhat remarkable to compare the CalSil-only debris bed pictures (Figures 6.13 and 6.14) with their dry mass and retrieval fraction. Nominally only 10% of the material was retained on the screen (observed rust material from the loop is included in the measured dry mass).

The water mass consideration can also theoretically be used to determine a representative porosity assuming the debris bed is completely saturated with no interstitial air. The higher head loss debris beds may be expected to have a lower porosity. The density of water, ρ_H , is taken as 1 g/mL. The representative porosity of the debris bed, ϕ_W , can then be determined from

$$\phi_W = \left(1 - \frac{m_D}{m_W} \right) \frac{\rho_W}{\rho_H} \quad (6.2)$$

where ρ_W is the wet debris bed density computed from

Table 6.9. Debris Bed Measured Mass from Benchtop Investigation of NUKON/CalSil Debris Beds

Test Number	Test Case	Wet Mass (g)	Dry Mass (g)	Dry Solid Retrieval Fraction of Target	Water Fraction Eq. (6.1)	Dry Debris Bed Porosity Eq. (6.5)
051214_NC_1234_B1	1A	65.27 ^(a)	10.76 ^(a)	0.87	0.84	0.91
051214_NC_1234_B2	1B	64.01 ^(a)	10.17 ^(a)	0.82	0.84	0.92
051215_NC_1234_B1	2A	72.98	11.58	0.94	0.84	0.94
051215_NC_1234_B2	2B	97.39	11.42	0.93	0.88	No h ^(b)
051216_NC_1234_B1	2C	65.3	11.66	0.94	0.82	0.94
051227_CO_0411x_B1	3A	N/A ^(a)	1.49 ^(a)	0.08	N/A	No h ^(b)
051227_CO_1763_B2	3B	19.36	2.26	0.13	0.88	No h ^(b)
051228_NC_1234_B1	4A	63.16	10.15	0.82	0.84	0.92
051228_NC_1234_B2	4B	62.92	10.33	0.84	0.84	0.92
051228_NC_1234_B3	4C	64.26	9.6	0.78	0.85	0.93
060207_NC_1234_B1	NA	64.2	9.3	0.75	0.86	0.94
060303_NC_1234_B2	NA	66.22	9.44	0.76	0.86	0.92

(a) Rust debris from loop observed in/on debris bed.
(b) No height measurement, see Table 6.8.

$$\rho_w = \frac{m_w}{\frac{\pi}{4}d^2h} \quad (6.3)$$

where d is the test section diameter (4 in.) and h is the debris bed body height. Imperfections in the debris bed and the rim are neglected. Calculation of the representative porosity using Eq. (6.2) and (6.3) from the data of Tables 6.8 and 6.9 is rendered suspect, however, when porosities greater than 1 are achieved.

Consider, therefore, that the bulk wet density may be expressed by

$$\rho_w = \frac{1}{\frac{1-w_H}{\rho_s} + \frac{w_H}{\rho_H}} \quad (6.4)$$

where ρ_s is the dry solid density. Also, the density of the dry debris material, assuming relatively constant particulate to fiber mass ratios between the respective debris beds, should be relatively constant. In application of Eq. (6.3) and (6.4), the dry debris material density is computed to range from -1.5 to 3.3 g/mL. Because this is a nonsensical result, and the solid density should in fact be relatively constant, the nonphysical results from Eq. (6.2) are understandable and not considered further.

Consider instead the average porosity of the dry debris bed, which may be evaluated from

$$\phi_D = 1 - \frac{m_D}{\frac{\pi}{4}d^2h\rho_s} \quad (6.5)$$

With a representative dry solid density of 3 g/mL, relatively consistent results are achieved (see Table 6.9). A representative constant dry solid density of 3 g/mL is chosen loosely based on data from Zigler et al. (1995), Shaffer et al. (2005), Weast (1975) and preliminary PNNL work. An attempt was made to minimize the error of the difference between ρ_w from Eq. (6.3) and (6.4) by solving for ρ_s ; convergence was not achievable. Acknowledging the uncertainties of the analysis, the average porosity of the Case 2 debris beds appears to be only slightly elevated over the Case 1 and Case 4 debris beds in keeping with, but having a surprisingly small difference with regard to, the head loss results. The apparent relatively constant average porosity does make sense in relation to the argument that the formation conditions in terms of particulate distribution play a significant role. To reiterate, it is suggested that, when added during the debris bed formation, particulate may be collected in the flow paths by selective mass transport as opposed to being more homogeneously distributed from a premixed condition.

The apparent structural strength issue is not explained by examination of the average porosity. Insight into the internal structure of the debris bed may possibly be gained by a literature review of the relative strength of fiber particulate matrixes as related to their inner structure. It is striking to note that the Case 1 debris beds are apparently weaker than NUKON-only debris beds. Consider that the Case 1 debris beds consist of CalSil deposited onto a preformed NUKON-only debris bed. Apparently, therefore, the addition of CalSil to a preformed NUKON debris bed weakens or changes the structure of a NUKON debris bed with respect to post test handling. Contrary to this observation, testing in the benchtop loop

has repeatedly shown that a formed NUKON-only debris bed will rupture if subjected to no-flow conditions while still submerged. However, the apparent weaker (based on post test handling) 051228_NC_1234_B3 NUKON/CalSil debris bed sat submerged at no-flow conditions during retrieval for approximately 10 minutes (water in the test section above the debris bed had to be siphoned out; there was no flow through the debris bed with approximately 2.5 ft of water on it). The observations with respect to structural strength may be related to the compressibility of the debris beds and changes that may occur when the differential pressure is removed and the debris bed is no longer submerged (removed from the water).

6.3.2 Investigation Conclusions

The results of the benchtop tests discussed herein support the conclusion that the elevated head loss results observed in the initial benchtop tests as well as large-scale Series 1 tests 051123_NC_2181_L1 and 051128_NC_2776_L2 were due to slight differences in CalSil and NUKON debris introduction process/sequences. All investigated changes in loading sequences resulted in divergent head loss results. The investigated debris loading sequences were ranked from the highest measured head loss to the lowest as follows:

1. CalSil introduction followed by the introduction of NUKON after a slight time lag (Case 4). Increasing the lag time between the introduction of the CalSil and NUKON increased the resultant head loss.
2. CalSil introduction onto a preformed NUKON-only debris bed (Case 1).
3. Premixed NUKON and CalSil (Case 2) had the lowest measured head loss of the NUKON and CalSil sequences investigated.

These debris loading sequence issues should be considered in terms of both the statistically meaningful results with regard to repeatability, conservatism of the results for real applications in terms of a safety-basis use, and identification of required correlation parameters. The data suggest, in accordance with other particulate filtration studies, that the particulate-to-fiber mass ratio (i.e., internal decrease in debris bed porosity due to the addition/buildup of particulate) has a more significant effect on the resulting head loss than just the formation of a closely packed layer of particulate on the surface of the debris bed.

Other test sequences such as additional variations in the time lag for Case 4, CalSil debris bed formation followed by the addition of NUKON, CalSil addition followed by NUKON followed by CalSil, and sequential tests may provide additional information. Insight into the underlying physical phenomena may be achieved through bed sectioning and associated analyses as well as debris deposition modeling and packing/porosity calculations based on particulate and fiber size distributions.

6.4 Debris Bed Sectioning

Debris beds 060303_NC_1234_B2 and 060516_NC_1234_B1 generated in the benchtop loop as part of the load sequence evaluation (Section 6.3) were selected for cross-sectional analysis. Both debris beds had a target CalSil mass loading of 507 g/m² and a target NUKON mass loading of 1015 g/m², for a total target mass loading of 1522 g/m². This is essentially the same target mass loading as test cases NC12 and NC13. Debris bed 060303_NC_1234_B2 had 76% of the target mass retained on the screen for a retrieved mass loading of 1164 g/m². The final dry mass for bed 060516_NC_1234_B1 is not available;

however, other benchtop debris beds with the same mass target mass loading subjected to repeat tests of the test procedure used for 060516_NC_1234_B1 had an average of 86% of the target mass retained on the screen for an average retrieved mass loading of 1306 g/m².

Debris bed 060516_NC_1234_B1 was generated to Case 1 test conditions (refer to Section 6.3.1) with a complete NUKON debris bed formed before introducing the CalSil debris. Bed 060303_NC_1234_B2 was generated to Case 4 test conditions with a 30 second lag time between the introduction of the CalSil and NUKON debris materials.

After being dried at 90°C, the debris beds were impregnated with an epoxy resin and sectioned; cross-sectional samples were imaged using SEM, as described in Section 2.5.3.3. The samples were taken along the center wire of the square grid and along a diagonal, as shown in Figure 6.28. A photograph of the mounted samples for bed 060516_NC_1234_B1 is shown in Figure 6.29. A series of images was taken through the depth and along the top surface for each sample.

Under visual examination, both debris beds appeared to consist of three distinct regions: the wire support, a thick region with high porosity, and a very thin high-density region on the upstream (inlet) surface of the debris bed. A series of SEM images for each of the last two regions is shown in Figures 6.30 through 6.33 for bed 060303_NC_1234_B2 and Figures 6.34 through 6.36 for bed 060516_NC_1234_B1. The orientation of the images is such that the vertical axis of the debris bed appears horizontal in the image with the direction of flow through the debris bed having been from right to left in the image.

The porous center region shown in Figures 6.30 and 6.31 consists almost entirely of cylindrical NUKON fibers ranging from 5 to 15 microns in diameter, based on analyses of SEM photos. The elliptical cross-sectional shapes indicate where a fiber is at an angle with respect to the cut surface. Based on the images, it appears the predominant orientation of the fibers is approximately parallel to the debris bed surface (assumed to be at right angles to the direction of flow). The light-shaded areas indicate CalSil material. The center region also includes gaps (voids) between the NUKON fiber regions, as shown in Figure 6.31. One possible explanation for these gaps is that the procedure for flooding the sample with epoxy induced separation. Another possible explanation, since the benchtop did not have the ability to increase the static pressure of the loop to maintain gas in solution, is that the void may have been created by a gas bubble forming within or at the base of the debris bed as the pressure drop increased. If the bubble was formed at the bottom of the bed, it may have migrated upward in the bed as the flow was reduced or during the debris bed retrieval process.

Digital analysis of the SEM images indicate that the porous center regions, excluding gaps, consist of a NUKON fiber concentration of 6.1 ± 1.7 vol% (060303_NC_1234_B2) and 8.3 ± 1.9 vol% (060516_NC_1234_B1) and a CalSil concentration of 1.4 ± 0.6 vol% (060303_NC_1234_B2) and 3.7 ± 1.2 vol% (060516_NC_1234_B1). These concentrations are consistent throughout the center porous region of the bed, with no discernable trend as a function of location. The thickness of the center porous region is approximately 8.2 and 4.5 mm, respectively. The total thickness of the debris beds is 8.7 and 5.5 mm, respectively.

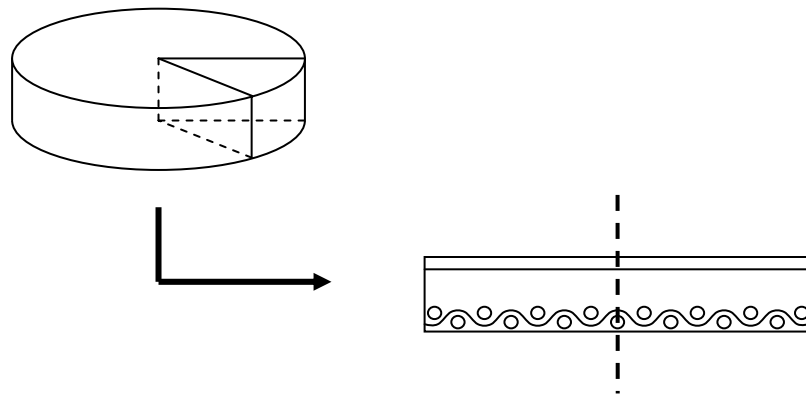


Figure 6.28. Schematic of Debris Bed Cross-Section Used for SEM Imaging



Figure 6.29. Mounted Debris Bed Samples Used for SEM Imaging

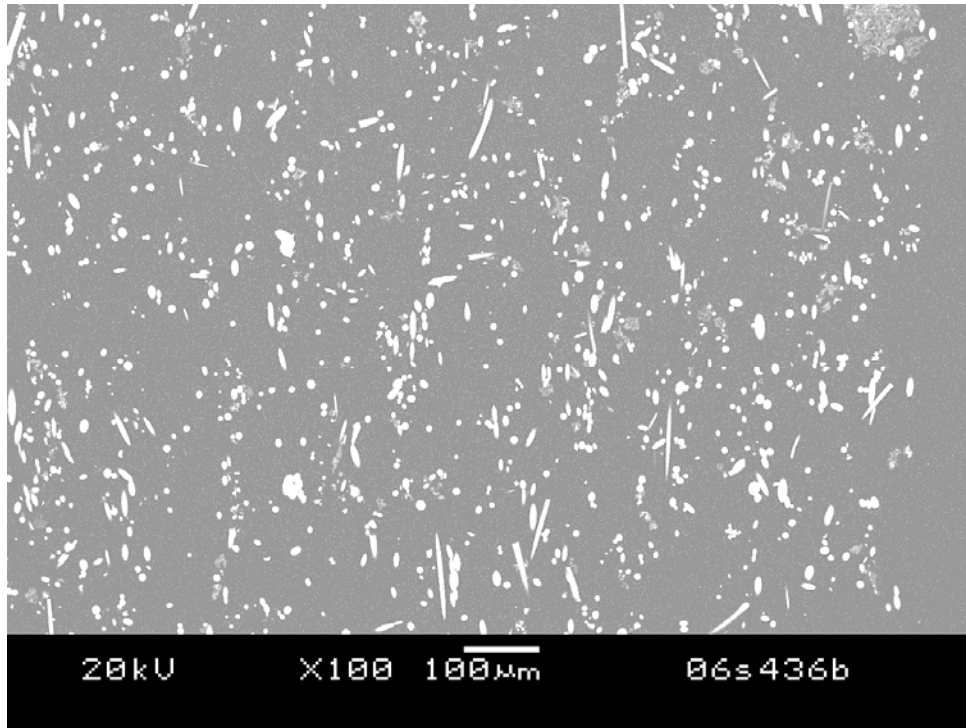


Figure 6.30. SEM Image of the NUKON Fiber Region in Debris Bed 060303_NC_1234_B2 (Case 4)

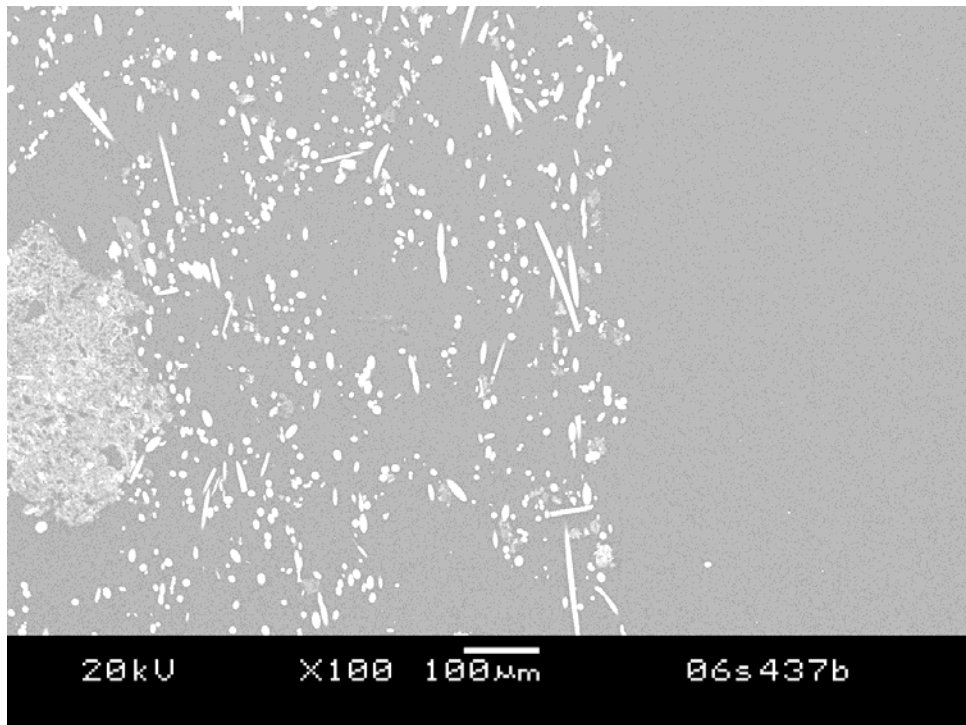


Figure 6.31. SEM Image of NUKON Fiber Region in Debris Bed 060303_NC_1234_B2 (Case 4) Showing Gap or Void Region

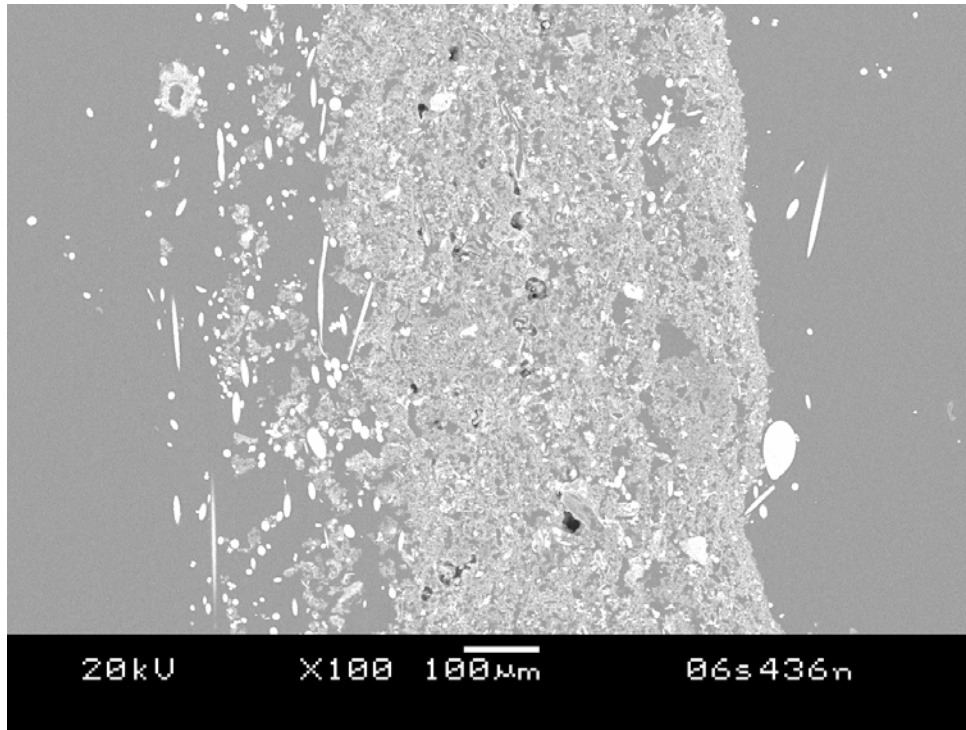


Figure 6.32. SEM Image of the CalSil Surface Layer for Debris Bed 060303_NC_1234_B2 (Case 4)

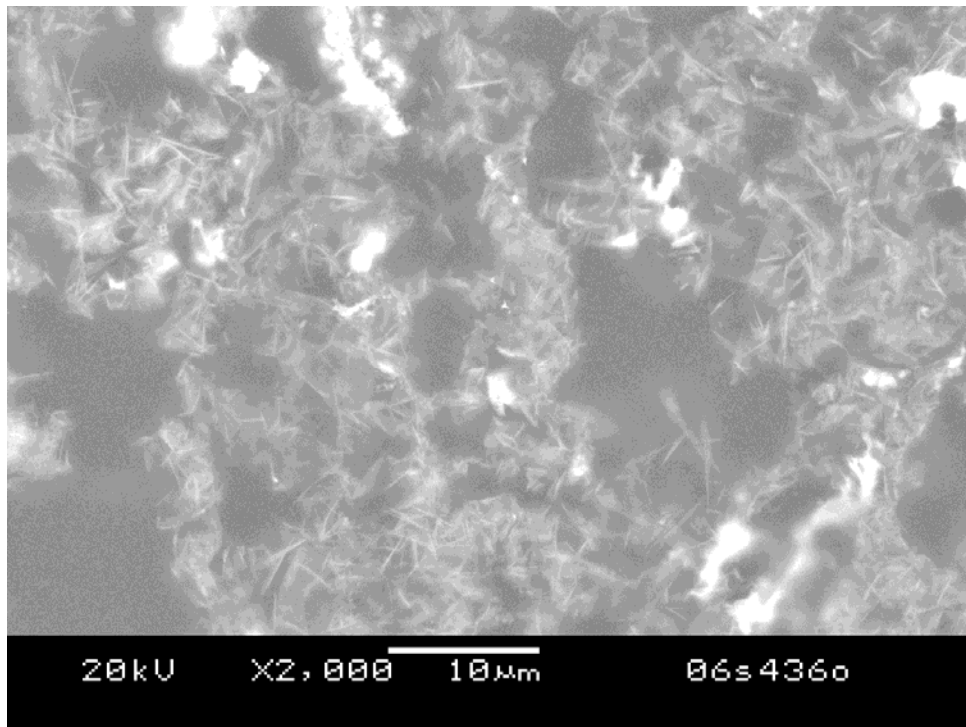


Figure 6.33. High-Magnification SEM Image of the CalSil Surface Layer for Debris Bed 060303_NC_1234_B2 (Case 4)

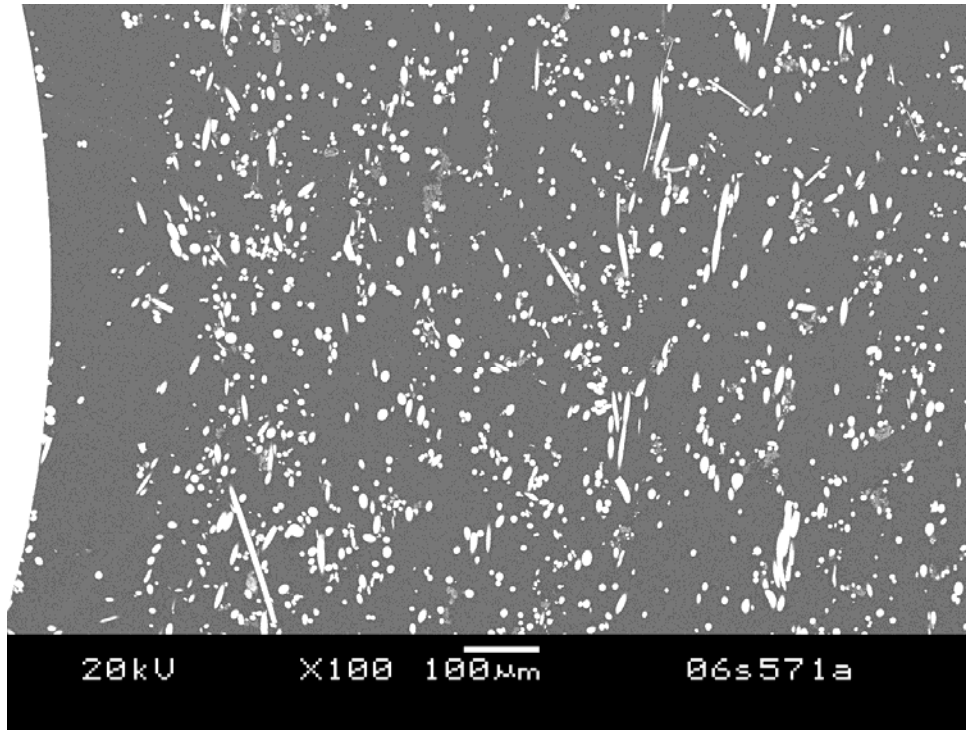


Figure 6.34. NUKON Fibers near Metal Grid for Debris Bed 060516_NC_1234_B1 (Case 1)

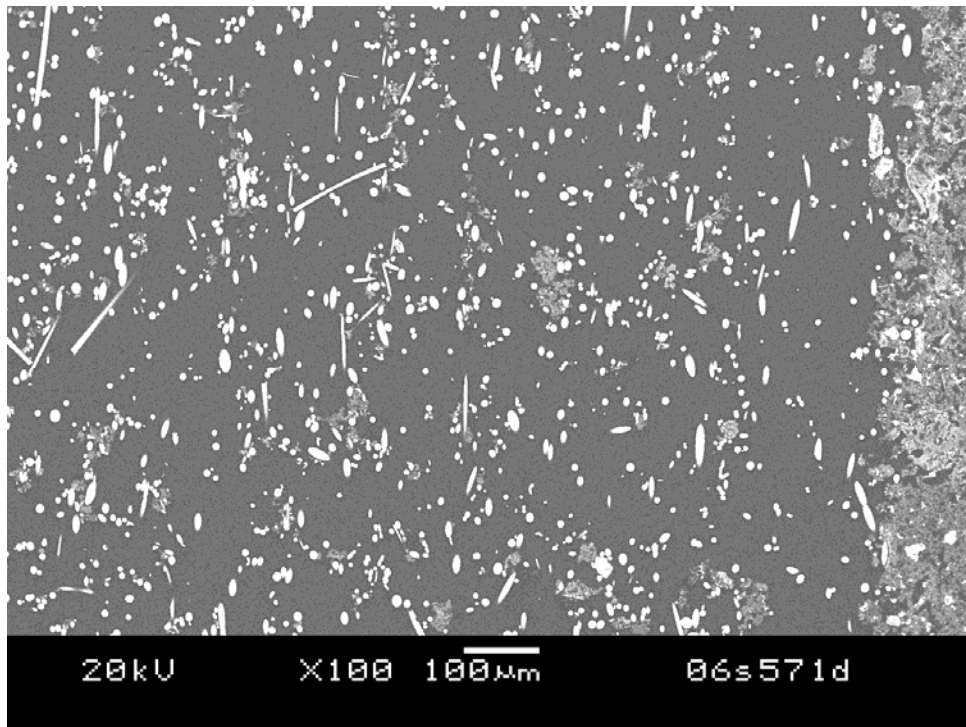


Figure 6.35. NUKON Fibers near Surface Region for Debris Bed 060516_NC_1234_B1 (Case 1)

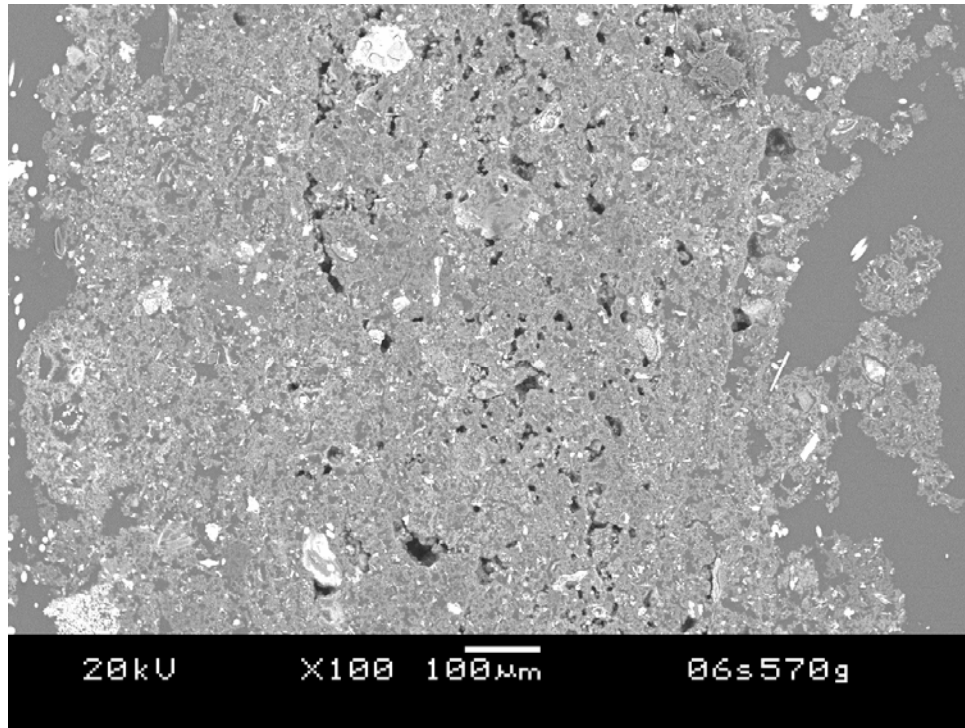


Figure 6.36. Cross-Section of Surface Region (CalSil layer) for Debris Bed 060516_NC_1234_B1 (Case 1)

The high-density surface layer shown in Figures 6.32 and 6.33 consists primarily of CalSil particulate supported by NUKON fibers. The layer is relatively uniform across the debris bed with measured thicknesses of 0.52 ± 0.06 mm and 1.05 ± 0.09 mm, respectively. Digital image analysis results indicate that the surface layer consists of CalSil concentrations of 59 ± 7 vol% (060303_NC_1234_B2) and 64 ± 4 vol% (060516_NC_1234_B1) and a NUKON fiber concentration of 6.5 ± 0.5 vol% and 5.5 ± 0.6 vol%, respectively. Figure 6.33 is a high-magnification SEM image of the CalSil surface layer. Much of the calcium silicate has the form of micron sized needle-like crystals that have agglomerated together.

The structure of the two debris beds suggests a sequence of filtration mechanisms. The original wire grid is not effective in capturing the CalSil particles, but the long aspect ratio NUKON fibers begin to form a mat on the grid surface. The particles continue to pass through the grid until the density of the fiber mat increases to the point where the gaps are roughly the size of the particle diameters. The fiber mat then acts as the particle filter and the surface layer begins to form.

The composition results presented for the porous center region are for a bed that is not loaded and compressed. The NUKON fibers may have elastic properties that allow the bed to change its structure in response to forces resulting from the flow resistance of the surface layer. The dynamic behavior of the fiber mat due to pressure fluctuations may also allow the release of CalSil particles trapped in the center region.

The total flow resistance of the debris bed is determined by the permeability and thickness of both the center and surface regions under flow conditions. The center region resistance will be relatively insensitive to the applied flow rate. However, the thickness and permeability of the center region will

decrease significantly as the flow rate increases. The flow resistance of the surface layer will result in a lithostatic load compressing the fiber bed. The increase in fiber density will result in a lower permeability and higher flow resistance in the center region. This resistance adds to the lithostatic load on the downstream fiber bed, compressing it even further.

A major difference between the two debris beds is the thickness of the fiber bed center region, which is approximately 8.2 mm (060303_NC_1234_B2) and 4.5 mm (060516_NC_1234_B1), not quite a factor of 2. The second bed also has a significantly higher concentration of CalSil particles, which could interfere with the compression and sealing of the bed. The use of microscale simulations may be used to determine the permeability of both the surface region and the fiber bed region as a function of compression. This information, along with the elastic strength of the NUKON fibers, could be used to predict the overall flow resistance of the debris bed under different flow conditions.

6.5 Flow History

Head loss for a given screen approach velocity has been observed to increase as the velocity is cycled through the test range and returns to the given velocity either as part of a ramp up or ramp down of the velocity sequence (see Sections 6.1–6.3). Section 5.3 describes the velocity matrixes applied for the various test series. Flow history, the time and flow a debris bed has been subjected to prior to attaining a specific velocity, has also been observed to have an impact on the measured head loss (see head loss data in Section 6.2 of complete and truncated velocity matrixes). Specific repeated-cycle benchtop tests have been conducted to investigate the magnitude of the effect of flow history on the debris bed head. The tests were conducted using test condition 1a (NUKON-only, target debris loading 1681.4 g/m²).

6.5.1 Test Conditions

Tests were conducted in the PNNL benchtop loop (Section 2.3) using test procedures similar to those described in Section 5.3. The non-boiled NUKON debris was prepared to an R4 value of 11 ± 1 for each test. The target debris loading of 1681.4 g/m² corresponds to 13.63 g of NUKON debris in the 4 in.-diameter test section of the benchtop loop. All tests employed 5-mesh screen as the test screen material, which is described in Section 2.2.

The initial screen approach velocity was 0.20 ft/sec, and the velocity was allowed to decay over the 20-minute bed formation time (constant pump speed), resulting in approximately 27 circulations through the loop. The steady-state criterion for bed formation and at each subsequent velocity was taken as less than a 2-in.-H₂O change in head loss over a 2-minute period. Repeated cycling through the screen approach velocity matrix (0.20, 0.45, and 0.75 ft/sec screen approach velocities) was conducted. Extended half-hour hold periods at constant screen approach velocities (same as cycling points) were also performed. Two flow history tests were performed, 060418_NO_1363_B1 and 060419_NO_1363_B1.

6.5.2 Test Results

Head loss results as a function of screen approach velocity for flow history tests 060418_NO_1363_B1 and 060419_NO_1363_B1 are presented in Table 6.10. The approximate 20% difference in test results compares with similar test comparisons observed in Sections 6.1 and 6.2. For each flow history test, the head loss at a given screen approach velocity increased with the number of cycles (refer to Table 6.10 and Figures 6.37 and 6.38). The average increase in head loss with cycling is typically at a maximum for cycles 1–3, as observed in Table 6.11. It may also be observed from Table 6.11 that the average change in head loss per velocity cycle was typically greater at the higher screen approach velocities.

Table 6.10. 060418_NO_1363_B1 and 060419_NO_1363_B1 Flow History Tests Data

Test		060418_NO_1363_B1	060419_NO_1363_B1
Test Phase ^(a)	Screen Approach Velocity (ft/sec)	Head Loss (in. H ₂ O)	Head Loss (in. H ₂ O)
Ramp up 1	0.2	41	37
	0.45	120	102
	0.75	236	197
Ramp Down 1	0.45	128	105
	0.2	49	40
	0.45	128	105
Ramp up 2	0.45	128	105
	0.75	244	203
	0.45	132	108
Ramp Down 2	0.45	132	108
	0.2	51	41
	0.45	131	108
Ramp up 3	0.45	131	108
	0.75	249	206
	0.45	134	110
Ramp Down 3	0.45	134	110
	0.2	51	41
	0.2 (T)	51, 52	41, 43
T1	0.45 (T)	135, 135	111, 112
	0.75 (T)	256, 256	213, 211
	0.2	53	43
Ramp up 4	0.45	137	111
	0.75	260	213
	0.45	140	113
Ramp Down 4	0.45	140	113
	0.2	54	43
	0.45	139	112
Ramp up 5	0.45	139	112
	0.75	262	214
	0.45	141	115
Ramp Down 5	0.45	141	115
	0.2	54	43
	0.45	140	114
Ramp up 6	0.45	140	114
	0.75	266	216
	0.45	142	115
Ramp Down 6	0.45	142	115
	0.2	55	44
	0.2 (T)	55, 57	44, 46
T2	0.45 (T)	145, 146	118, 118
	0.75 (T)	276, 276	225, 222
	0.2	57	45
Ramp up 7	0.45	147	117
	0.75	278	223
	0.45	149	119
Ramp Down 7	0.45	149	119
	0.2	58	45
	0.45	149	117
Ramp up 8	0.45	149	117
	0.75	280	223
	0.45	150	119
Ramp Down 8	0.45	150	119
	0.2	58	45
	0.45	150	119
Ramp up 9	0.45	150	119
	0.75	281	224
	0.45	152	120
Ramp Down 9	0.45	152	120
	0.2	59	46
	0.2 (T)	59, 61	46, 48
T3	0.45 (T)	155, 156	122, 123
	0.75 (T)	293, 291	232, 228

(a) T1 = T2 = T3 = 0.5 hour hold period. Double entries indicate the head loss at the beginning and end of the hold periods, respectively.

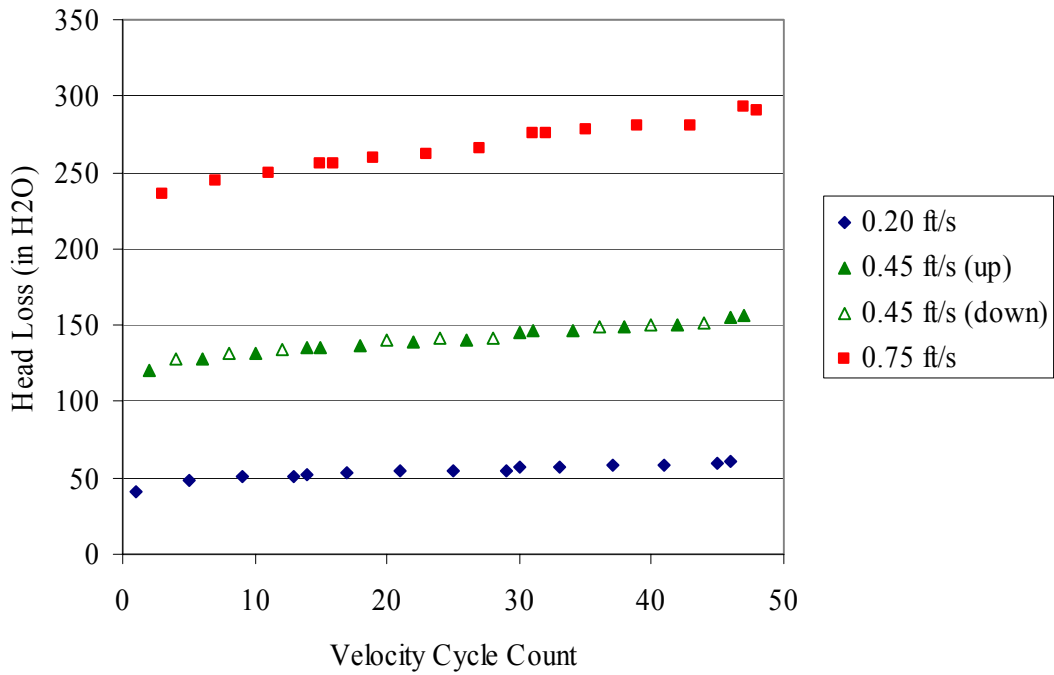


Figure 6.37. 060418_NO_1363_B1 Head Loss as a Function of the Velocity Cycle Count (number of cycles of velocity ramp up and ramp down completed)

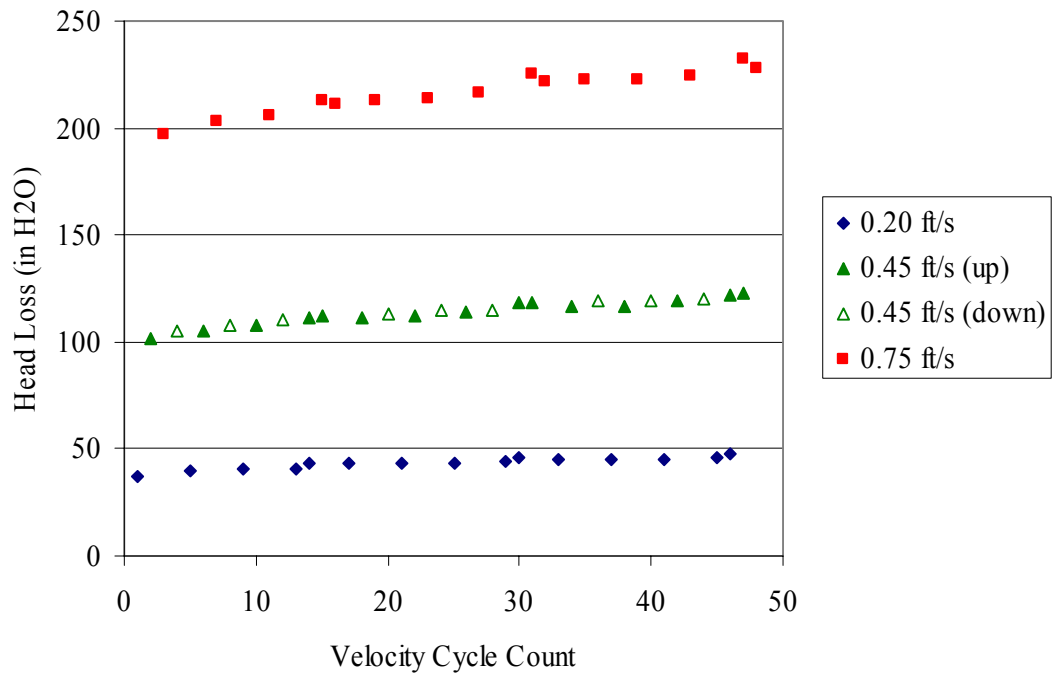


Figure 6.38. 060419_NO_1363_B1 Head Loss as a Function of Velocity Cycle Count (number of cycles of velocity ramp up and ramp down completed)

Table 6.11. Average Change in Head Loss per Velocity Cycle

Parameter	Average Change in Head Loss per Velocity Cycle Count (in H ₂ O/Cycle)		
Screen Approach Velocity (ft/sec)	0.20	0.45	0.75
Test	060418_NO_1363_B1		
Cycles 1–3	3.3	5.0	6.7
Cycles 4–6	0.7	2.7	2.0
Cycles 7–9	0.7	1.3	5.0
Test	060419_NO_1363_B1		
Cycles 1–3	1.3	3.0	5.3
Cycles 4–6	0.3	2.3	4.0
Cycles 7–9	0.3	1.7	3.0

The results from the half-hour hold periods at constant screen approach velocities indicate a different trend (see Table 6.10); it appears that at the higher velocities the head loss remains constant or decreases over the hold period.

The representative approximate debris bed body heights and dry debris bed masses for debris beds of the flow history tests are provided in Table 6.12. Similar height and mass results lead to essentially equivalent computed bulk densities. The debris bed appearances in Figures 6.39 and 6.40 are similar as well.

Table 6.12. 060418_NO_1363_B1 and 060419_NO_1363_B1 Flow History Tests Debris Bed Data

Test	Approximate Measured Debris Bed Body Height (in)	Dry Debris Bed Mass (g)	Computed Density (g/mL)
060418_NO_1363_B1	0.39	13.23	0.16
060419_NO_1363_B1	0.39	13.03	0.16

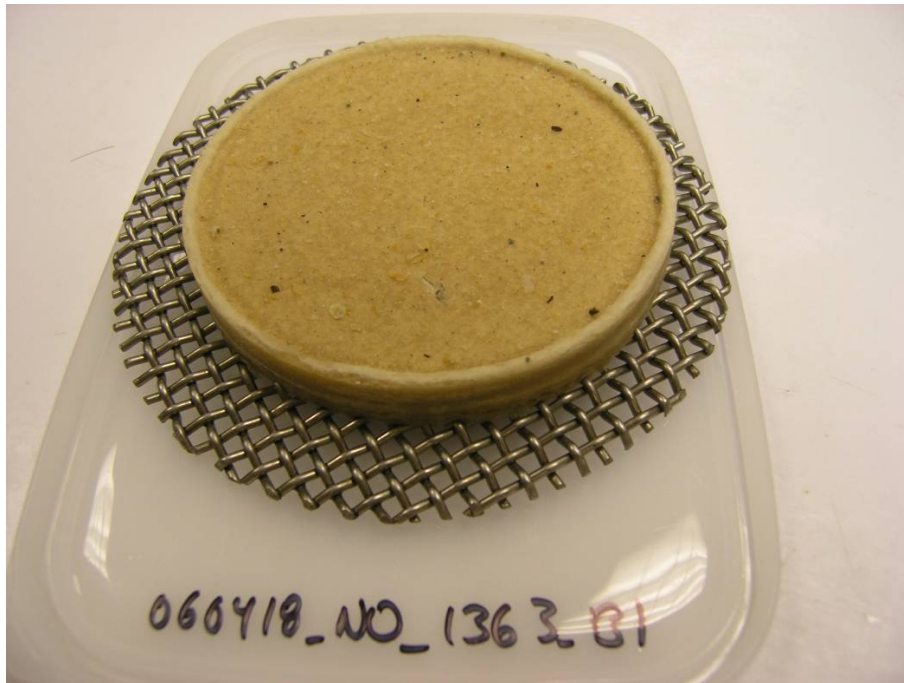


Figure 6.39. 060418_NO_1363_B1 Flow History Test



Figure 6.40. 060419_NO_1363_B1 Flow History Test

7.0 Results of Large-Scale Tests

This section presents the results of the pressure-drop measurements made in the large-scale loop. The large-scale tests were conducted in four test phases: Series 1, Benchmark, Series 2, and Coatings Tests (refer to Section 5.1 for the description of the test matrixes). The test results are presented for the following five types of debris beds:

- Screen only with no debris added, Section 7.1
- NUKON only, Section 7.2
- CalSil only, Section 7.3
- Combinations of NUKON and CalSil (denoted NUKON/CalSil), Section 7.4
- Coatings material tests, Section 7.5.

Results from the benchtop loop are presented for comparative purposes where appropriate. The bulk of the results from the benchtop loop are presented in Sections 3 and 6.

The discussion of the different types of debris beds includes results from multiple test series. As discussed in Section 5.3, there were slight differences in the test procedures applied to the various test series. The most significant differences are summarized below.

- Approach velocity during debris bed formation. Four Series 1 tests used an initial debris bed formation velocity of 0.2 ft/sec (0.06 m/s). The pump speed was then left constant, and the velocity declined as the pressure drop across the accumulating debris bed increased. For the remainder of the test program, the bed formation velocity was maintained at 0.1 ft/sec (0.03 m/s) throughout the bed formation process. Faster approach velocities of up to 0.8 ft/sec (0.24 m/s) were used for the coating tests (see Section 7.5). The majority of the testing conducted in the benchtop loop used a screen approach velocity of 0.2 ft/sec (0.06 m/s).
- Velocity sequence. The velocity sequence to which debris beds were subjected during testing was changed from one test series to another. Debris beds generated during the Series 1 tests were subjected to velocities at least 3 times the maximum velocity tested during the Benchmark or Series 2 tests. The velocities tested during Series 1 produced pressure drops at the higher velocities in excess of 400 in. H₂O (app 14.4 psi [99.3 kPa]). Due to perceived NPSH margins of typical centrifugal pumps, obtaining pressure drops in excess of 1 atm (14.7 psi [101.3 kPa]) was subsequently determined not to be of interest. Following the Series 1 tests, perforated plate was used exclusively for the remaining tests because this material better represented configurations being proposed by utilities for the resolution of GSI-191. Therefore, the combination of the perforated plate and the perceived NPSH margins of typical pumps motivated alterations to the velocity sequence used for the Benchmark and Series 2 tests, resulting in a lower range of approach velocities. Section 6.5 discusses the effects of the debris bed flow history on measured pressure drops. Comparisons of pressure drop measurements for different debris beds at various approach velocities should consider the complete flow history to which the debris beds were subjected.
- Filtering following debris bed formation. A 10- μ m bag filter was included in the test loop to remove suspended debris material from the flow following debris bed formation. Because debris beds compress as the approach velocity increases, it was anticipated that the filtering efficiency of a

compressed debris bed would increase with increasing approach velocity. As a result, the debris bed mass could be a function of the approach velocity and flow history (velocity cycle). Filtering after the completion of debris bed formation was only applied to the Series 2 tests.

- The Series 1 tests were conducted to simulate as closely as possible the test conditions of the 2004 LANL test conditions (Shaffer et al. 2005). No filtering was used by LANL following debris-bed formation; therefore, no filtering was applied during the Series 1 tests.
 - The Benchmark tests were conducted to obtain measurements that could be compared with those from a test loop at ANL (Kasza et al. 2006). The ANL tests, and therefore the Benchmark tests, applied no filtering following debris bed formation.
 - During the Series 2 and Coatings tests, the test fluid was passed through the filter housing at the completion of the first ramp up in the screen approach velocity to reduce the amount of suspended material and attempt to maintain a fairly constant mass on the debris bed through the remainder of the test.
- Debris preparation. The debris preparation used for the Benchmark tests used the R4 metric to match the debris preparation performed by ANL. Therefore, the prepared NUKON may have been slightly coarser for the Benchmark tests than for the Series 1 and 2 tests (see Section 5.1.2).
 - Screen material. The Series 1 tests used the 5-mesh woven cloth and the Benchmark, Series 2, and Coatings tests used the 1/8-in.-hole perforated plate. (Section 2.2 describes these screen materials in detail.) Section 7.1 compares the pressure drop measured across the screen materials.

Two additional factors that should be considered when comparing tests or evaluating trends are:

- The ratio of the retained debris loading to the target debris loading
- The flow regime (laminar, transition, or turbulent) existing in the test section when the pressure drop measurements were made.

The target debris loading is the amount of debris material introduced into the test loop; the retrieved debris bed loading is the dried mass of the retrieved debris bed and represents the amount of material on the screen at the end of the test. During testing, the debris bed was allowed to form until a steady-state condition was obtained with respect to measured pressure drop (refer to Section 5.3). However, even with a steady-state condition, it is possible for debris material to be suspended in the flow and pass through the debris bed. With an increase or decrease in the approach velocity, the debris bed may contract or expand, resulting in debris material being retained or lost, respectively. When comparing debris beds of the same retrieved mass, the initial target mass needs to be considered. If two debris beds have similar retrieved masses but different initial target masses were used to generate them, the potential exists for the debris bed with the higher initial target mass to be coarser and have a higher void fraction.

Turbulent flow is characterized by mixing action that results from eddies throughout the flow field. Most naturally observed flows, such as rivers and wind, exhibit turbulent flow. Laminar flow is a very uniform stable flow consisting of layers (lamina) of fluid gliding by each other. The streamlines of the flow are parallel, and there is no intense mixing. Any disturbances to the flow are readily damped out. Laminar flow is observed when pouring honey. Transition flow defines conditions in which neither fully laminar nor turbulent flow exists. The flow will tend to be unsteady and intermittent. Turbulent slugs of flow will be followed by intervals of near-laminar flow.

For the same debris bed and fluid properties, different pressure drop measurements can be obtained under each of the three flow regimes. One way to accomplish this is to obtain measurements from test sections of different diameter. While measurements taken in laminar or turbulent flow conditions will be repeatable, measurements taken under conditions of transition flow may yield inconsistent results.

To evaluate which flow regime is present, the Reynolds number (Re) is used. The Re is a nondimensional number that provides a relative ratio of the inertial to viscous forces existing in the flow. Re is a function of the fluid velocity, U, dynamic viscosity, μ , density, ρ , and pipe diameter, D. For pipe flow, Re is defined as

$$Re = \frac{U\rho D}{\mu} \quad (7.1)$$

For pipe flow, a $Re \geq 4000$ will produce turbulent flow, and a $Re \leq 1500$ can be assumed to yield laminar flow. For the condition of $1500 \leq Re \leq 4000$, the potential exists for transition flow to be present.

During testing, the pressure drop was evaluated at nominal temperatures of 68°F (20°C), 129°F (54°C), and 180°F (82°C). The fluid density and viscosity are temperature dependent. The flow regime present should be considered when comparing pressure drop measurements taken at different temperatures or from different test loops. Table 7.1 contains the velocity range in which the large-scale test section may have contained transition flow conditions for each nominal temperature tested.

Table 7.1. Velocity Range in Which a Transition Flow Regime May Exist for Each Nominal Test Temperature

Flow Regime	Re Used to Determine Velocity Limit	Critical Velocities for 68°F (20°C) ft/sec (m/s)	Critical Velocities for 129°F (54°C) ft/sec (m/s)	Critical Velocities for 180°F (82°C) ft/sec (m/s)
Condition defining upper bound of laminar flow	1500	0.032 (0.0098)	0.017 (0.0051)	0.011 (0.0035)
Condition defining lower bound of turbulent flow	4000	0.085 (0.0260)	0.044 (0.0136)	0.030 (0.0093)

In Sections 7.1 through 7.5, tables are presented that list all of the large-scale tests conducted for a particular debris loading condition. The tables include the test case, test series, and test ID for each associated large-scale test conducted. The test series and test ID are presented in Section 5.1. The test ID is used to identify the associated Quick Look report in Appendixes G through K. The Quick Look reports tend to reference the target debris loadings when presenting the results. In this section, test case numbers are assigned, and the results are compared relative to the retrieved debris bed mass loading.

The tables for each test condition also indicate whether a complete debris bed was formed. The formation of debris beds was characterized as complete, channeling formed, or incomplete. A complete debris bed means that following debris bed formation the entire screen and all flow areas through the screen were completely and uniformly covered. The designation “channeling formed” indicates that, at the completion of debris bed formation a complete debris bed existed, but through execution of the velocity sequence, channels were formed in the debris bed. An incomplete debris bed refers to a test condition in which a complete debris bed was never observed at any point during the test.

During the experiments, the head loss across the debris beds was measured in units of in. of H₂O at 68°F (20°C). In this section, the term pressure drop is used interchangeably with the term head loss. To convert the experimental measurements of head loss in inches of H₂O at 68°F (20°C) to pressure drop in units of psi, use the following:

$$P = \gamma h C \quad (7.2)$$

where

P = pressure in psi

γ = 62.214 lbf/ft³ specific weight of water @ 68°F

h = measured head loss in in. H₂O @ 68°F

C = 1ft³/1728 in.³ conversion factor.

In presenting the test results, less emphasis is placed on the results for incomplete debris beds. Sections 7.1 through 7.5 present the test results for each type of debris bed. Each section evaluates the effects of debris loading on the pressure drop and debris-bed height. Data on the effect of fluid temperature on the measured pressure drop are also presented. The Quick Look reports in Appendixes G through J contain the specific test conditions, the measured head loss as a function of velocity, and the measured debris bed heights for each of the tests.

7.1 Large-Scale Results of Screen-Only Tests

Testing was conducted to obtain baseline measurements of the pressure drop across the 5-mesh screen and perforated plate (1/8-in.-diameter holes) with no debris material present. Tables 7.2 and 7.3 list the screen only (SO) and plate only (PO) test cases conducted.

Table 7.2. PNNL Large-Scale Screen-Only Tests Conducted

Test Case	Test Series	Test ID	Target Debris Bed NUKON Loading (g/m ²)	Target Debris Bed CalSil Loading (g/m ²)	CalSil to NUKON Ratio	Total Target Debris Bed Loading (g/m ²)	Nom. Temp (°F)	Screen or Plate	Debris Bed Formed
SO1	1	051114_SO_0000_L1	0	0	N/A	0	70	screen	N/A
SO2	1	051128_SO_0000_L1	0	0	N/A	0	70	screen	N/A

Table 7.3. PNNL Large-Scale Plate-Only Tests Conducted

Test Case	Test Series	Test ID	Target Debris Bed NUKON Loading (g/m ²)	Target Debris Bed CalSil Loading (g/m ²)	CalSil to NUKO N Ratio	Total Target Debris Bed Loading (g/m ²)	Nom. Temp. (°F)	Screen or Plate	Debris Bed Formed
PO1	2	060804_PO_0000_LP1	0	0	N/A	0	83	plate	N/A
PO2	2	060804_PO_0000_LP2	0	0	N/A	0	131	plate	N/A
PO3	2	060805_PO_0000_LP1	0	0	N/A	0	179	plate	N/A

Measurements of the pressure drop across the bare 5-mesh screen were first taken for SO1 using a 0-to-30-in.-H₂O DP transmitter at a nominal temperature of 20°C. The fluid temperature ranged from 63°F (17°C) to 75°F (24°C) during testing. The small values obtained (<2 in. H₂O) indicated a transmitter with a lower span should be used. Test Case SO2 was a repeat of SO1 using a 0-5 in.-H₂O DP transmitter. Similar measurements were taken during test case PO1 for the bare perforated plate. The results for the pressure drop as a function of velocity for test cases SO1, SO2, and PO1 are presented in Figure 7.1 without error bars. The data series are identified by the test case and the range of the DP transmitter used to acquire the readings. Error bars for the data are included in Figure 7.2.

Comparing the cases of SO2 and PO1, the perforated plate material appears more restrictive than the 5-mesh screen. The measurements taken for SO1 tend to yield the same conclusion. All of the SO1 measurements were less than 7% of the full-scale reading for the 0-to-30-in. DP transmitter, and the main conclusion obtained is that a lower range transmitter needed to be employed.

The recorded pressure drops for all of the velocities tested for the SO and PO cases are included in the Quick Look reports in Appendix G. For comparison, the values of the measured head loss at approach velocities common to all of the tests are presented in Table 7.4

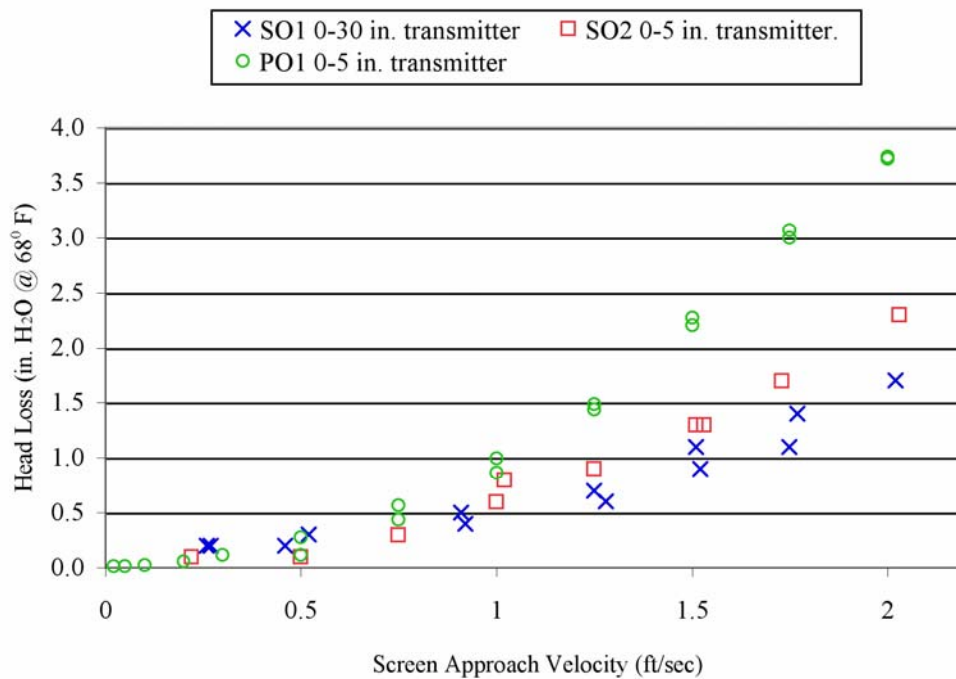


Figure 7.1. Pressure Drop as a Function of Screen Approach Velocity for the Bare Screen and Bare Perforated Plate Without Error Bars

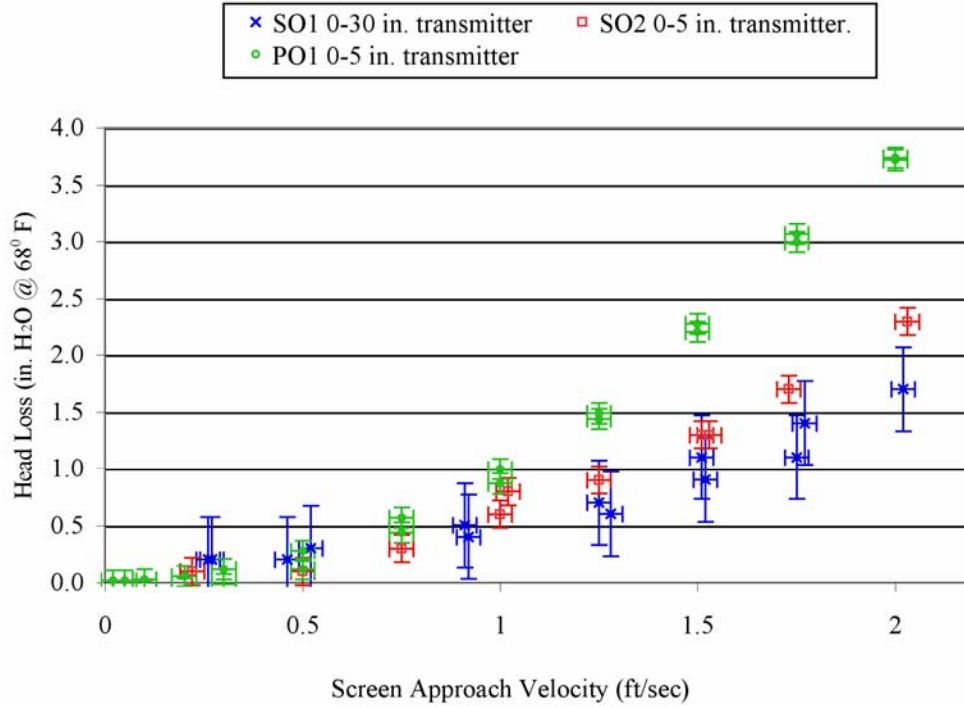


Figure 7.2. Pressure Drop as a Function of Approach Velocity for the Bare Screen and Bare Perforated Plate with Error Bars

Table 7.4. Comparison of Head Loss Measurements for Bare Screen and Bare Plate at Selected Screen Approach Velocities (temperature and zero offset corrections applied)

Screen Approach Velocity ±0.03 ft/sec	Test Cases		
	Pressure Drop Measurements for SO2 0.1 ± in. H ₂ O @ 68°F (psi)		Pressure Drop Measurements for PO1 ^(a) 0.1 ± in. H ₂ O @ 68°F (psi)
0.20–0.22	0.1 (0.00)		0.0 (0.00) 0.1 (0.00)
0.50	0.1 (0.00)		0.1 (0.00) 0.3 (0.01)
1.00	0.8 ^(a) (0.03)	0.6 ^(a) (0.02)	0.9 (0.03) 1.0 (0.04)
2.01–2.03	2.3 (0.08)		3.7 (0.13) 3.7 (0.13)

(a) Different head loss measurements were obtained for the same approach velocity. First measurements were obtained when incrementally ramping up the flow rate and the others when incrementally ramping down the flow rate.

7.1.1 Temperature Effects for Bare Perforated Plate

Because testing of debris beds generated on 5-mesh screens was not performed at elevated temperatures, no data were obtained for the bare screen at the elevated temperatures. Test cases PO2 and PO3 were performed at temperatures of 131°F (55°C) and 179°F (81°C), respectively, and are presented along with the results of PO1 in Figure 7.3 without error bars displayed. Figure 7.4 is a repeat of Figure 7.3 with the error bars included. The results have been corrected for the temperature difference between the DP manifold fluid and the test loop fluid. While lower head losses were expected at higher temperatures due to the reduced fluid viscosity and density, no significant differences were observed in the results measured for the different temperatures.

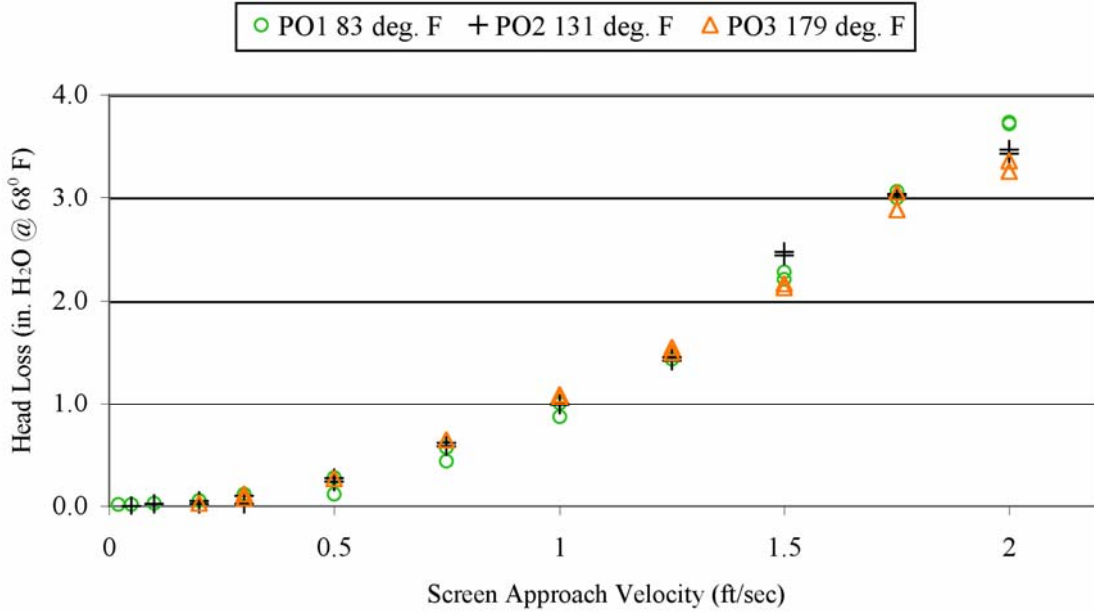


Figure 7.3. Comparison of Head Loss Across Bare Perforated Plate with 1/8-in. Holes as a Function of Screen Approach Velocity for Nominal Temperatures of 83°F (28°C), 131°F (55°C), and 179°F (81°C) Without Error Bars

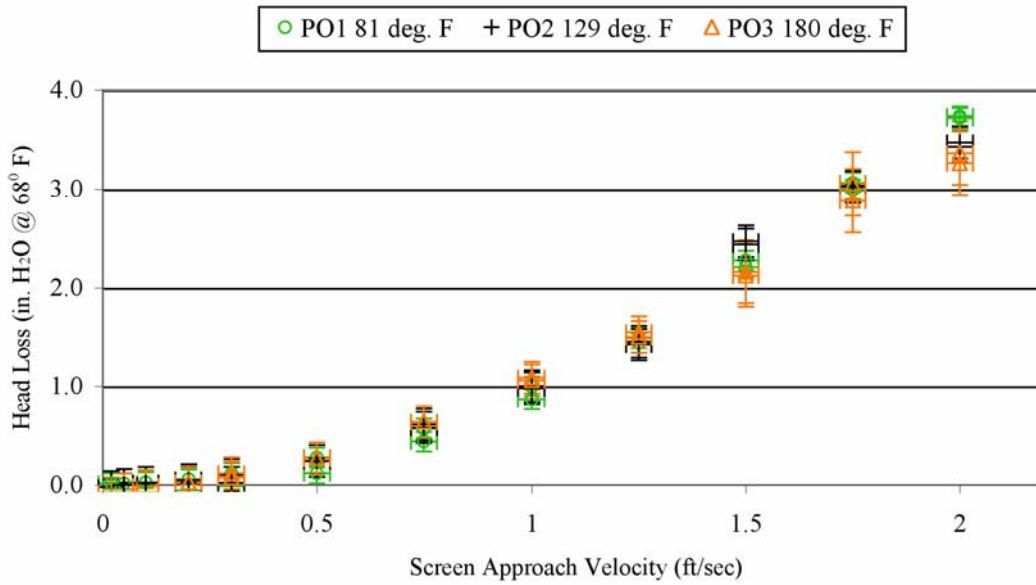


Figure 7.4. Comparison of Head Loss Across Bare Perforated Plate with 1/8-in. Holes as a Function of Screen Approach Velocity for Nominal Temperatures of 83°F (28°C), 131°F (55°C), and 179°F (81°C) with Error Bars

The recorded pressure drops for all velocities tested are included in Quick Look reports in Appendix G. For comparison, the values of the measured head loss at approach velocities common to all of the tests are

presented in Table 7.5. Due to the relatively low flow rate of the loop and the centralized location of the band heaters, the uncertainty of the loop temperature throughout the tests is $\pm 8^\circ\text{F}$ (4.4°C). The maximum uncertainty occurs at the low flow condition due to the cooling that occurs before fluid circulates back through the heaters. At 0.02 ft/sec (0.006 m/s), the loop circulation time was approximately 50 min.

Table 7.5. Comparison of Head Loss Measurements of Bare Plate at 83°F (28°C), 131°F (55°C), and 179°F (81°C) for Selected Screen Approach Velocities

Screen Approach Velocity ± 0.03 ft/sec	Test Case					
	Pressure Drop Measurements for PO1 ^(a) Fluid Temp = 83°F (28°C) ± 0.10 in. H ₂ O ^(b) (psi)		Pressure Drop Measurements for PO2 ^(a) Fluid Temp = 131°F (55°C) ± 0.16 in. H ₂ O ^(b) (psi)		Pressure Drop Measurements for PO3 ^(a) Fluid Temp = 179°F (81°C) ± 0.16 in. H ₂ O ^(b) (psi)	
0.20	0.00 (0.00)	0.06 (0.002)	0.02 (0.001)	0.05 (0.002)	0.00 (0.00)	0.03 (0.001)
0.50	0.12 (0.004)	0.28 (0.010)	0.24 (0.009)	0.27 (0.010)	0.27 (0.010)	0.27 (0.010)
1.00	0.87 (0.031)	1.00 (0.036)	0.98 (0.035)	1.00 (0.036)	1.06 (0.038)	1.09 (0.039)
2.00	3.72 (0.134)	3.74 (0.135)	3.47 (0.125)	3.43 (0.124)	3.36 ^(c) (0.121)	3.26 ^(c) (0.118)

(a) Different head loss measurements were obtained for the same approach velocity. First measurements were obtained when incrementally ramping up the flow rate and the others when incrementally ramping down the flow rate.
(b) Head loss measurements are referenced to H₂O at 68°F (20°C).
(c) Measurements have an uncertainty of ± 0.33 in. H₂O @ 68°F. Increased uncertainty is due to higher range instrument required to make measurements.

7.2 Large-Scale Results of NUKON Debris Beds

The NUKON-only cases provided the baseline conditions for evaluating debris bed pressure drop and the effects associated with debris loading, fluid temperature, and flow history. The single constituent debris bed condition reduced the complexity associated with debris bed formation resulting from multiple constituents (e.g., debris loading sequence).

Table 7.6 contains the test matrix of NUKON-only conditions completed during the test program. Cases NO4 and NO5 were conducted as part of the Series 1 tests and are repeat tests. For these cases, the initial bed formation velocity was set to 0.2 ft/sec (0.06 m/s) and the test-loop pump speed held constant. The screen approach velocity was then allowed to decrease with the increasing debris bed resistance throughout the course of bed formation.

Cases NO1, NO2, NO3a were all conducted in the same manner at ambient temperature. Cases NO3b and NO3c are a continuation of the test that generated the debris bed for case NO3a and were conducted at elevated temperatures of 129°F (54°C) and 180°F (82°C), respectively. For cases NO6a through NO7b, the debris bed was generated at elevated temperatures. The results of the cases conducted at elevated temperatures are discussed in Section 7.2.2. Bed height measurements of the debris beds are presented in Section 7.2.1. All of the mass loadings for NUKON-only debris beds tested in the large-scale loop formed complete debris beds.

As discussed in Section 5.3, the debris bed formation process was allowed to take place until a steady-state pressure drop was achieved. Following the formation of the debris bed, a velocity sequence was executed in which the screen approach velocity was incrementally ramped up and down with steady-state measurements of head loss taken at each pre-established velocity. As discussed in Section 6.5, the pressure drop was not only a function of the approach velocity but also the flow history to which the

debris bed had been subjected. For the NUKON-only tests, most repeat points for a given velocity resulted in an increase in the measured head loss. The results of Test Case NO4 provide an example of this phenomenon. Figure 7.5 is a plot of head loss as a function of screen approach velocity for the measurements obtained during the velocity ramp up phases of Test Case NO4. In examining the values obtained for velocities greater than 0.8 ft/sec, it is readily observed that the head loss increased with each consecutive ramp up of velocity.

The data provided in Figure 7.5 provide an example of the degree of repeatability that can be expected for head loss measurements obtained for the same debris bed formation conditions. The efforts put forth to control the debris preparation and debris introduction processes were made in an attempt to evaluate the variability of the debris bed formation process. Given the same debris prepared to a similar degree of fragmentation or disassociation and introduced to the screen at a similar concentration and rate, the question was whether the arrangement of the debris material on the screen would vary enough to create significant differences in the measured head loss.

Test Cases NO4 and NO5 were repeat tests performed in the large-scale loop, both with a target mass loading of 1645 g/m². The retrieved mass loading for Test Case NO4 was approximately 4% higher than that for NO5. Figure 7.6 contains head loss measurements from test Cases NO4 and NO5 from bed formation through the second ramp down. Due to the velocities selected for NO5, no data points were collected for ramp down 2 (the peak velocity at the end of ramp up 2 was followed by the minimum velocity initiating ramp up 3). Head loss measurements obtained in the benchtop loop for two tests with similar debris loadings are compared with those of NO4 and NO5 in Figure 7.7.

The results presented in Figures 7.6 and 7.7 demonstrate that reasonable repeatability was obtained between debris beds of similar composition. The lowest head loss of NOBT1 corresponds to the debris bed with the lowest retrieved mass loading. Table 7.7 compares head loss measurements from Test Cases NO4, NO5, NOBT1, and NOBT2 for velocities common to the tests. The uncertainty of benchtop measurements is greater than that obtained from the large-scale loop due to different instrumentation.

Tests NO1, NO2, NO3a, NO4, and NO5 were all conducted at ambient temperature (approximately 70°F [21°C]) over a range of debris loadings. Figure 7.8 is a plot of the head loss versus ramp up 2 screen approach velocity for the varying NUKON-only debris loadings up to a screen approach velocity of 1 ft/sec (0.3 m/s). Only the Series 1 tests exceeded screen approach velocities of 0.2 ft/sec (0.06 m/s); therefore, Figure 7.9 presents the data from Figure 7.8 between 0 and 0.3 ft/sec. Values of head loss for screen approach velocities of 0.02, 0.1, and 0.2 ft/sec are presented in Table 7.8. The transition flow regime for ambient temperature is predicted to exist between 0.03 ft/sec (0.01 m/s) and 0.08 ft/sec (0.02 m/s), and no measurements in this range were taken for data presented in Figures 7.8 and 7.9.

The majority of the results presented in Figures 7.8 and 7.9 and Table 7.8 indicate that the head loss correlates well with increases in debris mass loading. An inconsistency in the trend is observed for the case of NO3 at a screen approach velocity of 0.2 ft/sec (0.6 m/s). The head loss obtained for NO3a at an approach velocity of 0.2 ft/sec (0.6 m/s) appears to follow the trend when compared to the results of NO1 and NO2; however, it appears high when compared to the data from NO4 and NO5. Measurements of 59 and 60 in. H₂O at 0.2 ft/sec were obtained during ramp up 1 and ramp up 3 of test NO3a; the uncertainties associated with the head loss measurements are too small to account for similar measurements being obtained for NO3a, NO4, and NO5.

Table 7.6. Target Test Matrix for Large-Scale NUKON-Only Debris Bed Tests

Test Case	Test Series	Test ID	Target Debris Bed NUKON Loading (g/m ²)	Target Debris Bed CalSil Loading (g/m ²)	CalSil to NUKON Ratio	Total Target Debris Bed Loading (g/m ²)	Total Retrieved Debris Bed Loading (±8 g/m ²)	Nom. Temp. (°C)	Screen or Plate	Complete Debris Bed Formed
NO1	BM	060321_NO_0405_LP1	217	0	0.00	217	171	21	plate	yes
NO2	BM	060313_NO_1349_LP1	724	0	0.00	724	576	21	plate	yes
NO3a	2	060425_NO_2703_LP1	1450	0	0.00	1450	1244	21	plate	yes
NO3b	2	060425_NO_2703_LP2	1450	0	0.00	1450	1244	54	plate	yes
NO3c	2	060425_NO_2703_LP3	1450	0	0.00	1450	1244	82	plate	yes
NO4 ^(a)	1	051108_NO_3067_L1	1645 ^(d)	0	0.00	1645	1788	21	screen	yes
NO5 ^(a)	1	060125_NO_3067_L1	1645 ^(d)	0	0.00	1645	1719	21	screen	yes
NO6a ^(b)	2	060731_NO_2703_LP1	1450	0	0.00	1450	1250	54	plate	yes
NO6b ^(b)	2	060731_NO_2703_LP2	1450	0	0.00	1450	1250	27	plate	yes
NO7a ^(b)	2	060802_NO_2703_LP1	1450	0	0.00	1450	1190	82	plate	yes
NO7b ^(b)	2	060802_NO_2703_LP2	1450	0	0.00	1450	1190	55	plate	yes
NOBT1 ^(c)	N/A	080305_NO_1363_1	1681	0	0.00	1681	1665	26	screen	yes
NOBT2 ^(c)	N/A	081505_NO_1363_1	1681	0	0.00	1681	1702	33	screen	yes

(a) Initial screen approach velocity during debris-bed formation = 0.2 ft/sec as opposed to a constant 0.1 ft/sec.
 (b) Debris bed formation took place at elevated temperature.
 (c) Tests conducted in the benchtop loop.
 (d) Target mass loading was intended to be the same as for Test Condition 1a, 1681 g/m². However, a value of 6 in. instead of 6.065 in. was used for the test section diameter in calculating the required mass of NUKON needed for the test.

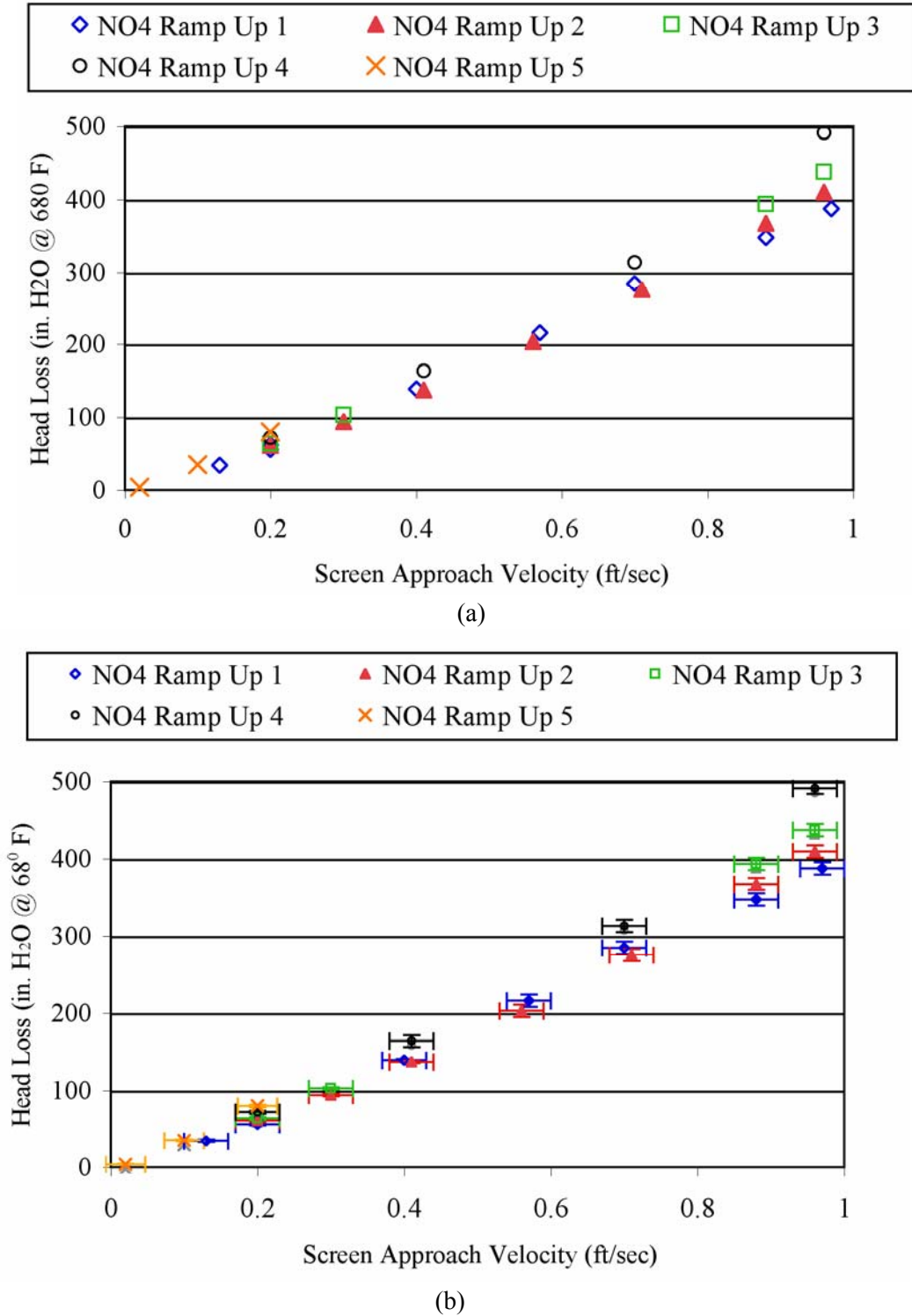


Figure 7.5. Head Loss Across Debris Bed as a Function of Screen Approach Velocity for Test Case NO4. The NUKON-only debris bed has a retrieved debris loading of 1788 g/m^2 . The plot contains only head loss measurements obtained during the ramp up portions of the velocity sequence at ambient temperature (a and b are the same plot with and without error bars, respectively).

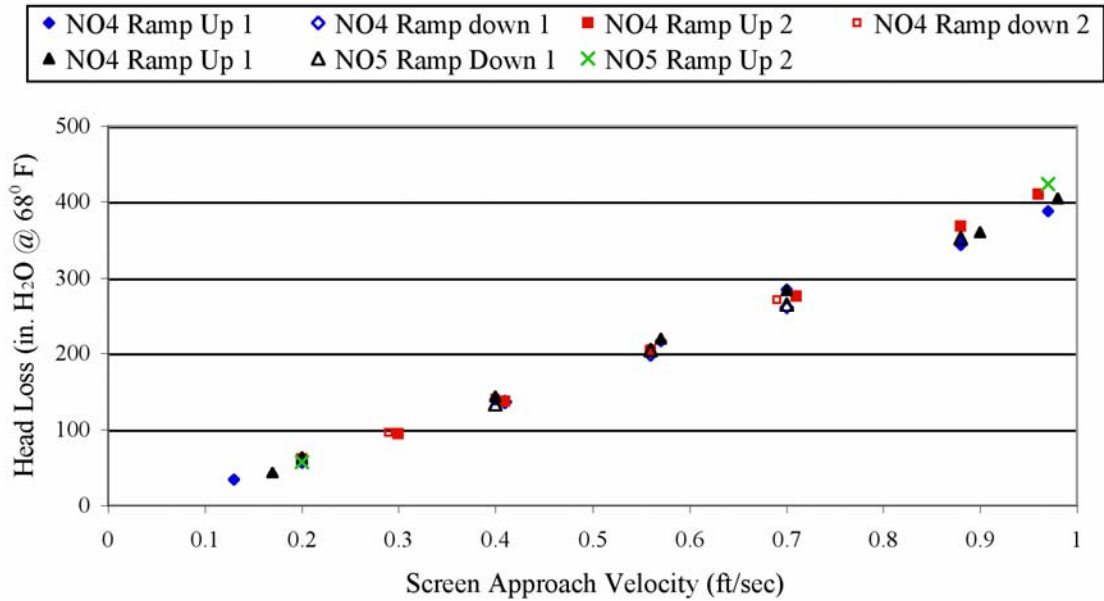


Figure 7.6. Comparison of Head Loss as a Function of Screen Approach Velocity for Repeat Test Cases NO4 and NO5. The retrieved mass loadings for NO4 and NO5 were 1788 and 1719 g/m², respectively. The data presented are from the first two velocity cycles for each test.

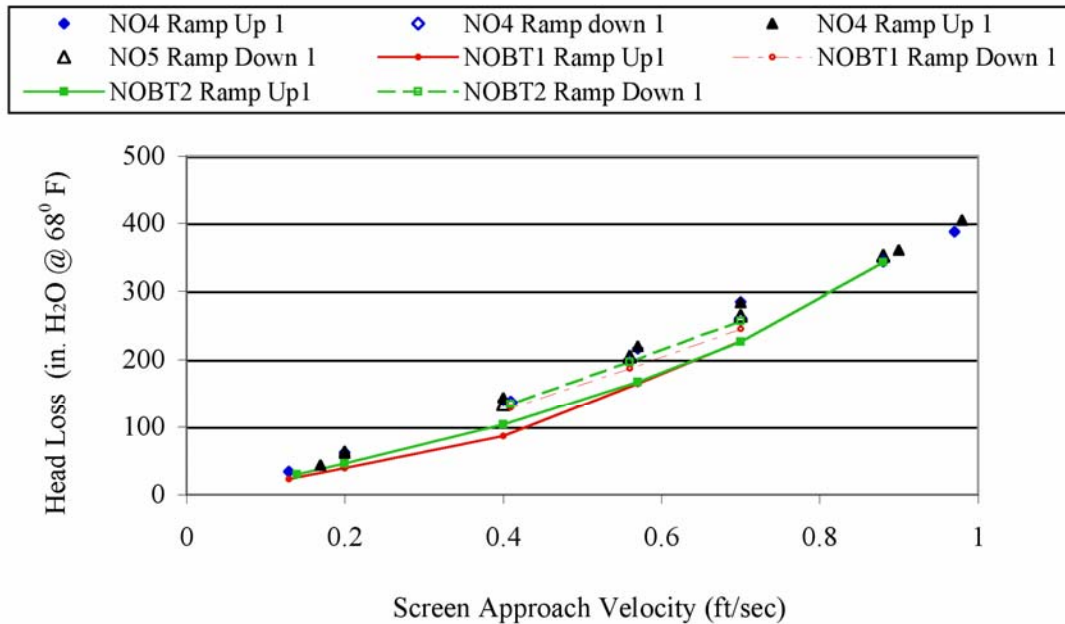


Figure 7.7. Comparison of Large-Scale and Benchtop Loop Results for NUKON-Only Test Condition 1a. The retrieved mass loadings for Test Cases NO4, NO5, NOBT1, and NOBT2 were 1788, 1729, 1665, and 1702 g/m², respectively. Data are from the first ramp up and ramp down of each velocity sequence.

Table 7.7. Comparison of Measured Head Loss at Selected Velocities for Test Condition 1a Debris Beds Generated in Both the Large-Scale and Benchtop Loops at Ambient Temperature

Screen Approach Velocity (ft/sec)	Test Case and Phase of Velocity Sequence							
	NO4 ^(a) Ramp up 1 (±1.6 in. H ₂ O) ^(c)	NO4 ^(a) Ramp down 1 (±1.6 in. H ₂ O) ^(c)	NO5 ^(a) Ramp up 1 (±1.6 in. H ₂ O) ^(c)	NO5 ^(a) Ramp down 1 (±1.6 in. H ₂ O) ^(c)	NOBT1 ^(b) Ramp up 1 (±11 in. H ₂ O) ^(c)	NOBT1 ^(b) Ramp down 1 (±11 in. H ₂ O) ^(c)	NOBT1 ^(b) Ramp up 1 (±11 in. H ₂ O) ^(c)	NOBT2 ^(b) Ramp down 1 (±11 in. H ₂ O) ^(c)
0.20	62	--	63	--	--	--	--	--
0.25	--	--	--	--	55	65	62	84
0.40-0.41	139	136	143	133	106	128	114	147
0.70	285	261	284	265	--	--	--	--
0.96-0.98	388	--	404	--	--	--	--	--
Retrieved mass loading (±8 g/m ²)	1788	1788	1729	1729	1665	1665	1702	1702

(a) Tests conducted in the large-scale test loop.
(b) Tests conducted in the benchtop test loop.
(c) Head loss measurements are referenced to H₂O at 68°F (20°C).

The percent of the target mass retained on the screen also does not explain the higher than anticipated head loss measured for the case of NO3a. Slightly less than 80% of the target mass was retained for NO1 and NO2 compared with 86% for NO3a. It should be noted that after the head loss measurements were made at ambient temperature, two additional complete velocity sequences were run for loop temperatures of 129°F (54°C) and 180°F (82°C) prior to the retrieval of the NO3a debris bed. In comparison, the debris beds for NO4 and NO5 were slightly above 100% target mass retained due to small amounts of additional debris.¹

A major difference between the debris beds of NO1, NO2, and NO3a and those from NO4 and NO5 is the bed formation velocity. A constant screen approach velocity of 0.1 ft/sec (0.03 m/s) was maintained throughout the bed formation process of tests NO1, NO2, and NO3a. For the debris beds of NO4 and NO5, as well as those from NOBT1 and NOBT2, the screen approach velocity was initially set to 0.2 ft/sec (0.06 m/s) and allowed to decrease as the resistance of the debris bed increased during the buildup of debris.

It is plausible that starting with a screen approach velocity of 0.1 ft/sec (0.03 m/s) allowed debris material to settle within the loop or be transported at a slower rate. The settling of debris segregates debris material by size. This in turn results in the initial debris bed being generated with material of a different size distribution than what was initially introduced into the loop. Following the initial bed formation process, the screen approach velocity was increased, allowing settled material to be resuspended and deposited on the debris bed. During inspection of the test loop between NUKON-only tests, no deposits of NUKON material were observed.

The term “initial debris bed” describes the debris bed formed when steady-state conditions were reached at the end of the debris bed formation process. The potential exists for both suspended and settled

¹ During the Series 1 tests, process water from the lab was used as opposed to DI water. The test loop also contained a temporary fitting due to the back ordering of a malfunctioned component. The temporary component and process water resulted in small amounts of contaminants such as rust being retained on the debris bed.

material to be added to the debris bed during ramp up 1. As the approach velocity is increased, the debris bed compresses and becomes more efficient at retaining fine debris that may be suspended in the flow when steady-state conditions are achieved for the initial debris bed. The increased velocity within the loop also allows settled debris to be resuspended and to become deposited on the top of the debris bed. Visual observations made during testing tend to indicate this phenomenon occurred. For the Series 2 tests, filtration was performed at the peak velocity of ramp up 1 to reduce the amount of debris that could be added to the debris bed afterward.

The tests conducted with an initial screen approach velocity of 0.2 ft/sec (0.06 m/s) would have experienced less material settling and thus less segregation of the debris than a debris bed generated at a constant approach velocity of 0.1 ft/sec (0.03 m/s). Therefore, the difference in the debris bed formation velocity could influence the structure of the bed and its corresponding flow resistance. In developing a debris preparation process, it was demonstrated that changing the size distribution of the debris (i.e., changing the R4 value for the material) would affect the measured head loss (refer to Section 3.2). It has also been demonstrated that changing the sequence at which material arrives or is retained on the screen can affect the resulting head loss.

Therefore, it is suggested that the difference in debris bed formation velocity might explain the inconsistency observed in comparing the results of test NO3a with those from NO4 and NO5. Based on this explanation, it is possible that the NO1, NO2, and NO3a beds may have all generated lower head losses had they been created with a faster screen approach velocity. This is only a suggested explanation. Additional testing would be necessary to validate the impact of changing the velocity at which the debris bed is formed.

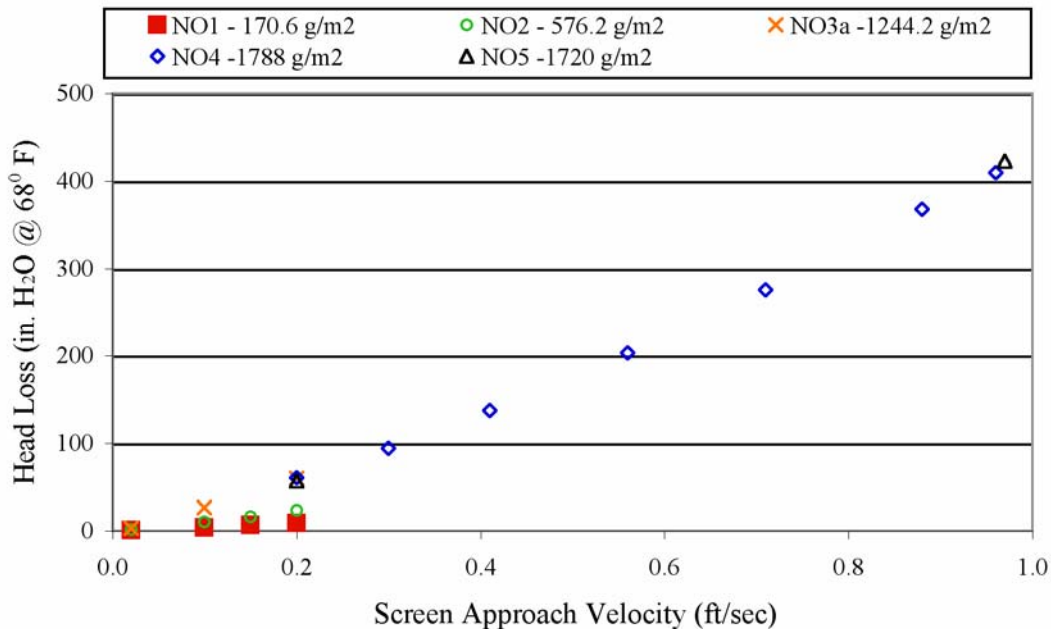


Figure 7.8. Head Loss Across the NUKON-Only Debris Beds as a Function of Screen Approach Velocity During the Ramp up 2 Portion of Each Velocity Sequence. The tests were all conducted at ambient temperature.

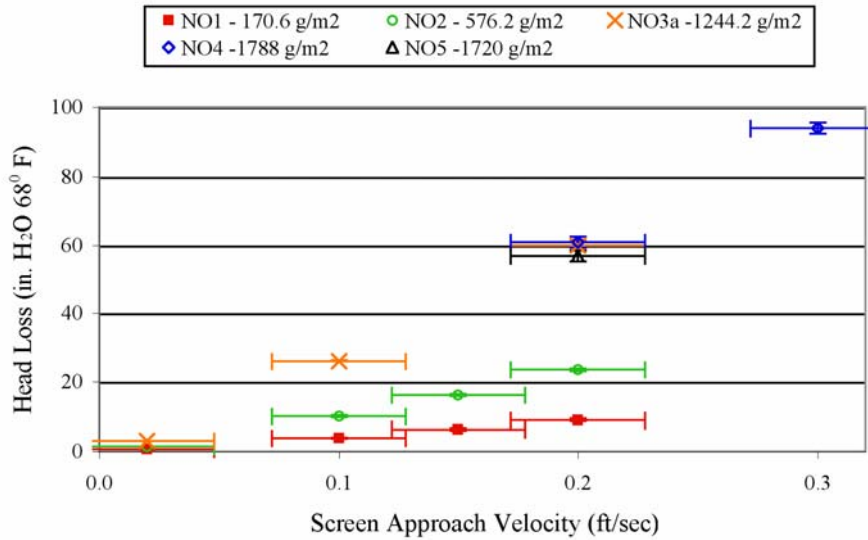


Figure 7.9. Head Loss Across the NUKON-Only Debris Beds as a Function of Screen Approach Velocity During the Ramp up 2 Portion of Each Velocity Sequence. Error bars for head loss are smaller than the symbols used. The tests were all conducted at ambient temperature.

Table 7.8. Comparison of Measured Head Loss at Selected Velocities for NUKON-Only Debris Beds Generated and Evaluated at Ambient Temperature

Screen Approach Velocity (ft/sec)	Test Case				
	NO1 Ramp up 2 (in. H ₂ O) ^(a)	NO2 Ramp up 2 (in. H ₂ O) ^(a)	NO3a Ramp up 2 (in. H ₂ O) ^(a)	NO4 ^(a) Ramp up 2 (±1.6 in. H ₂ O) ^(a)	NO5 ^(b) Ramp up 2 (±1.6 in. H ₂ O) ^(a)
0.02	0.6 ^(c)	1.4 ^(c)	3.0 ^(c)	--	--
0.1	3.9 ^(c)	10.0 ^(d)	26.0 ^(d)	--	--
0.2	8.9 ^(d)	23.5 ^(d)	60.1 ^(e)	60.9	57.0
Retrieved mass loading (±8 g/m ²)	171	576	1244	1788	1720

(a) Head loss measurements are referenced to H₂O at 68°F (20°C).
 (b) Initial screen approach velocity during debris-bed formation = 0.2 ft/sec as opposed to a constant 0.1 ft/sec.
 (c) (±0.12 in. H₂O).
 (d) (±0.34 in. H₂O).
 (e) (±1.6 in. H₂O).

7.2.1 Debris Bed Height Measurements from NUKON-Only Tests

As discussed in Section 5, three types of debris bed height measurements were taken during the test program. For all of the debris beds that were successfully retrieved, manual post-test debris bed measurements were taken. These measurements were taken after the test loop had been drained and while the debris bed was still in the test section. This method provided fairly accurate (± 0.03 in. [± 0.7 mm]) dimensions. However, the bed had been drained, and no correlation could be drawn between debris bed height under flow and the post-test dimensions of the drained debris bed. These measurements for the

NUKON-only debris beds are compared in this section. For those debris beds that were successfully retrieved, the actual measurements are included in the individual Quick Look reports (Appendix H).

In situ manual debris bed height measurements were taken during testing by an operator observing the surface of the debris bed through the TTS wall and comparing the elevation of the bed to a scale taped to the side of the TTS. For the bulk of the test, this method provided repeat measurements of the elevation of the annular rim of the debris bed at the wall of the test section. However, the outer rim of the debris bed was higher than the surface of the main body of the debris bed and precluded direct sighting of the bed surface when viewing in a horizontal plane. Attempts were made to obtain the elevation of the main body of the debris bed through the rim using back lighting. By back lighting, the surface of the debris bed was indicated by the line above which the back lighting showed through and below which the back lighting was absent. Due to the configuration and location of the mating seam for the top and bottom halves of the TTS, it was difficult to make bed height measurements of even the rim that were less than approximately 0.3 in. (8 mm) in height. For measuring the debris bed surface, this method was considered unreliable because multiple operators often reported varying results. The manual in situ measurements of debris bed height are reported in the individual Quick Look reports (Appendix H) but are not discussed in this section. Parameters affecting these measurements include the operator taking the measurements and the characteristics of the debris bed associated with the attenuation and reflection of light.

In situ debris bed height measurements were also taken via the optical triangulation method. Photographs of the debris beds were taken at each steady-state condition of the velocity sequence for post-test analysis. Due to the time and effort associated with analyzing the digital pictures, only a limited set of selected pictures was analyzed for each test. Additional pictures could be evaluated at a later date. Depending on the extent of the photo analysis, the elevation of specific points can be obtained or the entire topography of the debris bed surface can be mapped. In some instances, the optical triangulation pictures were not in focus due to opaqueness of the flow or a temporary change in lighting. Only pictures that are completely in focus can be analyzed. The optical triangulation system was not fully functional for the Series 1 tests except for Test NO5. The examination of the optical triangulation measurements will be the main focus of this section.

From measurements of debris bed height and dry retrieved bed mass, the bulk density of the debris in the bed can be calculated. Table 7.8 contains all the bed height measurements obtained with optical triangulation from the NUKON-only test cases. Table 7.8 also contains the calculated bulk dry density of the debris beds for all of the test conditions in which the photo imaging analysis was performed. The values of bulk dry debris bed density reported in Table 7.8 were obtained by calculating the debris bed volume using the product of the cross-sectional area of the test section and the average body height obtained from the optical triangulation measurements.

As expected, the height of debris beds tended to increase with retained mass loading on the screen. Figure 7.10 presents the debris bed height as a function of the screen approach velocity for the photos analyzed from Tests NO1, NO2, and NO3a. Based on the plot, for a given approach velocity, the debris bed height is relatively proportional to the debris mass loadings. A slight decrease in the bed height with increasing approach velocity is also observed.

A change in the bed formation velocity, as in the previous section, affected the observed trends in the data. The bed height measurements obtained from Test NO5 are plotted in Figure 7.11 along with the data from Figure 7.10. The results again indicate that the bed formation velocity impacts the structure of

Table 7.9. In Situ Debris Bed Height Measurements and Calculated Density Obtained from Optical Triangulation Measurements

Test Case	Retrieved Debris Bed Mass Loading ($\pm 4 \text{ g/m}^2$)	Screen Approach Velocity ($\pm 0.3 \text{ ft/sec}$)	Test Phase	Rim Ht ($\pm 0.03 \text{ in.}$)	Body Center Ht ($\pm 0.03 \text{ in.}$)	Average Body Ht ($\pm 0.03 \text{ in.}$)	Body Diameter ($\pm 0.03 \text{ in.}$)	Vol of Body (in.^3)	Bulk Dry Debris Bed Density ($\pm 0.02 \text{ g/mL}$)
NO1	170.6	0.10	RD1	0.18	0.12	0.08	5.55	1.94	0.084
		0.02	RD1	0.20	0.15	0.12	5.59	2.95	0.056
		0.20	RU2	0.20	0.12	0.10	5.60	2.46	0.067
		0.10	RU4	0.18	0.11	0.10	5.54	2.41	0.067
NO2	576.2	0.10	RD1	0.63	0.31	0.30	4.48	4.72	0.076
		0.02	RD1	0.60	0.33	0.32	4.47	5.03	0.071
		0.20	RU2	0.48	0.20	0.17	4.11	2.26	0.133
		0.20	RU3	0.45	0.18	0.17	4.29	2.46	0.133
		0.02	RD4	0.57	0.22	0.20	4.17	2.74	0.113
		0.10	RU4	0.46	0.18	0.17	4.10	2.25	0.133
		0.10	RU1	0.72	0.40	0.38	4.44	5.88	0.129
NO3a	1244.2	0.20	RU1	0.66	0.35	0.33	4.54	5.34	0.148
		0.02	RD2	0.71	0.43	0.41	4.72	7.17	0.119
		0.10	RU3	0.64	0.37	0.35	4.72	6.13	0.140
		0.20	RU3	0.61	0.31	0.29	4.72	5.07	0.169
		0.10	RD3	0.61	0.35	0.33	4.98	6.42	0.148
		0.02	RD3	0.67	0.40	0.38	4.86	7.05	0.129
		0.10	RU4	0.62	0.34	0.32	4.88	5.99	0.153
		0.20	RU1	0.57	0.34	0.32	4.96	6.19	0.153
NO3c	1244.2	0.02	RD1	0.66	0.42	0.40	4.84	7.37	0.122
		0.02	RD3	0.64	0.42	0.40	4.89	7.52	0.122
		0.96	RU4	0.36	0.26	0.27	5.24	5.82	0.251
NO5 ¹	1719.5	0.98	RU1	0.44	0.32	0.32	5.10	6.54	0.212
		0.05	RD4	0.44	0.32	0.32	5.28	6.99	0.212
		0.18	BF	0.62	0.42	0.42	4.45	6.52	0.161
		0.10	RU1	0.64	0.50	0.48	5.24	10.37	0.103
NO6a	1250.1	0.20	RU1	0.49	0.31	0.29	5.11	5.95	0.170
		0.20	RU3	0.50	0.31	0.29	5.09	5.91	0.170
		0.02	RD3	0.50	0.40	0.38	5.30	8.39	0.130
		0.10	RU4	0.50	0.33	0.31	5.14	6.42	0.159
		0.20	RU1	0.20	0.49	0.23	0.21	5.08	0.214
NO6b	1250.1	0.10	RU2	0.10	0.48	0.28	0.26	5.18	0.176

Table 7.9. (contd)

Test Case	Retrieved Debris Bed Mass Loading (±4 g/m ²)	Screen Approach Velocity (±0.3 ft/sec)	Test Phase	Rim Ht (±0.03 in.)	Body Center Ht (±0.03 in.)	Average Body Ht (±0.03 in.)	Body Diameter (±0.03 in.)	Vol of Body (in. ³)	Bulk Dry Debris Bed Density (±0.02 g/mL)
NO7a	1190.5	0.10	RU1	0.71	0.63	0.61	5.50	14.50	0.077
		0.20	RU1	0.65	0.52	0.50	5.52	11.95	0.094
		0.20	RU3	0.57	0.46	0.44	5.38	10.02	0.107
		0.10	RD3	0.57	0.46	0.44	5.49	10.42	0.107
		0.02	RD3	0.58	0.56	0.54	5.70	13.80	0.087
NO7b	1190.5	0.20	RU1	0.50	0.32	0.30	5.24	6.46	0.156
		0.10	RU2	0.50	0.33	0.31	5.18	6.53	0.151

¹ Debris bed formed with an initial screen approach velocity of 0.2 ft/sec as opposed to a constant 0.1 ft/sec

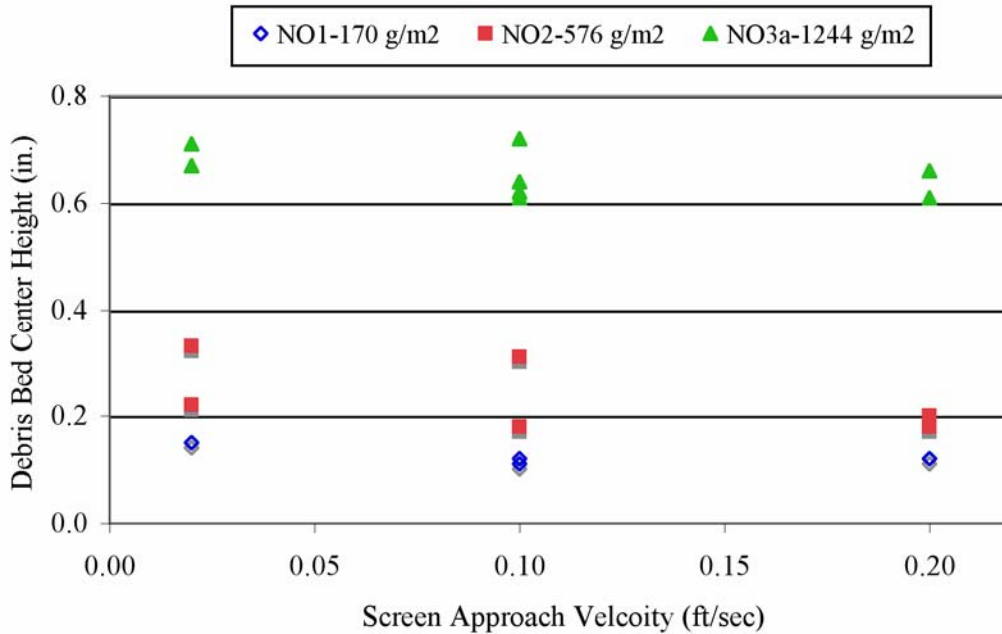


Figure 7.10. Center Height of Debris Beds from Tests NO1, NO2, and NO3a as a Function of Screen Approach Velocity. Tests NO1, NO2, and NO3a were all formed at a constant screen approach velocity of 0.1 ft/sec.

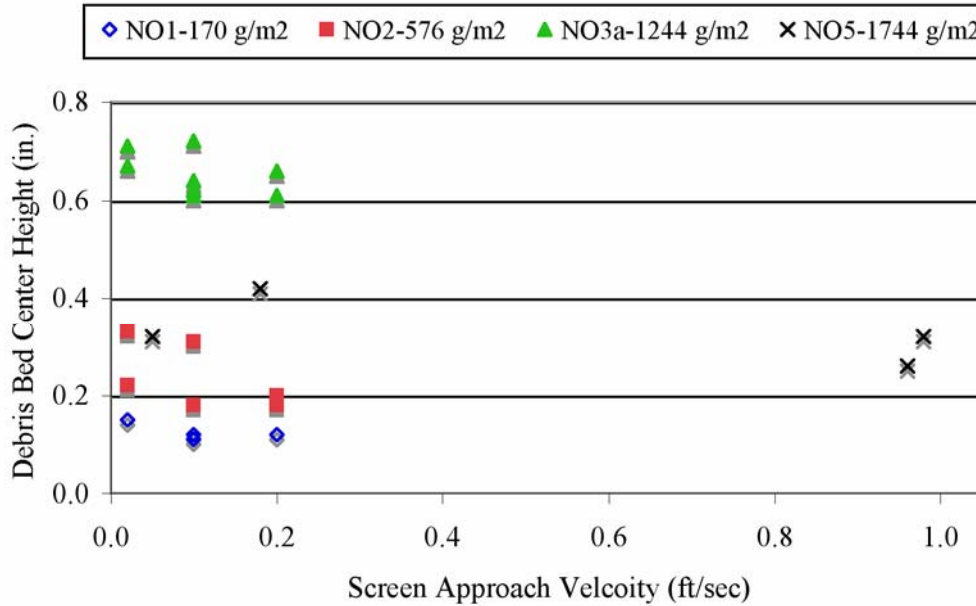


Figure 7.11. Center Height of Debris Beds from Tests NO1, NO2, NO3a, and NO5 as a Function of Screen Approach Velocity. Tests NO1, NO2, and NO3a were all formed at a constant screen approach velocity of 0.1 ft/sec and test NO5 at an initial velocity of 0.2 ft/sec.

the debris bed. Comparing the calculated bulk dry debris bed densities, from Table 7.8 for the tests plotted in Figures 7.10 and 7.11, the density of the debris bed from Test NO5 is seen to be approximately 1.2 to 4.5 times greater than that calculated for NO1, NO2, or NO3a. Considering the retrieved mass loadings for debris beds NO3a and NO5 along with the head loss data plotted in Figure 7.9, the higher-density cases did not correspond to the cases of highest head loss.

Figure 7.12 is a plot of the dry bulk density as a function of the retrieved debris bed mass loading for constant screen approach velocities. All of the data plotted is from debris beds generated with a screen approach velocity of 0.1 ft/sec (0.03 m/s). The relative bulk density of the debris beds is largest at the highest retrieved mass loadings. However, for the limited number of retrieved mass loadings obtained, no definitive relationship between the bulk density and the retrieved mass loading is observed.

The head loss across the debris bed is plotted as a function of the calculated bulk dry debris bed density for constant screen approach velocities in Figure 7.13. For all cases plotted the bed formation velocity was 0.1 ft/sec. The observed trends indicate that the bulk density increases with the screen approach velocity, and the head loss increases with the relative bulk density. Again it is noted that this trend is observed only for test cases having the same bed formation velocity (0.1 ft/sec).

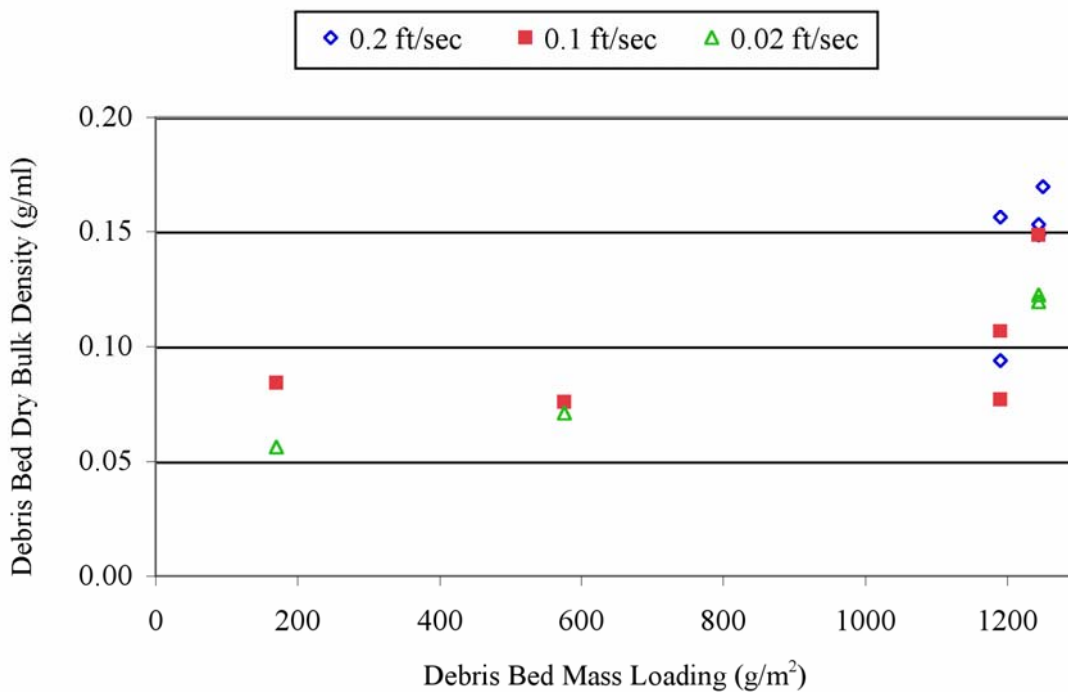


Figure 7.12. Debris Bed Dry Bulk Density as a Function of Mass Loading for the NUKON-Only Debris Beds Created and Tested at Ambient Temperature. The data presented were obtained during the first two cycles of the velocity sequence for each test. For the data plotted, debris beds were formed at 0.1 ft/sec.

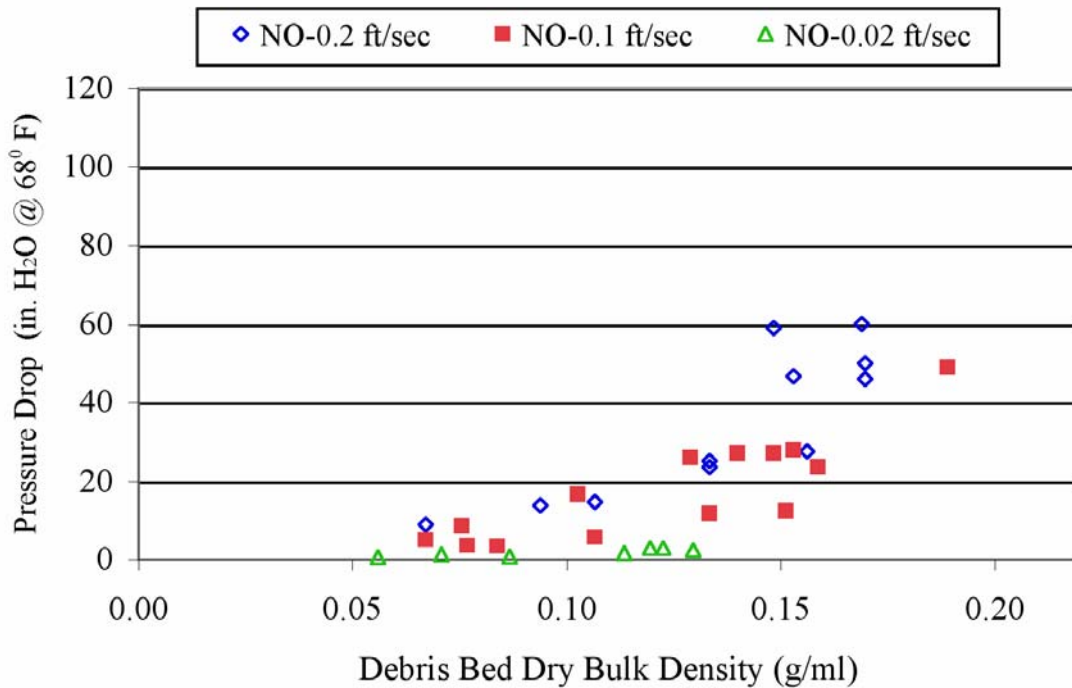


Figure 7.13. Pressure Drop Across NUKON-Only Debris Beds as a Function of Dry Bulk Density for Screen Approach Velocities of 0.02, 0.1 and 0.2 ft/sec. Debris beds were formed at a screen approach velocity of 0.1 ft/sec and tested at ambient temperature.

7.2.2 Temperature Effects on NUKON-Only Debris Beds

The initial Series 2 tests conducted to evaluate the effects of temperature on head loss consisted of elevating the loop temperature after a test at ambient temperature had been completed. The nominal elevated temperatures at which testing was performed were 129°F (54°C) and 180°F (82°C). This resulted in the measurements at elevated temperature being obtained with the debris beds having been subjected to substantially more flow history than when measurements were taken at ambient temperature. For NUKON-only, tests NO3b and NO3c were conducted in this manner. After evaluating the initial results obtained at elevated temperature, it was decided that additional tests should be conducted to further examine the effects of temperature.

For the additional tests, the debris beds were generated at the elevated test temperatures of 129°F (54°C) and 180°F (82°C). The initial head loss measurements were then taken at the temperature at which the debris bed was formed. Following the completion of the initial velocity sequence, the loop temperature was reduced and a truncated velocity sequence was executed. For NUKON-only, tests NO6a through NO7b were conducted in this manner. For Tests, NO6a and NO7a, the debris beds were generated at 129°F (54°C) and 180°F (82°C), respectively, and the full Series 2 velocity sequence was executed. Test NO6b was conducted using the debris bed generated during test NO6a with the loop temperature reduced to 81°F (27°C). Test NO7b was conducted using the debris bed generated during test NO7a with the loop temperature reduced to 131°F (55°C).

It was anticipated, based on conversations with the vendors of the debris material, that fluid temperatures between 68°F (20°C) and 180°F (82°C) would have negligible effects on the physical/chemical makeup of debris material. However, it is unknown what effect the temperature has on the material properties of the fibers (e.g., flexibility). It was also expected that increases in the fluid temperature would decrease the measured head loss due to the reduction in fluid viscosity and density.

The effects of temperature are first evaluated by examining the temperature history for individual tests. Comparisons will then be made for data sets obtained at a similar temperature. Additional parameters impacting the attempt to isolate the effects of temperature include the flow history of a debris bed and the temperature at which the debris bed was generated. For the plots used to present the head loss data, the data sets will be labeled in the legend as NO#-DTC-BF-BTC, where NO# = the test case number, DTC = the temperature at which head loss data were taken (°C), BF stands for bed formation, BTC = the temperature at which the debris bed was formed (°C). For example, NO6b-27C-BF-54C is the data taken at 27°C for test case NO6b, and the debris bed was formed at a temperature of 54°C.

For evaluating temperature effects, three NUKON-only debris beds were generated as part of Tests NO3a, NO6a, and NO7a. Refer to Section 5.3 for a description of how the testing at elevated temperatures was conducted. Figures 7.14, 7.15, and 7.16 contain the head loss data from ramp up 2 for tests NO3a, NO6a, and NO7a along with the corresponding follow-on tests conducted for each debris bed at various temperatures.

In Figure 7.14, it can be seen that the initial increase in temperature from 24° to 53°C was unexpectedly accompanied by a slight increase in head loss. The subsequent rise in temperature to 82°C resulted in a decrease in head loss. For tests NO6a and NO7a, the reduction in loop temperature for the resulting follow-on tests resulted in a corresponding increase in head loss.

Figures 7.14, 7.15, and 7.16 each contain the temperature history for a single debris bed. Each debris bed was generated at a different loop temperature. The expected decrease in head loss for increasing temperature was observed for all test cases except NO3b. The same head loss data is again presented by comparing data sets collected at the same loop temperature. Figures 7.17, 7.18, and 7.19 contain the results obtained at ambient temperature, 54°C, and 82°C, respectively.

The results presented in Figures 7.18 and 7.19 indicate that an increase in the bed formation velocity decreases the resulting head losses. However, the results of Test Case NO6b in Figure 7.17 do not follow this trend. If the calculated dry bulk densities from Table 7.9 are examined, it is observed that the head loss increases with increasing bulk density regardless of the bed formation temperature.

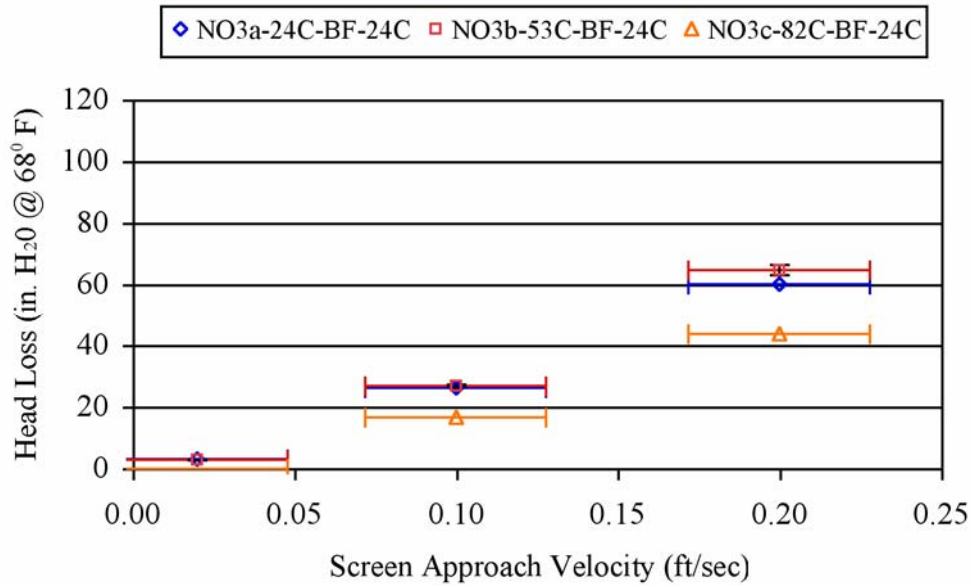


Figure 7.14. Head Loss as a Function of Screen Approach Velocity for the NUKON-Only Debris Bed Formed at 24°C. The retrieved mass loading was 1244 g/m². Tests NO3a, NO3b and NO3c were conducted sequentially at temperatures of 24°, 54°, and 82°C, respectively.

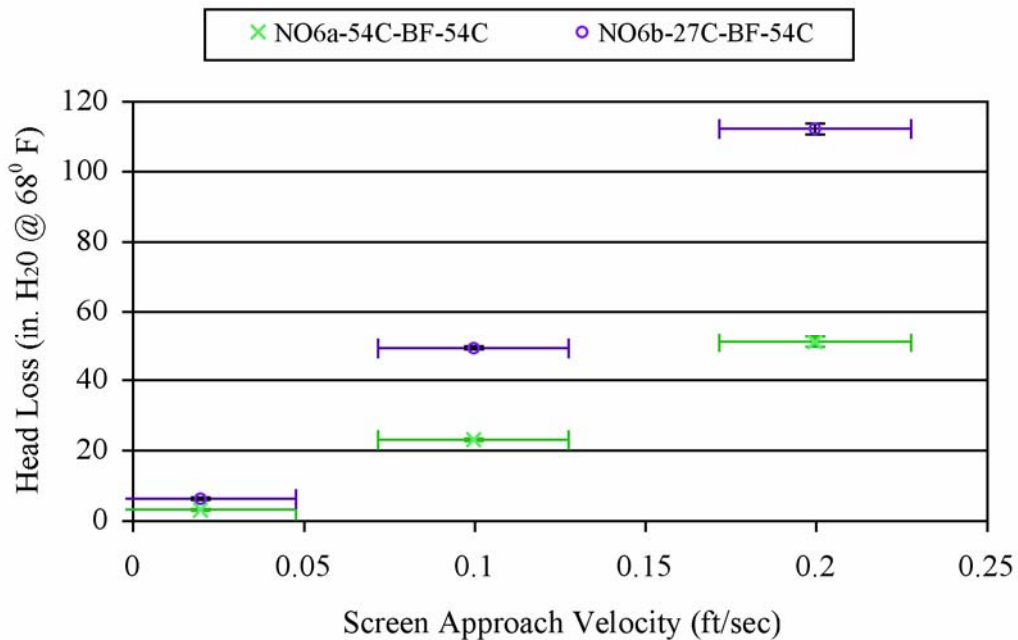


Figure 7.15. Head Loss as a Function of Screen Approach Velocity for the NUKON-Only Debris Bed Formed at 54°C. The retrieved mass loading was 1250 g/m². Tests NO6a and NO6b were conducted sequentially at temperatures of 54° and 27°C, respectively.

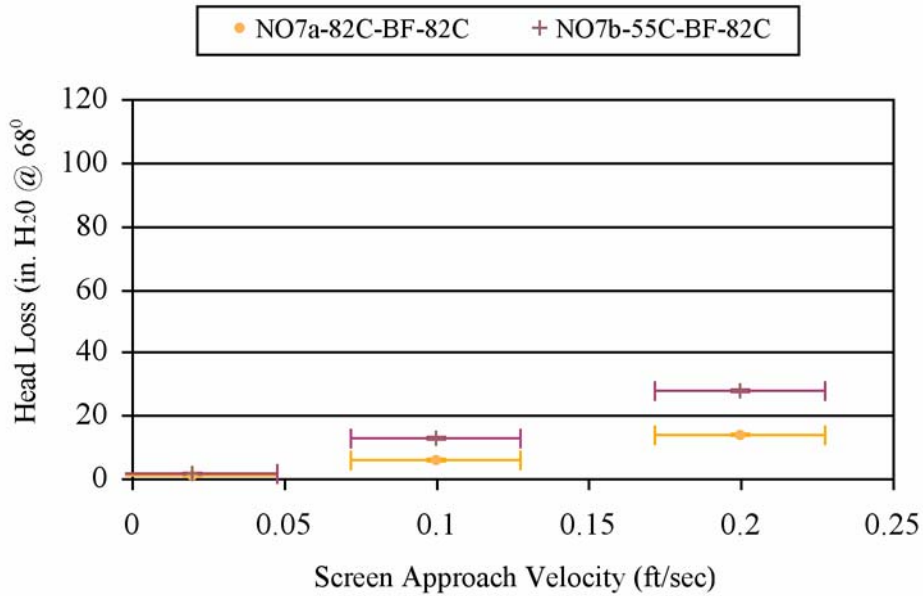


Figure 7.16. Head Loss as a Function of Screen Approach Velocity for the NUKON-Only Debris Bed Formed at 82°C. The retrieved mass loading was 1244 g/m². Tests NO7a and NO7b were conducted sequentially at temperatures of 82° and 55°C, respectively.

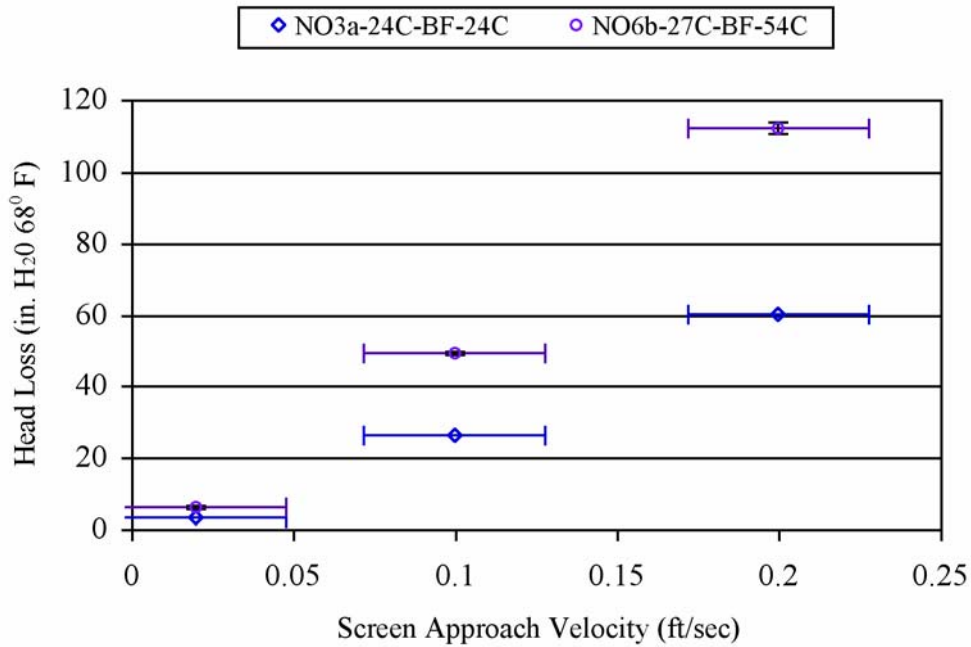


Figure 7.17. Head Loss as a Function of Screen Approach Velocity for the NUKON-Only Debris Bed Tests Conducted at Ambient Temperature. The retrieved mass loading for cases NO3a and NO6b were 1244 g/m² and 1250 g/m², respectively.

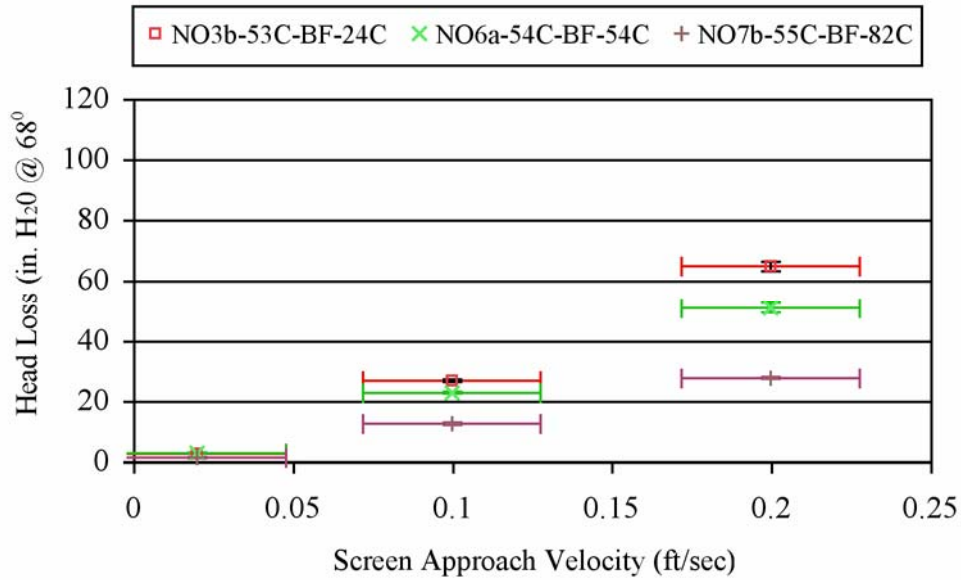


Figure 7.18. Head Loss as a Function of Screen Approach Velocity for the NUKON-Only Debris Bed Tests Conducted at Approximately 54°C. The retrieved mass loading for cases NO3b, NO6a, and NO1 were 1244 g/m², 1250 g/m², and 1191 g/m², respectively.

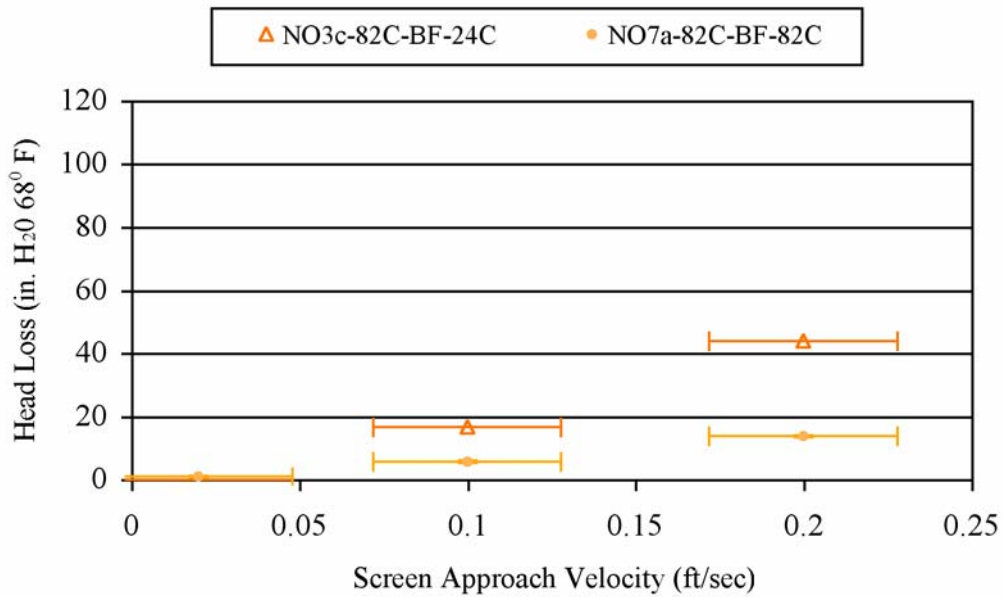


Figure 7.19. Head Loss as a Function of Screen Approach Velocity for the NUKON-Only Debris Bed Tests Conducted at Approximately 82°C. The retrieved mass loading for cases NO3c, and NO7a were 1244 g/m² and 1191 g/m², respectively.

7.3 Results of CalSil-Only Debris Bed Tests

PNNL testing for CalSil-only debris beds was initiated in the benchtop loop to assess what CalSil mass loading would be required to achieve a complete debris bed. The initial benchtop tests were conducted with both the 5-mesh woven cloth and the perforated plate with 1/8-in. holes. Based on the benchtop test results, a mass loading of 4350 g/m² was chosen for the only CalSil-only test condition conducted in the large-scale loop. The large-scale test condition was evaluated for fluid temperatures of 21°, 54°, and 82°C. None of the CalSil target mass loadings tested by PNNL produced a complete debris bed. For all of the CalSil-only tests conducted, the target mass retained on the screen ranged from 5 to 17%.

Tables 7.10 and 7.11 list the large-scale and benchtop CalSil only tests conducted, respectively. The tables include the target mass loadings, retrieved dry mass loadings, and percentages of the target mass loading retrieved on the screen. The benchtop tests are included because their results were used to determine the mass loading for the large-scale tests and are the reason only one large-scale CalSil-only debris bed test was attempted. Test cases are numbered in ascending order of target CalSil mass loading.

The various debris loading scenarios used and the observations obtained from the CalSil tests are presented in Section 7.3.1. The limited head loss measurements from the incomplete CalSil debris beds are presented in Section 7.3.2. Section 7.3.3 discusses the head loss results obtained at elevated fluid temperatures. Because no complete debris beds were formed, none of the photos taken with the optical triangulation system were analyzed for bed height measurements. Therefore, no debris bed height measurements or associated debris bed relative bulk densities are presented for the CalSil-only test cases.

Table 7.10. PNNL Large-Scale CalSil-Only Debris Bed Tests

Test Case	Test Series	Test ID	Target Debris Bed CalSil Loading (g/m ²)	CalSil to NUKON Mass Ratio	Total Target Debris Bed Loading (g/m ²)	Total Retrieved Dry Debris Bed Mass Loading (g/m ²)	Target Mass Loading Retained on Screen (%)	Nominal Temp. (°C)	Screen or Plate	Debris Bed Formed
CO1a	2	060512_CO_8108_LP1	4350	N/A	4350	434	10	21	plate	no
CO1b	2	060512_CO_8108_LP2	4350	N/A	4350	434	10	54	plate	no
CO1c	2	060512_CO_8108_LP3	4350	N/A	4350	434	10	82	plate	no

Table 7.11. PNNL Benchtop CalSil-Only Debris Bed Tests

Test Case	Test Series	Test ID	Target Debris Bed CalSil Loading (g/m ²)	CalSil to NUKON Mass Ratio	Total Target Debris Bed Loading (g/m ²)	Total Retrieved Dry Debris Bed Mass Loading (g/m ²)	Target Mass Loading Retained on Screen (%)	Nominal Temp. (°C)	Screen or Plate	Debris Bed Formed
COBT1 ^(a)	N/A	060406_CO_1176_BP1	1450	N/A	1450	79	5 ^(a)	21	plate	no
COBT2	N/A	060510_CO_1469_BP1	1812	N/A	1812	237	13	21	plate	no
COBT3 ^(b)	N/A	051227_CO_0411x_B1	2174	N/A	2174	184	9 ²	26	screen	no
COBT4	N/A	051227_CO_1763_B2	2174	N/A	2174	279	13	26	screen	no
COBT5	N/A	060510_CO_1763_BP2	2175	N/A	2175	292	13	23	plate	no
COBT6	N/A	060510_CO_2351_BP3	2900	N/A	2900	390	13	22	plate	no
COBT7	N/A	060511_CO_3527_B2	4350	N/A	4350	724	17	22	plate	no

(a) Debris bed disturbed during retrieval. Therefore retrieved mass does include all of the debris material retained on the screen.

(b) Debris incrementally added to the loop in a total of 5 separate batches to obtain the total mass loading.

7.3.1 CalSil Debris Bed Formation

The initial CalSil tests conducted were COBT3 (051227_CO_0411x_B1) and COBT4 (051227_CO_1763_B2). The final target mass loading for both tests was the maximum CalSil loading that had been proposed by the NRC for the Series 1 test matrix. These tests were performed as part of the

load sequence evaluation using the 5-mesh screen. Subsection 6.3.1.2 contains a description of the tests and photos of the two retrieved debris beds (Figures 6.13 and 6.14).

For COBT3, the CalSil debris was added incrementally by recharging the debris injection line five times. For COBT4, the total mass of CalSil was added to the debris injection line at one time and a single debris introduction procedure was executed. While neither test formed a complete debris bed, COBT4 with the single introduction of debris material retained approximately 50% more material than the incremental addition of the debris employed for COBT3. This limited evidence suggests that bulk-loading (single introduction) of the target CalSil mass may have a greater probability of forming a complete CalSil-only debris bed than performing incremental additions to achieve the total target CalSil mass loading. This is the expected result since the bulk-loading would result in the debris having being at a higher concentration when it reached the screen. The higher debris concentration promotes retention on the screen.

Figure 7.20 shows the underside (downstream side, discharge) of the COBT3 debris bed. From the photo one can observe how the CalSil material is wrapped completely around the wires of the screen material. This phenomenon was not observed for the NUKON-only tests presented in Section 7.2.

Test COBT1 was conducted to assess whether the peak CalSil mass loading specified by the NRC in the proposed Series 2 test matrix (NRC 2006) would form a complete debris bed on the perforated plate. The initial screen approach velocity for bed formation was 0.1 ft/sec, which was maintained for approximately 13 calculated loop circulations (approximately 20 minutes) without forming a debris bed. The screen approach velocity was then increased to 0.2 ft/sec for approximately an additional 26 calculated loop circulations (approximately 20 minutes) in an attempt to mobilize any settled CalSil material.

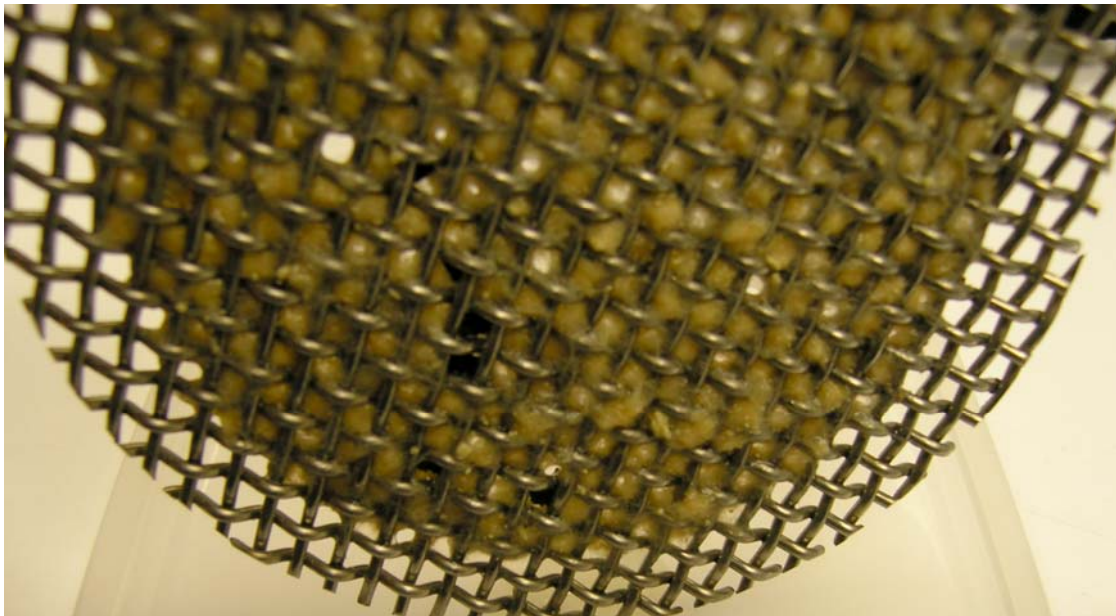


Figure 7.20. Underside of Incomplete Debris Bed from COBT3 Showing How CalSil Material was Completely Entangled with Some Screen Wires in Test 051227_CO_0411x_BP1. Target CalSil mass loading =2174 g/m², retrieved CalSil mass loading = 184 g/m², 9% of target mass retained on screen, debris bed formed in benchtop test loop.

The higher velocity increased the amount of debris that accumulated on the perforated plate based on visual observations. After about one circulation of the flow loop (approximately 45 sec), the resuspended CalSil material appeared to fill up the holes/openings of the incomplete debris bed. However, a complete debris bed was apparently not sustained. The test section then became very murky, making it extremely difficult to observe the debris bed. The presence of similar amounts (as judged by visual observation) of CalSil debris both above and below the perforated plate may indicate that suspended CalSil was passing uninhibited through the perforated plate or possibly being deposited on the plate but also being lost from the debris bed at a similar rate. Because of the very murky test section, it was not possible to observe whether the holes/openings in the perforated plate were re-exposed. After 20 minutes at 0.2 ft/sec, the debris bed was judged, based on visual observation, to still be incomplete.

During the retrieval of the debris bed for COBT1, a potentially significant portion of the retained CalSil debris was visually observed to be flushed off the screen. Figure 7.20 is a photo of that portion of the retrieved debris bed considered to have experienced the least disturbance. The retrieved mass loading reported in Table 7.11 is known to be less than the amount retained on the screen during the test.

Additional benchtop tests were conducted with progressively larger CalSil mass loadings in an attempt to determine the target mass loading sufficient to generate a complete debris bed in the large-scale test loop. The results of subsequent tests were used to determine the mass loading for the following test. Tests COBT2, COBT5, COBT6, and COBT7 were conducted with target mass loadings 1.25, 1.5, 2.0, and 3.0 times the mass loading of COBT1, respectively. None of the tested mass loadings yielded a complete debris bed. The retrieved debris beds from these tests are pictured in Figures 7.21 through 7.24. The specifications for each test are detailed in the Quick Look reports of Appendix I.



Figure 7.21. Incomplete Debris Bed from COBT1, Test 060406_CO_1176_BP1. NOTE: Debris bed was disturbed during retrieval. The lower half of the photo was not representative of the screen coverage achieved in the test loop and therefore was omitted from the figure. Target CalSil mass loading = 1450 g/m², retrieved CalSil mass loading = 79 g/m² (reduced due to disruption of debris bed during retrieval), 5% of target mass retained on screen, debris bed formed in the benchtop test loop.



Figure 7.22. Incomplete Debris Bed from COBT2, Test 060510_CO_1469_BP1. Target CalSil mass loading = 1812 g/m², retrieved CalSil mass loading = 237 g/m², 13% of target mass retained on screen, debris bed formed in benchtop test loop.



Figure 7.23. Incomplete Debris Bed from COBT5, Test 060510_CO_1763_BP2. Target CalSil mass loading = 2175 g/m², retrieved CalSil mass loading = 292 g/m², 13% of target mass retained on screen, debris bed formed in the benchtop test loop.



Figure 7.24. Incomplete Debris Bed from COBT6, Test 060510_CO_2351_BP3. Target CalSil mass loading = 2900 g/m², retrieved CalSil mass loading = 390 g/m², 13% of target mass retained on screen, debris bed formed in the benchtop test loop.

It was speculated, based on the thickness and appearance of the debris bed retrieved from COBT7, that the potentially nonuniform flow profile in the benchtop loop upstream of the test screen could be creating an uneven distribution of CalSil debris at the surface of the perforated plate. Examining Figure 7.25, the majority of perforated plate appears to be covered with a substantial thickness of debris material. No evidence of the plate hole pattern is observed on the surface of the debris bed. The topography of the surface of the debris bed and the fact that all of the open channels are located on one side of the debris bed indicate the approaching flow stream may have possessed a substantial swirl component that inhibited the formation of a complete debris bed. The relatively longer section of straight pipe upstream of the test screen in the large-scale loop would eliminate this phenomenon. Therefore, it was postulated that a mass loading of 4350 g/m² would be sufficient to generate a complete debris bed in the large-scale loop.

The mass loading of 4350 g/m² was used for conducting CO1a in the large-scale loop. Test cases CO1b and CO1c were conducted with the same debris bed at fluid temperatures of 54° and 82°C, respectively. At no time during any of the three tests was a complete debris bed visually observed. Figure 7.26 is an upstream photo of the retrieved debris bed from test condition CO1. The open channels in Figure 7.26 are distributed throughout the debris bed in contrast to those of the benchtop debris bed pictured in Figure 7.25. The head loss results obtained for CO1a through CO1c are presented in the next two sections.

The CalSil debris beds had debris extruded through the holes of the perforated plate. The majority of the material protruding through the holes appeared to be at the location of open channels. Figure 7.27 is the underside of the perforated plate retrieved from the benchtop test COBT7. Side views of the debris beds and perforated plates from tests COBT7 and CO1 are presented in Figure 7.28. Minimal entangling (attaching to debris from other holes) of the debris material extruded through the holes was observed. This contrasts with the appearance of the material on the underside of the 5-mesh woven wire observed after tests COBT3 and COBT4 in Figure 7.20. The topography of the debris bed surface in the region of the channels can also be seen in Figure 7.28.



Figure 7.25. Incomplete Debris Bed from COBT7, Test 060511_CO_3527_BP2. Target CalSil mass loading = 4350 g/m^2 , retrieved CalSil mass loading = 724 g/m^2 , 17% of target mass retained on screen, debris bed formed in the benchtop test loop.



Figure 7.26. Incomplete Debris Bed from Test Condition CO1, Tests 060510_CO_8108_LP1 Through LP3. Debris bed pictured within TTS, target CalSil mass loading = 4350 g/m^2 , retrieved CalSil mass loading = 434 g/m^2 , 10% of target mass retained on screen, debris bed formed in large-scale test loop.

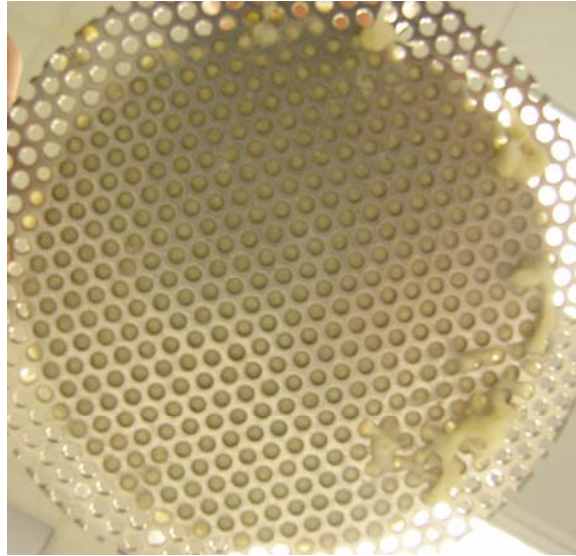
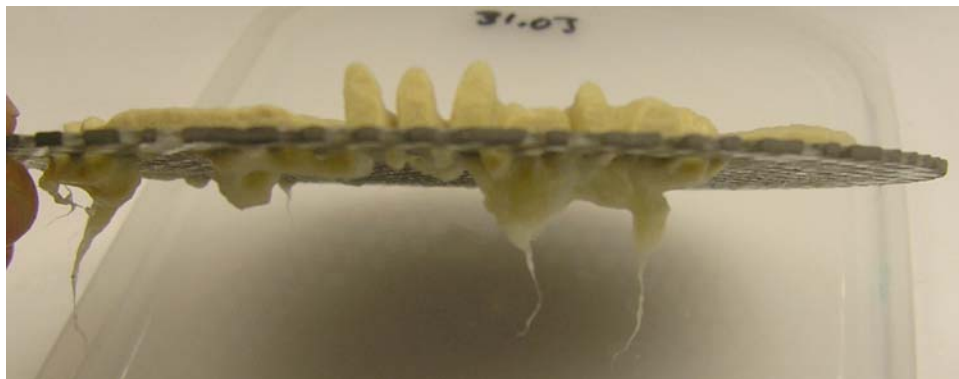
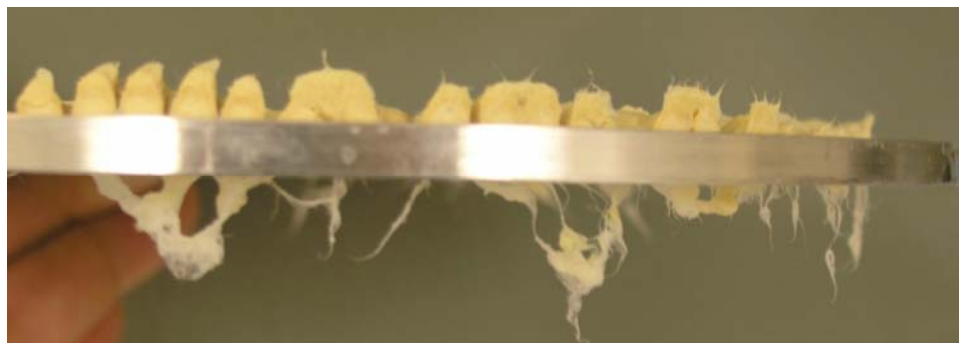


Figure 7.27. Extruded Debris Viewed from the Underside of the Perforated Plate after Benchtop Test COBT7. Retrieved mass loading was 724 g/m^2 , debris extruded through some of the plate holes but was not entangled with the plate (refer to Figure 7.20).



a.



b.

Figure 7.28. Side Views of the Debris Bed and Perforated Plate for Large-Scale and Benchtop Test Cases CO1 and COBT7. Target mass loadings of 4350 g/m^2 debris on the underside of the perforated plate were extruded through the holes in the plate. Figure 7.28a is from COBT 7 with a retrieved mass loading of 724 g/m^2 ; Figure 7.28b is from CO1 with a retrieved mass loading of 434 g/m^2 .

Tables 7.10 and 7.11 also list the percent of the target CalSil mass loading that was retained on each debris screen. Despite significant changes in the target mass loading, test cases COBT2, COBT4, COBT5, and COBT6 all retained 13% of the introduced CalSil. Test Case COBT1 is not a good comparison because it was disturbed during retrieval; neither is Test Case COBT3 because it was formed using incremental addition of the debris. The other benchtop case, COBT7, had a mass loading 2.4 times that of COBT2 and still only retained 17% of the introduced CalSil. In addition, the large-scale test case, CO1, retained 10% of the initial CalSil. This similarity in the retained mass fraction of introduced material indicates that additional CalSil loading does not lead to increased retention.

Having the same fraction of debris retained on the screen over a range of target mass loadings indicates a critical particle size may exist for retention. The CalSil material is made up of 4% by mass fibrous material. If 100% of the CalSil fiber material is retained on the screen, the critical particle size for retention could be approximated using the CalSil particle size data from Section 3.2.2.

7.3.2 Pressure Measurements for CalSil-Only Debris Beds

The benchtop loop had only a single differential pressure transmitter with a range of 0 to 1000 in. H₂O (in. H₂O @ 68°F). Therefore, the resolution and uncertainty of the benchtop measurements are not as good as those obtained from the large-scale loop. The greatest impact is for low pressure drops in the lower 1% of the transmitter range (<10 in. H₂O).

The pressure drop as a function of the screen approach velocity is presented in Figure 7.29 for the large-scale test conducted at ambient temperature, CO1a. The plot contains the data for all four ramp ups in velocity and the first ramp down. Other than ramp up 1, the results were repeatable from one ramp up to another. The increase in pressure observed for the NUKON-only debris beds for repeated cycling of the approach velocity was not observed, which may be because the CalSil-only debris beds were incomplete.

Figure 7.30 compares the pressure drop as a function of the screen approach velocity for benchtop cases COBT2, COBT5, COBT6, and COBT7 and the large-scale case CO1a. The legend of the plot contains the retrieved mass loading after each test case number. The plotted results indicate that, even for the incomplete debris beds, the head loss increases with increasing mass loading.

The pressure drop data for COBT3 and COBT4 was obtained at higher screen approach velocities so a good comparison cannot be made (Section 6.3.1.2). Test Case COBT1 was conducted to determine whether a complete CalSil-only debris bed could be formed, and minimal head loss data were recorded. Following bed formation at 0.1 ft/sec for COBT1, the pressure drop indication was still 0 in. H₂O. After the extended bed formation at 0.2 ft/sec, the indicated pressure drop was 0.1 in. H₂O.

The pressure drop as a function of the retrieved mass loading is plotted in Figure 7.31 for constant velocities of 0.1 and 0.2 ft/sec for the same test cases as plotted in Figures 7.30. The plot in Figure 7.31 indicates how the large-scale and benchtop results compare. Despite the incomplete debris beds, the large-scale data appear to fit well with the benchtop data at both 0.1 and 0.2 ft/sec.

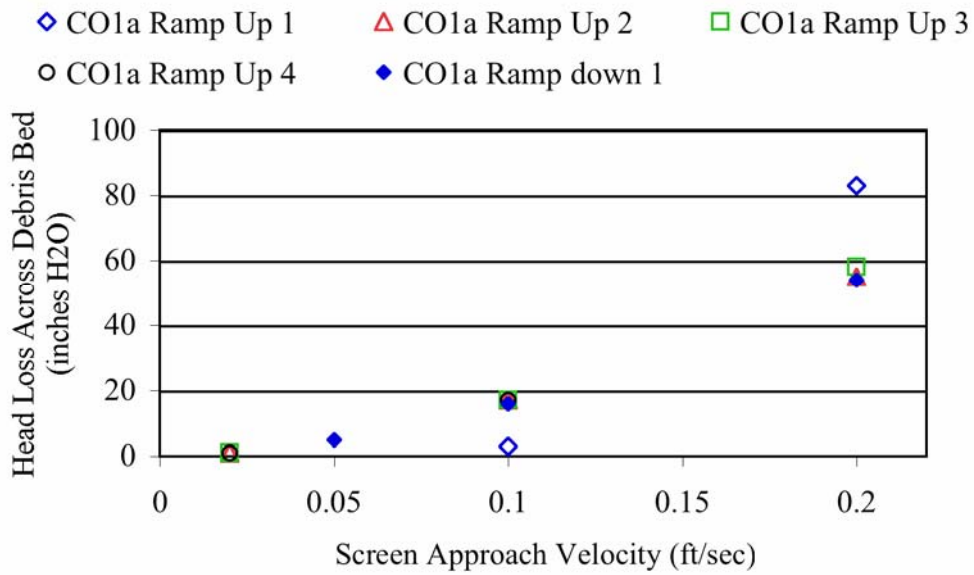


Figure 7.29. Pressure Drop as a Function of the Screen Approach Velocity for CO1a, with a Target CalSil Mass Loading of 4350 g/m² and a Retrieved Mass Loading of 434 g/m². Head loss data are from the Quick Look report for 060512_CO_8108_LP1 in Appendix I.

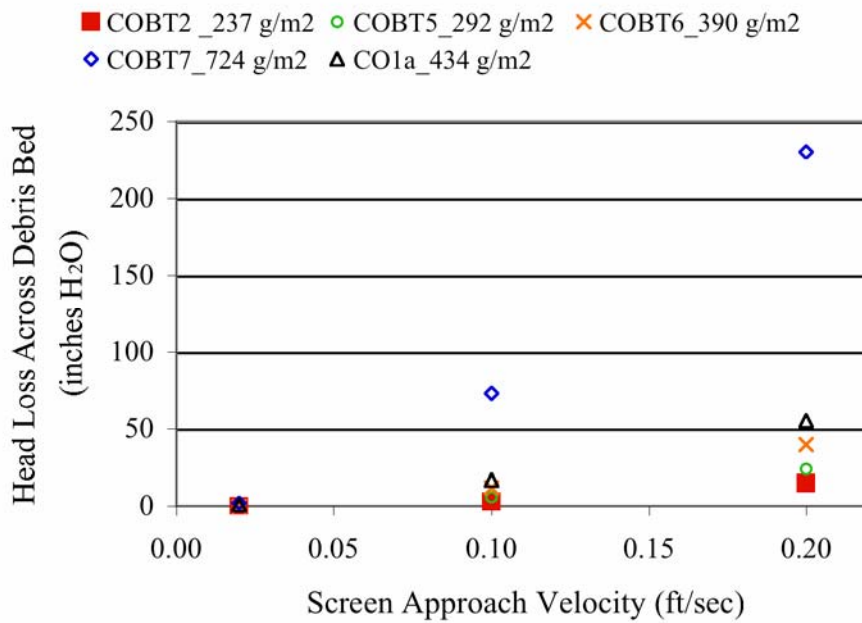


Figure 7.30. Pressure Drop as a Function of Screen Approach Velocity for Benchtop Tests COBT2, COBT5, COBT6, and COBT7 and Large-Scale Test CO1a. Head loss data are from the Quick Look report for 060512_CO_8108_LP1 in Appendix I.

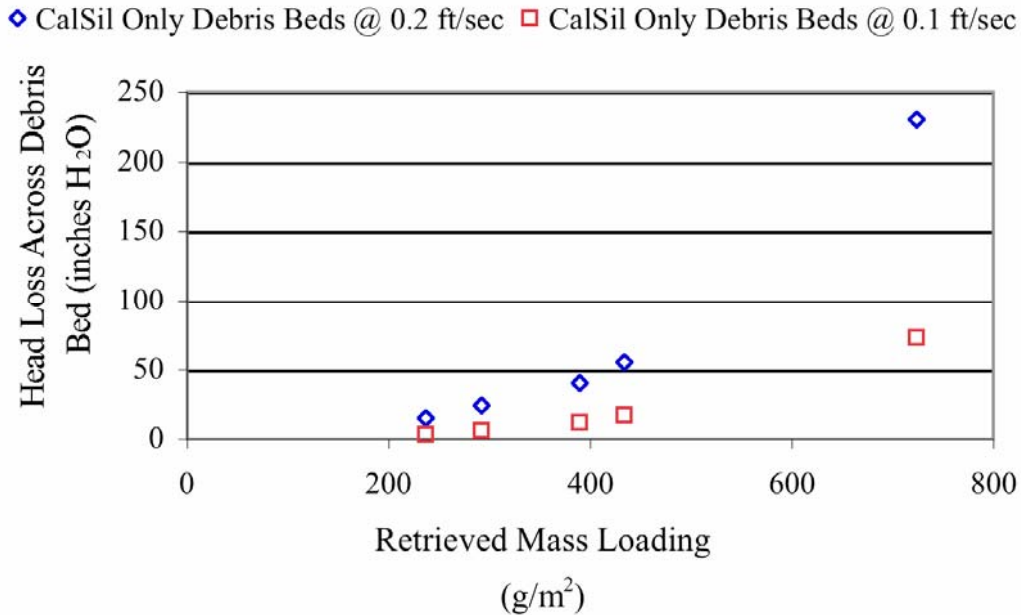


Figure 7.31. Pressure Drop as a Function of Retrieved Mass Loading at Constant Screen Approach Velocities of 0.1 and 0.2 ft/sec. Data plotted for benchtop tests COBT2, COBT5, COBT6, and COBT7 and large-scale test CO1a. Head loss data from Quick Look report for 060512_CO_8108_LP1 in Appendix I.

7.3.3 Temperature Effects on CalSil-Only Debris Beds

The CalSil for test case CO1a was introduced at a fluid temperature of approximately 70°F (21°C). Following the execution of the velocity sequence, the fluid temperature was raised to 129°F (54°C) and the velocity sequence again executed to obtain the steady state measurements for CO1b. The process was again repeated by raising the fluid temperature to 180°F (82°C) to obtain the measurements for CO1c.

The head loss measurements for CO1b were essentially the same as for CO1b without the variations observed in ramp up 1 for CO1a. However, the pressure drop measurements obtained for CO1c yielded an increase in pressure with each velocity cycle. For a screen approach velocity of 0.2 ft/sec, the resulting head loss was 53, 69, and 74 in. H₂O for ramp ups 1 through 3. It is unclear exactly what caused the increase in head loss, and it is assumed that the debris bed retained additional mass, debris material redistributed within the bed (e.g., surface material flowed over an open channel), or the debris properties changed as a function of temperature.

Head loss data are plotted in Figure 7.32 for velocity ramp up 2 of the three temperature cases of test condition CO1. Velocity ramp down 1 has been included for CO1c due to unexplained changes observed for ramp up 2. The other three data sets indicate no measurable change in head loss due to changes in fluid temperature. The effects may be the result of not only the elevated temperature but also the temperature history (i.e., time at temperature and time associated with fluid heat up).

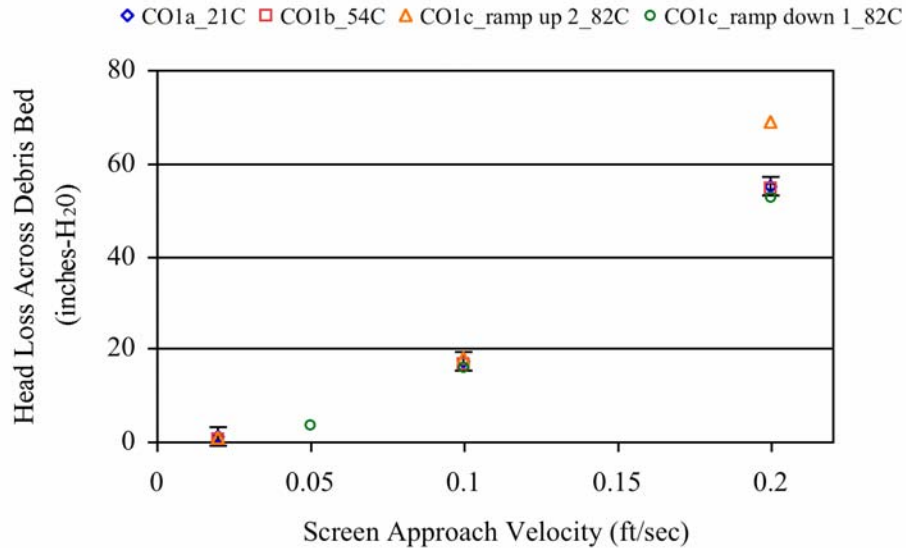


Figure 7.32. Pressure Drop as a Function of Screen Approach Velocity for Test Condition CO1. Target CalSil mass loading was 4350 g/m² and retrieved mass loading was 434 g/m². Test cases CO1a, CO1b, and CO1c were conducted at fluid temperatures of 21°, 54°, and 82°C, respectively. Data for velocity ramp up 2 except as noted for CO1c. Head loss data are from Quick Look report for 060512_CO_8108_LP1 in Appendix I.

7.4 Large-Scale Results for Debris Beds Containing NUKON and CalSil

Sections 7.2 and 7.3 presented the results of the single constituent tests conducted with NUKON-only and CalSil-only debris beds, respectively. The results presented in this section are for tests conducted with both NUKON and CalSil (referred to as NUKON/CalSil or NC) being introduced to the test loop at the same time. Table 7.12 contains the target test matrix for the NUKON/CalSil tests, the dry retrieved mass loadings of the retrieved debris beds, the nominal temperatures at which testing was conducted, the screen materials used, and indication of whether a complete debris bed was formed. An overview of the test matrix completed is provided in Section 7.4.1.

From the results of the NUKON-only tests presented in Section 7.2, it was observed that parameters influencing the debris bed head loss included the mass loading, the flow history, the fluid temperature, the relative bulk density of the debris bed determined from measurements of the debris bed height, and potentially the bed formation velocity. Having a second debris constituent potentially adds the mass loading for the individual constituents and the associated mass ratio of the constituents as parameters influencing the head loss across the debris bed.

The target test matrix was based on a parametric study of the target mass loadings of the constituents and the assumption that the either all of the mass would be retained on the screen or at least the ratio of the debris constituent masses retained on the screen would be similar to the target ratio. In Section 7.2, the results of the NUKON-only tests were presented relative to the retrieved mass loading of NUKON. The same presentation is used for the CalSil in Section 7.3. To evaluate the effects of CalSil being added to the NUKON, the masses of the individual constituents should be determined. Following a preliminary

Table 7.12. Target Test Matrix for Large-Scale NUKON/CalSil Debris Bed Tests

Test Case	Test Series	Test ID	Target Debris Bed NUKON Loading (g/m ²)	Target Debris Bed CalSil Loading (g/m ²)	Target CalSil to NUKON Ratio	Total Target Debris Bed Loading (g/m ²)	Total Retrieved Debris Bed Loading (±8 g/m ²)	Nominal Temp. (°C)	Screen or Plate	Complete Debris Bed Formed
NC1	2	060427_NC_0252_LP1	108	27	0.25	135	56	21	plate	no
NC2	2	060428_NC_0453_LP1	108	135	1.25	243	94	21	plate	no
NC3 ^(a)	1	051110_NC_0595_L1	213	106	0.50	326	217	21	screen	yes
NC4	2	060509_NC_0505_LP1	217	54	0.25	271	209	21	plate	yes
NC5a	2	060426_NC_0708_LP1	217	163	0.75	380	213	21	plate	yes
NC5b	2	060426_NC_0708_LP2	217	163	0.75	380	213	82	plate	yes
NC6a	2	060517_NC_0808_LP1	217	217	1.00	434	297	21	plate	yes
NC6b	2	060517_NC_0808_LP2	217	217	1.00	434	297	82	plate	yes
NC7	1	051121_NC_1586_L1	568	284	0.50	851	729	21	screen	yes
NC8	BM	060323_NC_1619_LP1	724	145	0.20	869	646	21	plate	yes
NC9	2	060331_NC_2024_LP1	724	362	0.50	1086	732	21	plate	yes
NC10 ^(b)	2	060404_NC_2698_LP1	724	724	1.00	1448	862	21	plate	yes
NC11	1	051123_NC_2181_L1	780	390	0.50	1170	1034	21	screen	yes
NC12	1	051117_NC_2776_L1	993	496	0.50	1489	1334	21	screen	yes
NC13	1	051128_NC_2776_L2	993	496	0.50	1489	1260	21	screen	yes
NC14 ^(a)	1	051115_NC_4098_L1	1419	780	0.55	2199	1924	21	screen	yes
NC15a ^(c)	2	060807_NC_0708_LP1	217	163	0.75	380	261	54	plate	yes
NC15b ^(c)	2	060807_NC_0708_LP2	217	163	0.75	380	261	36	plate	yes
NC16a ^(c)	2	060809_NC_0708_LP1	217	163	0.75	380	160	82	plate	yes
NC16b ^(c)	2	060809_NC_0708_LP2	217	163	0.75	380	160	54	plate	yes
NC17a ^(c)	2	060817_NC_2024_LP1	724	362	0.50	1086	811	54	plate	yes
NC17b ^(c)	2	060817_NC_2024_LP2	724	362	0.50	1086	811	29	plate	yes

(a) Initial screen approach velocity during debris-bed formation = 0.2 ft/sec as opposed to a constant 0.1 ft/sec.
(b) Debris bed essentially plugged screen (head loss > 750 in. H₂O) at completion of bed formation process.
(c) Debris bed formed at an elevated fluid temperature.

investigation, the process of dissolving the debris beds in hydrochloric acid and detecting the concentration of calcium using a calcium ISE (Sections 2.5.4.2 and 5.3), was chosen for determining the mass loading of CalSil. The results of this assessment are presented in Section 7.4.2.

Optical triangulation was used to obtain in situ debris bed height measurements for the Benchmark and Series 2 tests. These measurements, along with a comparison of the relative bulk density of the debris beds, are presented in Section 7.4.3. Post-test measurements of the debris bed height are also presented in Section 7.4.3 to provide a comparison of the Series 1 tests, which did not have the optical triangulation system available, and the Benchmark and Series 2 tests. As discussed earlier, in situ manual measurements of the debris bed height could not always be obtained and are not discussed in this section. The data for the NUKON/CalSil debris bed measurements made are in the Quick Look reports in Appendix J.

The head loss measurements obtained for all velocity sequences completed for each NUKON/CalSil debris bed are contained in the Quick Look reports of Appendix J. Section 7.4.4 provides an overview and a comparison of the NUKON/CalSil head loss measurements and is not intended to provide data for all of the measurements, which can be obtained from the Quick Look reports.

As with the NUKON-only tests, fluid temperature effects were evaluated using two different test methods. The results of the testing conducted at elevated fluid temperatures are presented in Section 7.4.5. The test descriptions, initial conditions, debris bed photos, and test measurements for the CalSil/NUKON debris beds are contained in the Quick Look reports of Appendix J.

7.4.1 Overview of the NUKON/CalSil Test Matrix

Debris injection into the large-scale loop was conducted for seventeen NUKON/CalSil debris target conditions. From the 17 debris bed target conditions, 22 tests were conducted. The multiple tests conducted for a single debris bed are the result of changing the test loop fluid temperature and executing a second velocity matrix. The test case numbers for cases NC1 through NC14 are ordered first for ascending target NUKON mass loading followed by increasing target CalSil mass loading. For debris bed conditions having multiple tests conducted with the same debris bed, a lower case letter is used to designate the sequential order of the tests (e.g., Test Cases NC5a and NC5b were conducted with the same debris bed, with Test NC5a being conducted prior to Test NC5b). Test cases 15 through 17 are additional test conditions that are numbered in the order in which they were completed.

For the six Series 1 NUKON/CalSil tests, the CalSil and NUKON were prepared separately and introduced into the loop using independent injection loops for each constituent. The constituents were introduced into the test loop simultaneously but had no interaction prior to entry into the main line of the test loop. Based on the variation in the head loss measurements relative to the target mass loadings obtained between tests from the Series 1 tests, it was postulated that the Series 1 debris introduction procedure created variability in the sequence in which debris arrives at the test screen. To examine the variation observed in the Series 1 head loss measurements, the debris loading sequence investigation presented in Section 6.3 was conducted. Following the investigation of the loading sequence, the NRC staff decided that future tests, Benchmark and Series 2, would be conducted by premixing the debris constituents before introducing them into the test loop. The Series 1 test also used the 5-mesh screen (woven wire cloth), and the Benchmark and Series 2 tests used the perforated plate with 1/8-in. holes.

As discussed, the initial screen approach velocity for bed formation at the start of the Series 1 tests was 0.2 ft/sec (0.06 m/s), which was subsequently changed by NRC staff to a constant 0.1 ft/sec (0.03 m/s) after four large-scale tests were conducted. Two of the NUKON/CalSil tests, NC3 and NC14, had debris beds form with an initial screen approach velocity of 0.2 ft/sec (0.06 m/s). As indicated in Table 7.12, tests NC7 and NC 11 through NC 13 were formed at a constant screen approach velocity of 0.1 ft/sec (0.03 m/s) but with simultaneous introduction (not premixed) of debris constituents.

The two CalSil/NUKON tests with the lowest retrieved mass loading, NC1 and NC2, did not generate complete debris beds. Figures 7.33 and 7.34 are photos of the incomplete debris beds from NC1 and NC2, respectively. The target NUKON loading for both NC1 and NC2 was 108 g/mL while the total retrieved mass loadings were 56.3 and 94.4 g/mL, respectively. Based on the photos, it appears that approximately the same fraction of the screen is covered with debris for both tests despite NC2 having approximately 80% more mass. It appears again, based on the results of Section 7.3, that the formation of a complete debris bed is dependent on the mass loading of NUKON. The lowest target mass loading at which a complete NUKON-only debris bed was formed was 217 g/mL for NO1, which had a total retrieved mass loading of 171 g/mL. The lowest target NUKON loading from the NUKON/CalSil tests that generated a complete debris bed was 213 g/mL from NC13. The retrieved mass loading of NUKON



Figure 7.33. Incomplete Debris Bed Retrieved from Test NC1 with a Retrieved Mass Loading of 56.3 g/m^2 . The target mass loading was 108 g/m^2 NUKON, 27 g/m^2 CalSil, and 135 g/m^2 total.

for Test NC13 is discussed in Section 7.4.2. Testing was not conducted to determine the actual minimum debris loading conditions at which complete debris beds could be formed.



Figure 7.34. Incomplete Debris Bed Retrieved from Test NC2 with a Retrieved Mass Loading of 94.4 g/m^2 . Target mass loading was 108 g/m^2 NUKON, 135 g/m^2 CalSil, and 243 g/m^2 total.

Test NC6a appeared to have formed a complete debris bed at the end of the bed formation process; however, channeling occurred during the initial ramp up in velocity. The target NUKON loading for NC6a was 217 g/mL. The effect of the CalSil loading on the formation of the debris bed is discussed further in Section 7.4.2 with the presentation of the CalSil mass measurements. Due to the effort required to obtain measurements from the CalSil dissolution process, the debris beds from NC1 and NC2 were not assessed for CalSil mass content. Test NC16a yielded the lowest retrieved mass loading for a complete NUKON/ CalSil debris bed at 160 g/mL. Figure 7.35 is a photo of the debris bed retrieved following completion of tests NC16a and NC16b. The hole pattern of the perforated plate is visible on the debris bed surface.

Three tests were conducted for CalSil to NUKON mass ratios greater than 0.75, one of which was the incomplete debris bed of NC2. Of those three tests, NC10 had both the greatest target mass loading, 1448 g/mL, and retrieved mass loading, 862 g/mL. At the completion of bed formation at 0.1 ft/sec (0.03 m/s), the head loss measured for NC10 was 749 in. H₂O at 68°F. The measured head loss was greater than the range of interest for this test program; and therefore, the debris bed was assumed to be plugged and additional measurements were not taken. This test case is discussed further in Section 7.4.2, but head loss measurements from NC10 are not presented in Section 7.4.4.

Head loss measurements were obtained at elevated fluid temperatures (>50°C) for tests NC5b, NC6b, NC15a, NC16a, NC16b, and NC17a; the debris beds for tests NC15a through NC 17b were generated at elevated temperatures. The head loss measurements for the tests conducted at elevated fluid temperatures are presented in Section 7.4.5.

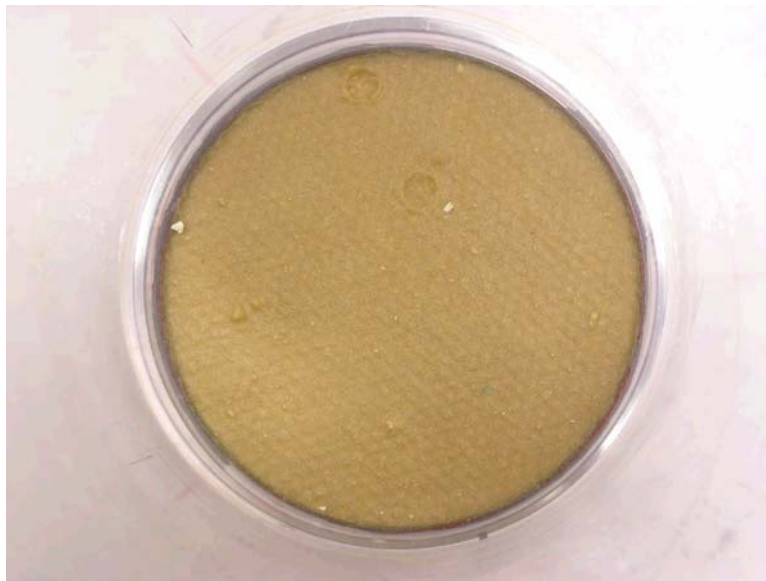


Figure 7.35. Upstream View of Top of Debris Bed from Test Condition NC16. Target mass loadings were 217 g/m² NUKON and 163 g/m² CalSil; total retrieved mass loading was 160 g/m². This is the smallest retrieved mass loading of the CalSil/NUKON test cases to form a complete debris bed. Test cases NC16a and NC16b were completed before bed retrieval. The two divots/craters in the upper of half of the photo are the result of disturbances to the debris bed during post-test retrieval. The surface texture of the debris bed is the hole pattern of the perforated plate being telegraphed through the debris material.

7.4.2 Results of Debris Bed Dissolution to Assess CalSil Mass Content

The mass of CalSil in a retrieved debris bed was determined from two methods referred to as the “mass method” and “chemical dissolution.” The mass method used the dry masses of the constituents introduced to the loop and the dry mass of the retrieved debris bed to calculate an upper and lower bound for the possible quantity of CalSil retained in a debris bed. The predicted CalSil mass loading was obtained from the mass method. Chemical dissolution obtained the final mass from voltage measurements taken with calcium ISE probes in prepared samples of the dissolved debris beds. The ISE probe voltage was experimentally correlated to the CalSil concentration. (See subsection 2.5.4.2 for a brief overview of the ISE probe and Section 5.3 for a summary of the procedure used to determine the CalSil mass in the debris bed.) The calculated CalSil mass loading was obtained from chemical dissolution. The values reported for the retrieved CalSil mass loading and used to compare the NUKON/CalSil test cases are based on the following assumptions.

- No residual CalSil existed in the loop at the start of a test, and the mass of CalSil existing in the debris bed cannot be greater than the mass of CalSil introduced to the loop for the test.
- The mass loading of NUKON in the debris bed is assumed to be equal to the retrieved total dry mass loading minus the CalSil mass loading obtained from chemical dissolution. The minimum mass of CalSil possible in a debris bed can be determined from the post-test measurement of the dry debris bed mass assuming all of the introduced NUKON was retained in the debris bed. The total mass of the retrieved debris bed may be potentially influenced by retained contaminants (debris from previous tests, system debris, etc.), thus affecting the determination of the predicted minimum CalSil mass present in the debris bed. For this section, it is assumed that the debris beds contained no contaminants.
- All of the CalSil fiber material, assumed to be 4% by mass based on information provided by the CalSil vendor during phone conversations with PNNL staff (refer to Section 3), contained in the mass of CalSil introduced into the test loop for a head loss test is retained in a complete debris bed. The performance standards used to generate the correlation between ISE probe voltage and the concentration of CalSil were made with CalSil material having a uniform ratio of calcium silicate to fiber material. Debris beds containing only a fraction of the CalSil introduced into the loop have a different ratio of calcium silicate to fiber material than existed in the performance standards. However, it is assumed the difference in fiber content is not detected by calcium ISE probes. Therefore, the values for CalSil mass loading obtained from the inverse regression have been corrected based on the assumption that 100% of the CalSil fiber material introduced into the test loop was captured by the debris beds.
- Results from earlier “design of experiment” tests indicated that the presence of NUKON during CalSil dissolution can influence the results. Additionally, the amount of hydrochloric acid (HCl) used to dissolve the debris beds may have a slight influence on CalSil mass estimates. For the design of experiment tests, it is not certain whether dissolution kinetics, analysis techniques, or other effects impacted the results. Acknowledging these uncertainties, preliminary unreviewed data from CalSil dissolution in the presence of NUKON indicates that, at lower mass ratios (not quantifiably defined) of CalSil to NUKON the CalSil mass estimates can be lower than the true values. The difference has been indicated to be as much as 35%. The potential effect of the mass of HCl on CalSil mass estimates in debris beds is included in this difference. Additional investigation would be required to quantify these effects. The current analysis has not considered these possible influences.

Based on these assumptions, the CalSil mass loadings for the complete NUKON/CalSil debris beds are presented in Table 7.13. From the mass method, only upper and lower bounding values are presented. Two values for CalSil mass loading obtained from the chemical dissolution method are presented in the table; column 5 contains the CalSil mass loading determined directly from the calcium ISE probe readings, and the values in column six have been corrected assuming 100% of the fiber contained in the CalSil material introduced into the test loop was retained in the debris bed. Upper and lower bounding values are provided for the CalSil mass loadings corrected for the additional CalSil fiber. The lower and upper bound values were obtained from the 95% upper and lower inverse confidence limits obtained for the inverse linear regression used to transform ISE probe voltage readings to CalSil concentration. The CalSil mass loadings provided in Table 7.13 that have been corrected for the additional CalSil fiber are used to present and compare the test results throughout the remainder of the report.

Table 7.13 also includes the mass percent of the target CalSil retained in the debris bed and the mass fraction of retained CalSil predicted to consist of the CalSil fiber. The lower the percent of CalSil retained in the debris bed, the greater the predicted mass fraction of fiber making up the retained CalSil. The predicted NUKON mass loading and the mass ratio of CalSil to NUKON are also included in the table and are obtained from the CalSil mass loading corrected for the additional CalSil fiber. The upper and lower bounds of the CalSil to NUKON mass ratio were obtained from the upper and lower bounding CalSil mass loadings reported in columns 7 and 8, respectively.

Incomplete debris beds were formed for Test Cases NC1 and NC2; therefore, no chemical dissolution of the retrieved debris bed was performed. Test Cases NC1 and NC2 are included in Table 7.13 for completeness and to simplify comparisons with Table 7.12.

Accounting for the additional CalSil fiber has the greatest impact on the results of test cases with the lowest percentage of initial CalSil material introduced into the loop being retained in the debris bed such as cases NC5 and NC16. For both NC5 and NC16, the CalSil assessment predicted that 5% of the initial CalSil material was retained in the debris bed. Correcting for the additional CalSil fiber increased the predicted amount of CalSil retained in both debris beds to 11%, which is a 120% increase. For cases NC8 and NC15, the correction for fiber increased the predicted value for retained CalSil by 25 and 33%, respectively. For all other cases, the correction increased the predicted amount of retained CalSil by 8% or less.

The retrieved CalSil mass loadings determined by chemical dissolution were expected to fall within the range of the minimum and maximum CalSil amounts predicted from the mass method. Twelve of the 15 debris beds that underwent chemical dissolution had predicted CalSil mass loadings falling within the range predicted by the mass method. Of those 12 cases, all but one, NC12, had the upper and lower bounding values based on the 95% confidence interval falling within the range of the mass measurements. Test case NC 12 had a predicted CalSil mass loading of 343 g/m² and a lower limit of 292 g/m² compared to a lower limit of 341 g/m² predicted by the mass method.

NC7, NC11, and NC15 were the three cases with CalSil mass loadings predicted by chemical dissolution to be below the lower bound values for CalSil mass loading determined from the mass method (refer to Table 7.13). For cases NC7 and NC11, the upper bound values of CalSil mass loading lie within the range obtained from the mass method.

Table 7.13. Retrieved Mass Loading of CalSil in the CalSil/NUKON Debris Beds

Test Case	Total Retrieved Debris Bed Loading (± 4 g/m ²)	CalSil Mass Loading Based on Mass Method		CalSil Mass Loading Based on Chemical Dissolution (g/m ²)	Values Below Corrected Assuming 100% of CalSil Fiber Retained in Debris Bed ^(a)									
		Upper Bound (g/m ²)	Lower Bound (g/m ²)		CalSil Mass Loading Based on Chemical Dissolution			Mass of Initial CalSil Retained in Debris Bed (%)	Mass of Retained CalSil Made up of Fiber ^(a) (%)	NUKON Loading (g/m ²)	CalSil to NUKON Mass Ratio			
					Reported CalSil Mass Loading (g/m ²)	Upper Bound from 95% Upper Inverse Confidence Limit (g/m ²)	Lower Bound from 95% Lower Inverse Confidence Limit (g/m ²)				Reported Ratio	Upper Bound	Lower Bound	
		NC1	56		27	0	N/A	N/A	N/A	N/A	N/A	N/A	N/A	N/A
NC2	94	94	0	N/A	N/A	N/A	N/A	N/A	N/A	N/A	N/A	N/A	N/A	N/A
NC3 ^(b,c)	217	106	4	47	49	56	42	46	9	168	0.29	0.35	0.24	
NC4	209	54	0	25	26	27	25	48	8	183	0.14	0.15	0.14	
NC5a	213	163	0	5	11	11	11	7	59	202	0.05	0.06	0.05	
NC5b	213	163	0	5	11	11	11	7	59	202	0.05	0.06	0.05	
NC6a	297	217	80	80	85	88	83	39	10	212	0.40	0.42	0.39	
NC6b	297	217	80	80	85	88	83	39	10	212	0.40	0.42	0.39	
NC7 ^(d)	729	284	161	150	155	178	132	55	7	574	0.27	0.32	0.22	
NC8	646	145	0	20	25	26	24	17	23	621	0.04	0.04	0.04	
NC9	732	362	8	132	141	145	138	39	10	591	0.24	0.25	0.23	
NC10 ^(c)	862	724	138	339	354	365	344	49	8	508	0.70	0.73	0.66	
NC11 ^(d)	1034	390	254	236	242	279	206	62	6	792	0.31	0.37	0.25	
NC12	1334	496	341	337	343	395	292	69	6	991	0.35	0.42	0.28	
NC13	1260	496	267	327	334	384	284	67	6	926	0.36	0.44	0.29	
NC14 ^(b)	1924	780	505	667	671	772	571	86	5	1253	0.54	0.67	0.42	
NC15a ^(d)	261	163	44	18	24	25	23	15	27	237	0.10	0.11	0.10	
NC15b ^(d)	261	163	44	18	24	25	23	15	27	237	0.10	0.11	0.10	
NC16a	160	160	0	5	11	11	11	7	58	149	0.08	0.08	0.07	
NC16b	160	160	0	5	11	11	11	7	58	149	0.08	0.08	0.07	
NC17a	811	362	87	120	129	133	126	36	11	681	0.19	0.20	0.18	
NC17b	811	362	87	120	129	133	126	36	11	681	0.19	0.20	0.18	

(a) CalSil material assumed to contain 4% by mass fiber.

(b) Initial screen approach velocity during debris bed formation = 0.2 ft/sec as opposed to a constant 0.1 ft/sec.

(c) Debris bed essentially plugged screen (head loss > 750 in. H₂O) at completion of bed formation process.

(d) The CalSil mass loading predicted by the chemical dissolution process is less than the lower bound CalSil mass loading determined from the "mass measurements."

Case NC15 provides the one exception in which there is no overlap between the ranges of CalSil mass loading predicted from the mass method and calculated by chemical dissolution. From chemical dissolution, the CalSil mass loading was determined to be $25 \pm 2 \text{ g/m}^2$, compared with the lower and upper bounds from the mass method calculated to be 44 and 163 g/m^2 , respectively. Based on the results of both the mass method and chemical dissolution, the CalSil to NUKON mass ratio was between 0.07 and 0.11, which is one of the four lowest mass ratios obtained. The debris bed was calculated to have retained only 15% of the target CalSil mass. The CalSil mass loading determined from the chemical dissolution is only 57% of the lower bound obtained from the mass method. This deviance significantly exceeds the 35% difference in CalSil estimates compared to true values that was observed during the design of experiment tests for the low CalSil-to-NUKON mass ratios discussed above. Other than uncertainties or chemical effects not investigated, the discrepancy between the CalSil mass loadings obtained from the mass method and chemical dissolution for Test Case NC15 cannot be explained at this time.

Figure 7.36 contains plots of the percent target mass loading obtained, percent target CalSil mass retained, and the CalSil-to-NUKON retrieved mass ratio obtained from the retrieved debris bed as a function of the retrieved dry mass loading. The percent target mass loading obtained is the percentage of the initial mass introduced into the test loop retrieved in the final dry debris bed. The percent target CalSil retained in the debris bed is based on the chemical dissolution calculations of the mass of CalSil retained in the debris bed (corrected for fiber content) and the mass of CalSil initially introduced to the test loop. The CalSil-to-NUKON mass ratio plotted in Figure 7.36 is based on the chemical dissolution measurements of the mass of CalSil retained in the debris bed (corrected for fiber content) and the dry mass of the retrieved debris bed. This is the mass ratio predicted to exist in the final debris bed retrieved from the test loop. From Figure 7.36, the percentage of initial CalSil introduced into the test loop that is retained in the debris bed and the retrieved CalSil to NUKON mass ratio is observed to increase with the retrieved mass loading on the test screen.

The data for NC10, the only large-scale test case that was considered to be plugged, are also included in Figure 7.36. NC10 had 49% of the target CalSil loading retained in the debris bed and a retrieved CalSil-to-NUKON mass ratio of 0.70. This was the largest mass ratio obtained for the 15 debris beds evaluated. NC10 had an initial target CalSil to NUKON mass ratio of 1. In Section 6.3, observations of significant variability in measured head loss for high target CalSil-to-NUKON mass ratio beds obtained during benchtop testing were discussed. During the benchtop tests, extreme variability was observed in the resulting head losses for initial mass ratios greater than 0.5. Debris beds generated with the same initial conditions and target mass loadings were observed to yield head losses that varied by almost an order of magnitude.

The target CalSil-to-NUKON mass loadings are added to the Figure 7.36 plot in Figure 7.37. Inspecting Figure 7.37, the following observations are made:

- The greater the total mass loading, the closer the retrieved CalSil-to-NUKON mass ratio is to the target mass ratio. For case NC14 at a retrieved mass loading of 1924 g/m^2 , the target mass ratio was 0.55 and the retrieved mass ratio was 0.54.
- NC10 had the highest target mass loading of the three cases (NC2, NC6, and NC10; refer to Table 7.12) with target CalSil-to-NUKON mass ratios exceeding 0.75 and was the only test case to have a CalSil-to-NUKON retrieved mass ratio in excess of 0.54, refer to Table 7.13.
- Of the test cases having retrieved mass loadings greater than 900 g/m^2 , none had target CalSil-to-NUKON mass loadings greater than 0.55.

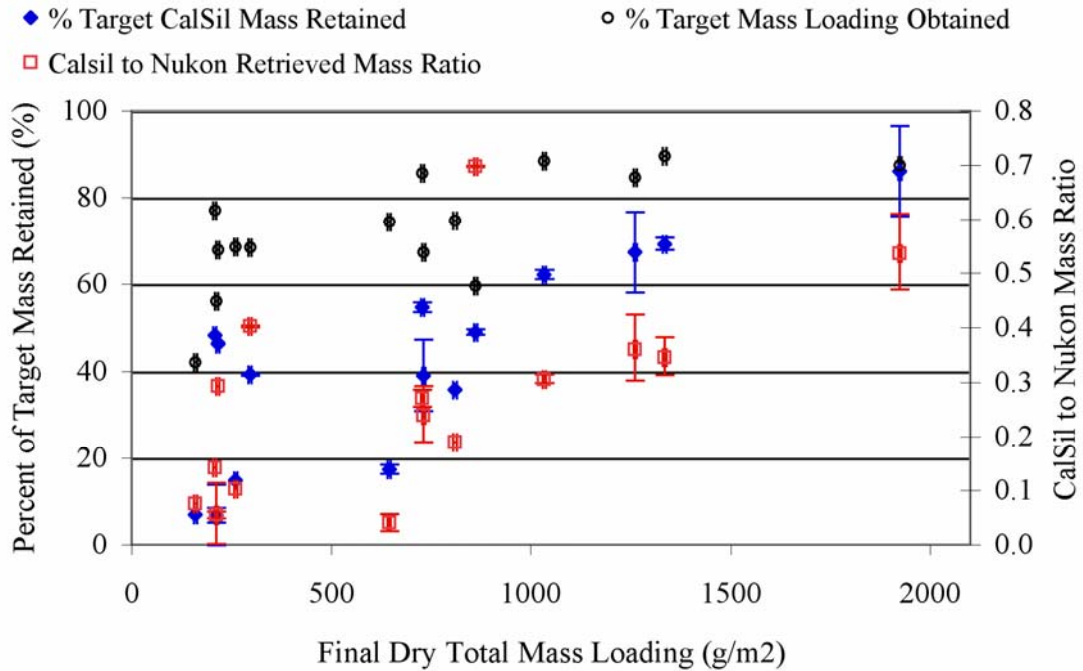


Figure 7.36. Percent Target CalSil Mass and Percent Total Target Mass Loading Retained in the Debris Bed as a Function of the Retrieved Dry Mass Loading. The CalSil-to-NUKON retrieved mass ratio is also plotted. Data are for 15 CalSil/NUKON debris beds that were assessed via chemical dissolution; data presented in Table 7.13

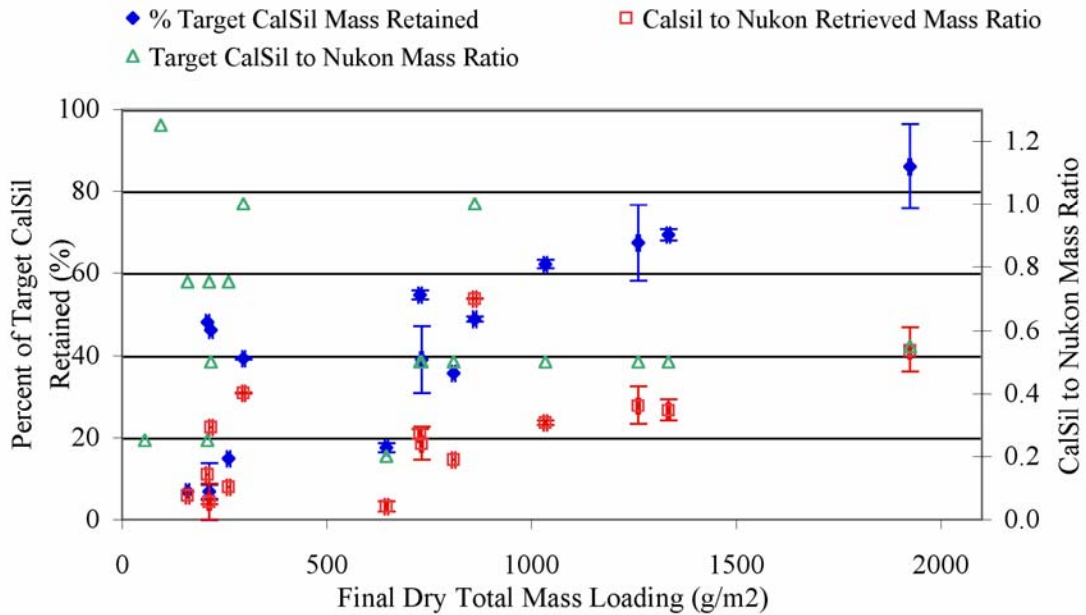


Figure 7.37. Percent Target CalSil Mass and CalSil-to-NUKON Retrieved Mass Ratio Obtained from the Retrieved Debris Bed as a Function of the Total Retrieved Dry Debris Bed Mass Loading. The target CalSil-to-NUKON mass ratio is also plotted as a function of the total retrieved mass loading. Data are for 15 CalSil/NUKON debris beds that were assessed via chemical dissolution; data are presented in Table 7.13

It is unknown whether additional large-scale test cases exhibiting plugged behavior would have been encountered if higher CalSil/NUKON ratios had been tested at the higher mass loadings. The results again indicate that the NUKON mass loading needs to be sufficient to retain the CalSil. The question is again raised as to whether a critical retrieved CalSil/ NUKON mass ratio exists for which the debris bed becomes plugged or saturated. It is unclear to what extent the target CalSil-to-NUKON mass ratio affects the amount of retained CalSil in the debris bed. Test Cases NC3, NC4, NC5, NC15, and NC16 each had a target NUKON mass loading of approximately 217 g/m², and Test Cases NC8, NC9, NC10, and NC17 had a target NUKON mass loading of 724 g/m². Tables 7.14 and 7.15 compare the target mass ratio to the percentage of CalSil retained in the debris bed for the NUKON loadings of 217 g/m² and 724 g/m², respectively.

It was initially postulated that an increase in the CalSil mass loading would increase the amount of CalSil retained in the debris bed. Two scenarios were considered:

- The addition of CalSil to the debris bed would increase the capture efficiency of the debris bed, resulting in a reduction of the average particle size retained in the debris bed.
- The NUKON is only capable of retaining CalSil down to a critical particle size, and additional CalSil does not improve the capture efficiency of the debris bed to act as a filter. This scenario seems more plausible considering the results of Section 7.4.3, in which approximately the same mass fraction of CalSil debris is captured on the perforated plate regardless of the target mass loading of CalSil introduced to the test loop.

Table 7.14. Comparison of Percent of Target CalSil Retained in Debris Bed with Target CalSil-to-NUKON Mass Ratio for a Target NUKON Mass Loading of 217 g/m²

Test Case	Target NUKON Mass Loading (g/m ²)	Target CalSil to NUKON Mass Ratio	Target CalSil Mass Retained in Debris Bed (%)	Retrieved CalSil Mass Loading (g/m ²)	Retrieved Total Mass Loading (g/m ²)
NC4	217	0.25	48	26	209
NC3 ^(a)	213	0.50	46	49	217
NC5	217	0.75	7	11	213
NC16 ^(b)	217	0.75	7	11	160
NC15 ^(b)	217	0.75	15	24	261

(a) Debris bed generated with a bed formation velocity of 0.2 ft/sec.
(b) Debris bed formed at elevated temperature.

Table 7.15. Comparison of Percent of Target CalSil Retained in Debris Bed with Target CalSil-to-NUKON Mass Ratio for Target NUKON Mass Loading of 724 g/m²

Test Case	Target NUKON Mass Loading (g/m ²)	Target CalSil to NUKON Mass Ratio	Target CalSil Mass Retained in Debris Bed (%)	Retrieved CalSil Mass Loading (g/m ²)	Retrieved Total Mass Loading (g/m ²)
NC8	724	0.20	17	25	646
NC9	724	0.50	39	141	732
NC17 ^(a)	724	0.50	36	129	811
NC10 ^(b)	724	1.00	49	354	862

(a) Debris bed formed at elevated temperature.
(b) Debris bed plugged at the completion of debris bed formation.

The results of Table 7.14 do not support the postulated effect of increased CalSil loading on CalSil retention, but instead indicate that an increase in the target CalSil-to-NUKON mass ratio inhibits the

retention of CalSil in the debris bed. However, the results of Table 7.15 indicate the opposite trend; an increase in the target CalSil-to-NUKON mass ratio corresponds to an increase in the percentage of the target CalSil that was retained in the debris bed and an increase in the actual CalSil mass loading. The opposing trends exhibited in these two tables appear to be due to the difference in the retrieved debris bed mass loadings.

Another observation that can be made from the results presented in Tables 7.14 and 7.15 is the similarity in the final CalSil loading obtained from test cases with identical target mass loadings. Cases NC5, NC15, and NC16 formed debris beds at fluid temperatures of 21°, 54°, and 82°C, respectively, but all three had target mass loadings of 217 g/m² NUKON and 163 g/m² CalSil. The three cases retained 7 to 15% of the target CalSil and had CalSil mass loadings between 11 and 24 g/m². NC15 had the largest CalSil mass and total mass loadings of the three cases. However, the increase in total mass loading is not accounted for by the increase in retained CalSil. Additional NUKON should have been retained in the debris bed. It is not known whether the additional CalSil contributed to the retention of the additional NUKON material.

Both of the other two cases presented in Table 7.14, NC4 and NC3, retained more CalSil despite having target CalSil mass loadings 33 and 67% of the target loadings for cases NC5, NC15, and NC16. It appears as if the higher concentration of CalSil present at the initiation of debris bed formation inhibited the NUKON from being as efficient in retaining (filtering) the CalSil. It was observed during benchtop testing that NUKON-only debris beds were fairly durable when retrieved from the test section and readily stayed intact. However, for the same NUKON mass loading, retrieved debris beds seemed to become more fragile and harder to keep intact with increased CalSil mass loading. The observation was that CalSil appeared to weaken or disrupt the structural integrity of the debris bed with respect to post-test handling. It is unclear whether the benchtop test observations are relevant to the results for CalSil retention presented in Table 7.14. Without further investigation, the effect of the target CalSil loading on the amount of CalSil retained in the debris bed is inconclusive. It is speculated that the CalSil may interfere with the interaction of the NUKON fiber.

With regard to the observations of similarity in the final CalSil mass loadings, cases NC9 and NC17 had target mass loadings of 724 g/m² NUKON and 362 g/m² CalSil. These two cases retained 39 and 36% of the target CalSil despite having debris beds generated at different temperatures. Despite NC9 retaining approximately 10% more CalSil than NC17, the total retrieved mass loading for NC9 was approximately 10% less than that of NC17.

7.4.3 Debris Bed Height for NUKON/CalSil Test Cases

As discussed in Section 5, three types of debris bed height measurements were taken during the test program. A description of each of the debris bed height measurements is provided in Section 7.2.1. For review, the three types of height measurements are listed below.

1. Manual post-test debris bed measurements taken with the retrieved debris bed and TTS removed from the test loop
2. In situ manual debris bed height measurements taken by an operator looking (sighting across) through the side of the TTS
3. In situ debris bed measurements obtained via post-test analysis of photos taken during testing using the optical triangulation system.

All of the debris bed height measurements are contained in the Quick Look reports of Appendix J. The optical triangulation system was not operational during the Series 1 NUKON/CalSil tests, which include test cases NC3, NC7, and NC11 through NC14. Like the NUKON-only test cases of Section 7.2.1, the comparison of the optical triangulation measurements is the main focus of this section. The post-test measurements for the debris bed rim and center heights are presented to provide a comparison to the Series 1 tests. The results of the in situ manual measurements are not discussed in this report.

Table 7.16 contains all the bed height measurements obtained with optical triangulation from the NUKON/CalSil test cases. From the measurements of debris bed height and the dry retrieved bed mass, a relative bulk density of the debris material in the bed can be calculated. Table 7.16 contains the calculated bulk dry density of the debris beds for all of the test conditions in which the photo imaging analysis was performed. The values of bulk dry debris bed density reported in Table 7.16 were obtained by calculating the debris bed volume using the product of cross-sectional area of the test section and the average body height obtained from the optical triangulation measurements. The average body height is the average height of the debris bed excluding the area covered by the debris bed rim. Therefore, the volume of debris material included in the rim is excluded from the calculation of the relative density while the mass of the material is included. The calculated density is considered a relative density to be used for comparing test cases and should not be considered an absolute density.

Table 7.16. In Situ Debris Bed Height Measurements and Calculated Density Obtained from Optical Triangulation Measurements

Test Case	Retrieved Debris Bed Mass Loading ($\pm 4 \text{ g/m}^2$)	Screen Approach Velocity ($\pm 0.3 \text{ ft/sec}$)	Test Phase	Rim Height ($\pm 0.03 \text{ in.}$)	Body Center Height ($\pm 0.03 \text{ in.}$)	Average Body Height ($\pm 0.03 \text{ in.}$)	Body Diameter ($\pm 0.03 \text{ in.}$)	Relative Bulk Dry Debris Bed Density Based on Optical Triangulation Bed ht (g/mL)
NC1	56	N/A	N/A	N/A	N/A	N/A	N/A	N/A
NC2	94	N/A	N/A	N/A	N/A	N/A	N/A	N/A
NC3 ¹	217	N/A	N/A	N/A	N/A	N/A	N/A	N/A
NC4	209	0.10	RU1	0.21	0.13	0.11	5.11	0.075
NC4	209	0.20	RU1	0.20	0.11	0.09	5.23	0.091
NC4	209	0.20	RU3	0.18	0.10	0.08	5.38	0.103
NC4	209	0.02	RD3	0.19	0.12	0.10	5.32	0.082
NC4	209	0.10	RU4	0.18	0.11	0.09	5.32	0.091
NC5a	213	0.10	RU1	0.24	0.10	0.08	5.30	0.105
NC5a	213	0.20	RU1	0.22	0.08	0.06	5.18	0.140
NC5a	213	0.02	RD1	0.22	0.10	0.08	5.27	0.105
NC5a	213	0.20	RU2	0.22	0.07	0.05	5.31	0.168
NC5a	213	0.10	RU4	0.22	0.07	0.05	5.25	0.168
NC5b	213	0.20	RU3	0.20	0.06	0.04	5.32	0.210
NC6a	297	0.10	RU1	0.29	0.11	0.09	5.18	0.130
NC6a	297	0.20	RU1	0.21	0.05	0.03	5.42	0.390
NC6a	297	0.02	RD1	0.23	0.09	0.07	5.17	0.167
NC6a	297	0.10	RU2	0.22	0.07	0.05	5.29	0.234
NC6b	297	0.20	RU1	0.23	0.07	0.05	5.19	0.234
NC6b	297	0.02	RD1	0.24	0.10	0.08	5.29	0.146
NC7	729	N/A	N/A	N/A	N/A	N/A	N/A	N/A

Table 7.16 (contd)

Test Case	Retrieved Debris Bed Mass Loading ($\pm 4 \text{ g/m}^2$)	Screen Approach Velocity ($\pm 0.3 \text{ ft/sec}$)	Test Phase	Rim Height ($\pm 0.03 \text{ in.}$)	Body Center Height ($\pm 0.03 \text{ in.}$)	Average Body Height ($\pm 0.03 \text{ in.}$)	Body Diameter ($\pm 0.03 \text{ in.}$)	Relative Bulk Dry Debris Bed Density Based on Optical Triangulation Bed ht (g/mL)
NC8	646	0.10	RD1	0.64	0.36	0.34	4.39	0.075
NC8	646	0.02	RD1	0.59	0.36	0.34	4.44	0.075
NC8	646	0.20	RU2	0.52	0.25	0.23	4.66	0.111
NC8	646	0.10	RU4	0.52	0.25	0.23	4.57	0.111
NC9	732	0.10	RU1	0.40	0.18	0.16	4.61	0.180
NC9	732	0.20	RU1 nf	0.40	0.18	0.16	4.58	0.180
NC9	732	0.02	RD1	0.42	0.26	0.24	4.78	0.120
NC9	732	0.10	RU4	0.36	0.18	0.16	4.60	0.180
NC10	862	0.10	DP1 noSS	0.44	0.22	0.20	4.52	0.170
NC10	862	0.01	BF plus	0.40	0.17	0.16	4.72	0.212
NC11	1034	N/A	N/A	N/A	N/A	N/A	N/A	N/A
NC12	1334	N/A	N/A	N/A	N/A	N/A	N/A	N/A
NC13	1260	N/A	N/A	N/A	N/A	N/A	N/A	N/A
NC14	1924	N/A	N/A	N/A	N/A	N/A	N/A	N/A
NC15a	261	0.10	RU1	0.20	0.09	0.07	5.23	0.118
NC15a	261	0.20	RU1	0.21	0.08	0.06	5.27	0.131
NC15a	261	0.02	RD2	0.20	0.08	0.06	5.25	0.132
NC15a	261	0.10	RU3	0.20	0.07	0.05	5.37	0.155
NC15b	261	0.20	RU1	0.17	0.04	0.02	5.42	0.292
NC15b	261	0.10	RU2	0.17	0.05	0.03	5.59	0.254
NC16a	160	0.10	RU1	0.10	0.08	0.06	5.81	0.105
NC16a	160	0.20	RU1	0.09	0.06	0.04	5.78	0.157
NC16a	160	0.20	RU3	0.09	0.06	0.04	5.77	0.157
NC16a	160	0.02	RD3	0.10	0.08	0.06	5.67	0.105
NC16a	160	0.10	RU4	0.09	0.06	0.04	5.85	0.157
NC16b	160	0.20	RU1	0.07	0.05	0.03	5.86	0.210
NC16b	160	0.10	RU2	0.07	0.05	0.03	5.88	0.210
NC17a	811	0.10	RU1	0.40	0.34	0.32	5.48	0.100
NC17a	811	0.20	RU1	0.34	0.28	0.26	5.25	0.123
NC17a	811	0.20	RU3	0.25	0.19	0.17	5.43	0.188
NC17a	811	0.02	RD3	0.28	0.20	0.18	5.47	0.177
NC17a	811	0.10	RU4	0.26	0.20	0.18	5.49	0.177
NC17b	811	0.20	RU1	0.22	0.16	0.14	5.44	0.228
NC17b	811	0.10	RU2	0.22	0.14	0.12	5.56	0.266

Reviewing Table 7.12, five test cases formed complete debris beds, were formed and tested according to Series 2 procedures, and were generated at ambient fluid temperature: NC4, NC5a, NC6a, NC8, and NC9. Three of these, NC4, NC9, and NC8, bound the range of retrieved mass loadings for the five cases, and the debris bed height is plotted for them as a function of the screen approach velocity in Figure 7.38. In the legend of the plot, the test case number is followed by the predicted CalSil mass loading and the total retrieved debris loading. Like the NUKON-only condition, for a specific velocity the debris bed

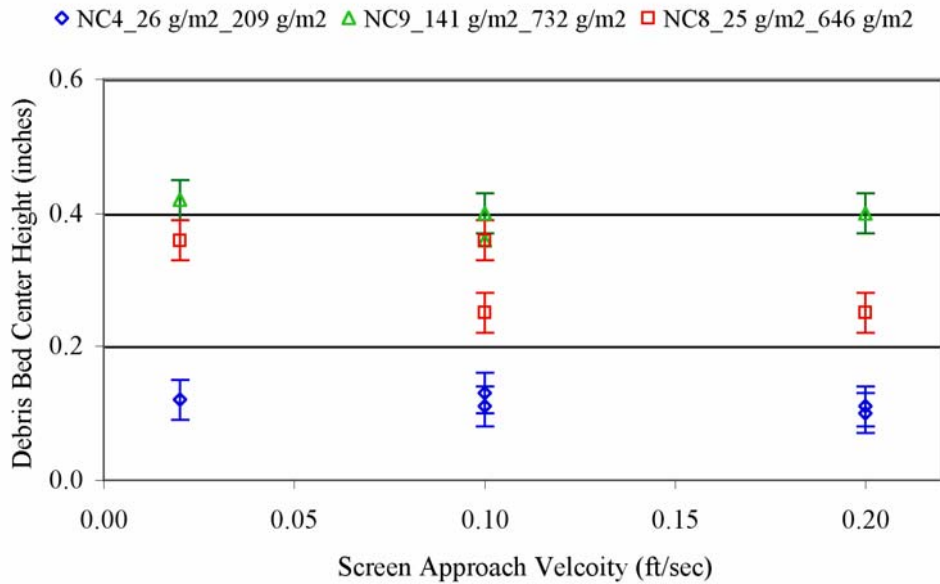


Figure 7.38. Debris Bed Center Height as a Function of Screen Approach Velocity for Three Retrieved Mass Loadings. Data for Series 2 test cases NC4, NC8, and NC9, with debris beds formed at ambient temperature; debris bed height measurements obtained from optical triangulation and presented in Tables 7.16.

height increases with an increase in the total debris bed mass loading. For each debris bed mass loading in Figure 7.38, bed height appears to decrease slightly with an increase in screen approach velocity.

In Section 7.2 the relative debris bed density calculated from the debris bed height appeared to be a significant parameter influencing the pressure drop across the debris bed. For the NUKON/CalSil cases, 6 of the 15 complete debris beds were created from the Series 1 tests, which did not have the capability for optical triangulation to obtain in situ debris bed height measurements. Table 7.17 contains the post-test debris bed height measurements for the 15 complete NUKON/CalSil debris beds and the in situ debris bed measurements obtained at 0.02 ft/sec. The relative debris bed densities have been calculated for both sets of measurements in an attempt to correlate the post-test relative densities with those obtained from measurements made at 0.02 ft/sec.

The test cases in Table 7.17 have been entered in the order of ascending relative bulk density based on the post-test manual measurements. Examining the relative bulk densities obtained from the in situ optical triangulation measurements in the order they are listed, it is apparent that no correlation can be made between the post-test debris bed measurement and the optical triangulation measurements obtained at 0.02 ft/sec. No agreement is observed in the ordering of the relative density obtained from the two debris bed height measurement techniques. It is unknown whether the retrieval process, which requires draining the test section, or simply the relaxation of the debris beds following the removal of the pressure differential unpredictably changes the relative density of the post-test debris beds. This lack of a correlation means only the Series 2 test cases can be used to evaluate the effects of the relative debris bed density on the pressure drop across the debris bed.

Table 7.17. Comparison of Post-Test Manual Measurements and In Situ Measurements from Optical Triangulation of Debris Bed Height and the Corresponding Calculated Relative Densities. Test cases arranged by ascending relative bulk density calculated from post-test measurements.

Test Case	Retrieved Debris Bed Mass Loading ($\pm 4 \text{ g/m}^2$)	CalSil Mass Loading Based on ISE Readings (g/m^2)	Based on In Situ Optical Triangulation Measurements			Based on Post Test Manual Measurements		
			Debris Bed Center Height (in.)	Debris Bed Rim Height (in.)	Relative Bulk Dry Debris Bed Density (g/mL)	Debris Bed Center Height (in.)	Debris Bed Rim Height (in.)	Relative Bulk Dry Debris Bed Density (g/mL)
NC15a	261	18	0.08	0.20	0.171	0.15	0.40	0.068
NC7	729	150	#N/A	#N/A	#N/A	0.36	0.13	0.080
NC14	1924	667	#N/A	#N/A	#N/A	0.92	0.36	0.082
NC13	1260	327	#N/A	#N/A	#N/A	0.55	0.25	0.090
NC12	1334	337	#N/A	#N/A	#N/A	0.47	0.23	0.112
NC11	1034	236	#N/A	#N/A	#N/A	0.35	0.12	0.116
NC8	646	20	0.36	0.59	0.075	0.21	0.51	0.121
NC17a	811	120	0.20	0.28	0.177	0.23	0.29	0.139
NC3 ¹	217	47	#N/A	#N/A	#N/A	0.06	0.16	0.142
NC6b	297	80	0.10	0.24	0.146	0.08	0.12	0.146
NC6a	297	80	0.09	0.23	0.167	0.08	0.12	0.146
NC4	209	25	0.12	0.19	0.082	0.05	0.22	0.164
NC9	732	132	0.26	0.42	0.120	0.15	0.33	0.192
NC5a	213	5	0.10	0.22	0.105	0.04	0.12	0.210
NC16a	160	5	0.08	0.10	0.105	#N/A	N/A	#N/A
NC10	862	339	0.17	0.40	0.212	#N/A	N/A	#N/A
NC1	56	#N/A	#N/A	#N/A	#N/A	#N/A	#N/A	#N/A
NC2	94	#N/A	#N/A	#N/A	#N/A	#N/A	#N/A	#N/A

In Section 7.2.1, Figure 7.12, the larger relative bulk densities ($> 0.1 \text{ g/mL}$) only occurred at the higher debris bed mass loadings ($> 1100 \text{ g/mL}$). Figure 7.39 plots the debris bed bulk density as a function of the retrieved debris bed mass loading for constant screen approach velocities of 0.02, 0.1, and 0.2 ft/sec from the Series 2 test cases for debris beds formed at ambient temperature. Test Cases NC4, NC5a, NC6a, NC8, and NC9 are included in the plot, and data are presented in Table 7.16. These five test cases were all formed at a constant 0.1 ft/sec and at ambient temperature, according to the Series 2 test procedures and subjected to the same velocity sequence (see Section 5.3). No indication of a trend in the data is observed.

The Series 2 NUKON/CalSil tests consisted of lower retrieved mass loadings than were obtained for the NUKON-only tests. Any effect of mass loading on the bulk density may not occur except at higher mass loadings. The bulk densities of the NUKON/CalSil tests were also higher than those of the NUKON-only test, which is expected with the addition of the CalSil particulate material. Both the CalSil mass loading and the CalSil-to-NUKON mass ratio are additional parameters for the NUKON/CalSil cases that did not exist for the NUKON-only tests. Figures 7.40 and 7.41 contain the same test conditions from Table 7.16 that were presented in Figure 7.39 to evaluate the bulk debris bed density as a function of the CalSil mass loading and CalSil/NUKON mass ratio, respectively. No trend is observed for the bulk density as a function of the CalSil mass loading; however, Figure 7.41 indicates the bulk density increases with an increase in the CalSil/NUKON mass ratio. This trend is expected due to the potential for CalSil particulate to be captured in the interstitial space of a NUKON debris bed. However, additional data points are needed before a definitive conclusion can be drawn.

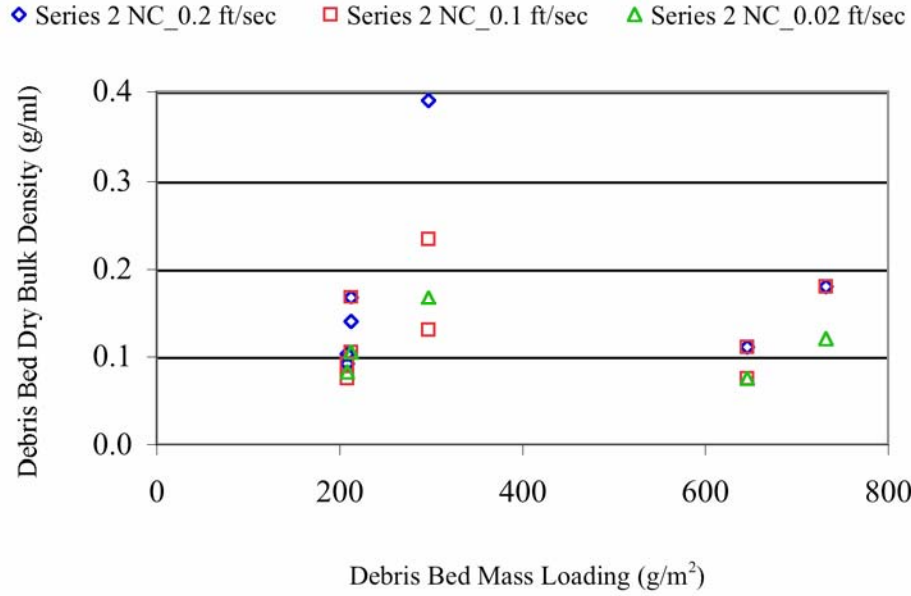


Figure 7.39. Debris Bed Dry Bulk Density as a Function of the Retrieved Debris Bed Mass Loading for Constant Screen Approach Velocities of 0.02, 0.1, and 0.2 ft/sec. Data are from Table 716 for Test Cases NC4, NC5a, NC6a, NC8, and NC9, which are all Series 2 test cases with debris beds formed at ambient temperature.

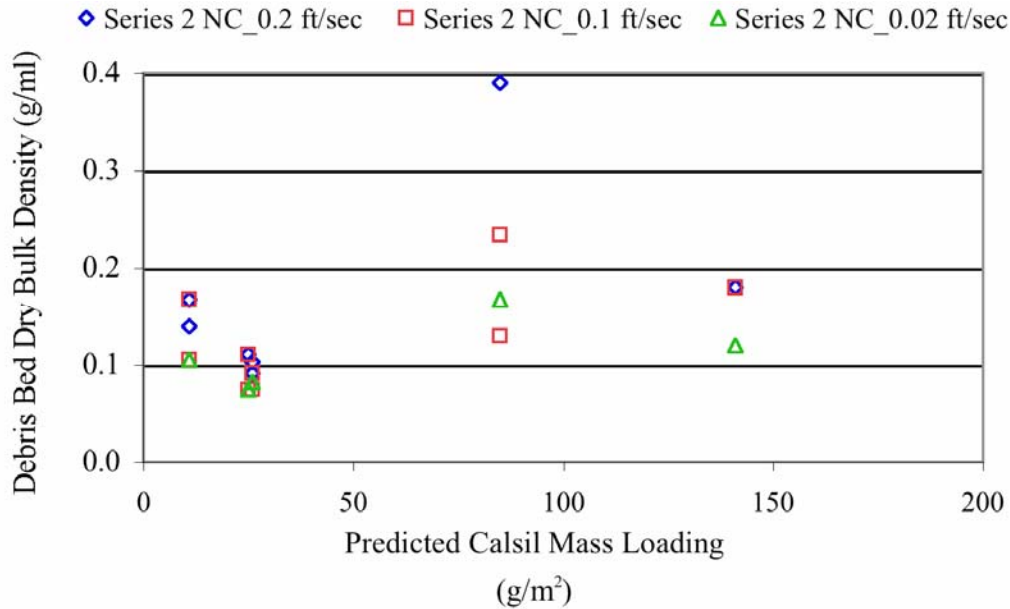


Figure 7.40. Debris Bed Bulk Density as a Function of the Predicted CalSil Mass Loading for Constant Screen Approach Velocities 0.02, 0.1, and 0.2 ft/sec. Data are from Table 716 for Test Cases NC4, NC5a, NC6a, NC8, and NC9, which are all Series 2 test cases with debris beds formed at ambient temperature.

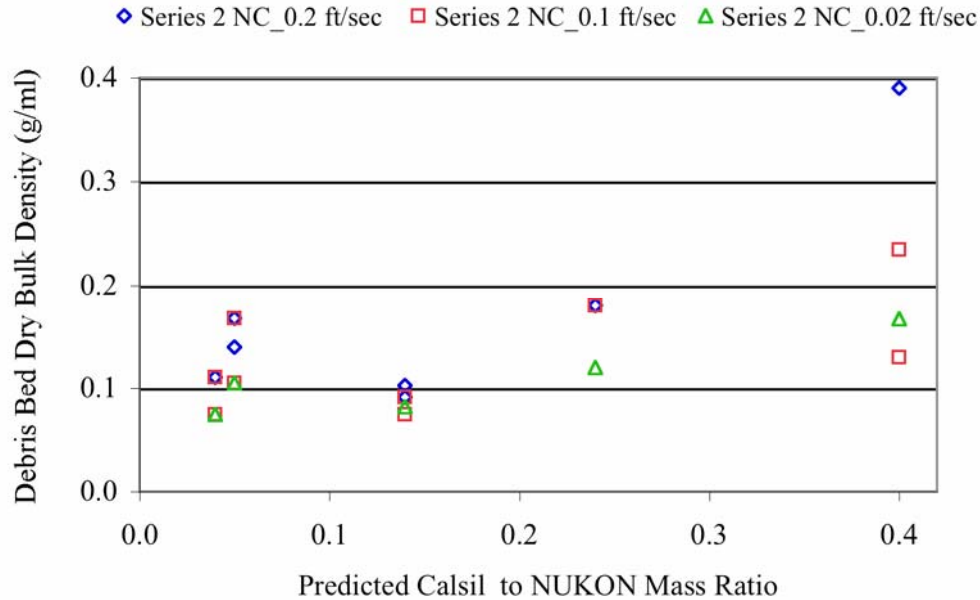


Figure 7.41. Debris Bed Bulk Density as a Function of the Predicted CalSil to NUKON Mass Ratio for Constant Screen Approach Velocities of 0.02, 0.1, and 0.2 ft/sec. Data are from Table 716 for Test Cases NC4, NC5a, NC6a, NC8, and NC9, which are all Series 2 test cases with debris beds formed at ambient temperature.

Based on these results, the effects of the bulk density and CalSil mass ratio on the debris bed pressure drop are examined in the next section.

7.4.4 Head Loss Measurements for NUKON/CalSil Debris Beds at Ambient Temperature

This section provides an overview of the head loss data obtained at ambient fluid temperature for debris beds generated at ambient fluid temperatures. The pressure drop measurements obtained at elevated fluid temperatures or for debris beds generated at elevated temperatures are presented in Section 7.4.5. Test cases NC1 and NC2 did not generate complete debris beds, so pressure drop data for these cases are not included. The debris bed formed for case NC10 essentially plugged the test section during debris bed formation. A head loss of 749 in. H₂O was measured at a screen approach velocity of 0.1 ft/sec near the end of the bed formation process. Due to the high pressure drop, the planned velocity sequence was not executed for case NC10.

Based on the distribution of retrieved debris bed mass loadings, the test cases are separated into three groups for presenting results. Group 1 test cases have retrieved mass loadings between 160 and 297 g/m² and consist of cases NC3, NC4, NC5a, and NC6a. The elevated temperature cases for test condition NC15 and NC16 also fall into the range of Group 1. Group 2 cases have retrieved mass loadings between 646 and 811 g/m² and consist of cases NC7, NC8, and NC9. The elevated temperature cases for test condition NC17 also fall into the range of Group 2. Group 3 test cases have retrieved mass loadings between 1034 and 1924 g/m² and consist of cases NC11 through NC14. Group 3 consists of only Series 1 test cases, which have no optical triangulation measurements from which to calculate the debris bed relative bulk density. There are also no elevated temperature cases associated with Group 3.

Tables 7.18, 7.19, and 7.20 contain the retrieved mass loading, CalSil mass loading, NUKON mass loading, CalSil-to-NUKON mass ratio, and debris bed bulk densities at 0.02, 0.1, and 0.2 ft/sec for test case groups 1, 2, and 3, respectively. Each test case was subjected to a velocity sequence that consisted of cycling the screen approach velocity up and down (refer to Section 5.3).

Table 7.18. NUKON/CalSil Group 1 Test Case Debris Bed Properties (total mass loadings between 160 and 297 g/m²)

Test Case	Nominal Temp (°C)	Retrieved Mass Loading	Calculated CalSil Loading (g/m ²)	Calculated NUKON Loading (g/m ²)	Calculated CalSil to NUKON Mass Ratio	Bulk Densities Calculated from Optical Triangulation Debris Bed Heights ^(a)		
						@ 0.02 ft/sec (g/mL)	@ 0.1 ft/sec (g/mL)	@ 0.2 ft/sec (g/mL)
NC3 ^(b,c)	21	217	49	168	0.29	N/A	N/A	N/A
NC4	21	209	26	183	0.14	0.082	0.075 0.091	0.091 0.103
NC5a	21	213	11	202	0.05	0.105	0.105 0.168	0.140 0.168
NC6a	21	297	85	212	0.40	0.167	0.130 0.234	0.390
Elevated Temperature Cases								
NC15b	36	261	24	237	0.10	N/A	0.342	0.513
NC15a	54	261	24	237	0.10	0.171	0.147 0.205	0.171
NC16b	54	160	11	149	0.08	N/A	0.210	0.210
NC5b	82	213	11	202	0.05	N/A	N/A	0.210
NC6b	82	297	85	212	0.40	0.146	N/A	0.234
NC16a	82	160	11	149	0.08	0.105	0.105 0.157	0.157 0.157
(a) Multiple densities are listed for velocities that had multiple optical triangulation photos analyzed from different velocity cycles. The densities are listed in the order they occurred in the velocity sequence.								
(b) Test case from Series 1, no optical triangulation measurements								
(c) Debris bed formed at an initial screen approach velocity of 0.2 ft/sec.								

Table 7.19. NUKON/CalSil Group 2 Debris Bed Properties (total mass loadings between 646 and 811 g/m²)

Test Case	Nominal Temp (°C)	Retrieved Mass Loading	Calculated CalSil Loading (g/m ²)	Calculated NUKON Loading (g/m ²)	Calculated CalSil to NUKON Mass Ratio	Bulk Densities Calculated from Optical Triangulation Debris Bed Heights ^(a)		
						@ 0.02 ft/sec (g/mL)	@ 0.1 ft/sec (g/mL)	@ 0.2 ft/sec (g/mL)
NC7 ^(b)	21	729	155	574	0.27	N/A	N/A	N/A
NC8	21	646	25	621	0.04	0.075	0.075 0.111	0.111 0.111
NC9	21	732	141	591	0.24	0.120	0.180 0.180	0.180 0.180
Elevated Temperature Cases								
NC17b	29	811	129	681	0.19	N/A	0.266	0.228
NC17a	54	811	129	681	0.19	0.177	0.100 0.177	0.123 0.188
(a) Multiple densities are listed for velocities that had multiple optical triangulation photos analyzed from different velocity cycles. The densities are listed in the order they occurred in the velocity sequence.								
(b) Test case from Series 1, no optical triangulation measurements.								

Table 7.20. NUKON/CalSil Group 3 Debris Bed Properties (total mass loadings between 1034 and 1924 g/m²)

Test Case	Nominal Temp (°C)	Retrieved Mass Loading	Calculated CalSil Loading (g/m ²)	Calculated NUKON Loading (g/m ²)	Calculated CalSil to NUKON Mass Ratio	Bulk Densities Calculated from Optical Triangulation Debris Bed Heights ^(a)		
						@ 0.02 ft/sec (g/mL)	@ 0.1 ft/sec (g/mL)	@ 0.2 ft/sec (g/mL)
NC11 ^(a)	21	1034	242	792	0.31	N/A	N/A	N/A
NC12 ^(a)	21	1334	343	991	0.35	N/A	N/A	N/A
NC13 ^(a)	21	1260	334	926	0.36	N/A	N/A	N/A
NC14 ^(a,b)	21	1924	671	1253	0.54	N/A	N/A	N/A

(a) Test case from Series 1, no optical triangulation measurements.
(b) Debris bed formed at an initial screen approach velocity of 0.2 ft/sec.

Like the NUKON tests, in these tests the pressure drop continued to increase with each cycling of the velocity. Based on the cycling of the debris bed height measured with the optical triangulation and the visual observations of fine debris material periodically exiting from the downstream side of the debris bed, it is postulated that the cycling of the screen approach velocity allowed the CalSil material within the debris bed to migrate deeper into the bed and possibly to be transported through the debris bed. This rearranging of the debris constituents may account for the increase in head loss with each velocity cycle.

Figures 7.42 and 7.43 are plots of head loss as a function of screen approach velocity for several velocity cycles. These figures provide examples of the increase in head loss experienced with each velocity cycle. NC7 is a Series 1 test case; NC9 is a Series 2 test case. For Series 2, the test fluid was filtered after ramp up 1. No filtering occurred during the Series 1 tests. The Series 2 results from Figure 7.43 indicate that increases in head loss following ramp up 1 during the Series 1 tests were not due entirely to the addition of recirculated debris material. The increase in head loss with each velocity cycle demonstrates the impact of flow history on the pressure drop across the debris bed. (For additional discussion of the effects of flow history; see Section 6.5.) To reduce the effects of flow history and minimize the effects of recirculated debris addition, the head loss measurements obtained during ramp up 2 of the velocity sequence are used throughout this section to compare results from different test cases.

Based on the results presented in Sections 7.2, 7.4.2, and 7.4.3, the head loss across the debris bed is evaluated as a function of the retrieved debris bed mass loading, the debris bed relative bulk density, and the calculated (based on chemical dissolution) CalSil-to-NUKON mass ratio in Figures 7.44, 7.45, and 7.46, respectively. The data used to generate the three figures are from Table 7.13, Table 7.16, and the Quick Look reports in Appendix J and are plotted for constant screen approach velocities of 0.02, 0.1, and 0.2 ft/sec. The plots of the debris bed head loss as a function of mass loading and of CalSil-to-NUKON mass ratio, Figures 7.44 and 7.46, contain Series 1 data, which has been identified on the plots. The Series 1 debris beds were generated using simultaneous introduction of debris constituents, while pre-mixed constituents were used for the Series 2 tests. Test cases NC3 and NC14 have been omitted from the Series 1 data used to generate the plots because the debris beds for these cases were formed with an initial screen approach velocity of 0.2 ft/sec (0.06 m/s). The pressure drop as a function of mass ratio has been plotted both with and without Series 1 data for clarity because Series 2 data were obtained over a lower range of head losses.

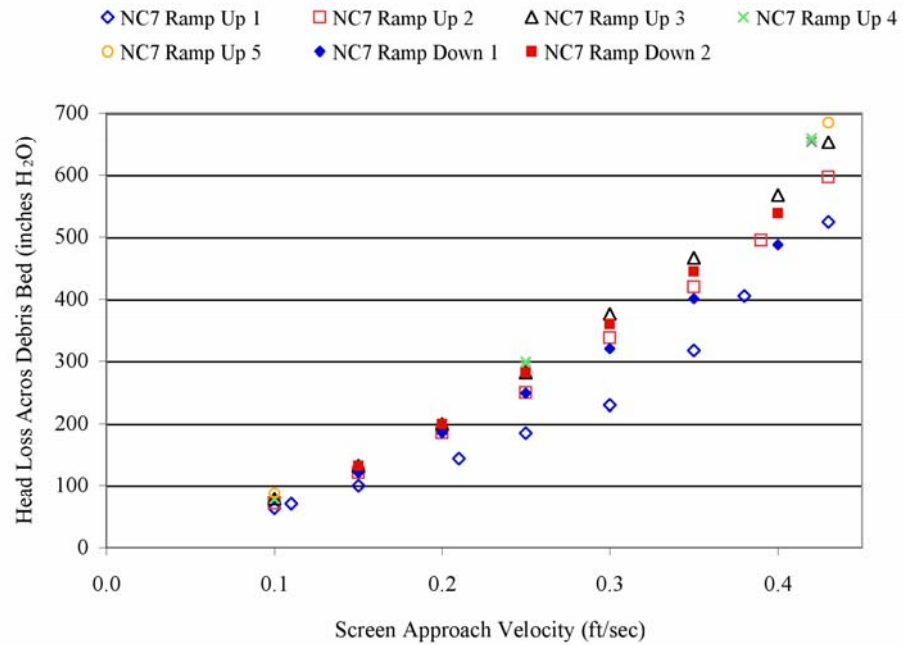


Figure 7.42. Debris Bed Head Loss from NC7 as a Function of Screen Approach Velocity for Five Ramp ups and the First Two Ramp Downs in the Screen Approach. NC7 is a Series 1 test case with data presented in the Quick Look report for PNNL Test 051121_NC_1586_L1, which is included in Appendix J.

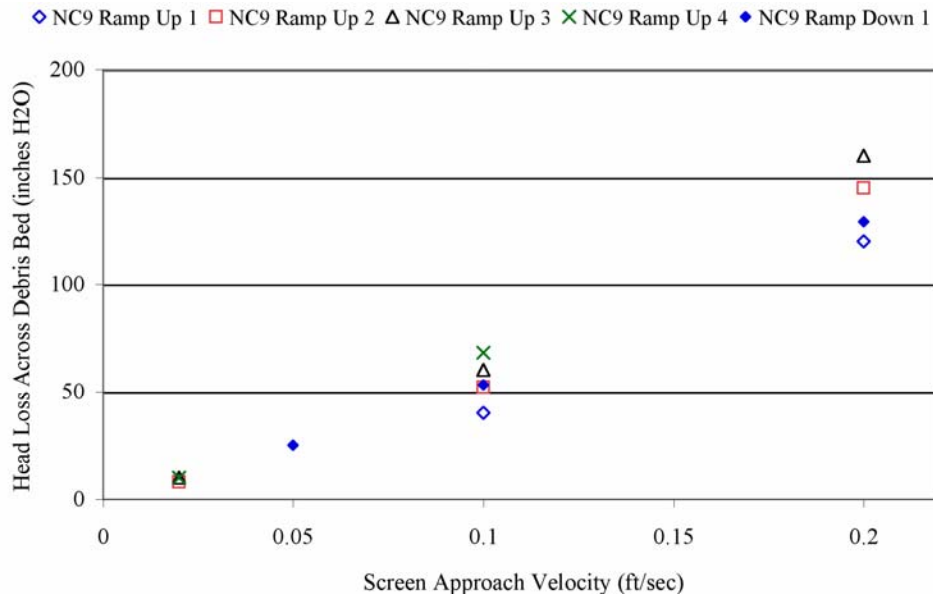


Figure 7.43. Debris Bed Head Loss from NC9 as a Function of Screen Approach Velocity for Four Ramp ups and the First Ramp Down in the Screen Approach Velocity. NC9 is a Series 2 test case with data presented in the Quick Look report for PNNL Test 060331_NC_2024_L1, which is included in Appendix J.

The head loss as a function of the debris bed relative bulk density presented in Figure 7.45 contains only Series 2 data since the optical triangulation measurements were not available for the Series 1 tests. The plot was created using the results of Test Cases NC4, NC5a, NC6a, NC8, and NC9.

From Figure 7.44, definitive trend in the data for the head loss as a function of the retrieved mass loading is observed for either the Series 1 or Series 2 data. As was observed for the NUKON-only test cases, Figure 7.45 indicates that for the NUKON/CalSil test cases the resulting pressure drop across the debris bed increases with an increase in the relative bulk density of the debris bed. The relationship between the debris bed pressure drop and the CalSil-to-NUKON mass ratio is not as obvious in Figure 7.46. Examining the Series 2 data in Figure 7.46b, the pressure drop appears to increase with an increase in the mass ratio. However, due to the limited number of points and the spread in the data further investigation is needed to draw final conclusions. No trend was observed between the debris bed pressure drop and calculated CalSil mass loading (plot not shown).

The individual test cases in each group of tests defined by Tables 7.18 through 7.20 will be compared using the ramp up 2 pressure data in Figures 7.47 through 7.50. For each test case listed in the legend of the plots, the calculated CalSil loading, the total mass loading, and the CalSil-to-NUKON mass ratio follows the test case. For example, NC4_26 g/m²_209 g/m²_0.14 is for test case NC 4, which had a CalSil mass loading of 26 g/m², a total retrieved mass loading of 209 g/m², and a CalSil to NUKON mass ratio of 0.14.

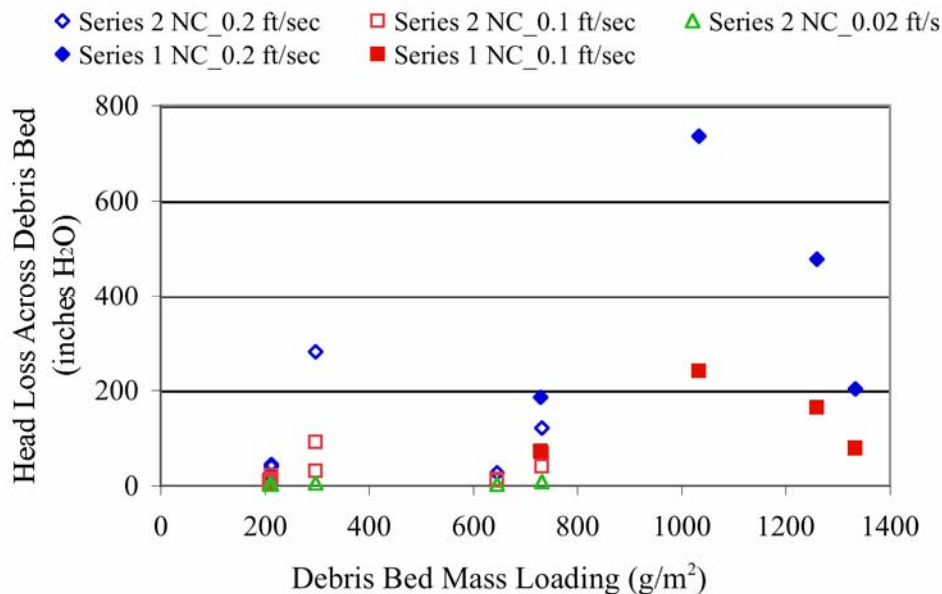


Figure 7.44. Plot of the Pressure Drop Across the Debris Bed as a Function of the Retrieved Debris Bed Mass Loading for Constant Screen Approach Velocities of 0.02, 0.1, and 0.2 ft/sec. Data from both Series 1 and 2 test cases for debris beds formed at ambient temperature and a screen approach velocity of 0.1 ft/sec. Test Cases NC4, NC5a, NC6a, NC7, NC8, NC9, NC11, NC12, and NC13 are included in the plot; head loss data are from the Quick Look reports in Appendix J.

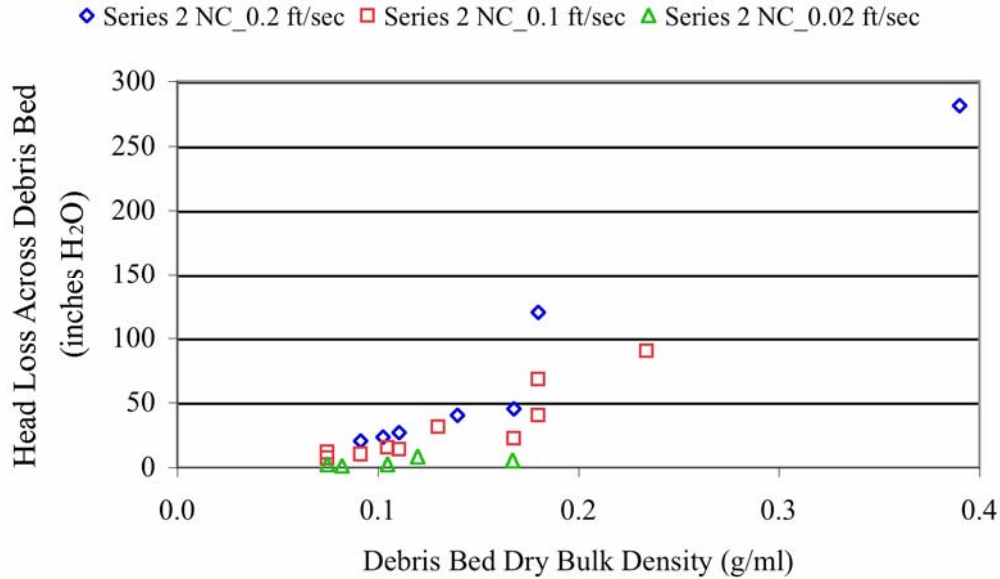
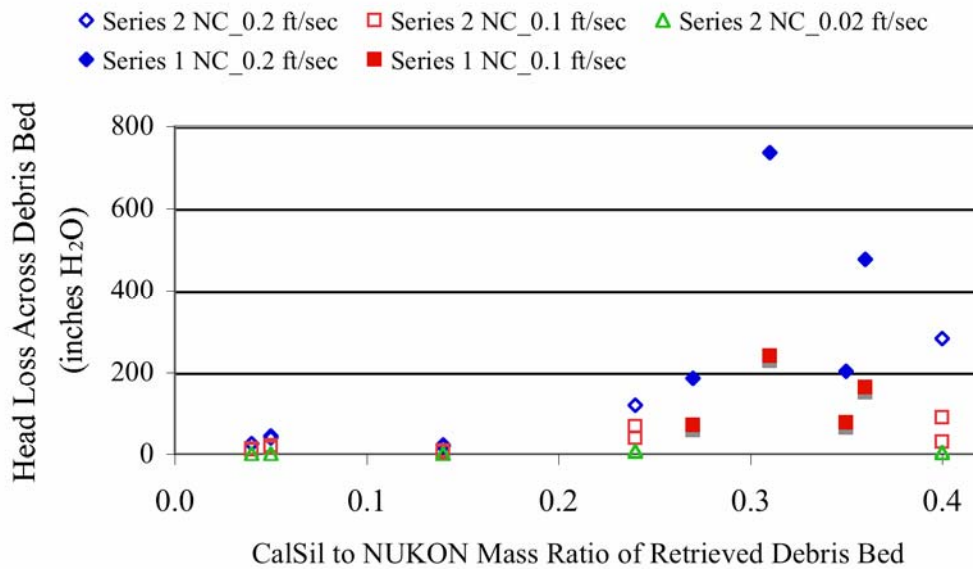


Figure 7.45. Plot of Debris Bed Pressure Drop as a Function of the Relative Debris Bed Bulk Density for Constant Screen Approach Velocities of 0.02, 0.1, and 0.2 ft/sec. Data from the Series 2 test cases with debris beds formed at ambient temperature. Test Cases NC4, NC5a, NC6a, NC8, and NC9 are included in the plot; data are from Table 7.16 and the Quick Look reports in Appendix J.

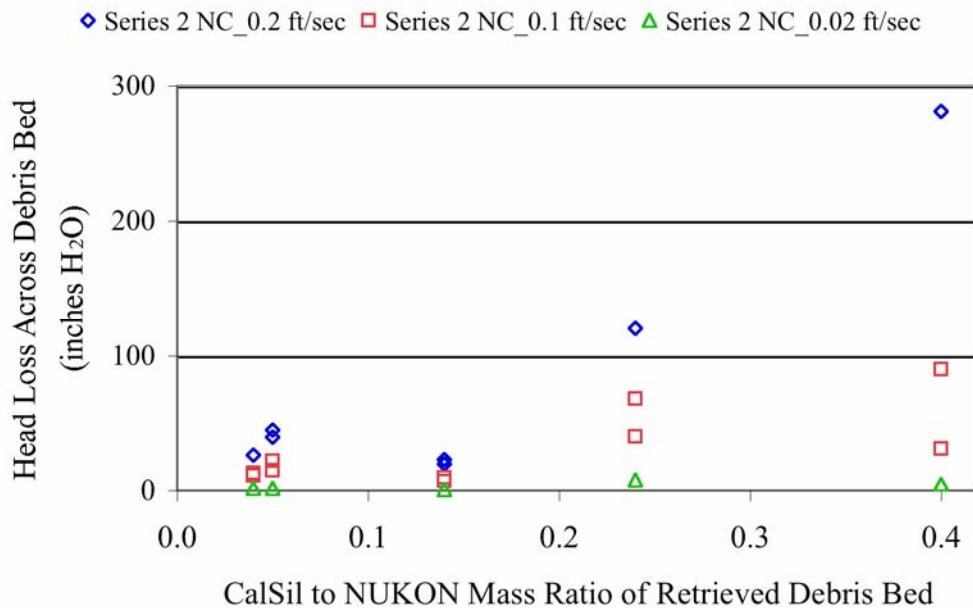
The head loss across the debris bed as a function of the screen approach velocity is plotted for Group 1 test cases in Figures 7.47 and 7.48. Figure 7.47 contains the Series 1 test case NC 3, which has been excluded from Figure 7.48 for simplifying the comparison between the remaining test cases. The NC3 debris bed was formed at an initial screen approach velocity of 0.2 ft/sec (0.06 m/s) and tested over a different range of screen approach velocities, which could skew the comparison with the other cases. There are also no optical triangulation debris bed heights and associated debris bed densities for NC3.

The four parameters considered in comparing the pressure drop measurements from the various test cases were the total mass loading, the CalSil mass loading, the CalSil-to-NUKON mass ratio, and the debris bed relative bulk density. The four test cases for Group 1 ranked from highest to lowest pressure drop are NC6a, NC5a, NC3, and NC4. Table 7.21 lists the 4 test cases of Group 1 and their ranking with respect to the four parameters listed above. Of the four parameters, only the ranking of the relative bulk densities corresponds to the order of the measured head losses. If NC3 is excluded due to the difference in the debris bed formation approach velocity, then the ranking of total mass loading also corresponds to the order of the measured head losses.

The head loss across the debris bed as a function of the screen approach velocity is plotted for Group 2 test cases in Figure 7.49. The four test cases for Group 2 ranked from highest to lowest pressure drop are NC17b, NC7, NC9, and NC8. Table 7.22 lists the 4 test cases of Group 2 and their ranking with respect to the four parameters listed above. Of the four parameters, only the ranking of the relative bulk densities corresponds to the order of the measured head losses. As with Group 1, if the Series 1 case, NC7, is excluded due to the difference in the screen approach velocity used for debris bed formation, then the ranking of retrieved total mass loading also corresponds to the order of the measured head losses.



(a) Includes both Series 1 and Series 2 data



(b) Includes only Series 2 data

Figure 7.46. Pressure Drop Across the Debris Bed as a Function of the Retrieved CalSil-to-NUKON Mass Ratio for Constant Screen Approach Velocities of 0.02, 0.1, and 0.2 ft/sec. Data provided from both Series 1 and 2 test cases with debris beds formed at ambient temperature and a screen approach velocity of 0.1 ft/sec. Test Cases NC4, NC5a, NC6a, NC8, and NC9 from Series 2 and NC7, NC11, NC12, and NC13 from Series 1 are included in the plot. Head loss data are from Quick Look reports in Appendix J.

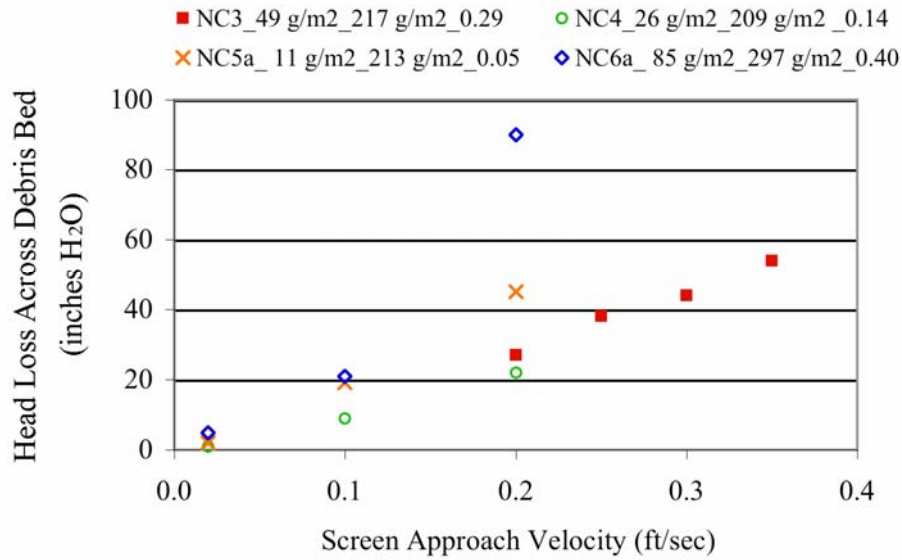


Figure 7.47. Pressure Drop Across the Debris Bed as a Function of the Screen Approach Velocity for Group 1 NUKON/CalSil Test Cases. Test Cases NC4, NC5a and NC6a are from Series 2 and were formed at ambient temperature with a screen approach velocity of 0.1 ft/sec. Test Case NC3 is from the Series 1 tests and was formed at ambient fluid temperature with an initial screen approach velocity of 0.2 ft/sec. The head loss data are from the Quick Look reports in Appendix J.

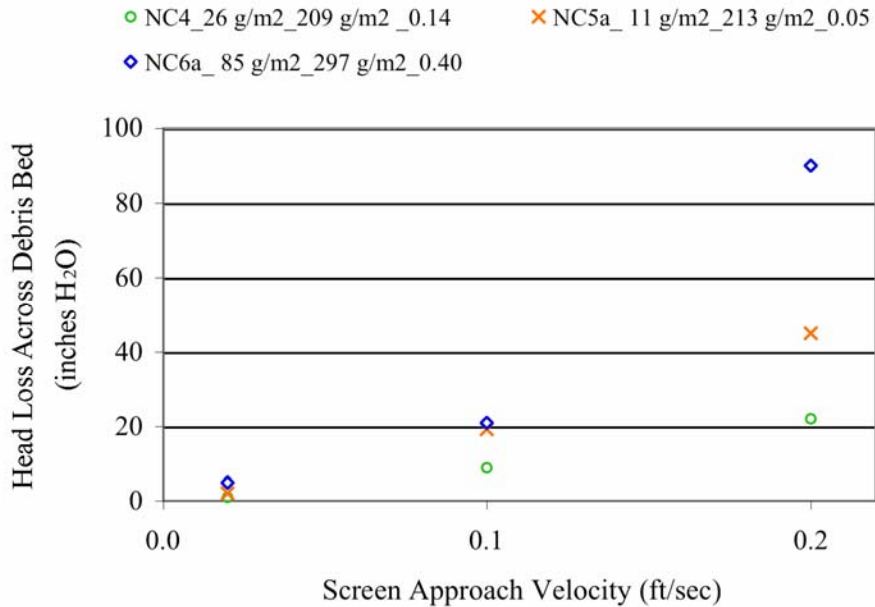


Figure 7.48. Pressure Drop Across the Debris Bed as a Function of the Screen Approach Velocity for Group 1, Series 2, NUKON/CalSil Test Cases. All debris beds were formed at ambient temperature with a screen approach velocity of 0.1 ft/sec. The head loss data are from the Quick Look reports in Appendix J

Table 7.21. Comparative Ranking (highest to lowest) of the Group 1 Test Cases with Respect to Head Loss Across the Debris Bed, Total Mass Loading, CalSil Mass Loading, CalSil-to-NUKON Mass Ratio, and Relative Bulk Density

Test Case Ranked in Order of Pressure Drop	Head Loss Across Debris Bed at 0.2 ft/sec (in. H ₂ O)	Ranking of Total Retrieved Dry Mass Loading	Ranking of Calculated CalSil Mass Loading	Ranking of CalSil- to-NUKON Mass Ratio	Ranking of Debris Bed Bulk Density
NC6a ^(a)	90	1	1	1	1
NC5a ^(a)	45	3	4	4	2
NC3 ^(b,c)	27	2	2	2	N/A
NC4 ^(a)	22	4	3	3	3

(a) Test case from Series 2.
 (b) Test case from Series 1.
 (c) Debris bed formed at an initial screen approach velocity of 0.2 ft/sec.

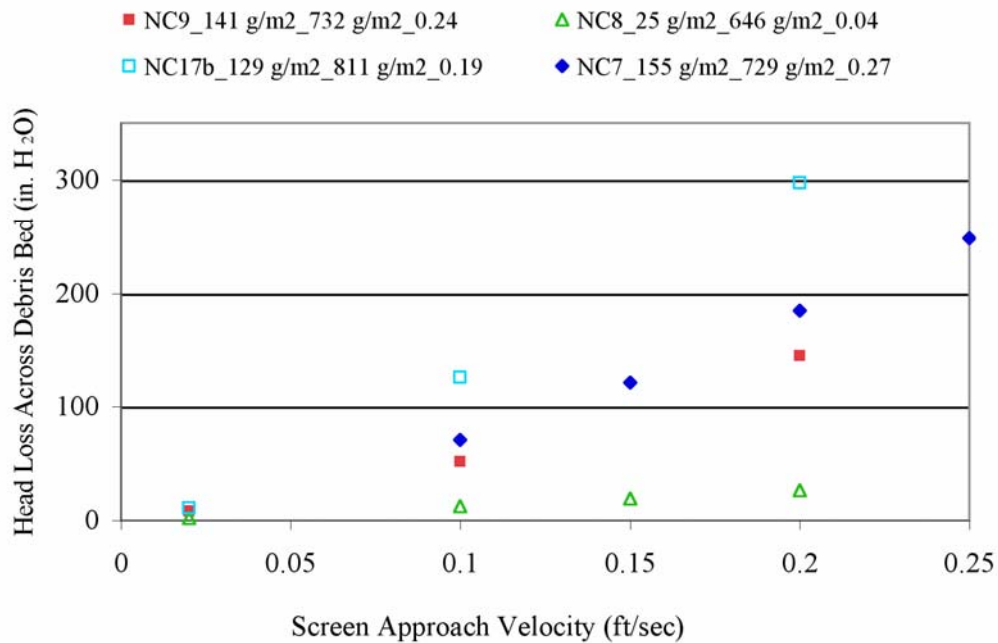


Figure 7.49. Pressure Drop Across the Debris Bed as a Function of the Screen Approach Velocity for Group 2 NUKON/CalSil Test Cases. Test Cases NC8, NC9 and NC17b are from Series 2 and were formed with a screen approach velocity of 0.1 ft/sec. Debris beds for NC8 and NC9 were formed at ambient temperature and the one for NC17b was formed at 54°C. Test Case NC7 is from the Series 1 tests and was formed at ambient fluid temperature with an initial screen approach velocity of 0.2 ft/sec. The head loss data are from the Quick Look reports in Appendix J.

Table 7.22. Comparative Ranking (highest to lowest) of the Group 2 Test Cases with Respect to Head Loss Across the Debris Bed, Total Mass Loading, CalSil Mass Loading, CalSil-to-NUKON Mass Ratio, and Relative Bulk Density

Test Case Ranked in Order of Pressure Drop	Head Loss Across Debris bed at 0.2 ft/sec (in. H ₂ O)	Ranking of Total Retrieved Dry Mass Loading	Ranking of Calculated CalSil Mass Loading	Ranking of CalSil-to-NUKON Mass Ratio	Ranking of Debris Bed Bulk Density
NC17b ^{(a)(b)}	298	1	3	3	1
NC7 ^(c)	185	3	1	1	N/A
NC9 ^(a)	145	2	2	2	2
NC8 ^(a)	26	4	4	4	3

(a) Test case from Series 2.
 (b) Debris bed formed at a fluid temperature of 54°C.
 (c) Test case from Series 1.

The head loss across the debris bed as a function of screen approach velocity is plotted for Group 3 in Figure 7.50. All four test cases are from Series 1 with the debris bed for NC14 formed at an initial screen approach velocity of 0.2 ft/sec compared to 0.1 ft/sec for the other three. No optical triangulation bed heights or associated densities are available for Group 3. The Group 3 test cases ranked from highest to lowest pressure drop are NC11, NC13, NC14, and NC12. Table 7.23 lists the relative ranking of the Group 3 test cases with respect to total retrieved mass loading, CalSil mass loading, and CalSil-to-NUKON mass ratio. Based on these rankings, no trend is observed. However, if NC14 is excluded due to its different bed formation velocity, both total mass loading and calculated CalSil loading decrease with increasing pressure drop. Analysis of these cases led to evaluation of the debris loading sequence discussed in Section 6.3. No elevated temperature cases were conducted for the mass loading range of Group 3; therefore, no discussion of Group 3 results is included in Section 7.4.5.

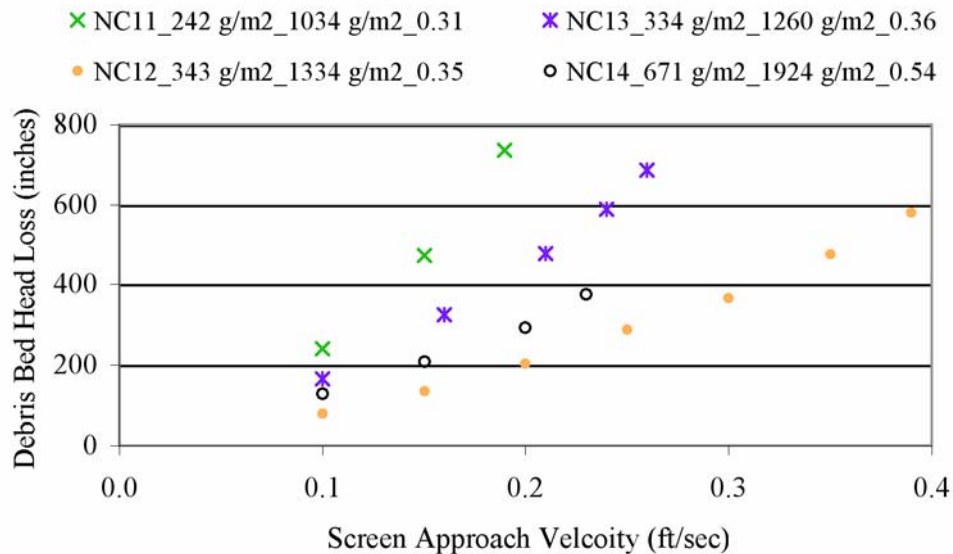


Figure 7.50. Pressure Drop Across Debris Bed as a Function of Screen Approach Velocity for Group 3, Series 1, NUKON/CalSil Test Cases. All debris beds were formed at ambient temperature with a screen approach velocity of 0.1 ft/sec. Head loss data are from the Quick Look reports in Appendix J.

Table 7.23. Comparative Ranking (Highest to Lowest) of the Group 3 Test Cases with Respect to Head Loss Across the Debris Bed, Total Mass Loading, CalSil Mass Loading, and CalSil-to-NUKON Mass Ratio

Test Case Ranked in order of Pressure drop	Head Loss Across the debris bed at 0.2 ft/sec (in. H ₂ O)	Ranking of Total Retrieved Dry Mass Loading	Ranking of Calculated CalSil Mass Loading	Ranking of CalSil to NUKON Mass Ratio	Ranking of Debris Bed Bulk Density
NC11 ^(a)	735	4	4	4	N/A
NC13 ^(a)	477	3	3	2	N/A
NC14 ^{(a)(b)}	292	1	1	1	N/A
NC12 ^(a)	203	2	2	3	N/A

(a) Test case from Series 1.
(b) Debris bed formed at an initial screen approach velocity of 0.2 ft/sec.

7.4.5 Head Loss Measurements for NUKON/CalSil Debris Beds at Elevated Temperatures

Two types of elevated temperature tests were conducted with NUKON/CalSil debris beds. The first elevated temperature tests were conducted by forming the debris bed at ambient fluid temperature, executing the velocity sequence at ambient fluid temperature, and then elevating the fluid temperature with the screen approach velocity maintained at approximately 0.1 ft/sec (0.3 m/s) and again taking data for the velocity sequence at the elevated temperature. Test cases NC5b and NC6b were performed this way to obtain data at 82°C and are part of Group 1 with their debris bed properties presented in Table 7.18. The results of elevated temperature tests NO4 and NO5 (refer to Section 7.2.2) raised concerns that the effects of flow history were masking any effects on the measured head loss resulting from the higher fluid temperature. Therefore, additional elevated temperature tests were conducted with debris beds formed at elevated temperatures.

The later elevated temperature tests consisted of raising the fluid temperature to the desired conditions prior to the introduction of debris material. The debris bed was formed and the velocity sequence executed at the raised temperature. At the completion of the first pass through the velocity sequence, the fluid temperature was cooled and a truncated velocity sequence executed at the reduced temperature. The debris beds for NC15a and NC16a had the same target debris loadings as test case NC5a and were formed at 129° and 180°F (54° and 82°C), respectively. NC15a and NC16a are part of Group 1. Their debris bed properties are presented in Table 7.18. The debris bed for NC17a was formed at 129°F (54°C) and had the same target mass loading as NC9. NC17a is part of Group 2; its associated debris bed properties are presented in Table 7.19.

The test cases listed in Tables 7.18 and 7.19 with identification numbers ending in “b” (e.g., NC5b) represent test cases that were conducted after an initial test and associated velocity sequence were run at a different temperature. The debris beds for these cases were also subjected to a prolonged period of flow (> 45 minutes) during fluid heat up or cool down prior to executing the velocity sequence and taking the associated steady-state pressure measurements. Test cases NC5b, NC15b, NC16b, and NC17b all yielded higher relative debris bed densities than the corresponding test cases conducted first with the same debris beds. The increase in the relative densities is another indication of the effect the flow history can have on the debris beds. Test Case NC6b was the lone exception, with debris bed densities less than those obtained from the bed height measurements for NC6a.

Identification of test cases used in the legends of plots are the same as described in Section 7.4.4 with the fluid temperature at which the head loss data was obtained added to the end of the identification. The reader is again reminded that all of the head loss data are reported in inches of H₂O @ 68°F. Figure 7.51 is a plot of the debris bed head loss as a function of the screen approach velocity for all the test conditions from Group 1 that include a test conducted at an elevated temperature. The results from four debris beds (test conditions NC5, NC6, NC15, and NC16) and eight test cases are presented in Figure 7.51. The same geometric shape is used to represent data points for the same debris bed. The hollow shape represents the test case conducted at the lower temperature and the filled in data point represents data obtained at the higher temperature. Despite the differences in flow history for all four debris beds, the lower temperature (i.e., higher fluid viscosity) test case yielded the higher pressure drop.

The Group 1 test cases conducted at 180°F (82°C) listed from highest to lowest pressure drop were NC6b, NC5b, and NC16a. Comparing the debris bed properties from Table 7.18 for the three test cases, the ranking from highest to lowest for the relative debris bed density and total mass loading corresponds to the order obtained for the pressure drop measurements.

Test cases NC15a and NC16b were conducted at 129°F (54°C) with NC15a producing the higher measurements for pressure drop. NC16b had a relative density greater than that for NC15a; however, the total mass loading for NC15a was 168% that for NC16b, 261 g/m² compared to 160 g/m².

The test cases conducted at ambient temperature from highest to lowest pressure drop were NC6a, NC15b, and NC5a, which corresponds to the ranking for total mass loading, CalSil mass loading, and CalSil-to-NUKON mass ratio. The relative density for the three debris beds did not correspond to the order of the pressure drops at an approach velocity of 0.2 ft/sec (0.06 m/s); however, it should be noted that test case NC15b, which had the largest relative density, was conducted at 97°F (36°C) compared to approximately 70°F (21°C) for test cases NC6b and NC16a. The greater fluid temperature of NC15b corresponds to a reduced fluid viscosity, which may account for the greater density case not yielding the largest pressure drop at 0.2 ft/sec (0.06 m/s). However, the highest pressure drop was obtained for test case NC15b at screen approach velocity of 0.1 ft/sec (0.03 m/s) (see Figure 7.51).

Visual observations indicated the debris beds generated at elevated temperatures did not appear to have rims as pronounced as comparable beds formed at ambient temperature. This observation could impact the relative densities calculated from the optical triangulation debris bed heights. The relative density measurements are obtained from the total retrieved mass, the debris bed volume calculated from the test section diameter, and the average body height obtained from the optical triangulation measurements. The average body height is the average height of the debris bed excluding the area covered by the debris bed rim. Therefore, the volume of debris material included in the rim is excluded from the calculation of the relative density, while the mass of the material is included.

The debris beds formed at an elevated fluid temperature, test cases NC15A, NC16a and NC17a, had relative rim heights that were a smaller percentage of the debris bed center height than those formed at ambient fluid temperatures. From Group 1, debris beds NC5a and NC6a formed at ambient temperature both had rims heights measured at 0.1 ft/sec that were 3.1 times the center height, respectively. In comparison, the Group 1 debris beds NC15a and NC16a formed at fluid temperatures of 129° and 130°F (54° and 82°C), respectively, had rims heights measured at 0.1 ft/sec that were 2.8 and 1.5 times the

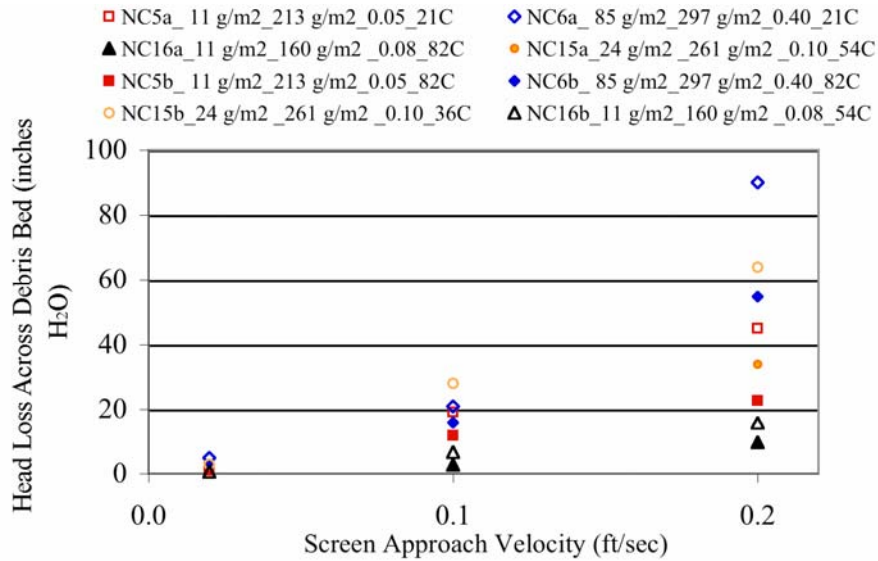


Figure 7.51. Plot of Pressure Drop Across the Debris Bed as a Function of Screen Approach Velocity for Group 1 Debris Beds Subjected to Testing at Elevated Fluid Temperatures. All test cases are from Series 2. The debris beds for conditions NC5 and NC6 were formed at ambient fluid temperature; debris beds for test conditions NC15 and NC16 were formed at fluid temperatures of 129° and 130°F (54° and 82°C), respectively. Head loss measurements are from Quick Look reports in Appendix J.

center height, respectively. Group 2 debris bed NC9 formed at ambient temperature had rim heights measured at 0.1 and 0.2 ft/sec that were 1.4 and 2.2 times the center height, respectively. In comparison, the Group 2 debris bed NC17a formed at a fluid temperature of 129°F (54°C) and had rim heights measured at 0.1 and 0.2 ft/sec that were 1.3 and 1.2 times the center height, respectively. The calculated densities are relative measurements used for comparing the different test cases and are not expected to represent true bulk densities. The variations in the relative rim height observed between debris beds formed at the different fluid temperatures indicate additional caution should be used when using the relative density to compare debris beds formed at different temperatures.

Figure 7.52 plots the debris bed head loss as a function of the screen approach velocity for the Group 2 test cases NC9, NC17a, and NC17b. The debris bed for NC17a was formed at a fluid temperature of 129°F (54°C) with the same target mass loading as NC9. For test condition NC17, the lower temperature (higher viscosity) case, NC17b, yielded larger pressure drop measurements. Comparing the ambient temperature cases of NC9 and NC17b, the test case with the larger mass loading and relative density, NC17b, yielded the higher head loss. Again, it is likely that the increased relative density obtained for NC17b is the result of the additional flow history resulting from the cool-down period and execution of the second velocity sequence.

The elevated temperature cases continue to support the trend that, for comparable mass loadings, the debris beds with the largest relative bulk density yielded the largest pressure drop measurements. The flow history resulting from periods of heating up and cooling down and repeating velocity sequences appears to impact the head loss measurements by increasing the relative density of the beds. Other than visual observations of the change in relative debris bed rim height, no conclusions have been drawn regarding changes to the debris bed resulting from forming it at an elevated temperature.

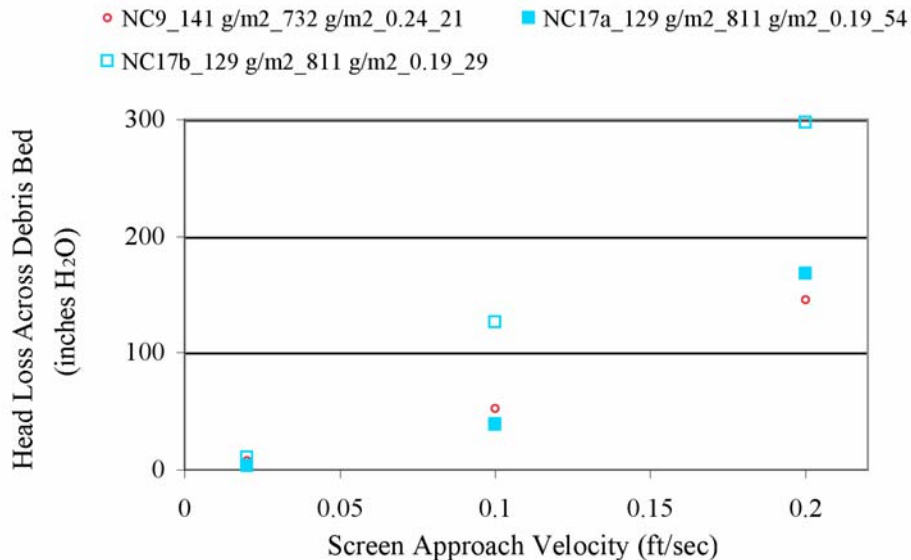


Figure 7.52. Pressure Drop Across Debris Bed as a Function of Screen Approach Velocity for Group 2 Debris Beds Associated with Elevated Temperature Test NC17a. Debris bed NC17 was formed at a fluid temperature of 129°F (54°C) and the same target mass loading as NC9, which was formed at a fluid temperature of 70°F (21°C). Head loss measurements are from Quick Look reports in Appendix J.

7.5 Coating Debris Bed Results

PNNL evaluated debris bed head loss for Ameron’s Amercoat 5450 alkyd topcoat (ALK) and Ameron's Dimetcote 6 inorganic zinc primer with Amercoat 90 epoxy topcoat (ZE) coatings as a function of screen approach velocity, flow history, and fluid temperature. The debris material was prepared as described in Section 4 to create processed and ¼-in. square chips for each coating type. The processed debris was the finer material with major and minor axis dimensions on the order of 0.05 to 0.15 in. (1.3 to 3.8 mm) and 0.05 to 0.10 in. (1.3 to 2.5 mm), respectively, for both the ALK and ZE coatings. The ¼-in. square chips were obtained by sieving and had major and minor axis dimensions on the order of; 0.1 to 0.45 in. (2.5 to 11 mm) and 0.1 to 0.3 in. (2.5 to 7.6 mm) for ALK and 0.3 to 0.6 in. (7.6 to 15 mm) and 0.15 to 0.3 in. (3.8 to 7.6 mm) for ZE, respectively. Size distributions for the four coating debris tested are provided in Appendix O.

Tests conducted with the ALK and ZE coatings are listed in Table 7.24. An ALK coating benchtop test, ALKBT, was initially conducted as a scoping test at 700 g/m² each of blender processed coating and ¼ in. square (also referred to as chips) coating (Section 4). Three large-scale tests, ALK1a, ALK1b, and ZE1, were conducted in the large-scale loop with equal target concentrations, 700 g/m² each, of processed coating and 1/4 in. square coating (see Section 4). Test ALK1b is a continuation of test ALK1a at an elevated fluid temperature. One additional test, ALK2, was conducted with only processed coating at the total target loading of 1,400 g/m².

In Section 7.5.1, determinations from the ALKBT benchtop test regarding the debris bed formation process are listed, and large-scale debris bed formation test procedures and observations are discussed. Coatings test results are discussed in Section 7.5.2.

Table 7.24. PNNL Coating Debris Tests Conducted

Test Case	Test ID	Target Debris Bed Processed Coating Loading (g/m ²)	Target Debris Bed ¼-in. sq. Coating Loading (g/m ²)	Total Target Debris Bed Loading (g/m ²)	Total Retrieved Debris Bed Loading (±8 g/m ²)	Nominal Fluid Temp. (°C)	Screen or Plate	Debris Bed Formed
ALK1a	060501_PQC_2609_LP1	700	700	1,400	807	18	plate	incomplete
ALK1b	060501_PQC_2609_LP2	700	700	1,400	807	82	plate	incomplete
ZE1	060504_PQZ_2609_LP1	700	700	1,400	794	21	plate	incomplete
ALKBT	060428_PQC_1136_BP1	700	700	1,400	762	21	plate	incomplete
ALK2	060502_POC_2609_LP1	1400	0	1,400	850	21	plate	incomplete

7.5.1 Coating Debris Bed Formation

The following items were determined from the initial ALKBT benchtop test:

- The paint chips when wet have a tendency to adhere easily to surfaces. Therefore, when premixing constituents, 1/4-inch square chips were placed dry in a mixing container and the other slurried constituents were added wet.
- A screen approach velocity of 0.1 ft/sec was not fast enough to transport the coating debris to the test screen. Initially, the benchtop injection line velocity was set to 0.8 ft/sec with a screen approach velocity of 0.1 ft/sec. Negligible paint chip material was visually observed to be transported to the test screen, even with significant line agitation. The paint chips exited the injection line as a saltation-type flow and immediately settled upon being introduced into a horizontal section of the main line. Some coating debris transport was achieved when the screen approach velocity was increased to approximately 1.5 ft/sec. Screen approach velocities for the coatings tests were greater than those used for the insulation materials (Sections 7.2–7.4)

From the latter observation in the benchtop test, the screen approach velocity for bed formation for the ALK1a and ALK1b coating test was set to the maximum velocity of the test matrix, 0.20 ft/sec (see Section 5 for test velocity matrixes). Some of the debris introduced to the loop was judged by visual observation of the flow to settle within the piping as opposed to collecting on the perforated plate. Thus, settled material was mobilized into the flow by tapping the horizontal flow region of the test loop at the debris injection level with a rubber hammer. Hammering was continued until some (usually a small amount) additional debris was observed to be mobilized. This hammer mobilization technique was conducted intermittently for approximately 20 minutes after debris injection.

Based on the debris bed formation conditions for tests ALK1a and ALK1b, the initial screen approach velocity for test ALK2 with processed-only coating debris was set to 0.30 ft/sec. At this screen approach velocity, essentially no debris was observed to be mobilized in the flow. Additionally, minimal processed ALK debris was visually observed retained on the perforated plate after the debris bed formation time of one hour. As noted for the ALK1a and ALK1b test, settled material was mobilized into the flow by tapping the horizontal flow region of the test loop at the debris injection level with a rubber hammer. This methodology, though apparently successful at mobilizing some portion of the particulate, was not used for test ALK2 because it was observed that the tapping released the processed-only particulate from the plate. Additional testing was conducted after completion of the truncated velocity matrix (see Section 5).

The additional testing for ALK2 consisted of incrementally raising the screen approach velocity to identify, if possible, when the settled (as inferred from the visually observed lack of debris on the plate or in the flow) was mobilized. The flow was then held for 45 minutes at this mobilization velocity to form, if possible, a complete debris bed, and filtration was again conducted. The maximum limit for flow rate was set to 140 gpm (corresponds to a screen approach velocity of 1.55 ft/sec) to preserve bag-filter integrity (see Section 2 for bag-filter description).

Cursory calculations were performed during the test in an attempt to quantify the expected solid volume fraction at complete mobilization of the injected debris into the flow. With a flowing loop volume of approximately 85 gallons, total processed ALK debris mass of 26.09 g (neglecting filtering given the limited indication of mobilization), and measured ALK density of approximately 1.04 g/mL, the solid volume fraction in the flow with homogenous mixing was calculated to be $< 0.01\%$ (mass fraction $8.1E-5$). Visual observation is therefore inadequate to determine total mobilization of the complete debris mass. Thus, the relative visually observed change in the solids content of the flow was used solely to judge mobilization effect. For a limited range of approach velocities (not thoroughly quantified) coatings material would appear to be entrained and held up (accumulate) in turbulent eddies just below the bed. Therefore, consideration was also given to ensuring an approach velocity sufficient to negate the trapping of debris particulate in the turbulence of the plate discharge. This was desired to ensure transport to the filter and negate the potential for settling upon reduction of the flow velocity.

The previous test conditions indicated that 0.3 ft/sec (all subsequently referenced velocities refer to the screen approach velocity) was insufficient to maintain suspension of the debris. Thus, it was not expected that 0.3 ft/sec would mobilize the settled particulate, and 0.4 ft/sec was selected as the initial elevated velocity. Limited particulate (hereafter to be taken as visually observed to be on the order of the prepared debris in size) was observed to be mobilized into the flow. The quantity of debris above and below the plate was judged to be similar, and no buildup was observed on the plate. Particulate was trapped below the screen. At this and subsequent velocities, the debris appeared to be evenly distributed throughout the loop; i.e., the observed concentration appeared constant for successive circulations (with time).

At 0.5 ft/sec, the quantity of particulate was observed to increase, a slight difference in concentration was observed in the upper (above the plate) and lower (below the plate) test sections, a slight buildup was observed on the plate, and particulate was trapped below the screen. At 0.6 ft/sec, the quantity of particulate in the flow was observed to significantly increase, a difference in concentration was observed between the upper and lower test sections, gradual buildup was observed on the plate, and the quantity of particulate trapped (mobilized) below the screen was reduced as trapped particulate was transported downstream.

The increase in particulate in the flow from 0.6 to 0.7 ft/sec was not as substantial as the increase from 0.5 to 0.6 ft/sec, particulate buildup was observed on the plate, and particulate was mobilized below the screen. Thus, the 45-minute second bed formation period was initiated. At the end of the 45 minute period, the particulate concentration was significantly reduced and particulate coated the plate surface leaving the majority of the perforations open. A velocity of 0.8 ft/sec was subsequently achieved. No increase in particulate concentration was observed, the flow was returned to 0.7 ft/sec, and the incomplete debris bed velocity test matrix was again employed.

The initial debris bed formation screen approach velocity for test ZE1 was maintained at 0.3 ft/sec. As with previous benchtop and large-scale coating debris tests, the mobilized debris for flow circulations immediately after the introduction of debris into the loop was judged by visual observation to be reduced by settling rather than collection on the plate. Thus, settled material was mobilized into the flow by

tapping the horizontal flow region of the test loop at the debris injection level with a rubber hammer. Eight tapping periods were conducted within 5 minutes of the debris introduction. By the eighth tapping period, material mobilization to the test section/plate was minimal as judged by visual observation.

At the end of the debris bed formation period at a screen approach velocity of 0.3 ft/sec, 1/4-in. square ZE debris on the perforated plate was visually observed to approximate the loaded amount. The debris bed was incomplete, with ~20% of the plate area exposed. The processed debris was visually observed to be passing through the plate (and the 1/4-in chips were retained thereon) during the early portion of the bed formation test phase. This processed debris concentration in the flow was visually observed to decrease with time without readily apparent buildup on the debris bed. Thus, it was judged to have settled in the loop. The screen approach velocity was therefore increased to 0.7 ft/sec (per test ALK2 description above). The processed particulate concentration in the flow was visually observed to increase, minimal 1/4-in. chip debris appeared mobilized, and the processed particulate collected on the plate over the 45-minute hold period, as judged by the visually observed increase on the plate and reduction of debris in the flow. The measured debris bed head loss increased by 60% (10 to 16 in. H₂O) over this period. The incomplete debris bed velocity matrix was subsequently employed.

7.5.2 Coating Debris Bed Results

A Quick-Look report providing the data sets for tests ALK1a, ALK1b, ZE1, and ALKBT is provided in Appendix K. The current presentation of results will focus on the effects of coating preparation, test repeatability, coating type comparison, and test fluid temperature. The effect of coating preparation is considered in subsection 7.5.2.1 for tests ALK1a and ALK2; test repeatability is examined through tests ALK1a and ALKBT in Section 7.5.2.2; coating type comparison (e.g., ALK to ZE) is provided in Section 7.5.2.3; and temperature effects are considered in Section 7.5.2.4. The uncertainties for the Coatings test are similar to those presented in Sections 7.2 through 7.4. Given that incomplete debris beds were formed for each test, uncertainties in the presented data are not detailed.

7.5.2.1 Coating Preparation

The effect of coating preparation (i.e., processed or 1/4-in. square chips debris) may be considered with regard to tests ALK1a and ALK2. The 3°C temperature difference for the nominal fluid temperature between the tests is neglected (Table 7.5.1).

As specified in Table 7.5.1, the total target debris loading for these tests was 1,400 g/m². Test ALK1a had 700 g/m² each of processed and 1/4-in. square chips coating, while the entire loading for ALK2 consisted of -processed coating. Differences in debris behavior during the debris bed formation periods are noted in Section 7.5.1. No data are available to evaluate or quantify the possible effects of flow histories.

Each debris bed was incomplete, as shown in Figures 7.53 and 7.54. The debris bed for test ALK2 was an extreme case, with the bulk of the perforations in the plate open to flow.¹ As expected due to the bed formation behavior, the combination of processed coating and 1/4-in. square chips for test ALK1a resulted in a larger head loss across the debris bed than for test ALK2 (Figure 7.55).² Test phase ramp up 2 for ALK1a and ramp up 1 of the truncated velocity matrix employed for ALK2 are shown.

¹ In Figure 7.54, the observable areas of blocked perforations were observed to be caused by contamination with 1/4-in. square coating ALK from the prior ALK1a and ALK1b test mobilized out of the test loop by the increased screen approach velocities used during debris bed formation for ALK2 (see Section 7.5.1).

² Results from the second test period (Section 7.5.1) of ALK2 are presented.

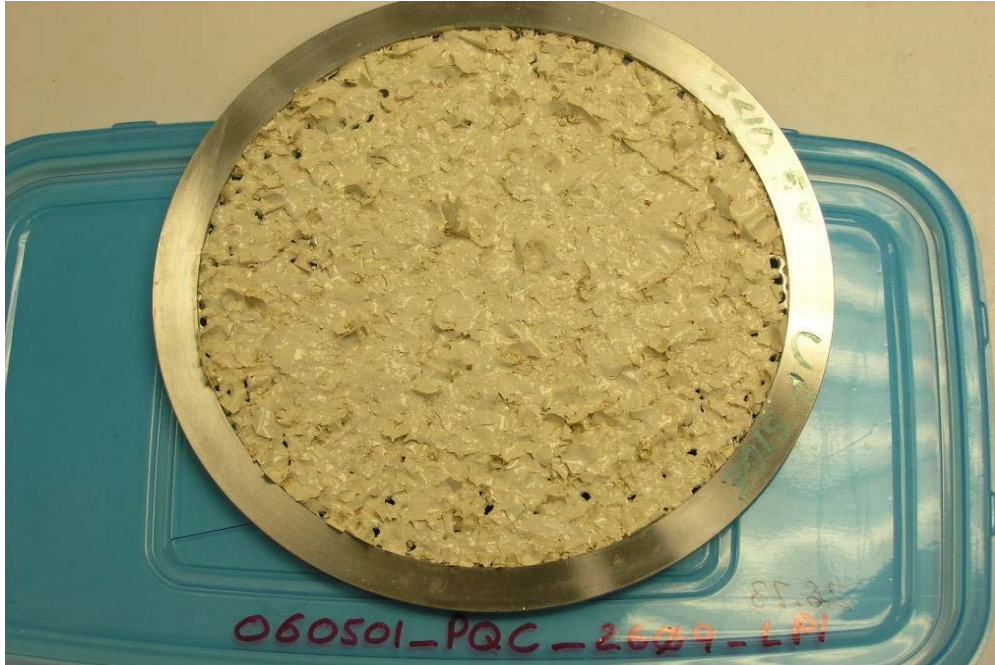


Figure 7.53. ALK1a Debris Bed After Retrieval from Test Section, Top View



Figure 7.54. ALK2 Debris Bed After Retrieval from Test Section, Top View

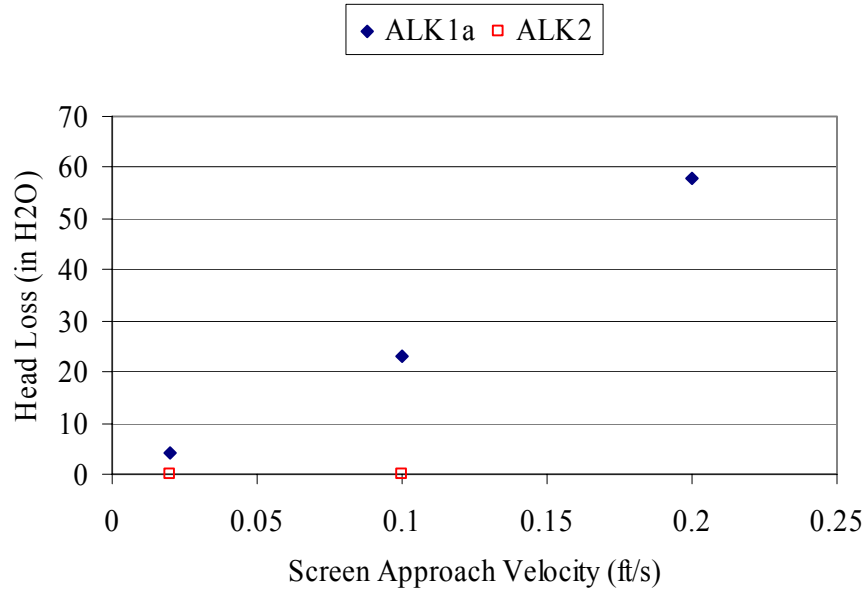


Figure 7.55. Head Loss Results for ALK1a and ALK2

The retrieved debris bed mass loadings for ALK1a and ALK2 were within about 5% of each other. The incomplete and varying debris bed surfaces preclude considerations based on the debris bed heights.

7.5.2.2 Coating Test Repeatability

Coating test repeatability, in terms of measured head loss for a given screen approach velocity, is considered for repeat velocity cycles within a single test and for repeated tests. Multiple velocity cycles were performed for tests ALK1a and ALK1b. As shown in Figure 7.56, the variability between the velocity cycles (ramp up 2 and 3 results are plotted for each test) is relatively minor (absolute value ~ 0 (10%) at 0.1 ft/sec, ~ 0 (5%) at 0.2 ft/sec), indicating stability (i.e., constant mass, porosity, etc. at or over the screen approach velocities) for the debris bed.

Repeat tests for the ALK coating were performed in the large scale, ALK1a, and benchtop, ALKBT, loops. The 3°C temperature difference for the nominal fluid temperature between the tests is neglected (Table 7.24). Each test had 700 g/m² each of processed coating and 1/4 in. square coating chips. The debris beds were formed under different flow conditions, and no data are available to evaluate or quantify the possible effects of the bed formation and flow histories.

As may be observed by comparison of Figures 7.53 and 7.57, the incomplete debris beds were similar in appearance, although the open channels and perforations were noticeably fewer for ALKBT. In Figure 7.58, test phase ramp up 2 head loss results are provided for each test. The higher head loss results for ALKBT are somewhat surprising given the higher retrieved debris bed loading of ALK1a, refer to Table 7.24, but may be expected with the relative completeness of the debris beds indicated above. This observation may be supported by considering that the maximum variability in the presented results. The variability of approximately 55% is up to 25% larger than that observed for comparisons of the NUKON-only large-scale and benchtop tests (Section 7.2). This difference is also substantially larger than the benchtop test comparisons in Section 6.1. The incomplete and varying debris bed surfaces preclude investigation of the head loss results based on the debris bed heights.

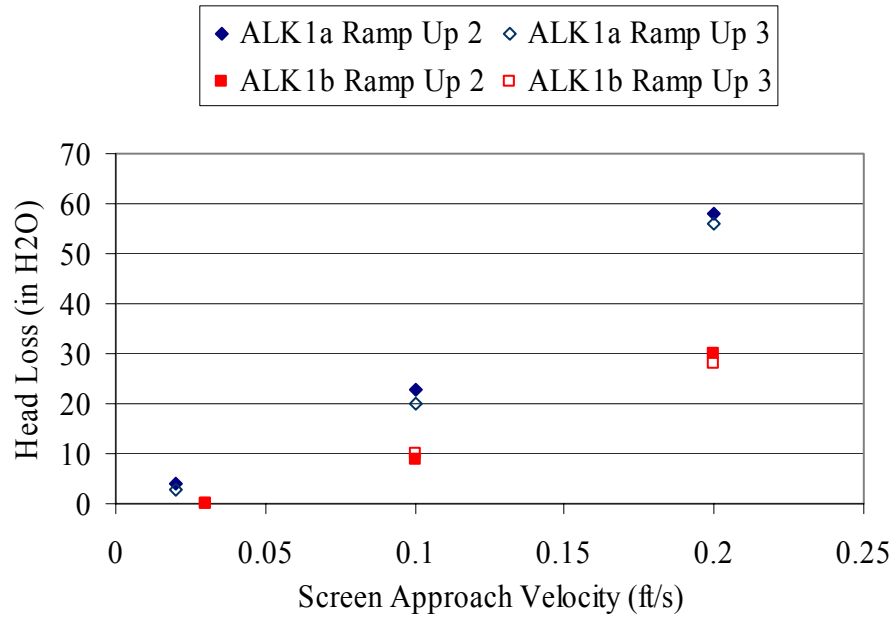


Figure 7.56. Head Loss Results for ALK1a and ALK2, Repeat Velocity Cycles

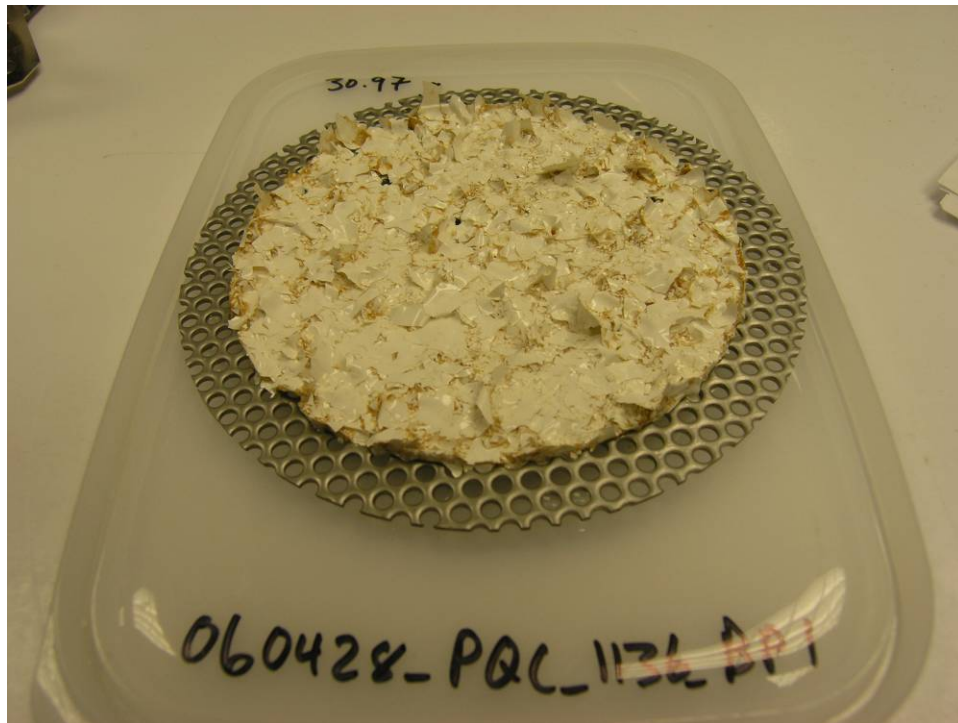


Figure 7.57. ALKBT Debris Bed After Retrieval from Test Section, Top View

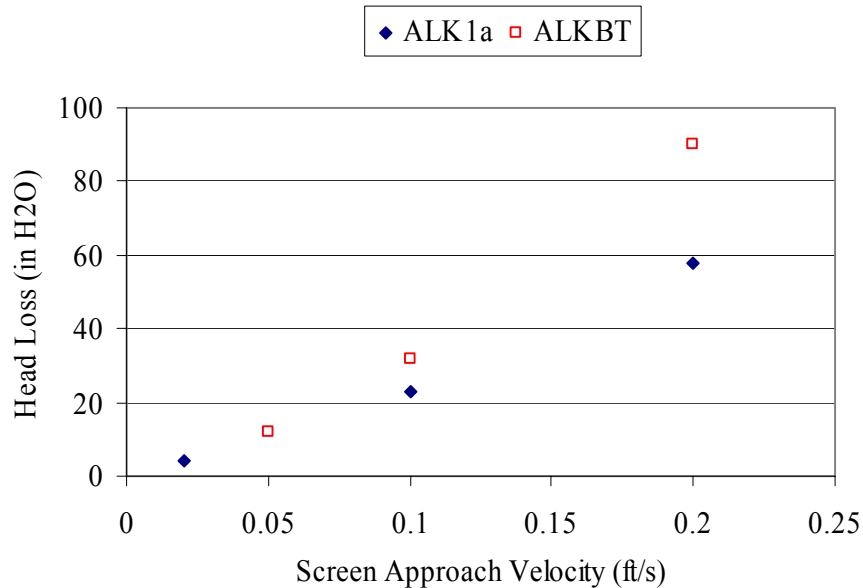


Figure 7.58. Head Loss Results for ALK1a and ALKBT

7.5.2.3 Coating Type Comparison

The head loss performance of debris beds with the same target debris loading and preparation but different coating materials was investigated. ALK was used for test ALK1a, and ZE was used for ZE1. ALK1a and ZE1 had 700 g/m² each of processed coating and 1/4-in. square coating chips for a total target debris loading of 1,400 g/m². The nominal fluid temperature difference, 3°C (from Table 7.24), is neglected. No data are available to evaluate or quantify the possible effects of bed formation and flow histories.

As described in Section 7.5.1, significantly different flow conditions were required for debris bed formation. The ALK coating debris types are thought to have been more homogeneously transported to and collected on the screen, while the ZE debris appeared to be segregated by the flow conditions. The ZE1 debris bed thus formed by deposition of the 1/4-in. square coating chips, and the processed coating was deposited only after a substantial increase in the screen approach velocity (Section 7.5.1).¹ Insufficient data exist to evaluate the possible effect of this observed variation.

The ZE1 debris bed shown in Figure 7.59 was substantially less complete than the ALK1a debris bed in Figure 7.53. Further, while the ALK1 debris bed was relatively easily removed from the screen as a complete intact bed after drying, the ZE1 debris bed was essentially a collection of separate debris pieces with no cohesiveness. It is uncertain what effect this observed integrity of the debris bed had on the resultant head loss, but clearly, as shown in Figure 7.60, the ALK1a debris bed head loss was substantially greater than that for ZE1. The head loss results presented are for test phases ramp up 2 and ramp up 1 for the ALK1a and ZE1 tests, respectively. The retrieved debris bed loading for ALK1a was 2% greater than that for ZE1. Considerations based on the debris bed heights are precluded by the incomplete and varying debris bed surfaces.

¹ It has been shown (see Section 6.3) that small variations in the loading sequence of fibrous and particulate insulation debris can have a significant impact on head loss results. Thus it may be reasonable to assume that a similar effect, uncertain in magnitude, may be achieved with coating debris. The varied nature of the ALK and ZE coating debris, and more significantly the incompleteness of the coating debris beds formed, possibly renders comparison of the loading sequence effects for ALK1a and ZE1 moot.

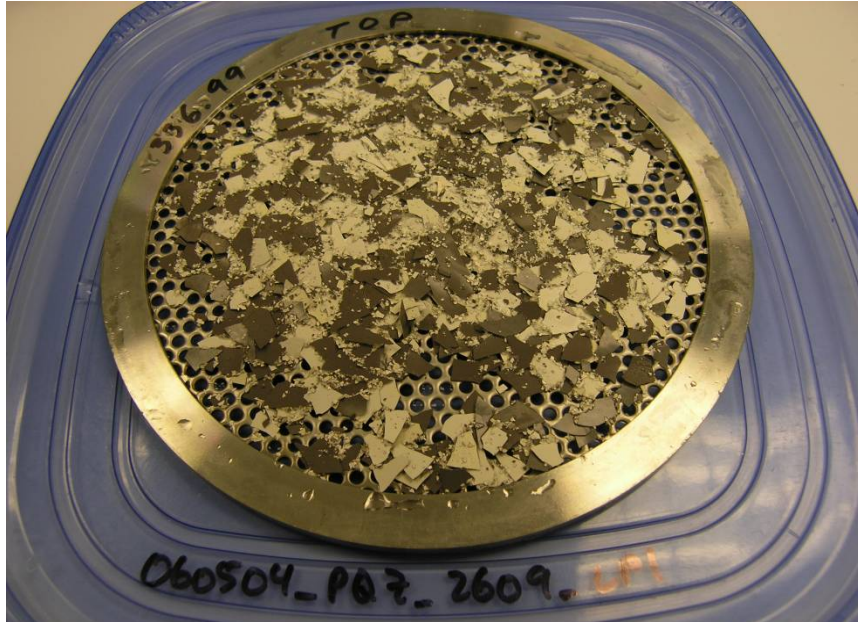


Figure 7.59. ZE1 Debris Bed After Retrieval from Test Section, Top View

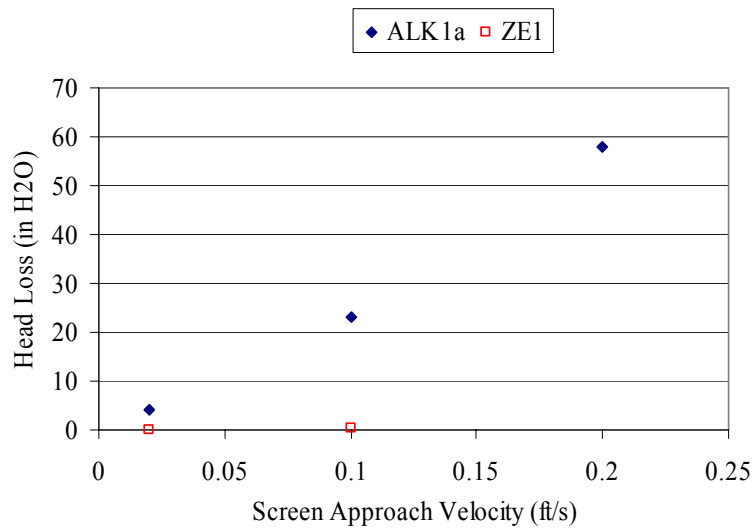


Figure 7.60. Head Loss Results for ALK1a and ZE1

7.5.2.4 Temperature Effects

The effect of varied fluid temperature on head loss as a function of screen approach velocity was investigated with tests ALK1a and ALK1b. As with specific NUKON-only and NUKON/CalSil debris beds, temperature effects testing was first conducted by performing debris bed formation and the completion of the velocity test matrix at ambient conditions (test ALK1a). The loop fluid was then heated to 82°C, whereupon the velocity matrix was repeated (test ALK1b). The effect of the flow history resulting from this approach is uncertain.

The head loss for ALK1b was reduced as compared to that for ALK1a, Figure 7.61. Data for test phase ramp up 2 is shown for each temperature.

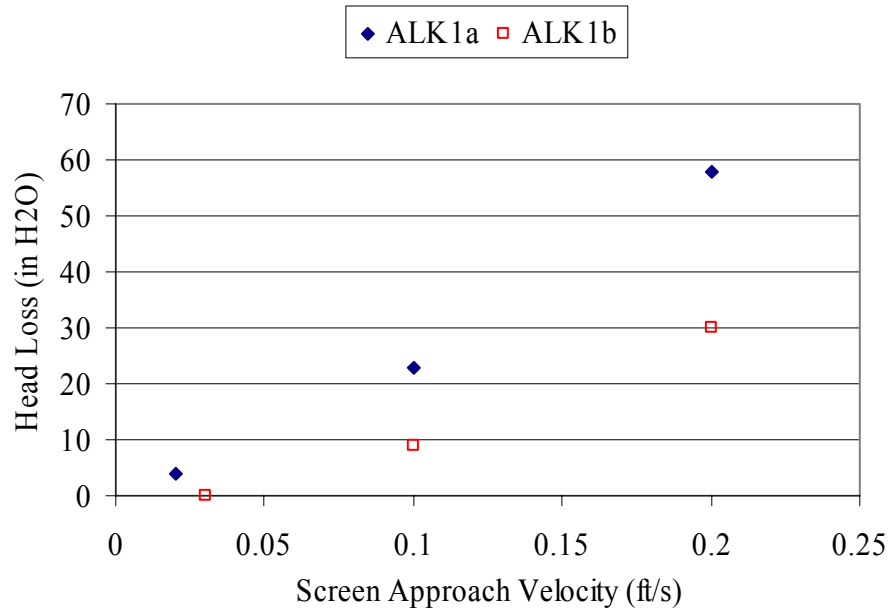


Figure 7.61. Head Loss Results for ALK1a and ALK1b

8.0 Discussion of Large Scale Results

This section discusses the results obtained from large-scale testing that were presented in Section 7. Comparisons are made between the results for different types of debris beds and test conditions. Final conclusions are presented in Section 9.

Under clean, debris-free conditions, the perforated plate with 1/8-inch holes had a greater resistance to flow than the 5-mesh woven wire cloth screen (referred to as the 5-mesh screen); however, the difference in pressure drop was small. At a screen approach velocity of 2.0 ft/sec, the perforated plate had a head loss of 3.7 in. H₂O (referenced to 68°F) compared with 2.3 in. H₂O for the 5-mesh screen. For a screen approach velocity of 0.2 ft/sec, both screen materials yielded head loss measurements on the order of 0.1 ± 0.1 ft/sec for clean water. Based on how the debris bed formed on the two types of screen material, it is unclear which material contributed higher flow resistance to a debris bed. The NUKON and NUKON/CalSil debris beds formed on the surface of the perforated plate with minimal material protruding through the perforations. The debris beds were easily removed from the perforated plates. For the CalSil-only tests (no complete debris beds formed), the debris appeared to have been extruded through holes in the perforated plate in the vicinity of open flow channels, but minimal entangling of the extruded material occurred.

On the 5-mesh screen, the debris appeared to become entangled with the woven wire. The least entanglement was experienced with NUKON-only debris beds. Additional effort was required to remove the debris beds from the 5-mesh woven wire screens, and after removal of a debris bed, additional effort was required to remove residual debris material that remained entangled with the woven wire.

For the bare screen materials, no significant changes in head loss were observed at elevated fluid temperatures of 129°F (54°C) and 180°F (82°C). Any difference in the measured pressure drop with respect to fluid temperature is considered to be indistinguishable within the resolution of the DAS at low head loss values.

The pressure drop data presented for ambient fluid temperatures (approx. 68° to 82°F [20° to 28°C]) were obtained for conditions of either fully turbulent or fully laminar pipe flow upstream of the debris bed. Only the data obtained at 0.05 ft/sec (0.02 m/s) for ambient fluid temperatures were predicted to have transition flow conditions upstream of the test screen. For the elevated fluid temperature tests at 129° and 180°C (54° and 82°C), the data presented for 0.02 ft/sec (0.01 m/s) were predicted to potentially have transition pipe flow conditions upstream of the debris bed. Higher approach velocities at the elevated temperature were predicted to produce fully turbulent pipe flow upstream of the test screen.

For the NUKON-only and NUKON/CalSil debris beds, the steady-state head loss achieved for each velocity condition tested tended to increase with each cycle of the velocity sequence. The continual changes observed in the pressure drop with each velocity cycle were greater than the uncertainty of the measurements. This phenomenon complicates the assessment of test repeatability. Because the debris beds were observed to compress and relax with changes in the screen approach velocity over multiple cycles, the potential existed for the structure of the debris beds to continually change as finer material migrated through the debris bed with oscillations in the debris bed height and associated bulk porosity.

For the NUKON-only tests, repeatability was obtained between large-scale tests NO4 and NO5, with both test cases exhibiting a similar increase in pressure drop with each velocity cycle. The large-scale results also compared well with benchtop loop results with similar mass loadings. All of the test cases used to assess the repeatability of the NUKON-only debris beds had an initial screen approach velocity of 0.2 ft/sec. After this assessment, the screen approach velocity for bed formation was changed to 0.1 ft/sec.

Based on the comparison made for the measured debris bed height as a function of screen approach velocity presented in Figures 7.10 and 7.11, the initial screen approach velocity used for bed formation appears to impact the resulting debris bed height and, hence, the relative bulk density. The debris bed in test NO5, which was formed with an initial screen approach velocity of 0.2 ft/sec, had a bed height similar to that of NO2 despite having a mass loading approximately three times greater.

Several factors may contribute to the differences observed in results obtained for the various screen approach velocities used for debris bed formation. At greater approach velocities, debris beds were observed to compress. The variation in the compression of a debris bed changes the filtration efficiency of the debris bed. Changes in the screen approach velocity may change the mass fraction of material that is retained within a debris bed. If a debris bed captures fewer fines during the initial stages of the bed formation process, a higher fraction of the smaller size material may not be captured until the bulk of the debris bed is formed or the screen approach velocity is increased. This would result in a higher fraction of fine debris being available for deposition in a thin surface layer, as discussed in Section 6.4.

Variations in the results obtained between test cases with different bed formation velocities may also be the result of the test loop geometry. A reduction in the screen approach velocity also reduces the flow rate throughout the test loop. The reduction in the flow rate may lead to material holdup or settling within the test loop. The size distribution of the held-up or settled material would differ from that of the bulk material introduced to the loop. This segregation of material would create a change in the debris loading sequence, which, based on the results of Section 6.3, can have a significant effect on the pressure drop across the debris bed. For the same screen approach velocity, the bed formation process could be altered depending on the line sizes of the test loop.

For the NUKON/CalSil tests, NC3 and NC14 were formed at the higher initial bed formation velocity of 0.2 ft/sec. Due to the potential differences in the debris load sequence and in the CalSil mass loadings compared with other NUKON/CalSil test cases, it is difficult to draw final conclusions regarding the impact of the initial bed formation velocity on the resulting head loss across the debris bed. NC14 had the greatest retrieved mass loading of any debris bed tested, but the measured pressure drops at 0.1 and 0.2 ft/sec were approximately 50 and 40% those obtained for NC11, which had approximately half the mass loading of NC14. These results indicate the importance of knowing the conditions for debris bed formation when comparing the results of different test cases.

For the same debris bed formation process, the pressure drop across the NUKON-only and CalSil-only debris beds increased with an increase in the retrieved mass loading. Figure 8.1 is a plot of the head loss across the debris bed as a function of the retrieved mass loading for the NUKON-only (denoted NO) and CalSil-only (denoted CO) test cases. The data are plotted for constant screen approach velocities of 0.1 and 0.2 ft/sec. The data plotted in Figure 8.1 are for the debris beds formed at ambient fluid temperatures. While none of the CalSil-only mass loadings tested developed complete debris beds, for the same retrieved mass loading the CalSil-only test cases still generated higher pressure drops than the NUKON-only cases, which were for complete debris beds (i.e. no channeling).

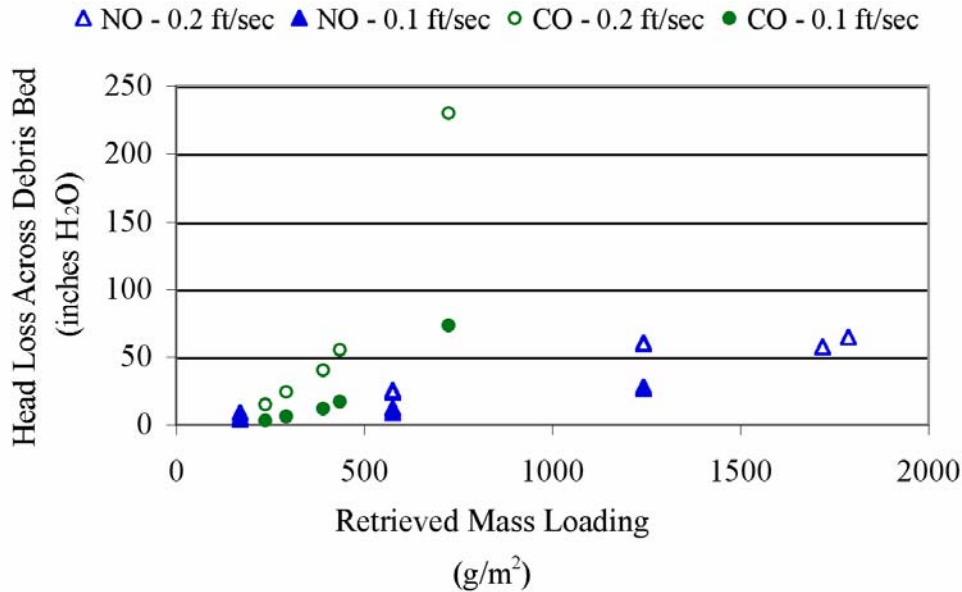


Figure 8.1. Pressure Drop Across the Debris Bed as a Function of the Retrieved Mass Loading for NUKON-Only (NO) and CalSil-Only (CO) Test Cases at Constant Velocities of 0.1 and 0.2 ft/sec. Test cases conducted at elevated fluid temperatures or with debris beds formed at elevated temperatures are excluded from the data. Data are from Tables 7.6 and 7.12 and the Quick Look reports in Appendixes H and I.

The pressure drops obtained for the CalSil-only tests combined with the results of the debris loadings, sequence investigation demonstrate what a difference the rearrangement of the debris constituents can have on the resulting pressure drop. In the benchtop loop, complete NUKON-only debris beds were formed on the 5-mesh screen that had retrieved mass loadings of 56 and 102 g/m². Thin fibrous beds such as these can provide a support structure for capturing CalSil, potentially creating a two-layer bed that, based on the test results, can have a significantly higher pressure drop than one using debris constituents that were premixed before introduction into the test loop.

For the loading sequence investigation, four scenarios were evaluated.

1. Formation of a NUKON-only debris bed prior to CalSil material being introduced into the test loop.
2. Premixing of the NUKON and CalSil debris constituents prior to introduction into the loop.
3. Formation of a CalSil-only debris bed followed by the addition of NUKON debris.
4. The addition of CalSil to the test loop with the addition of NUKON debris following after a short time (referred to as the lag time). The intent was to evaluate the formation of a debris bed resulting from the addition of NUKON to a flow stream that already contained well-dispersed CalSil material.

Scenario 4 yielded the highest-pressure drop measurements of the scenarios tested with the pressure drop reaching approximately 1000 in. H₂O in the benchtop loop and essentially exceeding the pump capacity. Scenario 1 yielded the next highest pressure drop measurements, followed by the results for the premixed condition of Scenario 2. As stated earlier, the results of Scenario 3 were not fully evaluated because a complete CalSil debris bed was never formed. The Series 2 tests were conducted using premixed debris for the NUKON/CalSil test cases.

The Series 1 tests attempted to simultaneously inject the separated debris constituents into the test loop. It is postulated that the variation in the resulting head loss with respect to the mass loading observed for the Series 1 NUKON/CalSil tests was due to variations created in the loading sequence of the debris on the screen. The simultaneous injection of the debris constituents was determined to create variations in the relative concentrations of the constituents in the main line just downstream of the point of debris injection. The loading sequence investigation not only demonstrated a variation in pressure drop resulting from changes in the debris loading sequence, it also demonstrated that repeatable results can be obtained for various loading sequences as long as the introduction sequence of the debris materials was controlled.

In Figure 8.2, the data from Figure 8.1 are plotted along with the pressure drop data from the NUKON/CalSil (denoted NC) debris beds formed under similar conditions. The head loss data presented in Figure 8.2 as a function of the retrieved debris bed mass loading is plotted for constant screen approach velocities of 0.1 ft/sec (0.03 m/s) and 0.2 ft/sec (0.06 m/s). Figure 8.2a includes both the Series 1 and Series 2 test cases; Figure 8.2b contains only the Series 2 test cases. The retrieved mass loadings of Series 1 tests are higher than those of Series 2 with minimal overlap between the two test series. Therefore, a good comparison of the pressure drop measurements obtained for the two debris-loading procedures cannot be made. The variations in the head loss measurements relative to the retrieved mass loading for the NUKON/CalSil test cases could be impacted by both the debris loadings sequence and the variations in the CalSil-to-NUKON mass ratio for each retrieved debris bed.

The results of Figure 8.2a and the fact that no complete CalSil-only debris beds were formed make it difficult to determine which debris bed condition would yield the highest pressure drop. Based on the results of the loading sequence evaluation, it is postulated that higher pressure drops can be obtained from a NUKON/CalSil debris bed then from a CalSil-only debris bed.

In both Sections 7.2 and 7.4, the pressure drop was shown to increase with an increase in the relative bulk density of the debris bed for the Series 2 test cases. Figure 8.3 compares the pressure drop across the debris bed as a function of the debris bed relative bulk density for both the NUKON-only and NUKON/CalSil debris beds. From Figure 8.3, the trend appears to hold for all of the Series 2 test cases, with the NUKON/CalSil debris beds appearing to yield a slightly higher pressure drop at a given mass loading (see Figure 8.2). Comparing Figures 8.2 and 8.3, it appears the pressure drop across the debris bed for a given bed formation procedure trends better with the debris bed relative bulk density than with the retrieved mass loading of the debris bed.

The pressure drop across a debris bed was anticipated to decrease with an increase in the fluid temperature due to the reduction in the fluid viscosity and density. While this was observed for a majority of the test cases, several instances occurred where the pressure drop increased with an increase in the fluid temperature. For both the NUKON-only and the NUKON/CalSil debris beds, these discrepancies in the measured head loss across a debris bed relative to the fluid temperature were accounted for by observed changes in the relative bulk density of the debris beds. It is assumed the change in debris bed density observed for some of the elevated temperature tests was the result of the additional flow history to which the debris bed was subjected.

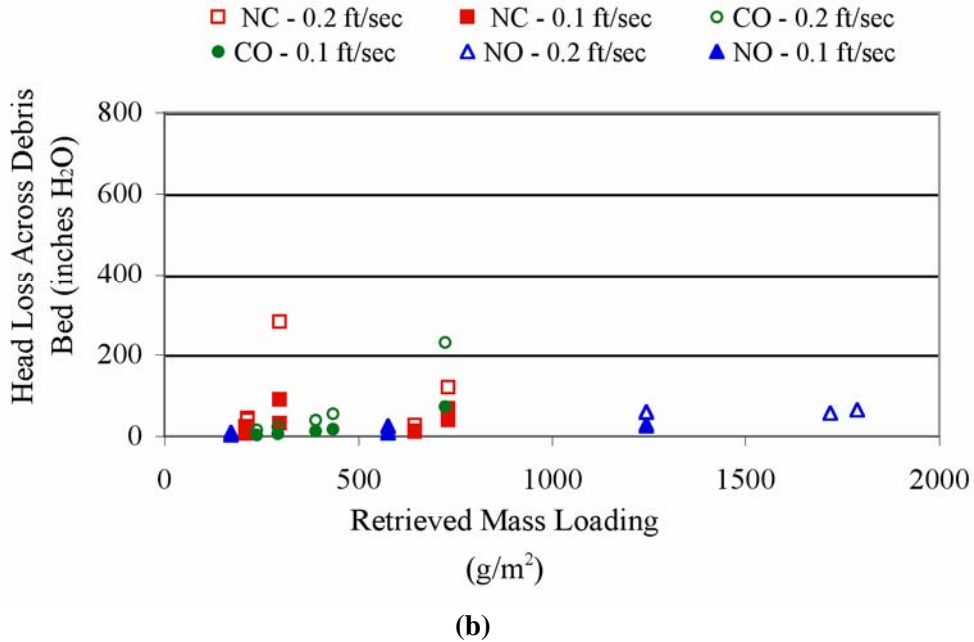
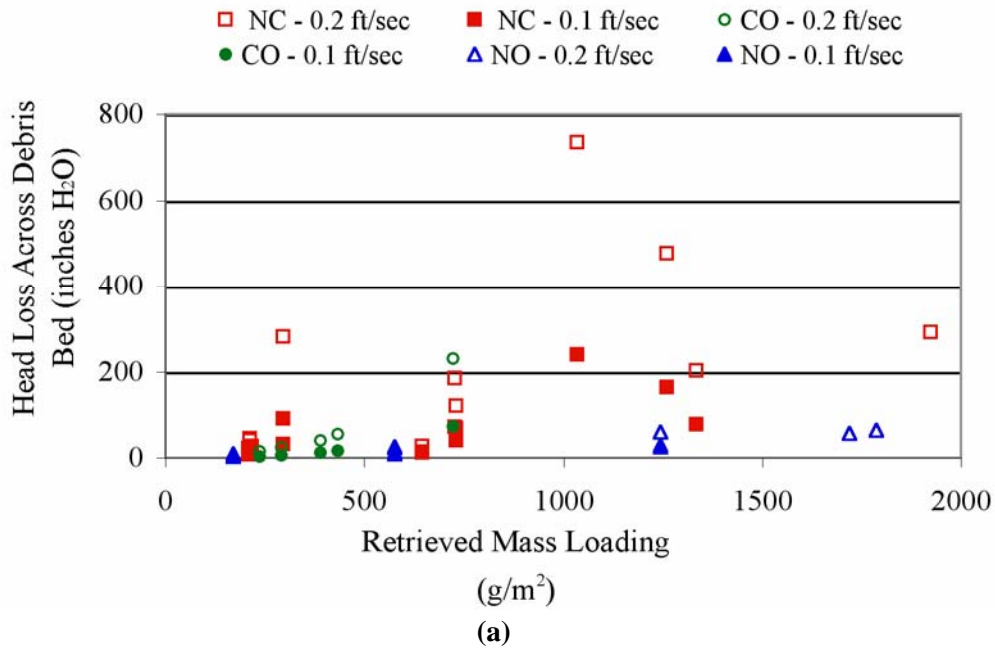


Figure 8.2. Pressure Drop Across the Debris as a Function of the Retrieved Mass Loading for NUKON-Only, CalSil-Only, and NUKON/CalSil (NC) Test Cases at Constant Velocities of 0.1 and 0.2 ft/sec. Test cases conducted at elevated fluid temperatures or with debris beds formed at elevated temperatures are excluded from the data. Figure 8.2a contains data from both Series 1 and 2 tests; Figure 8.2b contains only Series 2 data. Data taken from Tables 7.6, 7.10, 7.11, and 7.12 and Quick Look reports in Appendixes H, I, and J.

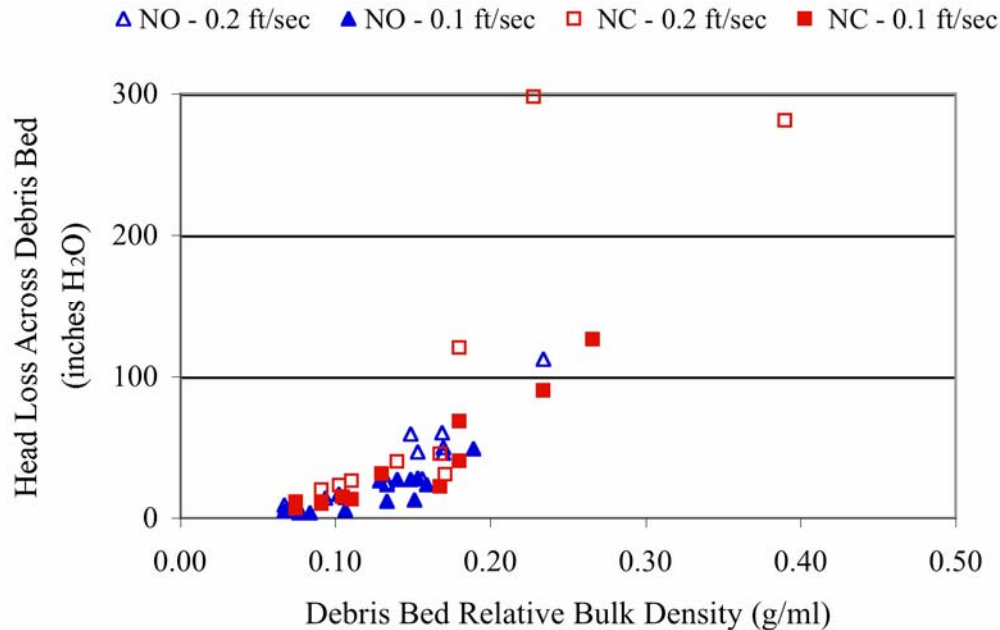


Figure 8.3. Pressure Drop Across the Debris Bed as a Function of the Debris Bed Relative Bulk Density for NUKON-Only and NUKON/CalSil Test Case at Constant Velocities of 0.1 and 0.2 ft/sec. Test cases conducted at elevated fluid temperatures or with debris beds formed at elevated temperatures are excluded from the data. The NUKON/CalSil Series 1 tests have not been included because no optical triangulation bed height measurements or associated densities exist. Data are from Tables 7.9 and 7.16 and the Quick Look reports in Appendixes I and J.

In Section 6.3, an example was provided to demonstrate that two debris beds of similar porosity (similar bulk density) could have significantly different flow resistances. However, these debris beds were generated using different load sequences. Based on the results of Sections 6.3, 7.2.1, 7.2.2, 7.4.4, and 7.4.5, it is postulated that, if two debris beds are formed with the same bed formation process, an increase in the relative density of the debris beds will correspond to an increase in the flow resistance.

The pressure drop measurements obtained from the two test scenarios used for the elevated temperature tests provided no indication of whether the fluid temperature had a significant effect on the formation of the debris bed. However, it is unclear whether subjecting the debris bed to an elevated temperature between 129° and 180°F (54° and 82°C) affects the CalSil content of the retrieved bed. Table 7.14 lists the percent of the target CalSil mass retained and the calculated retrieved CalSil mass loading for each of the Group 1 debris beds with a target NUKON mass loading of 217 g/m². Based on the results of Table 7.14, it appears that an increase in the CalSil-to-NUKON mass ratio reduced the mass of CalSil retained in the debris bed despite the target CalSil mass loading being higher.

The debris beds for NC4 and NC3 had CalSil-to-NUKON mass ratios of 0.25 and 0.50, respectively, and retained CalSil mass loadings of 26 and 49 g/m², respectively, which correspond to 48 and 46% of the target CalSil being retained. This compares to NC5, NC15, and NC16, which all had target CalSil-to-NUKON mass ratios of 0.75 and retained 11, 24, and 11 g/m² CalSil and 7, 15, and 7% of the target

CalSil, respectively. It has also been noted that the physical integrity (qualitatively assessed) of the retrieved NUKON/CalSil debris beds was observed to degrade with an increase in the CalSil mass loading. It is unclear whether this observed phenomenon is related to the ability of the debris material to form a debris bed.

However, the reduced retention of CalSil may be the result of testing at elevated fluid temperatures. The debris beds from NC5 and NC16 were subjected to a maximum fluid temperature of 180°F (82°C) and NC15 to a maximum fluid temperature of 129°F (54°C). The debris beds from NC3 and NC4 were only subjected to ambient temperature. Based on the Group 1 results, the higher the temperature, the lower the CalSil mass loading in the retrieved debris beds.

The debris bed from test condition NC17 was the other NUKON/CalSil bed subjected to an elevated temperature, 129°F (54°C). NC17 had a NUKON target mass loading of 724 g/m² and a target CalSil-to-NUKON mass ratio of 0.5. The same dramatic drop in retained CalSil was not observed for test condition NC17. This may be because the CalSil and NUKON mass loadings of NC17 were over twice and three times those of NC5, NC15, and NC16. The higher CalSil loading may result in a saturation level being reached, or the increased NUKON loading may counteract the reduction of CalSil at the elevated temperature by increasing the capture efficiency of the debris bed. The difference may also be due to the lower CalSil-to-NUKON mass ratio of 0.5. Due to the number of parameters in play, the limited number of test cases and limited ranges of parameters insufficient results were obtained to determine what caused the dramatic reduction in CalSil retention for test conditions NC5, NC15, and NC16.

9.0 Conclusions

To meet the objectives of this test program, PNNL fabricated large-scale and supporting benchtop test loops. A total 156 tests were conducted consisting of the following test conditions: 5 screen-only tests, 11 CalSil-only tests, 90 NUKON-only tests, 45 NUKON/CalSil tests, and 5 Coatings tests. Of the 156 tests, 43 were performed in the large-scale test loop, and 16 of those tests were conducted at elevated temperatures of 129° and 180°F (54° and 82°C). The large-scale tests were conducted in three series. The first series duplicated test conditions from the previous study conducted by LANL at the University of New Mexico (Shaffer et al. 2005).

All of the tests were conducted and completed according to documented test procedures. Test facility fabrication and operation was performed according to PNNL's Standards Based Management System. All safety, health, and environmental related requirements were satisfied in the execution of this test program, and no work-related injuries or instances of environmental impact occurred.

The following head loss data are provided for test cases with mass loadings on the order of 200 and 1300 g/m² for test cases of NUKON-only and NUKON/CalSil to provide a comparison of the differences observed between the two test conditions.

PNNL testing of NUKON-only debris beds with retrieved mass loadings of 171 and 1244 g/m² produced pressure drops of 0.3 psi (9 in. H₂O @ 68°F [23 cm H₂O @ 20°C]) and 2.2 psi (60 in. H₂O @ 68°F [152 cm H₂O @ 20°C]), respectively, at screen approach velocities of 0.2 ft/sec (0.06 m/s). Repeatable head loss measurements were obtained for the NUKON-only results. The flow history effects created slight increases in pressure drop with each velocity cycle, but these increases were observed in repeat tests. Good comparisons were also obtained between the pressure drop measurements from the large-scale and benchtop loops.

The NUKON/CalSil debris bed with a retrieved mass loading of 209 g/m² (containing 183 g/m² NUKON and 26 g/m² CalSil) and a screen approach velocity of 0.2 ft/sec (0.06 m/s) yielded a pressure drop of 0.8 psi (23 in. H₂O @ 68°F [58 cm H₂O @ 20°C]). For the CalSil/NUKON test cases, there were fewer opportunities to evaluate repeatability because the introduction of a target mass loading does not guarantee the same retained mass loading or ratio of constituents in the debris bed. To obtain a repeat case for a NUKON/CalSil debris bed, both the NUKON and CalSil mass loadings should be repeated. In addition, variations in the debris bed formation for cases of similar mass loadings can have significant effects on the resulting pressure drop. NUKON/CalSil debris beds having retrieved mass loadings of 1260 (926 g/m² NUKON and 334 g/m² CalSil [27 wt% CalSil]) and 1334 g/m² (991 g/m² NUKON and 343 g/m² CalSil [26 wt% CalSil]) produced pressure drops of 17.2 psi (477 in. H₂O @ 68°F [1212 cm H₂O @ 20°C]) and 7.3 psi (203 in. H₂O @ 68°F [516 cm H₂O @ 20°C]), respectively, at a screen approach velocity of 0.2 ft/sec.

Adjusting the debris loading procedure reduced variations in the results obtained for NUKON/CalSil debris beds and allowed comparable results in the benchtop loop to be obtained for various debris loading sequences. However, the CalSil content of the benchtop debris beds was not evaluated.

The work presented in Section 3 demonstrates that the debris preparation procedures yielded repeatable results. The R4 metric, while not quantifiable against other metrics used for debris characterization, provided a relative metric that allowed the debris preparation procedure to be adjusted, based on the debris concentration and the equipment being used, to yield prepared debris of similar consistency.

The particle size analysis conducted for CalSil debris demonstrated that similar particle size distributions were obtained over the range of CalSil concentrations prepared for introduction into the test loop.

The term complete is used to define debris beds that completely covered the screen and had no channeling through the debris bed. Debris beds that did not cover the entire screen or had channels (open flow passages) are referred to as incomplete. The appearance of the complete debris beds was uniform with a rim around the edge (at the wall of the test section) representative of what is expected for material deposited from a uniform steady pipe flow. The complete debris beds filled the entire cross-sectional area of the test section, with no gaps for flow to bypass the debris bed.

The increase in static pressure applied to the large-scale loop with the cover gas pressure maintained gas in solution with increases in the pressure drop across the debris bed. Therefore, the pressure drops measured in the large-scale loop are for two-phase (liquid and solids) flow with no gas present.

The in situ debris bed height measurements obtained with the optical triangulation system demonstrated that debris beds continued to compress and relax with changes in the screen approach velocity. The center height of a debris bed was observed to change typically on the order of 30% for an order of magnitude change in the screen approach velocity (0.2 to 0.02 ft/sec) with changes in bed height as much as 80% for some cases.

Post-test filtration and inspections of the test loop indicated that negligible amounts of NUKON and CalSil debris were left in the test loop. Test observations indicate that debris material was being held up within the loop during portions of the test. However, the peak flow rates appeared to be sufficient to transport the debris material within the test loop. The peak flow rates used during testing did not appear to be high enough to fully mobilize and transport all of the coatings materials.

The minimum retrieved mass loading obtained for a complete large-scale NUKON debris bed was 171 g/m² on the perforated plate, which was created with a target mass loading of 217 g/m². In the bench-top loop, complete debris beds were formed on the 5-mesh screen with target mass loadings of 107 g/m², which yielded retrieved mass loadings of 56 and 102 g/m². The minimum retrieved mass loading that formed a complete NUKON/CalSil debris bed was 160 g/m² on the perforated plate, which was calculated to have a NUKON mass loading of 149 g/m². This was the smallest NUKON mass loading obtained for any complete debris bed generated in the large-scale loop. NUKON/CalSil tests conducted with NUKON target debris loadings of 108 g/m² and target CalSil loadings of 27 and 135 g/m² failed to generate complete debris beds. Testing was not performed to determine the minimum mass loading at which debris beds could be formed.

Visual observations of the retrieved debris beds noted that the NUKON-only debris beds were very durable—they could be removed from the test screen and handled. However, for the same NUKON mass loading, the addition of CalSil debris appeared to reduce the durability or the physical integrity of the retrieved debris bed. It is unknown whether this observation has any relevance to the conditions

necessary to generate a complete debris bed. Similar target NUKON mass loadings for NUKON-only test conditions that generated complete debris beds were not adequate to form complete debris beds when additional CalSil mass was mixed with the NUKON prior to introduction into the loop for the NUKON/CalSil test cases.

PNNL CalSil-only tests with CalSil target mass loadings ranging from 1450 to 4350 g/m² yielded incomplete debris beds with retrieved mass loadings from 79 to 724 g/m². No complete CalSil-only debris beds were generated during this test program. All of the CalSil-only debris beds that were undisturbed during the retrieval process only retained from 10 to 17% of the target debris loading. The results of the CalSil-only and NUKON/CalSil tests indicate sufficient NUKON mass loading is necessary for a complete debris bed to be formed. The test plan was not designed to determine the minimum NUKON mass loading required for bed formation, nor could it be ascertained from the completed test matrix.

The results presented in Sections 3 and 6 demonstrate that the debris preparation procedure strongly influenced the resulting pressure drop across the debris bed. Other parameters shown to influence the head loss across the debris bed for a given retrieved mass loading include:

- The sequence in which debris material is loaded onto the screen. The loading sequence investigation and Series 1 NUKON/CalSil tests demonstrated that, for the same mass loading, the sequence in which the debris material was loaded on the screen could change the resulting head loss by more than an order of magnitude. The higher pressure drops were not fully quantified because they exceeded the limits of the instrumentation for both test loops and the pump capacity of the benchtop loop.

The debris loading sequence influenced multiple-constituent debris bed as well as the single-constituent beds. The CalSil-only test cases, COBT3 and COBT4, had the same target mass loading; however, the bulk loading in COBT4 (single introduction of debris) resulted in approximately 50% more mass being retained than the incremental loading of COBT3.

- The screen approach velocity used during debris bed formation. It is unclear how much of the influence of bed formation velocity is an artifact of test loop geometry. It has been postulated that if holdup or settling of debris occurs within the test loop during the test, the effect on the measured pressure drop may be as much as that of a change in the debris loading sequence due to segregation of material. All changes in the bed formation velocity may not result in a change in the measured pressure drops. A notable impact would occur if velocities within the test loop dropped below a critical velocity for transport or mobilization for the size range of a debris constituent.
- The flow history to which the debris bed has been subjected. The parameters contributing to the flow history include the magnitude of the screen approach velocity, the duration for which the debris bed is subjected to a flow condition, and the cycling or history of the screen approach velocity. The flow history contributes to changes in the debris bed structure. For the tested conditions the greatest impact appears to be that caused by cycling of the screen approach velocity.

It is postulated that the relaxing and contracting of the debris bed allows material to migrate through the bed. Some of the migrating debris may be released from the debris bed, circulate through the loop, and be recaptured by the debris bed. The migration of material could allow the debris bed to reorganize in a way which increases flow resistance. The migrating particulate would continue to pass through the debris bed until the flow carried individual particles to locations where they were

completely trapped despite relaxation of the debris bed. The returning particulate will enter the debris bed at points of preferential flow. As more and more material becomes permanently trapped within the debris bed, the head loss increases.

- The initial target mass loading. The initial target mass loading may impact the results in two ways. The absolute mass of material in the flow determines the amount of material present for a given size range. A critical size may exist for retention, and all smaller material may continue to pass through the debris bed with the flow or migrate through the bed with some critical holdup. The effects of the target mass could also impact the formation of the debris bed based on the effect of the concentration of debris material in the flow. The same target mass loadings may yield different results depending on the concentration of the debris approaching the screen. While the target mass loading appears to affect the results, it is unknown which phenomenon has the most significant effect.

The in situ bed height measurements obtained from optical triangulation allowed the relative bulk density of the debris beds to be calculated. The calculated density is associated with the bulk porosity of the debris bed and can be used to compare test cases and test conditions because the structure of the debris bed appears to change with changes in the screen approach velocity. The bulk density is not a controllable parameter but is a result of the bed formation process, flow history, and mass loading. The head loss for both the NUKON and NUKON/CalSil debris beds formed at ambient fluid temperature with a constant screen approach velocity of 0.1 ft/sec (0.03 m/s) increased with an increase in the relative bulk density. The trend also appeared to hold when NUKON-only and NUKON/CalSil beds were compared. The NUKON/CalSil debris beds tended to form debris beds with larger relative bulk densities. Over the entire range of Series 2 testing the trend appears to hold. The comparison could only be made for debris beds with in situ bed height measurements obtained from optical triangulation.

In most instances, an increase in fluid temperature (decrease in fluid viscosity) resulted in a decrease in pressure drop across the debris beds. The results were affected by the flow history applied to the debris beds during the time required to change the fluid temperature in the test loop. For cases where an increase in fluid temperature resulted in an increase in pressure drop, the discrepancy was explained by an increase in the relative bulk density of the debris bed.

Two NUKON/CalSil debris beds from the benchtop loop that were formed on the 5-mesh woven screen using different debris loading sequences were sectioned and examined using SEM. The SEM analysis identified three distinct layers within the debris beds: a surface CalSil layer, a center porous region, and the bottom wire support region. The uniform surface layer consisted mostly of CalSil particulate supported by NUKON fiber and comprised 6 and 19% of the total post-test debris bed heights for the two cases; however, the compressibility of the individual layers under flow is unknown. The volume percent of CalSil in the surface layer was calculated to be 59 and 64 vol%, and the NUKON fiber concentration was 6.5 and 5.5 vol% for the two beds, respectively.

The center region was very porous and uniform with elevation. The center layer of the two debris beds consisted of NUKON fiber concentrations of 6.1 and 8.3 vol% and CalSil concentrations of 1.4 and 1.9 vol%, respectively. The center porous region comprised approximately 93 and 81% of the total bed heights for the two cases. The cylindrical NUKON fibers ranged in diameter from 5 to 15 microns as determined from the SEM analysis.

The bare perforated plate had a higher flow resistance than the 5-mesh woven wire screen. At a screen approach velocity of 2.0 ft/sec (0.6 m/s), the pressure drop across the perforated plate and 5-mesh screen were 3.7 in. H₂O @ 68°F (9.4 cm H₂O @ 20°C) and 2.3 in. H₂O @ 68°F (5.8 cm H₂O @ 20°C), respectively. No noticeable differences in the head loss measurements were obtained between tests conducted with the perforated plate and 5-mesh screen. However, some differences were observed in how the debris material interacted with the two screen materials. The debris material was more likely to become entangled with the woven wire of the 5-mesh screen so that it was not just resting on the screen but engulfed parts of the wire mesh. Some material was extruded through the holes of the perforated plate, but the degree of entanglement was much less. Removing the debris beds from the perforated plate was easier than removal from the woven wire.

For the limited Coatings test series, the results indicated:

- For the same target mass loadings and debris preparation processes, ALK debris tended to form a more substantial debris bed than ZE material.
- To obtain retrieved mass loadings that are comparable between the ALK and ZE debris, the Coatings tests should be conducted with larger target mass loadings than were used in this test program.
- The structure of the coatings debris resulted in larger retrieved mass loadings being required to obtain pressure drops similar to those obtained in the CalSil and NUKON debris beds.

10.0 References

- Bonaca MV. October 18, 2004. *Safety Evaluation of the Industry Guidelines Related to Pressurized Water Reactor Sump Performance*. ACRSR-2097, U.S. Nuclear Regulatory Commission Advisory Committee on Reactor Safeguards, Washington, D.C.
- Brinkman KW and PW Brady. May 1994. *Results of Hydraulic Tests on ECCS Strainer Blockage and Material Transport in a BWR Suppression Pool*. EC-059-1006 Rev. 0, Pennsylvania Power & Light, Allentown, Pennsylvania.
- European Nuclear Society (ENS). September 18, 1992. ‘*Swedish N-Utilities Explain BWR Emergency Core Cooling Problem.*’ No. 358/92, ENS Nuclear News Network, <http://www.nuclearenergynews.com>.
- Kasza K, JH Park, B Fisher, J Oras, K Natesan, and WJ Shack. 2006. *Chemical Effects Head-Loss Research in Support of Generic Safety Issue 191*. NUREG/CR-6913, U.S. Nuclear Regulatory Commission, Washington D.C.
- Konstandopoulos AG. March 2000. *Fundamental Studies of Diesel Particulate Filters: Transient Loading, Regeneration and Aging*. 2000-01-1016. SAE 2000 World Congress, Detroit Michigan, SAE International, Warrendale, Pennsylvania.
- Krotiuk WJ. 2006. *Development of Pressure Drop Calculation Method for Debris-Covered Sump Screens in Support of Generic Safety Issue 191*. NUREG-1862, U.S. Nuclear Regulatory Commission, Washington D.C.
- Merkel GA, WA Cutler, T Tao, A Chiffey, P Phillips, MV Twigg, and A Walker. 2003. “New Cordierite Diesel Particulate Filters for Catalyzed and non-Catalyzed Applications.” *Proceedings of the 9th Diesel Engine Emissions Reduction Conference*, Newport, Rhode Island.
- Mizuno T and J Suzuki. 2004. “Development of a New DPNR Catalyst.” 2004-01-0578, *SAE 2004 World Congress*, Detroit, Michigan.
- NRC March 2006, *Head Loss Testing*. Office of Nuclear Regulatory Research Division of Engineering Technology Modification to Statement of Work, JCN: N6106.
- Perry Nuclear Power Plant (PNPP). May 1993. “*Excessive Strainer Differential Pressure Across the RHR Suction Strainer Could Have Compromised Long-Term Cooling During Post-LOCA Operation.*” Licensee Event Report 93-011, docket 50-440. Perry Nuclear Power Plant, Cleveland, Ohio.
- Rao DV and F Souto. June 1995. *Experimental Study of Head Loss and Filtration for LOCA Debris*. NUREG/CR-6367 (SEA Report No. 554-06-A.8), Science and Engineering Associates, Inc., Albuquerque, New Mexico.
- Shaffer CJ, MT Leonard, BC Letellier, DV Rao, WA Roesch, JD Madrid, AK Maji, K Howe, A Ghosh, and J Garcia. May 2005. *GSI-191: Experimental Studies of Loss-of Coolant Accident-Generated Debris Accumulation and Head Loss with Emphasis on the Effects of Calcium Silicate Insulation*. NUREG/CR-6874, U.S. Nuclear Regulatory Commission, Washington D.C.

U.S. Nuclear Regulatory Commission (NRC). 1996. *Generic Safety Issue (GSI) 191, Potential Impacts of Debris Blockage on Emergency Recirculation During Design-Basis Accidents at PWRs*. U.S. NRC, Washington, D.C.

Weast RC (editor). 1975. *Handbook of Chemistry and Physics*. CRC Press. Cleveland, Ohio.

Zigler G, J Brideau, DV Rao, CJ Shaffer, F Souto, and W Thomas. 1995. *Parametric Study of the Potential for BWR ECCS Strainer Blockage Due to LOCA Generated Debris*. NUREG/CR-6224, U.S. Nuclear Regulatory Commission, Washington, D.C.